

Engineering and Targeting Glycan Receptor Binding of Influenza A Virus Hemagglutinin

by

Akila Jayaraman

Master of Science in Biotechnology
University of Madras, 2002

SUBMITTED TO THE DEPARTMENT OF BIOLOGICAL ENGINEERING IN PARTIAL
FULFILLMENT OF THE REQUIREMENTS FOR THE DEGREE OF

DOCTOR OF PHILOSOPHY IN BIOLOGICAL ENGINEERING
AT THE
MASSACHUSETTS INSTITUTE OF TECHNOLOGY

June 2011

© 2011 Massachusetts Institute of Technology. All Rights Reserved.

Author

.....

Akila Jayaraman
Department of Biological Engineering
April 25, 2011

Certified by

.....

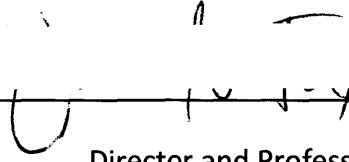
Ram Sasisekharan
Director & Edward Hood Taplin Professor of
Health Sciences & Technology
Thesis Supervisor

Accepted by

.....

Forest M. White
Associate Professor of Biological Engineering
Chair, Graduate Program

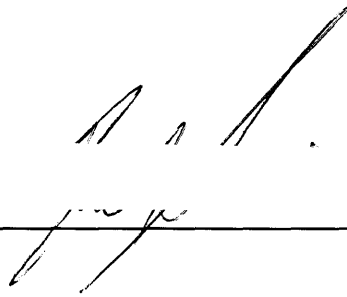
Thesis Committee members:



James G Fox
Director and Professor of Division of Comparative Medicine
Thesis Committee Chair



Ram Sasisekharan
Director & Edward Hood Taplin Professor of
Health Sciences & Technology
Thesis Supervisor



Zachary H Shriver
Vice President of Research,
Visterra, Inc.

Engineering and Targeting Glycan Receptor Binding of Influenza A virus Hemagglutinin

by

Akila Jayaraman

*Submitted to the Department of Biological Engineering on
April 29, 2011 in Partial Fulfillment of the Requirements
For the Degree of Doctor of Philosophy in Biological Engineering*

Abstract

The critical first step in the host infection by influenza A virus is the binding of the viral surface glycoprotein hemagglutinin (HA) to the sialylated glycan receptors terminated by N-acetylneuraminic acid (Neu5Ac) expressed on the host cell surface. Glycans terminating in Neu5Ac that is α 2-6 and α 2-3 linked to the penultimate galactose serve as receptors for human- and avian- adapted influenza A virus respectively. This thesis focuses on studying HA, glycan receptors and their interactions both in a biochemical and physiological context to understand the role of these interactions in influenza A virus pathogenesis.

The *first* Specific Aim of this thesis deals with understanding the molecular determinants of glycan receptor-binding specificity and affinity of HA (or avidity in the context of the whole virus) and how these properties govern antigenic drift and efficiency of airborne transmission. This approach contributed to uncovering the relationship between receptor-binding affinity and efficiency of transmission of the 2009 H1N1 pandemic influenza A virus and also predicting the evolution of this virus into a more transmissible strain.

The *second* Specific Aim of this thesis focuses on understanding the distribution of the glycan receptors for human-adapted HA (going beyond α 2-3/ α 2-6 linkages), in ferret (animal model for influenza research) and in human respiratory tracts. Based on this understanding, this part of the thesis contributed to developing new anti-viral strategies based on targeting the host glycan receptors (instead of the common strategies that directly target the viral proteins)

Overall, this thesis has provided functional insights into the role of HA-glycan interaction in viral pathogenesis. As part of this research, various tools and methods were developed. Further, such an approach paves way for elucidating the functional significance of important protein-glycan interactions in other disease models.

Thesis Supervisor: Ram Sasisekharan

Title: Director & Edward Hood Taplin Professor of Harvard Health Science & Technology

Technical Summary

Mammalian branched glycans that are present in the unique interface of cell surface and extracellular matrix (ECM) impinge on a variety of biological processes. One of the functions is to serve as receptors for recognition by glycan binding proteins on the surface of the pathogen. This is well exemplified in the case of human influenza A virus hemagglutinin (HA) that recognizes sialylated glycan receptors on the surface of tracheal epithelium. This HA-glycan interaction also determines the host restriction of influenza A viruses by virtue of the linkage specificity (between terminal sialic acid and the subterminal galactose) of HA to the glycan receptors.

In order to investigate the role of the HA-glycan interaction in viral pathogenicity, a multifaceted approach was used. This enabled gaining insights into both the molecular components viz, the glycan and the HA which further led to the understanding of its biological implication such as in transmissibility of the virus in human host.

1. Understanding the viral hemagglutinin (HA) in the context of its interaction with the host glycan receptors

Influenza A virus HA is the target of the host neutralizing antibody response. In order to escape the antibody response, the viral HA acquires antigenic drift mutation in and around the antigenic epitopes that prevents binding of the antibody. A careful analysis of these mutations, shed light into a new mechanism for viral escape of the host antibody response. A dose-dependent glycan array analysis of the escape mutants showed that mutants had increased binding avidity to the host glycan receptors as compared to the wild-type virus. Hence although the virus was able to bind the neutralizing antibody but due to an increased binding avidity to glycan receptors, the virus escaped the antibody response. This study hence provided a role for the receptor binding avidity in driving antigenic drift in influenza A virus.

Yet another mechanism by which the virus escapes the antibody response is by acquisition of new N-glycan sequons around the antigenic epitopes. The N-glycans would then sterically block the binding of the antibodies to the epitope. While analyzing such N-glycan sequons, conserved N-glycosylation sites were identified. One such site (at 91-93) was identified in H1 HA subtype. This site is located closer to the receptor binding domain (220-loop) of HA. Hence a potential role of the glycosylation site at 91 was analyzed using representative HAs from the 1918 pandemic. Recombinant HA lacking this glycosylation site was expressed and purified from insect cells. We found that lack of this glycosylation site led to a reduction or a complete loss of human receptor binding avidity and that there was no change in the binding of the glycan receptor by avian HA. This study provided a yet another role for site specific glycosylation (apart from antibody escape) on the receptor binding property of HA.

Given that receptor binding property of HA governs host restriction and species barrier, we next wanted to analyze its role in viral transmissibility using the 2009 H1N1 influenza A virus as a model system. We studied the transmissibility of the virus in

ferrets in collaboration with Dr. Terrence M Tumpey at the Centers for Disease Control. This study showed that the virus was inefficiently transmissible in ferrets as compared to seasonal and pandemic influenza A viruses. This was further corroborated by other epidemiological studies. We then analyzed the recombinant HA from a representative 2009 H1N1 virus (A/California/04/09 or CA04/09) on the glycan array platform. The HA showed a strict binding specificity to human receptor similar to the 1918 pandemic HA but had a reduced binding affinity as compared to the 1918 pandemic. This lower binding affinity could have resulted in a lower transmissibility of the virus. A closer examination of the HA showed a mismatched interaction network in the receptor binding site. Fixing the mismatch (by introducing a single or a triple mutation) in the RBS of the HA led to an increased binding affinity to the human receptors. The single mutant was tested for its transmissibility in ferrets (in collaboration with CDC). The single mutant had indeed acquired improved transmission efficiency in ferrets comparable to that of the seasonal and pandemic strains. This study provided a direct correlation between the receptor binding affinity of the HA to the transmissibility of the virus further emphasizing the functional significance of HA in viral pathogenicity.

2. Understanding glycan receptors in the context of its interaction with HA

Ferrets are widely used as animal models for studying influenza A viral pathogenesis and transmissibility. Though ferrets exhibit similar clinical symptoms of influenza A infection as that observed in humans, the viral tropism is different between ferrets and humans. Human-adapted influenza A viruses primarily target the upper respiratory tract in humans, while in ferrets, both upper and lower respiratory tract are targets. Viral tropism is governed by the distribution of host sialylated glycan receptors, which are recognized by influenza A virus hemagglutinin (HA). Although detailed structural characterization of glycan receptors in human upper respiratory tract was done previously, much less is known about the distribution of glycan receptors in the ferret respiratory tract. Hence we used a panel of plant lectins and recombinant HAs to stain ferret trachea (which represents the upper respiratory tract) and lung hilar region (which represents the lower respiratory tract). This lectin staining was further multiplexed with enzymes such as *Sialidase A* to identify specific glycan motif distribution in ferret respiratory tract. This study showed that the sialylated glycan receptors recognized by human-adapted HAs are predominantly distributed in submucosal gland of lung hilar region as a part of O-linked glycans. This is in contrast to human trachea where these glycan receptors are predominantly distributed in goblet cells as a part of O-linked glycans. Our study has implications in understanding influenza A viral pathogenesis in ferrets and also in employing ferrets as animal models for developing therapeutic strategies against influenza.

Based on the understanding of the glycan receptors for influenza A viruses, we have identified a plant lectin (PSL) from the mushroom *Polyporus squamosus*, which also binds to the receptors targeted by human influenza A viruses. We found that the N-terminal domain of PSL by itself (*rPSL-N*) inhibits infection of human influenza A viruses of H1 and H3 subtypes in MDCK cells. Hence we provide an alternate viable therapeutic strategy to combat influenza A infection.

Acknowledgements

The thesis work presented here wouldn't have been possible without the support and encouragement of several people whom I would like to acknowledge. First and foremost, I would like to express my sincere gratitude to my advisor Professor Ram Sasisekharan for believing in me and for challenging me with complex scientific problems during the course of my work in his lab. He gave me the opportunities to present my research work at various national and international conferences. Overall, working in Professor Sasisekharan's lab has not only enabled me gain scientific perspective but has also molded me into a better person instilled with confidence and patience.

I would like to thank my thesis committee Chair Professor James G Fox, for agreeing to be in my committee and also for providing me with insightful comments throughout my research work. His insightful comments on the project entitled "decoding the distribution of glycan receptors for human-adapted influenza A virus in ferret respiratory tract" enabled me to perform a comprehensive analysis of the glycan motifs present in ferret deep lung. He also provided me with the right set of ferret tissue sections for the analysis.

Dr. Zachary H Shriver, a member of my thesis committee was supportive and encouraging throughout my thesis work. His enthusiasm and a positive attitude really excited me to give closure to my projects. His inputs in the project involving the analysis of the receptor binding property of the 2009 H1N1 virus were seminal and enabled me to focus and wrap up the project in a timely fashion.

I had the unique opportunity to interact with Professor V. Sasisekharan who is a visiting faculty at MIT and a leading structural biophysicist. These interactions really helped me to appreciate the nuances of protein structure (in both hemagglutinins and lectins) in studies involving engineering of these proteins to achieve the desired glycan-binding properties. I really thank Professor V. Sasisekharan for his time and guidance.

My heartfelt gratitude goes to Dr. Karthik Viswanathan, my mentor and a great friend, with whom I first started working with after I joined the lab. He helped me get started in the lab and also taught me several techniques used in this thesis work. He was and still my "go-to" person if I have any questions on any of my scientific pursuit. It was really a pleasure working with Dr. Viswanathan. Aside from his scientific excellence, his wittiness would add smile in everyone's life in the lab.

I would like to extend my heartfelt gratitude to Dr. Rahul Raman who always responded patiently to any questions that I had in my research. Long scientific discussions also boosted my scientific curiosity and enabled me to think "outside-the-box". His inputs on rational structure-based engineering of viral hemagglutinin were seminal in understanding the receptor binding property of 2009 H1N1 influenza A virus.

I would like to extend my gratitude to our collaborators at the Centers for Disease Control (Dr. Terrance Tumpey and his research group) and at the National Institute for Allergy and Infectious Diseases (Dr. Jonathan M Yewdell and his research

group) whose contributions really helped in realizing the biological significance (through various animal models) of the structural and biochemical findings of my research.

I had fun working and mentoring Tadeusz Jan Kaczynski in the summer of 2009. Tad joined our lab as part of the HHMI-MIT program in Chemical Biology. He contributed to the project entitled "Site-specific N-glycosylation of influenza A HA: implications in glycan receptor binding" by troubleshooting expression of recombinant HA. His enthusiasm and hard work made mentoring for me a very fun-filled experience.

My time at MIT wouldn't have been more enjoyable and productive without the presence of excellent colleagues in the lab. I thank past members of the lab; Dr. Aarthi Chandrasekharan, Dr. Aravind Srinivasan and Dr. Dave Eavarone for teaching me new techniques. I would like to thank Dr. Vidya Subramaniam for helping me with plaque assays and for being a good friend. I would also like to thank Karunya and Carol for their friendship and for all the productive scientific discussions I had with them. I am also thankful to my classmate Luke Robinson for all the wonderful experience we had in discussing about the cool gadgets from Apple and for also organizing frequent outdoor trips/activities for the lab. I would like to thank the rest of my colleagues in the lab who have been extremely supportive and fun to work with: Uday, Jing, Beam, Troy, Andrew, Boris, Josh and Ras.

I would like to thank my professors in the Department of Biological Engineering for helping me build a strong foundation for solving complex biological problems. Professor Douglas A Lauffenburger, Head of the department, was my academic advisor when I entered the program in 2006. Professor Lauffenburger's guidance helped me navigate through my first year. The classes I took during the first year really shaped my scientific thinking and improved my communication skills. On this front I would really like to thank all of the professors who taught those classes. I was fortunate to be a teaching assistant (TA) for 20.440: Analysis of Biological Network as I had the fantastic opportunity to work with Professors Peter Dedon and Bevin Engelward. My TA experience helped me improve my teaching and mentoring skills.

My first year at MIT wouldn't have been so exciting without my BE classmates who were both supportive and fun to study with. Not to mention, the folks in the BE Headquarters, Dalia Fares, Mariann Murray and Susan Jaskela were really supportive and helpful when I had questions about my requirements in the BE program.

Overall, my experience wouldn't have been a pleasant one without the support from Ms. Ada Ziolkowski. I really thank you Ada for patiently responding to all my queries/concerns during my stay in the lab.

Last but not the least I would like to thank my parents (Amma and Appa) for giving me life and for instilling me with the right attitude to look at things. They have been seminal in encouraging me always and showing me that "sky is the limit". Their unconditional love combined with their constant support and encouragement in my life thus far has enabled me to achieve things that I wouldn't have by myself. I thank my husband, for his constant support, encouragement and for believing in me. He is someone whom I can confide on when I get lost. I thank my brother Mahesh, for our long discussions on life and philosophy and for his wittiness that brought smile into my life. I thank him for always being there for me. I thank my sister (Rama), and her family

especially my wonderful niece and nephew; Nithya and Akshay, who bring joy into my life. I express my thanks and gratitude to the rest of my extended family for their unsurpassed support.

Finally I thank GOD for giving me life and for providing me with wonderful opportunities in life.

Table of Contents

Abstract	5
Technical Summary	7
Acknowledgements.....	9
Table of Contents	13
List of Figures	16
List of Tables	19
Chapter 1. Introduction	21
1.1 Motivation	21
1.2 Influenza A virus.....	24
1.2.1 Influenza A virus: Biology and Pathogenesis.....	24
1.2.2 Viral proteins and their role in pathogenesis.....	26
1.2.3 Life Cycle of influenza A viruses	30
1.3 Host Cell Surface Glycans as receptors for Influenza A virus infection	32
1.4 Influenza A virus Hemagglutinin: Role in viral pathogenesis.....	37
1.4.1 HA structure:.....	38
1.4.2 HA and its role in membrane fusion events in influenza A virus life cycle:.....	39
1.4.3 Molecular insights into HA-glycan interaction:.....	41
1.5 Current tools to study HA-glycan interaction	43
1.5.1 RBC Agglutination Assay	44
1.5.2 Fetuin Binding Assay	45
1.5.3 Solid Phase Fetuin Capture Assay	45
1.5.4 Glycan Array Analysis	46
1.5.5 Flow Cytometry to analyze HA-glycan interaction.....	47
1.5.6 Other Methods to analyze HA-glycan interaction.....	48
1.5.7 Staining of relevant tissue sections with whole viruses and recombinant HA	48
1.6 Challenges associated with bridging HA-glycan interaction with viral pathogenesis..	49
1.7 A multifaceted approach to study HA – glycan interaction and to decode its role in viral pathogenesis.....	51
1.8 Thesis Outline and Specific Aims	62
Chapter 2. Hemagglutinin Receptor Binding Avidity Drives Influenza A Virus Antigenic Drift	63
2.1 Introduction	64
2.2 Antigenic structure of A/PR/8/34 or PR8 HA (H1 subtype).....	66
2.2.1 Antigenic sites Sa and Sb.....	66
2.2.2 Antigenic sites Ca (Ca ₁ , Ca ₂) and Cb	67
2.3 Receptor binding avidity and its role in driving antigenic drift	68
2.3.1 In vivo passaging of mouse-adapted A/PR/8/34 in immunized mice selects for single mutants in HA.....	68
2.3.2 Single HA mutants escape antibody response	70

2.3.3	Escape mutants acquire increased binding avidity to host glycan receptors	71
2.3.4	Further passaging of mutants in immunized and non-immunized mice.....	74
2.4	Discussion and Significance of this study	75
2.5	Published manuscript.....	80
Chapter 3. Site-specific N-glycosylation of influenza A HA: Implication in Glycan		
Receptor Binding		
3.1	Introduction	81
3.2	Identification of a new role for the N-glycan on the head domain HA.....	85
3.2.1	Identification of conserved glycosylation site in H1 HA.....	85
3.2.2	Effect of removal of N-glycan at 91 on the receptor binding property of H1 HA	89
3.2.3	Circular dichroism analysis of T93A mutant H1 HAs.....	95
3.2.4	Glycosylation analysis of H2 and H3 HAs	96
3.3	Discussion and Significance of this study	100
Chapter 4. Correlating Glycan Receptor Binding of the Pandemic 2009 H1N1 HA to		
Viral Transmissibility.....		
4.1	Introduction	103
4.2	Pathogenicity and Transmissibility of 2009 H1N1 influenza A viruses	106
4.2.1	Pathogenesis of 2009 H1N1 influenza A viruses in ferrets	107
4.2.2	Transmission of 2009 H1N1 influenza A viruses in ferrets.....	110
4.3	Glycan receptor binding property of 2009 H1N1 influenza A viruses.....	112
4.3.1	Biochemical characterization of glycan receptor binding property of 2009 H1N1 influenza A viruses.....	112
4.3.2	Biochemical characterization of glycan binding properties of natural variants of 2009 H1N1 virus	118
4.3.3	Fixing the mismatched interaction in the RBS of CA04/09 HA.....	121
4.4	Discussion and Significance of this study:	134
4.5	Published Manuscripts:	136
Chapter 5. Decoding the Distribution of Glycan Receptors for Human-Adapted		
Influenza A Viruses in Ferret Respiratory Tract.....		
5.1	Introduction	137
5.2	Lectins as tools to probe the distribution of glycan receptors in ferret respiratory tract	140
5.2.1	Hematoxylin and Eosin staining of Ferret Respiratory Tract tissue sections	141
5.2.2	O-linked glycans in ferret respiratory tract.....	142
5.2.3	α 2→6 glycan receptor distribution in ferret respiratory tract	143
5.2.4	α 2-3 glycan receptor distribution in ferret respiratory tract.....	144
5.2.5	Tropism of human influenza A HA and distribution of their glycan receptors in ferret respiratory tract	146
5.3	Discussion and significance of this study:	151
Chapter 6. Targeting Glycan Receptors of Influenza A virus: A Viable Alternative		
Strategy		
6.1	Introduction	155
6.1.1	Vaccines to prevent influenza A infection.....	156
6.1.2	Therapeutic strategies to combat influenza A infection	156
6.1.3	Plant lectins as tools to target host glycan receptor.....	159

6.2 Sambucus nigra agglutinin I or SNA-I to target host glycan receptor	159
6.2.1 Molecular structure of SNA-I	161
6.2.2 Homology modeling of SNA-I.....	162
6.2.3 Characterizing the glycan binding properties of native SNA-I	162
6.2.4 Engineering SNA-I to target glycan receptors	166
6.2.5 Functional characterization of the receptor binding properties of the engineered constructs of SNA-I	167
6.3 Lectin from the mushroom Polyporus squamosus (PSL) to target host glycan receptor	172
6.3.1 Molecular structure of PSL.....	172
6.3.2 Homology modeling of PSL	172
6.3.3 rPSL-N binds to the glycan receptors targeted by human-adapted influenza A viruses	175
6.3.4 Inhibition of influenza A virus infection by rPSL-N.....	181
6.3.5 PSL and not rPSL-N is cytotoxic to MDCK cells.....	186
6.3.6 <i>In vivo</i> studies with rPSL-N.....	187
6.4 Discussion and Significance of this study	189
Chapter 7. Summary and Significance of this Thesis	191
Appendix 1: Materials and Methods	195
A1.1 Materials and Methods for Chapter 2	195
A1.2 Materials and Methods for Chapter 3	199
A1.3 Materials and Methods for Chapter 4	203
A1.4 Materials and Methods for Chapter 5	208
A1.5 Material and Methods for Chapter 6.....	209
Abbreviations Used.....	215
Bibliography.....	217

List of Figures

Chapter 1 Introduction

Figure 1.1 Schematic representation of influenza A viruses.	25
Figure 1.2 Schematic representation of influenza A viral life cycle.	32
Figure 1.3 A schematic representation of N-glycosylation in endoplasmic reticulum (ER).	33
Figure 1.4 Glycans as recognition sites for pathogens.	34
Figure 1.5 Glycan receptors for influenza A HA in various hosts.	35
Figure 1.6 α 2-6 and α 2-3 sialylated glycan receptor distribution in human respiratory tract. . .	37
Figure 1.7 Molecular model of influenza A virus HA.	39
Figure 1.8 Ribbon diagram of the neutral and low pH forms of the HA.	40
Figure 1.9 Crystal structure of a representative H1N1 HA in complex with human receptor.	41
Figure 1.10 Molecular HA-Glycan receptor interactions.	43
Figure 1.11 Schematic representation of RBC agglutination assay.	44
Figure 1.12 Schematic representation of Fetuin Capture Assay. . .	46
Figure 1.13 Schematic representation of the glycan array platform.	48
Figure 1.14 Glycan topology influences HA-glycan interaction.	53
Figure 1.15 Glycan array assay to capture multivalent HA-glycan interactions.	56
Figure 1.16 Transmission experiments in ferrets.	60
Figure 1.17 A multifaceted approach to understanding HA-glycan interaction to correlate it with its biological function.	57

Chapter 2 HA receptor binding avidity drives influenza A virus antigenic drift

Figure 2.1 Antigenic sites on A/PR/8/34 (PR8) HA.	68
Figure 2.2 Scheme for <i>in vivo</i> passaging of PR8 in mice.	69
Figure 2.3 <i>In vivo</i> passaging of PR8 in vaccinated mice selects for single mutants in HA.	70
Figure 2.4 Location of amino acid mutations in <i>in vivo</i> selected influenza A viruses	70
Figure 2.5 Single HA mutants escape antibody response.	72
Figure 2.6 Glycan binding avidities of escape mutants.	73
Figure 2.8 Structural modeling of wild-type and mutant (E156K) PR8 HA with LSTc.....	76
Figure 2.7 A new mechanism to evade host immune response by influenza A viruses.	77
Figure 2.9 New model of antigenic drift in influenza A virus..	78

Chapter 3 Site-specific N-glycosylation of influenza A HA: implications in glycan receptor binding

Figure 3.1 Functional roles of influenza A HA glycosylation.	83
Figure 3.2 H1 HA ClustalW alignment.	87
Figure 3.3 Structure of 1918-Human H1 HA.	89
Figure 3.4 Effect of T93A mutation on AV18 receptor binding.	91
Figure 3.5 Effect of T93A mutation of SC18 receptor binding.	93
Figure 3.6 Effect of T93A mutation of NY18 receptor binding.	94
Figure 3.7 Effect of N91D mutation on AV18 receptor binding.	95
Figure 3.8 Circular Dichroism analysis of wild-type and mutant HAs.	96
Figure 3.9 H2 HA ClustalW alignment.	98
Figure 3.10 H3 HA ClustalW alignment.	99
Figure 3.11. Structure of a representative H3 HA (1963-Avian/Duck/Ukraine).	100

Chapter 4 Correlating Glycan Receptor Binding of the Pandemic 2009 H1N1 HA to Viral Transmissibility

Figure 4.1 Genesis of 2009 H1N1 swine flu virus.	100
Figure 4.2 Detection of H1N1 virus in ferret tissues.	108
Figure 4.3. Respiratory droplet transmissibility of H1N1 influenza viruses.	111
Figure 4.4. Direct contact transmissibility of H1N1 influenza viruses.	112
Figure 4.5 Direct glycan receptor binding of CA/04 and SC18 HA.	114
Figure 4.6. Correlation between α 2-6 binding affinity and respiratory droplet ferret transmission of H1N1.	115
Figure 4.7 Glycan array analysis with the wild-type CA04/09 virus (generated by reverse genetics).	116
Figure 4.8 Human respiratory tract tissue binding of CA04/09 HA.	117
Figure 4.9 Sialic acid specificity of CA04/09 HA	118
Figure 4.10 Role of Asp225 in human receptor binding of HA.	119
Figure 4.11 Dose dependent glycan array analysis of natural variants of 2009 H1N1 virus.	120
Figure 4.12 6'SLNLN binding curves for the natural variants of the 2009 H1N1 virus.	121
Figure 4.13 ClustalW Sequence alignment of CA04/09, SC18 and Bris07 HAs.	124
Figure 4.14 Fixing the mismatched interaction in RBS of CA04 HA.	125
Figure 4.15 Results from dose-dependent direct glycan-receptor binding assay (on the left) and human tracheal tissue binding assay (on the right).	128
Figure 4.16 Binding curves of mutant and wild-type HAs to 6'SLNLN.	129
Figure 4.17 Human tracheal Goblet cell staining by wild-type and mutant HAs.	124
Figure 4.18 Dose-dependent direct glycan array analysis of rgCA04/09 HA Ile219Lys mutant virus.	130
Figure 4.19 Respiratory droplet transmissibility of rgCA04/09 and rgCA04/09 HA Ile219Lys mutant virus.	133

Chapter 5 Decoding the distribution of glycan receptors for human-adapted influenza A virus in ferret respiratory tract

Figure 5.1 Regions of ferret respiratory tract analyzed in the study.	134
Figure 5.2 H & E stained images of tissue sections.	142
Figure 5.3 O-linked glycan distribution in ferret respiratory tract.	143
Figure 5.4 α 2-6 linked glycan distribution in ferret respiratory tract.	144
Figure 5.5 O-linked α 2-6 glycan distribution in ferret respiratory tract.	145
Figure 5.6 α 2-3 linked glycan distribution in ferret respiratory tract.	146
Figure 5.7 Glycan receptor distribution for recombinant Alb58 (H2) HA.	148
Figure 5.8 Glycan receptor distribution for recombinant SC18 (H1) HA.	149
Figure 5.9 Co-staining of recombinant Alb58 (H2) HA with Jacalin.	149
Figure 5.10 Sialic acid binding specificity of lectins.	150
Figure 5.11 Submucosal gland co-staining with Jacalin and Alb58 HA.	151
Figure 5.12 Mapping of glycan receptor distribution in ferret respiratory tract.	154

Chapter 6 Targeting the glycan receptors of human influenza A virus: A viable alternate strategy

Figure 6.1 Molecular structure of SNA-I 161	161
Figure 6.2 Glycan binding specificity of SNA-I. 164	164

Figure 6.3 Cellular tropism of SNA-I.	165
Figure 6.4 Strategies adopted for engineering SNA-I B chain.	166
Figure 6.5 Strategies to engineer SNA-I to target host glycan receptors for human influenza A viruses.	167
Figure 6.6 N-glycosylation sites on 42aa and 121aa protein constructs.	168
Figure 6.7 Purification of 42aa SNA-I construct.	169
Figure 6.8 Functional characterization of 42aa peptide.	171
Figure 6.9 Molecular structure of PSL and homology modeling of PSL.	174
Figure 6.10 Purification of <i>rPSL-N</i>	175
Figure 6.11 Glycan binding specificity of <i>rPSL-N</i> and native PSL.	178
Figure 6.12 Cellular tropism of <i>rPSL-N</i>	179
Figure 6.13 <i>rPSL-N</i> binds to the glycan receptors targeted by human influenza A viruses.	180
Figure 6.14 Experimental design for <i>rPSL-N</i> inhibition of influenza A infection.	183
Figure 6.15 <i>rPSL-N</i> inhibits infection of MDCK cells by influenza A viruses.	184
Figure 6.16 Standards for quantitative real time PCR.	185
Figure 6.17 Native PSL but not <i>rPSL-N</i> is highly cytotoxic to MDCK cells.	186
Figure 6.18 Survival curve of BALB/c mice treated with <i>rPSL-N</i>	188
Figure 6.19 Glycan array analysis with mouse-adapted CA04/09 (ma-CA04/09) virus.	188

Chapter 7 Summary and Significance of this Thesis

Figure 7.1 Overall summary of this thesis.	193
---	-----

Appendix 1 Materials and Methods

Figure A1.2 SDS-PAGE profile of recombinant HA purified by affinity chromatography	200
Figure A1.3 SDS-PAGE profile of mutant and wild-type recombinant HA (2009 H1N1) purified by affinity chromatography.....	204

List of Tables

Chapter 1 Motivation, Background and Specific Aims

Table 1.1 Glycan receptor binding specificity (identified by RBC agglutination assay) and respiratory droplet transmissibility of H1N1 influenza A viruses in ferrets	50
---	----

Chapter 3 Site-specific N-glycosylation of influenza A HA: implications in glycan receptor binding

Table 3.1 Evolution of H1N1 glycosylations.	88
--	----

Chapter 4 Understanding the 2009 H1N1 swine flu pandemic: correlating the glycan receptor binding of its HA to its transmissibility in ferrets

Table 4.1 Timeline of Swine flu Outbreak	106
Table 4.2: Replication and transmission of novel 2009 and seasonal H1N1 viruses in ferrets. ..	109
Table 4.3 Glycan binding residues of H1N1 HAs	123
Table 4.4 Replication and transmission of CA04/09 Ile219->Lys HA mutant virus in ferrets.....	132

Chapter 5 Decoding the distribution of glycan receptors for human-adapted influenza A virus in ferret respiratory tract

Table 5.1 Lectins and their glycan binding specificities.....	141
Table 5.2 Visual scoring of lectin staining intensity of various cell types in ferret upper (trachea) and lower (lung hilar region) tract.....	153

Chapter 6 Targeting the glycan receptors of human influenza A virus: A viable alternate strategy

Table 6.1 Rationale for Selection of SNA-I and PSL to target the glycan receptors of Influenza A virus	160
--	-----

Appendix 1 Materials and Methods

Table A1.2 Expanded nomenclature of glycans used in the glycan array	202
--	-----

Chapter 1. Introduction

1.1 Motivation

Annual influenza A epidemics results in about three to five million cases of severe illness, and about 250,000 to 500,000 deaths [<http://www.who.int/mediacentre/factsheets/fs211/en/index.html>]. Illnesses result in hospitalizations and deaths among high-risk groups (the very young, elderly or chronically ill). Epidemic viruses are derived from pandemic viruses by antigenic drift, gradual minor antigenic changes caused by point mutations in the viral coat proteins (hemagglutinin or HA and Neuraminidase or NA). Influenza epidemics are caused by A and B viruses, whereas pandemics are only caused by influenza A viruses. It has been estimated that there have been at least 13 pandemics in the last 500 years [1] including 3 scientifically well-documented ones in the 20th century; the Spanish flu of 1918 (H1N1), the Asian flu of 1957 (H2N2), and the Hong Kong flu of 1968 (caused by H3N2) and the first pandemic of the 21st century; swine flu pandemic of 2009 (caused by H1N1). There has been a significant reduction in the number of deaths caused due to pandemic and seasonal outbreaks. This has been possible due to the availability of better vaccine and anti-therapeutic strategies against influenza A viruses. But the “big” question that has to be answered is as follows: Is it possible to predict the emergence of future pandemic outbreaks? In this context it is important to understand the key molecular determinants of influenza A viral pathogenesis.

The critical first step in the host infection by influenza A virus is the binding of the viral surface glycoprotein hemagglutinin (HA) to sialylated glycan receptors, complex glycans terminated by *N*-acetylneuraminic acid (Neu5Ac) expressed on the host cell surface [2]. Glycans terminating in Neu5Ac that is $\alpha 2 \rightarrow 6$ -linked to the penultimate galactose are predominantly expressed in human upper respiratory epithelia and serve as receptors for human-adapted influenza A viruses (henceforth referred to as *human receptors*). On the other hand, glycans terminating in Neu5Ac that is $\alpha 2 \rightarrow 3$ -linked to the penultimate galactose, serve as receptors for the avian-adapted influenza viruses

(henceforth referred to as *avian receptors*). The HA-glycan receptor interaction is crucial for the human adaptation of influenza A viruses. Essentially a switch in the glycan receptor binding preference of the avian influenza A HA from $\alpha 2 \rightarrow 3$ to $\alpha 2 \rightarrow 6$ is known to be crucial in the human adaptation of the virus.

Currently, much of the influenza A research has taken a simplified view of the HA-glycan receptor interaction. HA-glycan interaction is a multivalent interaction, involving multiple HA molecules interacting with multiple glycan receptors. The current framework does not capture this multivalency associated with HA-glycan interaction and defines this interaction in a more qualitative way just based on the linkage specificity of the glycan receptor. Defining receptor specificity just based on terminal linkage undermines structural complexity of physiological glycan receptors. Hence it is challenging to correlate glycan-receptor specificity with molecular HA-glycan interactions as well as biological functions such as virulence and transmissibility of influenza A virus.

Motivated by the aforementioned challenges, this thesis work is aimed to further understand the subtle nuances associated with the HA-glycan interaction given its crucial role in influenza A pathogenesis. Given the complexities associated with the HA-glycan interaction, this thesis aims at teasing out this multivalent interaction by using a combination of three dimensional structural modeling and bioinformatics tools, biochemical analysis of the interaction followed by validation using *in vitro* and *in vivo* assays. Such an approach would not only enable understanding this critical interaction but can also pave way to the development of alternate antiviral strategies to combat influenza A infection.

The overall goal of this thesis is to

Elucidate the multifaceted role of influenza A virus hemagglutinin – host glycan receptor interaction to gain insight into its role in viral pathogenesis and for the development of alternate anti-viral strategies against influenza A infection

The remainder of this chapter provides insight into the current framework to understand influenza A hemagglutinin – host glycan receptor interaction and highlights the challenges that has to be addressed with the current framework. Building on this is the motivation of my research work, which paves way to the Specific Aims of this thesis.

Section 1.2 describes the biology and life cycle of Influenza A virus. Section 1.3 and 1.4 describes the two molecular components namely the viral hemagglutinin (HA) and the glycan receptors respectively. Following on Sections 1.3 and 1.4, Section 1.5 describes the currently available tools to analyze HA-glycan interaction. Building on this Section 1.6 provides an overview of the challenges associated with the current approach to study HA-glycan interaction. Section 1.7 provides an emphasis on taking a multifaceted approach to really correlate this critical molecular protein-glycan interaction to the viral pathogenesis. Towards this end this section also describes the tools that were developed in our lab and in this thesis to address the challenges mentioned in Section 1.6. Based on the motivation provided in Section 1.1 and the tools described in Section 1.7, Section 1.8 provides an overview of the Specific Aims and outline of this thesis.

1.2 *Influenza A virus*

1.2.1 *Influenza A virus: Biology and Pathogenesis*

Influenza A virus belongs to the family of *Orthomyxoviridae*. The structure of influenza A virus is somewhat variable, but the virion particles are usually spherical or ovoid in shape and 80 to 120nm in diameter. The genome consists of eight negative sense single stranded RNA segments encoding at least for 10 proteins (**Figure 1.1**). The influenza virion is an enveloped virus that derives its lipid bilayer from the plasma membrane of a host cells that it infects. There are three different proteins that are embedded in the lipid envelop of the virion: two glycoproteins (*neuraminidase* and *hemagglutinin*) and a transmembrane ion channel protein (M2). Underneath the lipid bilayer lies the matrix protein (M1), a major structural protein. Within the virus shell are eight viral ribonucleoprotein complexes (vRNP), each composed of viral RNA (vRNA) associated with the nucleoprotein NP and the three components of the viral RNA polymerase complex (polymerase basic protein 1 or PB1, Polymerase basic protein 2 or PB2 and polymerase acidic protein or PA). The NS1 protein, which counteracts the cellular interferon response, is synthesized from an unspliced mRNA, and a spliced mRNA yields the NS2, or NEP protein that mediates nuclear export of the vRNP complexes [3]. In addition, the recently identified PB1-F2 protein, which is encoded by the PB1 segment, is thought to play a role in viral pathogenicity [4-7].

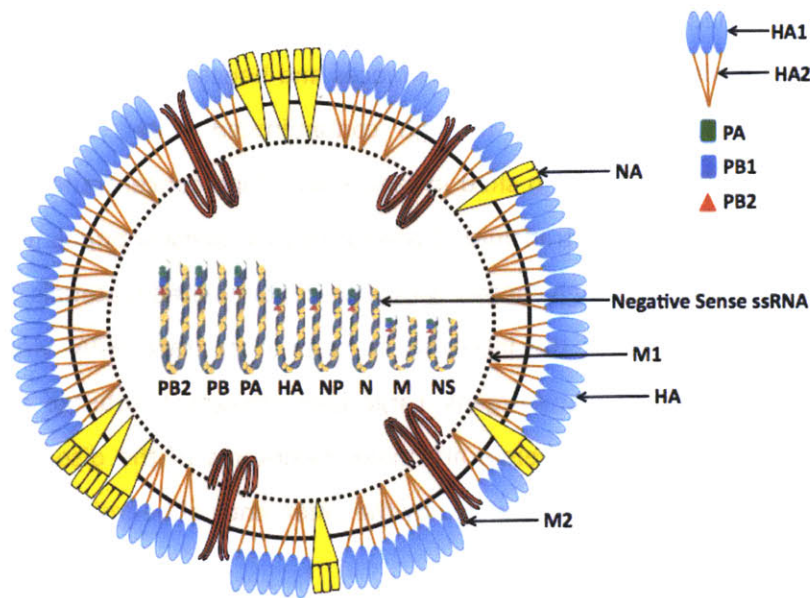


Figure 1.1 Schematic representation of influenza A viruses. The viral coat consists of three major proteins: hemagglutinin (HA), neuraminidase (NA) and matrix protein 2 (M2). The genome consists of eight negative sense single stranded RNA that interact with the components of the polymerase complex (PA, PB1 and PB2)

Human influenza infection is highly contagious that is transmitted by airborne route via respiratory droplet. Infection is usually confined to the respiratory tract. Replication occurs in the epithelia of the respiratory tract and normally reaches its peak 2-3 days after infection. The period of virus shedding is 5-7 days and may last with infants and children as long as 2 weeks. After an incubation time of 1-5 days, patients suffer from acute respiratory disease symptoms with headache, high fever, myalgia, nausea and malaise. Severe cases develop typically primary influenza pneumonia or combined viral-bacterial pneumonia. Persons usually at risk for complications during a seasonal epidemic are the elderly and patients with cardiovascular diseases, metabolic disorders or immunosuppression. Less frequent complications are myositis, myocarditis and Reye's syndrome, a severe disease with brain and liver involvement and usually lethal outcome.

Avian influenza A virus infection is different from that of the infection caused by human adapted influenza A virus. Low Pathogenic influenza A virus (LPAI) virus

replication is confined to the intestinal and respiratory tract resulting in mild disease or asymptomatic infection. Virus is shed in the faeces and hence the dissemination of the virus among aquatic birds occurs through contaminated water. High pathogenic influenza A viruses (HPAI) are also shed in faeces with high concentrations. However, these viruses are more readily transmitted among birds in densely populated flocks by the nasal and oral routes through contact with virus-contaminated materials. In contrast to the local LPAI infection of the intestinal or respiratory tract, HPAI viruses cause systemic infection affecting many organs. Large hemorrhages distributed all over the body, edema and cutaneous ischemia are major symptoms of the disease. The final stage of the infection can be characterized by the emergence of neurological signs, such as photophobia and dullness [8].

HPAI viruses have been found to specifically target lymphocytes and lymphoid tissues [9, 10], myocytes in the heart muscle [11] and endothelial cells [12]. Tropism to these cells may play an important pathogenic role in systemic virus dissemination and in the vascular leakage underlying hemorrhages and edema.

The role of various influenza A viral proteins and their role in viral pathogenesis is discussed in the following section.

1.2.2 *Viral proteins and their role in pathogenesis*

Viral glycoproteins:

The HA protein mediates virus binding to sialic acid receptor on the host cell surface and membrane fusion events in the life cycle of the virus (explained in detail in Section 1.4). The efficient release of new virions from the infected cells requires the removal of sialic acid by neuraminidase, another glycoprotein found in the lipid envelope of the virus. The receptor binding and receptor destroying properties of HA and NA, respectively, must be balanced [13, 14]. The NA stalk, which separates the head region with the enzymatic center from the transmembrane and cytoplasmic domains, varies in sequence and length, depending on the virus [15]. Typically, shortened stalks result in

less efficient virus release since the active site in the head region cannot efficiently access its substrates [16]. Compared to viruses with a long-stalk NA, viruses with a short stalk showed a decreased capacity to elute from RBCs and an increased virulence in mice [16]. Moreover, most recent highly pathogenic H5N1 viruses isolated from terrestrial poultry possess short NA stalks [17]. Influenza A virus HA and NA are the targets of the host antibody response (explained in detail in Chapter 2). In order to escape the neutralizing antibody response, the virus acquires mutations in its HA and NA and this further contributes to the antigenic drift mediated evolution of the virus.

Internal proteins:

There are seven internal proteins in influenza A virus: RNA polymerase (PB1, PB2 and PA), nucleoprotein (NP), matrix protein (M1 and M2), and non-structural proteins (NS1, NS2/NEP).

Viral RNA polymerase complex:

The polymerase proteins (PB1, PB2 and PA) form a heterotrimer bound to a short hairpin structure formed by the partially complementary terminal 5' and 3' untranslated regions (UTRs) of each segment. PB1 the central scaffold for trimer assembly, serves as RNA - dependent RNA polymerase. Short amino terminal (aa 1-15) and carboxy terminal (aa 685-757) sequences interacting with PA and PB2, respectively, are the only parts of PB1 currently known at atomic resolution [18]. PB2 functions in mRNA synthesis by binding host mRNA caps. The PB2 domains with known structure include an amino-terminal peptide (aa 1-35) that interacts with the carboxy-terminal end of PB1, the cap-binding domain (aa 320-483), a domain involved in host interaction carrying the adaptive mutation 627 (aa 538-678), followed by the carboxy terminal NLS domain (aa 678-759) the contains the classical bipartite nuclear localization sequence 736-RKRX12KRIR-755 [18].

While PA is necessary for a functional polymerase complex, including cap-snatching endonucleolytic cleavage of host RNAs, the biology of which is poorly understood [19]. The amino terminal domain of PA has been identified to have the

endonuclease activity. PA may have additional proteolytic activity and may also act as an elongation factor during RNA synthesis. A recent study suggested that the replication complex, particularly the PB1 protein, contributes to the virulence of the 1918 pandemic virus in ferrets [20].

Reverse genetics studies have shown that lysine at position 627 of PB2 (found in all highly pathogenic influenza A virus strains such as H5N1) determines high pathogenicity in mice, while glutamate at this position determines low pathogenicity [21]. However, the nature of the amino acid at position 627 of PB2 does not affect the cell tropism but its replicative ability in mice and probably in humans. PB2-Lys 627 is suggested to allow efficient replication not only in the lower but also in the upper tract of mammals, a feature that may facilitate transmission. PB2-Lys 627 mutation is known to facilitate the virus to adjust to physiological constraints such as differences in body temperature [22]. In fact, replacement of PB2-Lys 627 with Glu reduced the transmissibility of human influenza viruses in guinea pig model [23]. The amino acid at position 701 of PB2 has also emerged as a determinant of virulence [24, 25], a role probably related to its facilitation of binding of PB2 to importin α (a cellular nuclear import factor) in mammalian cells [26].

Recently, PB2 and HA proteins of the Spanish influenza virus were shown to be critical for droplet transmission [27].

Viral nucleoprotein (NP):

NP acts primarily as a single-strand RNA-binding protein and serves as a structural protein in the ribonucleoproteins (RNPs). In addition it plays an important role in transcription and in the trafficking of RNPs between the cytoplasm and nucleus. Influenza A virus RNA transcription and replication occur in the host cell nucleus, since this process is dependent on host cell RNA processing machinery. The process of being imported into the nucleus, exported back out to the cytoplasm, and then prevented from re-entering the nucleus also all appear to depend on the interaction of NP with host proteins.

Viral nonstructural (NS) protein:

The nonstructural 1 (NS1) protein has multiple functional domains, including N-terminal dsRNA binding (1-73) containing a nuclear localization signal (NLS), a central effector domain (73-207) containing a nuclear export signal, and a C-terminal region (207-230) containing a PDZ domain [28]. NS1 has pleiotropic functions, including dsRNA binding, enhancement of viral mRNA translation, inhibition of host mRNA processing and type I interferon antagonism [29]. As demonstrated by reverse genetics, the resistance to the antiviral effects of IFN and TNF- α is associated with glutamic acid at position 92 of NS1 protein. Also pigs infected with a virus containing Glu-92 in NS1 protein experience higher virus titers and body temperatures than those infected with a control virus [30, 31].

The NS2 protein (also referred to as nuclear export protein, NEP) is found in virions and facilitates nuclear export of viral RNP complexes.

PB1-F2 protein:

PB1-F2 is a small viral protein, which is encoded by PB1 gene by an alternative reading frame. PB1-F2 targets the mitochondrial inner membrane, and may play a role in apoptosis during influenza A virus infection. Recently, a single Asn66Ser mutation in the PB1-F2 protein was shown to increase virulence in mice by inhibiting early interferon response [32, 33].

M protein:

Segment 7 of influenza A viruses encodes the M1 matrix and the M2 ion channel proteins. M1 protein, one of the several late viral proteins, is involved in the export of viral ribonucleoproteins (vRNPs) from the nucleus into the cytosol for translation. Why M1 is essential for export of vRNPs from the nucleus to the cytosol is not clear. It may escort the vRNPs from the nucleus and through the nuclear pores, or it may be needed to release the bound vRNPs from the nuclear matrix. Another possibility is that, by associating with vRNPs in the cytosol, M1 may prevent their reimport into the nucleus [34].

M2 possesses proton channel activity that allows virion acidification for efficient uncoating after fusion in endosomes. Recently, M2 protein has been speculated to be involved in regulating cell death by inhibiting antiapoptotic macroautophagy [35].

1.2.3 *Life Cycle of influenza A viruses*

The life cycle of influenza virus is depicted schematically in **(Figure 1.2)** and comprises of the following key events.

1. **Binding:** The virus particle initially associates with a host cell surface by binding to sialic acid-containing glycan receptors
2. **Endocytosis:** The bound virus is endocytosed by one of four distinct mechanisms. Most internalization appears to be mediated by clathrin-coated pits, but internalization via caveolae, macropinocytosis, and by non-clathrin, non-caveolae pathways has also been described for influenza viruses [36].
3. **Fusion and Release of viral ribonucleoprotein:** Acidification of the endosome by the M2 ion channel matrix protein, promotes fusion of the viral and endosomal membranes mediated by the viral hemagglutinin (HA) protein, and the eventual release of the uncoated viral ribonucleoprotein complex into the cytosol of the host cell.
4. **Transport into the nucleus:** The ribonucleoprotein complex is transported through the nuclear pore into the nucleus.
5. **Replication:** Once in the nucleus, the incoming negative-sense viral RNA (vRNA) is transcribed into messenger RNA (mRNA) by a primer-dependent mechanism. Replication occurs via a two-step process. A full-length complementary RNA (cRNA), a positive-sense copy of the vRNA, is first made and this in turn is used as a template to produce more vRNA.
6. **Translation:** The newly synthesized vRNAs are exported into the cytoplasm by NEP or NS2 proteins, for translation, to make viral proteins.

- 7. Release of the viral particles:** The viral proteins are expressed and processed and eventually assemble with vRNAs at budding sites within the host cell membrane. The viral protein complexes and ribonucleoproteins are assembled into viral particles and bud from the host cell, enveloped in the host cell's membrane. The viral *neuraminidase* cleaves the sialic acid receptors on the surface of the host cell to prevent re-infection of the host cell and hence mediates the release of the newly formed virions.

The main focus of this thesis is to understand the first critical step in the viral life cycle, i.e., binding of the viral HA to the host cell surface glycan receptors and understand the factors governing this critical protein-glycan interaction. This thesis further investigates the structural and functional roles of viral HA and the host glycan receptors in the host adaptation of the virus and its implication in the transmissibility of the virus in human host. Building on the understanding of the host glycan receptors, this thesis also investigates an alternate strategy to target the glycan receptors to combat influenza A infection.

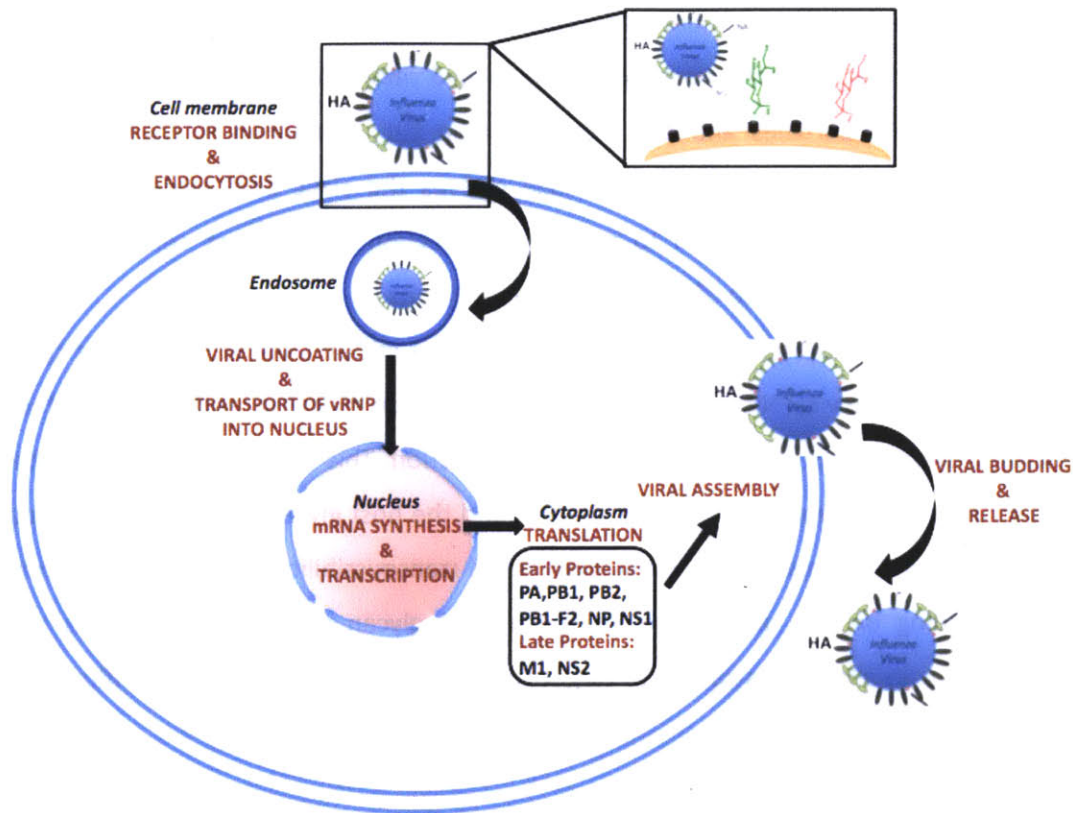


Figure 1.2 Schematic representation of influenza A viral life cycle. Influenza A virus hemagglutinin binds to the cell surface glycan receptors (shown in the inset) and mediates entry into the host cell by receptor mediated endocytosis. Due to the acidic pH of the endosomes, the virus undergoes uncoating and the viral ribonucleoprotein (vRNP) complexes are released into the cytoplasm and subsequently transported to the nucleus, where replication and transcription takes place. mRNAs are transported back to the cytoplasm for translation. Early viral proteins, which are required for replication and transcription, are transported back to the nucleus. Late proteins on the other hand, facilitate nuclear export of the newly synthesized vRNPs. The assembly and budding of the progeny virus occurs at the plasma membrane.

1.3 Host Cell Surface Glycans as receptors for Influenza A virus infection

Glycosylation is one of the key post-translational modification of proteins. Most well characterized pathways for the biosynthesis of major classes of glycans are confined within the ER and Golgi compartments. Thus, for example, newly synthesized proteins originating from the ER are either co-translationally or post-translationally modified with sugar chains at various stages in their itinerary toward their final

destinations. The glycosylation reactions usually use activated forms of monosaccharides (nucleotide sugars **Figure 1.3**), as donors for reactions that are catalyzed by *glycosyltransferases*. In proteins, glycosylation can be N- or O- linked depending on whether the glycan chain is added to the asparagine amine group or serine/threonine hydroxyl groups respectively. Glycosylation takes place in the endoplasmic reticulum and in the Golgi mediated by various enzymes.

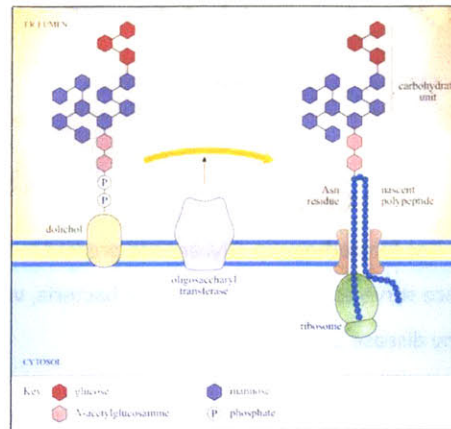


Figure 1.3 A schematic representation of N-glycosylation in endoplasmic reticulum (ER). The nascent polypeptide chain synthesized emerging from the ribosomes on the ER migrate into the ER and are processed by a series of enzymes. Figure adapted from <http://openlearn.open.ac.uk>

Glycans on proteins play an important role in proper folding of newly synthesized polypeptides in the endoplasmic reticulum (ER) and/or subsequent maintenance of protein solubility and conformation. Indeed if proteins are incorrectly glycosylated, they will fail to fold properly and/or exit the ER, being consigned instead to degradation in proteasomes. When present on cell surface, glycans also shield the underlying polypeptide from recognition by proteases and antibodies.

Since glycans on the glycoproteins are present in the unique interface of cell surface and extracellular matrix (ECM), apart from the aforementioned roles, they also serve as recognition sites (or receptors) for proteins on the surface of bacteria and viruses [37] (**Figure 1.4**). The specific binding of bacteria and virus particles to these glycan receptors on the host cell surface is a pre-requisite for evasion of host epithelium in order to gain entry into the host cell.

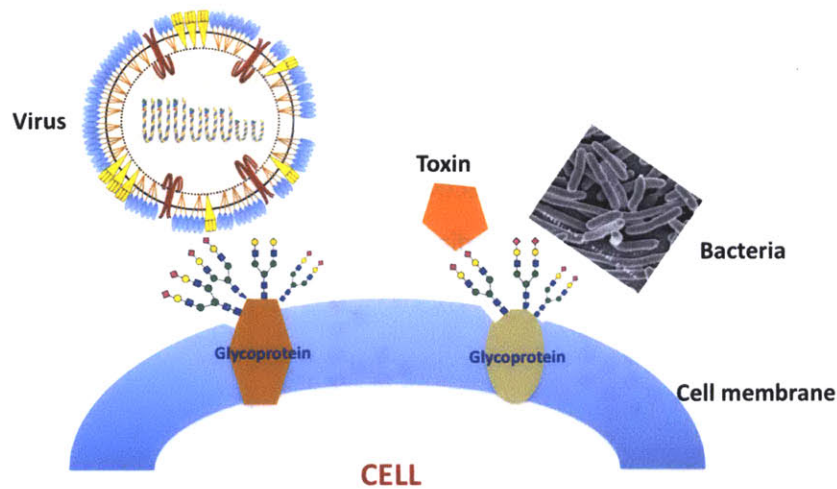


Figure 1.4 Glycans as recognition sites for pathogens. Glycans are present in the interface of cell surface-ECM (extracellular matrix) and hence serve as recognition sites for bacteria, virus and some toxins. This is responsible for tissue tropism of any disease pathogenesis.

One of the well-studied systems of host-pathogen interaction is that of influenza A virus. One of predominant viral coat proteins, hemagglutinin (HA) [explained in detail in Section 1.4.] is a glycan binding protein (or a lectin) which recognizes specific glycan receptors on the surface of host cell and mediates attachment, viral entry and membrane fusion events. The specificity of influenza A HA to specific host glycan receptor, determines the viral host adaptation and tissue tropism.

Influenza A viruses exist as commensals in the gut of waterfowl. The gut and respiratory tract of birds are known to predominantly express glycan receptors terminated by α 2-3 linked sialic acids (referred to as *avian receptors*) as shown in **Figure 1.5** [38-43]. Most avian viruses cause no or only mild disease symptoms. These low pathogenic avian influenza (LPAI) viruses comprising all subtypes are different from highly pathogenic avian influenza (HPAI) viruses such as H5 and H7, which have a polybasic HA cleavage site. HPAI viruses arise by introduction and circulation of H5 and H7 LPAI viruses in domestic poultry with subsequent mutations in the HA cleavage site [44, 45].

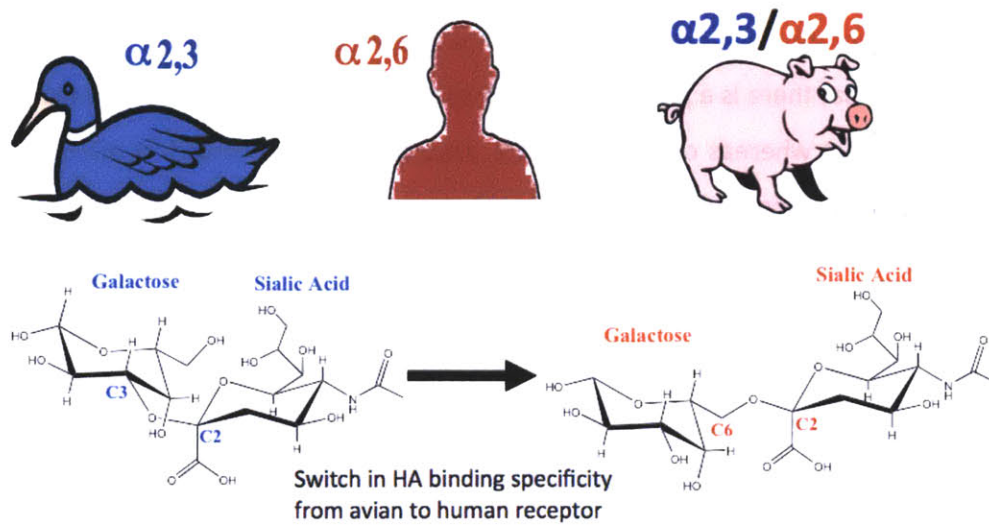


Figure 1.5 Glycan receptors for influenza A HA in various hosts. Sialic acid linked to galactose in either α 2-3 or α 2-6 linkages are the receptors for influenza A HA. Host restriction of the virus is determined by the glycan receptor distribution. The gut and respiratory tract of birds predominantly express α 2-3 glycans, which is in contrast to human respiratory tract, which express α 2-6 glycans. A switch in the receptor binding property of HA from α 2-3 to α 2-6 binding specificity is crucial for the human host adaptation of the virus. This host adaptation is facilitated by pigs, which express both α 2-3 and α 2-6 glycans in their gut and respiratory tract and are hence called as “mixing vessels”.

Since the host barrier is not an unsurmountable obstacle for LPAI viruses, they can occasionally be transmitted from their natural reservoir to terrestrial birds and mammals [46]. Most of these transmissions are transient and do not result in a stable new lineage [18]. Occasionally however, the viruses adapt to the new species and give rise to a new lineage. Adaptation requires multiple mutations and it may involve gene reassortment after coinfection with another virus. Influenza A viruses can adapt to human host and can cause infection in them.

The primary site of infection of influenza A viruses in humans is the upper respiratory tissues. Therefore the glycan receptors in the upper respiratory epithelia play a central role in mediating the host infection by the virus. It is known that these glycan receptors are terminated by α 2-6 linked sialic acids (referred to as *human*

receptors). Using plant lectins such as SNA-I (binds specifically to Neu5Ac α 2-6Gal/GalNAc motif [47]) and MAL-II (binds specifically to α 2-3 glycans), we and others have shown that there is a predominant expression of α 2-6 glycans in the human upper respiratory tract whereas α 2-3 glycans are predominantly expressed in the deep lung region (Figure 1.5 and Figure 1.6) [41, 48, 49].

Further to assess the influenza A viral tropism and to understand the distribution of the viral glycan receptors, Van Riel *et al*, determined the pattern of virus attachment by virus histochemistry of three human and three avian influenza A viruses in human nasal septum, conchae, nasopharynx, paranasal sinuses, and larynx. The human adapted influenza A viruses attached abundantly to ciliated epithelial cells and goblet cells throughout the upper respiratory tract. In contrast, the avian influenza A viruses, including the highly pathogenic H5N1 attached only rarely to epithelial cells or goblet cells. This was further corroborated by Chandrasekharan *et al* [48], using recombinant hemagglutinin (HA) expressed in insect cells, to stain various regions of human respiratory tract. HA from human adapted influenza A viruses showed predominant staining of the non-ciliated goblet cells and the ciliated epithelial cells in the upper respiratory tract indicating predominant distribution of α 2-6 glycans in the upper respiratory tract. In contrast HA from the avian influenza A viruses showed no staining of the human upper respiratory tract. The avian HA showed predominant staining of the deep lung alveolar tissue section indicating predominant expression of α 2-3 glycans in human deep lung or lower respiratory tract.

On the contrary, the epithelial cells of pig trachea contain both avian and human receptors [50]. Hence pigs are highly susceptible to infection by both the avian and human-adapted influenza A viruses [51]. Pigs may hence serve as “mixing vessel” for reassortment between avian and human influenza A viruses that can occasionally give rise to pandemic influenza A virus strains [52, 53].

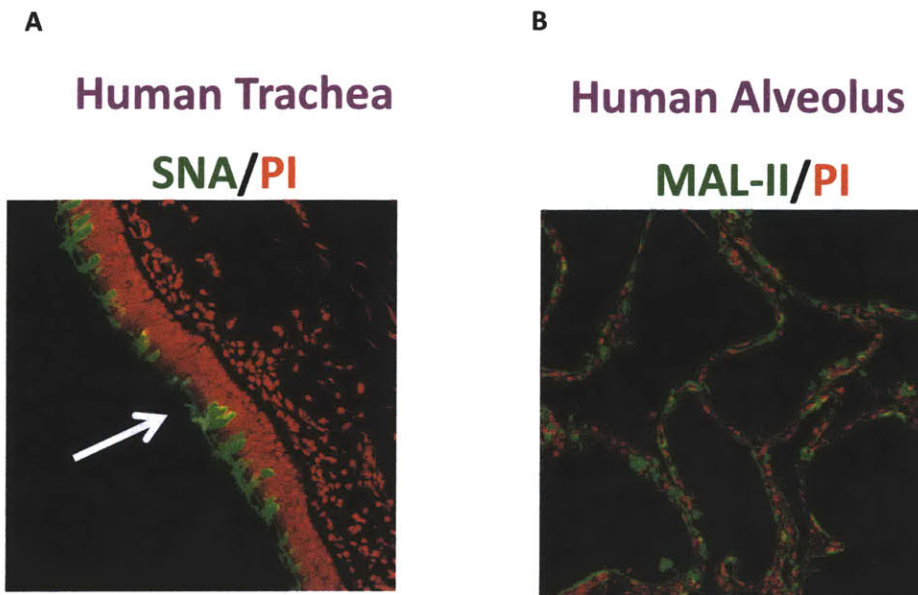


Figure 1.6 α 2-6 and α 2-3 sialylated glycan receptor distribution in human respiratory tract. SNA-I, a plant lectin, which binds to α 2-6 glycans showed highly specific binding to human tracheal apical surface ciliated and goblet cells (A). MAL-II, another plant lectin, which binds to α 2-3 glycans, showed highly specific binding to human alveolus (B). The nuclei were visualized by staining with propidium iodide (*red*). The lectin staining is visualized by a *green* staining of the tissue sections. Trachea and alveolus represent the upper and the lower respiratory tract in humans respectively.

1.4 *Influenza A virus Hemagglutinin: Role in viral pathogenesis*

The lipid envelope of influenza A virus consists of 2 major glycoproteins: Hemagglutinin (HA) and Neuraminidase (NA), both of which bind sialic acid [14]. As mentioned in Section 1.2, both these glycoproteins play an important role in the viral life cycle. Both HA and NA are the targets of the host neutralizing antibodies which block the viral infection [14]. As a result of this immune pressure, both HA and NA change their antigenic properties by acquiring mutations during evolution to evade the host antibody response. These antigenic differences are used to classify influenza A viruses into 16 HA (H1 – H16) and 9 NA (N1 – N9) subtypes.

Of the two glycoproteins, HA play crucial roles in the early stage of virus infection, including virus binding to host receptors, viral entry, and membrane fusion

[54]. The interaction of HA with the host glycan receptor plays a key role in the host adaptation of the influenza A virus.

1.4.1 *HA structure:*

HA is a trimer of identical subunits (**Figure 1.7**). HA is initially synthesized as a precursor, HA0, which trimerizes in the endoplasmic reticulum in association with chaperones and is transferred to the cell surface through the golgi apparatus. HA0 is proteolytically cleaved into the functional HA1 and HA2 subunits linked by a single disulfide bond. Cleavage of the precursor is essential for activation of membrane fusion potential and hence infectivity. For HAs of most subtypes, the site of cleavage is a single arginine residue, and cleavage occurs by an as yet unidentified enzyme. It has been speculated that this cleavage may be mediated by the serine protease, trypsin Clara, produced by Clara cells of bronchiolar epithelium [55, 56]. This enzyme shows recognition specificity for the sequence Q/E-X-R found at the cleavage sites of these HAs. HAT (human airway trypsin-like protease) and TMPRSS2 (transmembrane protease serine S1 member 2, also known as epitheliasin) are present in human airway epithelial cells and have been shown to be capable of cleaving HA having a monobasic cleavage site [57]. In agreement with this, TMPRSS2 and the related protease TMPRSS4 have been reported to cleave the HA of the 1918 H1N1 virus at a monobasic cleavage motif [58]. However, for many cell types, the protease(s) responsible for HA cleavage remain poorly defined.

In contrast, some members of the H5 and H7 subtypes (Highly Pathogenic Avian Influenza A viruses or HPAI) however have acquired multiple basic residues at the site of cleavage [59]. The HPAIs have 75% or higher mortality after experimental infection of chickens. Cleavage at these multibasic sites occur intracellularly and involves subtilisin-like enzymes that are active in the post-translational processing of hormone and growth factor precursors [60]. The furin recognition sequence R-X-R/K-R is a common feature of the inserted polybasic sequences. The wide tissue distribution of furin-like enzymes and the high efficiency of intracellular cleavage, compared with the extracellular cleavage, appear to be related to the widespread systemic and virulent infections caused by the

H5 and H7 viruses in birds and the localized outbreak of H5N1 infection in humans in Hong Kong in 1997 [61]. In all cases, enzymatic cleavage generates the N terminus of the “fusion peptide (FP)”, a conserved uncharged region of HA that plays an essential but undefined role in membrane fusion.

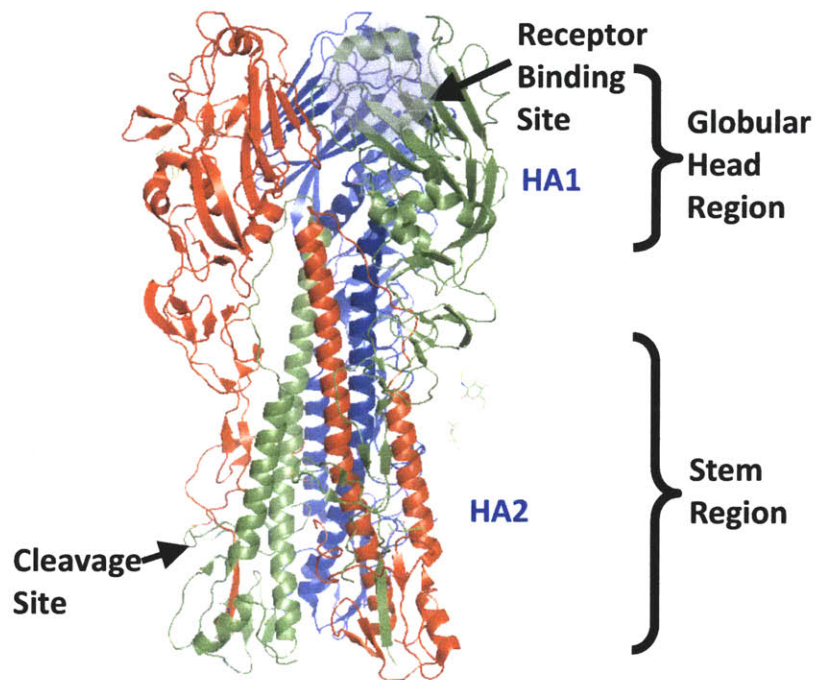


Figure 1.7 Molecular model of influenza A virus HA. Influenza A HA is a homotrimer consisting of a globular head region that harbors the receptor-binding site and a stem region that harbors the protease cleavage site. Each of the monomer is highlighted in *red*, *blue* and *green* respectively.

1.4.2 HA and its role in membrane fusion events in influenza A virus life cycle:

After binding to the host sialylated glycan receptor, influenza A virus is taken into cells by endocytosis. Within the endosomal compartment, the virion is exposed to the increasing acid pH 5-6, the HA protein undergoes irreversible conformational change from its metastable prefusion conformation to a low-pH hairpin structure involving extrusion of the “fusion peptide (FP)” from the interior of the HA2 at the neutral pH structure toward the endosomal membrane, promoting fusion of the viral and endosomal membranes (**Figure 1.8**) [62, 63]. X-ray crystallographic studies have demonstrated the extensive rearrangement of residues in HA2 at low pH with respect to

their relative orientation and coil-coil formation, loop-to-helix or helix-to-loop transitions [64, 65].

The interaction between FP and the target membrane leads to an extended intermediate that bridges the viral and cell membranes. Then the intermediate collapses by zipping up of the C-terminal part of the ectodomain alongside the trimer-clustered N-terminal part, which brings the two membranes into close proximity, resulting in formation of a hemifusion stalk. A fusion pore opens up through which the genetic material of influenza A virus is released into the host cell to generate new virions [62].

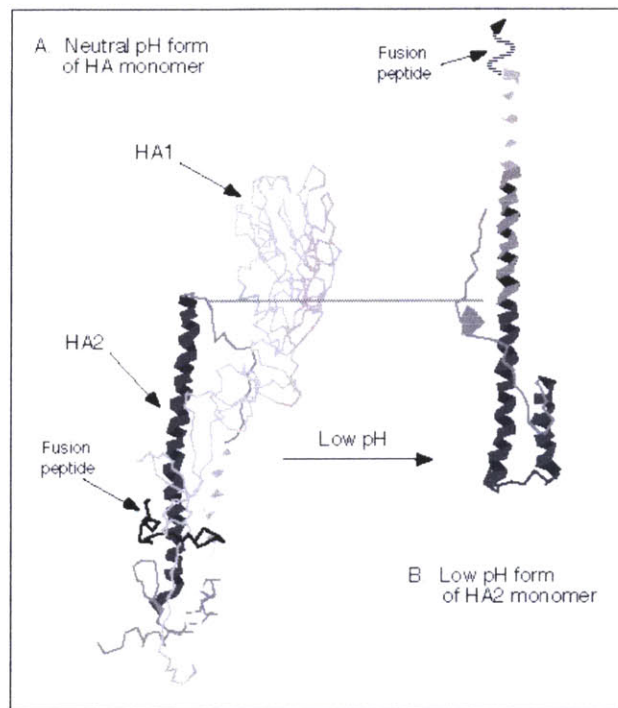


Figure 1.8 Ribbon diagram of the neutral and low pH forms of the HA. HA monomer at neutral pH is shown (A). Shown are HA1, HA2 and the central extended chain and the carboxy-terminal helix. At low pH (B) HA undergoes a major conformational change leading to the formation of an extended helix. The region of extended polypeptide chain between the N-terminal helix and the C-terminal helix is incorporated into the extended helix following acidification and the fusion peptide is exposed. This fusion peptide then interacts with the target membrane and enables membrane fusion.

Figure adapted from (<http://www.hiv.lanl.gov/content/sequence/HIV/REVIEWS/gp41.html>)

1.4.3 Molecular insights into HA-glycan interaction:

Each HA monomer contains a receptor – binding site (RBS) at its membrane distal tip, which has at its base, a number of conserved amino acids, Tyr-98, Trp-153, His-183 and Tyr-195, and at its edges, three conserved elements of secondary structure, the 130- and 220- loops and the 190 α -helix (**Figure 1.9**). Sialic acid is bound similarly in all HAs by hydrophobic interactions and by hydrogen bonds with the 130- and 220- loops and conserved amino acid in the base of the site.

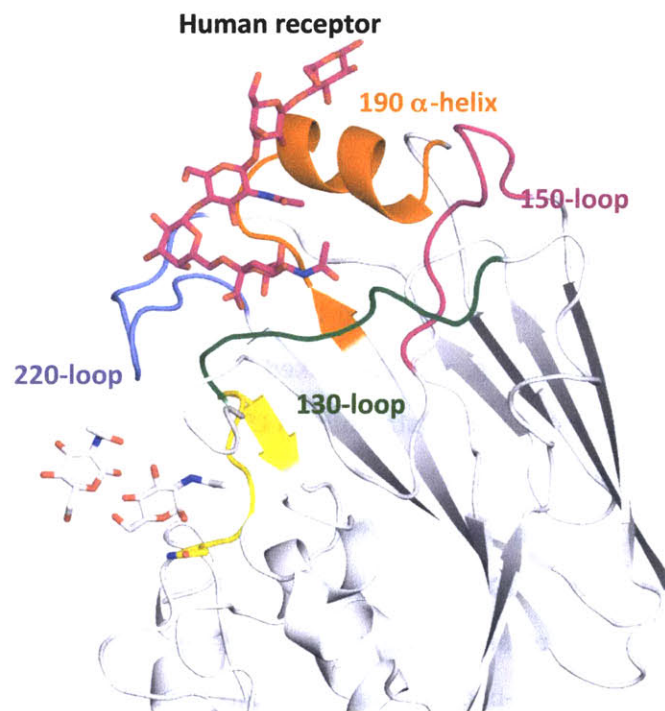


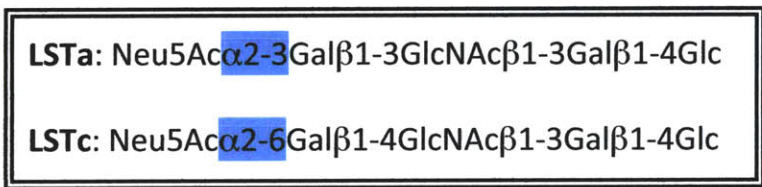
Figure 1.9 Crystal structure of a representative H1N1 HA in complex with human receptor. Shown is the crystal structure of HA from the 1918 pandemic A/South Carolina/1/18 or SC18. The protein was co-crystallized with LSTc (human receptor analog). Shown are the various loops (in various colors) and helix in the receptor binding site of the HA that interact with the glycan receptor.

The binding affinity of a single HA molecule to a single glycan receptor is in the mM range [66]. These estimates of low affinity imply that the tight binding of viruses to the cells during infection is mediated by the simultaneous interactions of a number of

HA molecules. In other words, HA-glycan interaction is *multivalent* similar to other protein-glycan interactions.

During antigenic variation, many amino acid sequence changes occur near the RBS on HA. Some of these influence receptor binding affinity and specificity. Such amino acid changes influence the specific interaction of HA with the sugars that are linked to sialic acid. The changes observed are different in H1 HA compared with H2 and H3 HAs. In H1 HA, mutations in residues 190 and 225 are important. An Asp190Glu and Asp225Gly double mutation in a prototypic H1 HA from the 1918 pandemic, A/South Carolina/1/18 or SC18, resulted in a complete switch from the human-like α 2-6 receptor binding preference to the avian-like α 2-3 receptor binding specificity [67]. In both H2 and H3 HAs, Gln226Leu and Gly228Ser are the major differences between avian and human viruses, with Gln226Leu observed in viruses isolated early in the pandemic.

X-ray crystal structures of several HA-ligand complexes have been determined in which the sialylpentasaccharide α 2-6 linked LSTc (the structure is shown below) was used as a human receptor analog, and α 2-3 linked LSTa (the structure is shown below) was used as an avian receptor analog (structure of LSTa and LSTc is shown below). In the complexes formed by all the human HAs with LSTc, the α 2-6 linkage between sialic acid and galactose adopts a *cis*-conformation in which the glycosidic oxygen faces out of the site (**Figure 1.9** and **Figure 1.10**). The galactose ring is oriented face on and together with C-6 presents a non-polar surface towards the base of the site. The bound oligosaccharide forms a folded-back structure and exits toward the right side of the site.



In avian H1, H2, H3 and H5 complexes with LSTa, the first three sugars of the avian receptor form a more extended chain in which galactose or Gal-2 (linked to sialic acid) is projected upwards, and the oligosaccharide exits site over the 220-loop, roughly

opposite to the direction taken by the folded human receptors. The α 2-3 linkage is in a *trans*-conformation, which exposes the glycosidic oxygen towards Gln-226 at the base of the site, and the Gal-2 is oriented edge on. The *trans*-conformation allows the formation of additional hydrogen bonds between the amine and carbonyl groups of Gln-226 and the 4-OH of Gal-2 and the glycosidic linkage oxygen. These interactions do not occur with human receptors, but this binding motif is common to all avian HAs.

In essence, the receptor binding pocket of the human adapted influenza A virus HA is more open than the avian HA binding pocket (**Figure 1.10B**). Hence unlike the human adapted HAs, the amino acids in avian HA that interact with the glycan receptor are conserved across all the avian HAs.

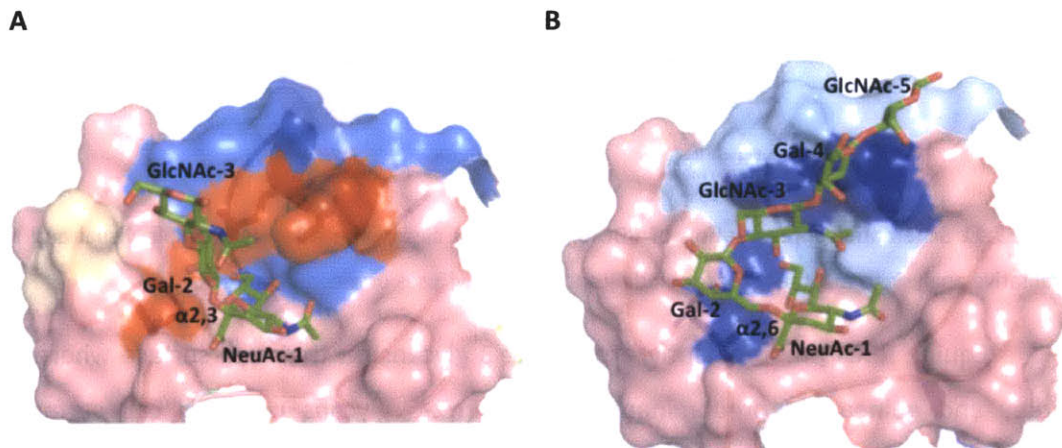


Figure 1.10 Molecular HA-Glycan receptor interactions. Shown are the HA-glycan receptor interactions for avian HA- α 2-3 glycan receptor (A) and human HA- α 2-6 glycan receptor (B). As seen from the figure, the avian HA receptor binding pocket is closed wherein the majority of the contacts are with the sialic acid linked α 2-3 to galactose. On the other hand, in case of the human HA, the receptor binding pocket is more open than avian HA due to its contact with sugars beyond the terminal sialic acid linked α 2-6 to the subterminal galactose (as shown in B).

1.5 Current tools to study HA-glycan interaction

A variety of biochemical assays are traditionally used to characterize HA-glycan interaction. This section highlights some of the pros and cons of these assays.

1.5.1 RBC Agglutination Assay

One of the earliest methods that still is used extensively to probe the glycan binding specificity of influenza A virus involves measuring the ability of the virus (through its HA) to agglutinate red blood cells (RBCs) as shown in **Figure 1.11**. RBCs from a variety of species such as chicken, turkey, horse, guinea pigs and humans are used for the assay due to their differential expression of α 2-3 and α 2-6 glycan receptors [67-71].

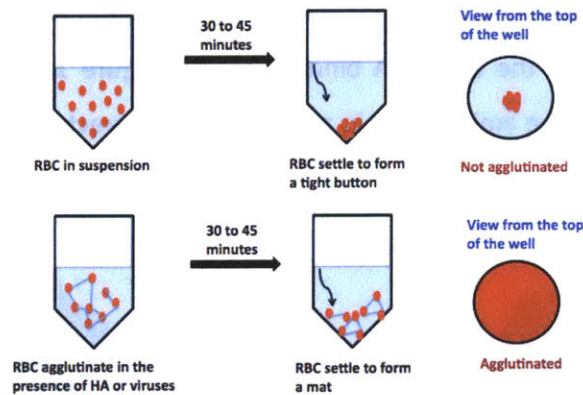


Figure 1.11 Schematic representation of RBC agglutination assay. The assay is a simple visual and a qualitative analysis to test the receptor binding specificity of viruses or recombinant HA.

Equine RBCs predominantly express α 2-3 glycans on their cell surface whereas turkey and guinea pig predominantly express α 2-6 glycans on their cell surface. Interestingly, chicken RBCs express both α 2-3 and α 2-6 glycans on their cell surface. To improve the specificity and the usefulness of the assay, the agglutination assay has been modified to include a step of complete desialylation of RBCs from a particular species followed by specific resialylation by either α 2-3 or α 2-6 sialyltransferase [72]. Agglutination assay is used extensively as it presents a simple approach for rapid analysis of influenza A virus. The visual read out further contributes to the easiness of the assay. Agglutination leads to a “matty” appearance of the RBCs as opposed to the non-agglutinated RBCs, which settle to form a tight button (**Figure 1.11**).

Though the agglutination assay is widely used, there are several drawbacks with the assay. *Firstly*, agglutination and other traditional hemagglutination assays define virus specificity according to the sialic acid linkage. However no information is obtained

on the virus specificity beyond the sialic acid linkage and hence probing the fine specificity of HA binding is not possible. *Secondly*, there is possibly substantial variability in the N- and O- linked cell surface glycans between different batches of between different batches of RBCs and related potential for variable response. This can skew results and mask any important specificity differences among viral strains. Additionally, the glycan structures on the cell surface of RBCs do not represent the glycan structures found on surface of human upper airway cells and hence are not physiologically relevant also this can undermine the diversity associated with the physiological glycan receptor [48].

1.5.2 *Fetuin Binding Assay*

Fetuin is a blood glycoprotein that is heavily glycosylated with N-glycans. Fetuin binding assay is based on competition for binding to solid phase immobilized virus between a horse radish peroxidase (HRP) conjugated fetuin, and unlabeled α 2-3 and α 2-6 sialyloligosaccharides [73]. The α 2-3 and α 2-6 sialyloligosaccharides are coupled to polyacrylamide, providing increased valency to compensate for the low HA affinity (mM range) for receptor analogues [74, 75]. Assays like these have been used to understand the diversity of receptor specificities of influenza A viruses from both birds and mammals [76-79] including H5 influenza A viruses [80]. Like the agglutination assays, fetuin binding assay also has several issues. *First*, measuring the binding of fixed viruses to glycans in solution is opposite to the physiological event where glycans are less mobile of the cell surface as compared with the virus. *Finally*, this assay is relatively a low throughput, and has been optimized for screening with whole viruses, thereby restricting the study of new pathogenic strains to specialized laboratories [81].

1.5.3 *Solid Phase Fetuin Capture Assay*

Subsequent development of fetuin binding assay has provided a wealth of information on the glycan binding properties of influenza A viruses (**Figure 1.12**). In

these assays, viruses are immobilized on fetuin-coated surfaces and their binding to various sialylated glycans (including polyvalent compounds) is evaluated [78, 79, 82, 83]. One of the major issues with the assay is the presentation of viruses, which is heterogeneous because the amount of virus captured on the plate depends on the binding of the viral HA to the sialylated glycans on fetuin. Moreover, similar to the fetuin binding assay, the binding event is opposite of the physiological event where the viruses in solution bind to the less mobile glycan receptors on the cell surface.

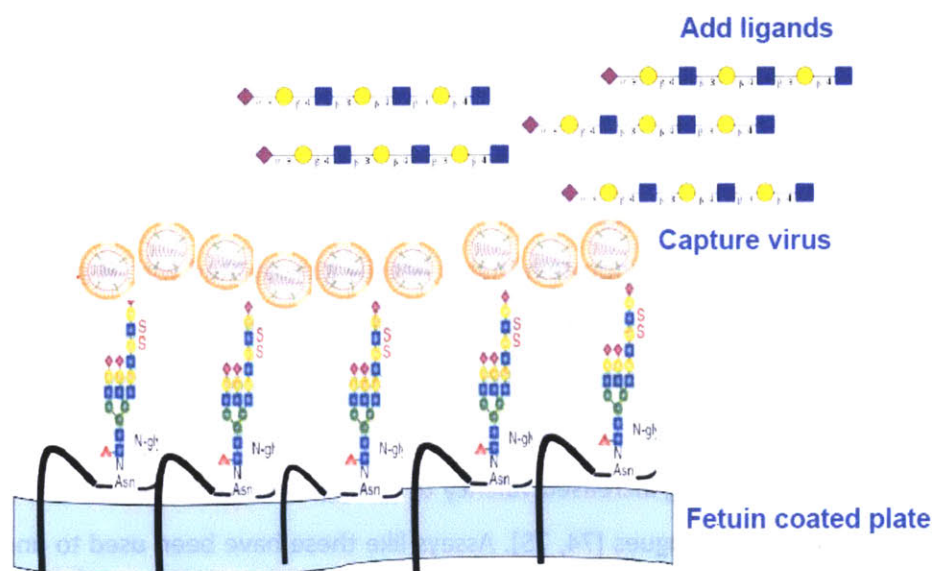


Figure 1.12 Schematic representation of Fetuin Capture Assay. Viruses can be captured on the fetuin coated plates through their interaction with the sialylated N-glycans on fetuin. Binding affinity constants can be estimated by adding varying concentrations of soluble ligands. This assay can also be used to estimate the potency of soluble sugar analogs that competitively inhibit binding of the virus to the glycan receptors.

1.5.4 Glycan Array Analysis

The recent advent of chemical and chemoenzymatic synthesis of glycans has led to the development of glycan array platform (**Figure 1.13**) [81, 84, 85]. Analogous to a DNA microarray platform, the glycan microarray platform consists of hundreds of synthetic glycan motifs (typically present on N- and O- linked glycoproteins and glycolipids) displayed on the surface of glass slide (sugars with amino terminal linkers are immobilized on amino-reactive N-hydroxysuccinimide activated glass slides by a

covalent amide bond). If the glycans are biotinylated, they can be immobilized on streptavidin-coated surfaces. Multiple types of arrays have been developed depending upon the source of glycans that are immobilized onto the surface. Recently a novel strategy for creating naturally derived glycan microarrays have been developed [86]. Such an approach will enable imprinting natural glycans extracted from the cell surface to be imprinted on a glycan array format thus allowing one to probe the glycan repertoire of a biological system. Further to improve the presentation of glycan similar to the physiological scenario, various strategies including the formation of neoglycolipids [87] and neoglycoprotein [85, 88].

More recently, the glycan array platforms developed by Consortium for Functional Glycomics (CFG) have been used to screen wild-type and mutant forms (mutations in HA) of intact viruses and recombinant HAs belonging to the H1, H2, H3, H5, H7 and H9 subtypes [89-92]. These studies have increased our understanding of HA binding to sialylated glycan receptors by mapping the effect of glycan modifications such as sulfation and fucosylation on the HA-glycan interactions. Glycan array analysis with whole viruses provides a quick snapshot of the various human and avian glycan receptors that are bound by the viral HA. Viruses are quantified as hemagglutination units (HAU) based on their ability to agglutinate RBCs. Since HAU is dependent on the binding affinity of the viral HA to the receptors on the surface of RBCs, it varies between different viruses. Hence it is challenging to compare the binding property of one virus (analyzed on the array) with that of another virus. Also this makes it challenging to quantify the affinity of HA for a specific glycan receptor.

1.5.5 *Flow Cytometry to analyze HA-glycan interaction*

Yet another technology that is being developed uses beads coated with specific glycan motifs to probe binding of fluorescently labeled whole viruses or recombinant HA (**unpublished results**). Binding can be analyzed by flow cytometry by measuring the fluorescence emanating from the bound virus or HA. This assay mimics the multivalent presentation of glycans on cell surface and hence is physiologically relevant.

1.5.6 *Other Methods to analyze HA-glycan interaction*

There are other (though not commonly used) methods to investigate HA-glycan interactions such as isothermal titration calorimetry and surface plasmon resonance (SPR), which have been used to determine equilibrium binding affinity constants and thermodynamic parameters for glycan-protein interactions [93, 94].

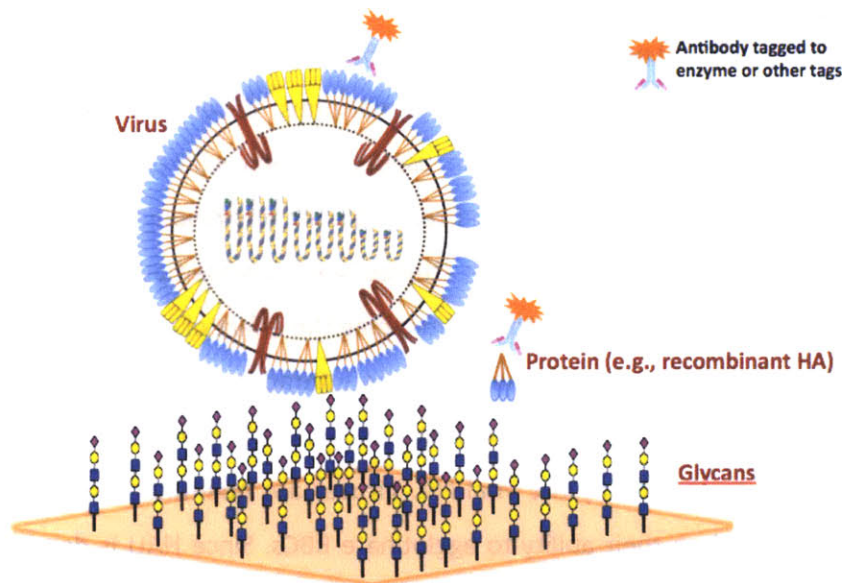


Figure 1.13 Schematic representation of the glycan array platform. Chemically synthesized enzymes can be immobilized to glass slides by chemical modification. Binding of whole viruses and proteins to specific glycans can be analyzed as shown above. Binding signals can be estimated by using a secondary antibody tagged to an enzyme or other chemiluminescent molecules.

1.5.7 *Staining of relevant tissue sections with whole viruses and recombinant HA*

One of the factors determining the pathogenicity of influenza A viruses is their tissue tropism. Human upper respiratory tract is the prime target of infection by human adapted influenza A virus. The variation in pathogenicity of influenza A viruses is speculated to be due to their differences in tropism to human upper respiratory tract. Hence in order to understand the tissue tropism of influenza A viruses, various strategies have been employed. Broadly, in order to understand the distribution of α 2-3

and α 2-6 glycans, fluorescently labeled plant lectins have been used to stain paraffinized human respiratory tract tissue section (**Figure 1.6**) [49]. Further, by looking at the pattern of virus attachment (PVA) to various regions of the paraffinized tissue sections from human upper respiratory tract, it was determined that the influenza A viruses that transmitted efficiently among humans attach abundantly to human upper respiratory tract, whereas inefficiently transmitted influenza A viruses attach rarely [38, 39, 41]. More recently, recombinant HA precomplexed with a primary antibody and a fluorescently labeled secondary antibody has been used to stain paraffinized human respiratory tract tissue sections [48]. This showed that the HA from human adapted influenza A viruses showed predominant staining of the goblet cells and ciliated epithelial cells of human trachea. On the contrary, recombinant HAs from avian influenza A viruses showed predominant staining of the human alveolar region (deep lung) [48, 95].

1.6 Challenges associated with bridging HA-glycan interaction with viral pathogenesis

In 1989 Peter Palese and colleagues developed a method termed as “reverse genetics” which allowed synthesis of whole influenza A virus from the cDNAs of individual virus genes [96, 97]. In addition to the advent of reverse genetics to understand influenza A virus biology, ferrets have emerged as a model system to study influenza A virus pathogenesis and contact and respiratory droplet modes of transmission [67, 98, 99]. Studies have shown that ferrets express similar glycan receptors as that of humans and that they exhibit similar symptoms upon influenza A viral infection [100].

Using reverse genetics, the pandemic 1918H1N1 viruses were reconstructed [101] and its virulence was tested in ferret animal model. This further enabled systematic exploration of the roles of various viral genes in the virulence and transmissibility of influenza A virus strains [102, 103].

A systematic study was performed involving single gene reassortments of the 1918 pandemic human H1N1 influenza A virus (A/South Carolina/1/18 or SC18) with a contemporary human H1N1 (A/Texas/36/91 or Tx91) virus in ferrets (**Table 1.1**). It was shown that the HA of SC18 had most profound effect on the virulence of the reassortment viruses followed by NA and PB1 genes [104]. Further, a single (NY18) or double (AV18) point mutation in the HA of SC18 resulted in a virus that was unable to transmit efficiently via respiratory droplet in the ferret model (**Table 1.1**). This prompted analyzing the glycan binding properties of these 1918 H1N1 HAs. RBC agglutination assay (described in *Section 1.5.1*) was used to characterize SC18 and it was found to be a strict α 2-6 binder, NY18 was a mixed α 2-3/ α 2-6 binder, and AV18 was a strict α 2-3 binder. Given the predominant distribution of α 2-3 glycans in the deep lung tissues of the human respiratory tract, both NY18 and AV18 are more likely to infect deep lung tissues. Since the NA of these α 2-3 binders is same as that of SC18, it might be inefficient at releasing the viral particles from the deep lung tissues, leading to lower virulence of these mutant viruses.

Table 1.1 Glycan receptor binding specificity (identified by RBC agglutination assay) and respiratory droplet transmissibility of H1N1 influenza A viruses in ferrets

<i>Virus Strain</i>	<i>Binding specificity to Sialic acid linkage</i>	<i>Transmission efficiency in ferrets</i>
A/South Carolina/1/18 or SC18	Only α 2-6	Efficient
AV18 (SC18 + 2 mutations)	Only α 2-3	None
NY18 (SC18 + 1 mutation)	α 2-3 and α 2-6	Inefficient
A/Texas/36/91 or TX91	α 2-3 and α 2-6	Efficient

By associating the inefficient virus transmissibility with the α 2-3 binding specificity of NY18 HA, it can be concluded that a loss of α 2-3 binding is necessary of efficient transmission but that the gain of α 2-6 glycan receptor binding is insufficient. In an apparent contradiction to this conclusion, TX91 also a mixed α 2-3/ α 2-6 binding H1N1 virus is able to transmit efficiently [67] (**Table 1.1**). Also in other studies with H7 and H9 viruses [89, 92]. it was observed that although some of the wild-type or HA mutant viruses showed substantial α 2-6 binding, none transmitted via respiratory droplets in

the ferret model. However, in the same experimental system, the control human adapted H3N2 viruses that showed similar α 2-6 binding specificity did transmit efficiently. Studies like these show that defining the glycan receptor binding specificity of HA only in term of α 2-3 or α 2-6 alone (based on RBC agglutination assay, glycan array etc.) makes it challenging to correlate the glycan binding specificity to human adaptation and viral virulence. Moreover, this also shows that there are additional factors that govern the glycan receptor binding specificity of HA and determine its role in influenza A virus infection and transmissibility in humans.

1.7 A multifaceted approach to study HA – glycan interaction and to decode its role in viral pathogenesis

In order to address the aforementioned challenges, it is important to integrate information from complementary set of approaches. Interfacing information obtained from structural modeling of HA-glycan interaction to their biochemical characterization and finally to correlate these with their biological significance in viral pathogenesis is the essence of such a multifaceted approach (**Figure 1.17**). Such an endeavor starts with understanding the properties of HA and the glycan receptors individually as two molecular components involved in HA-glycan interaction.

To understand HA, it is important to look at the primary sequence of HA and identify key amino acid sequences that play an important role in governing HA binding properties. This would involve comparing and aligning HA sequences from influenza A viruses infecting different hosts. This kind of an approach has enabled identifying sequences that are common to the viruses isolated from a specific host and how a change in the amino acid sequence at these regions can lead to new viral host adaptation (explained in detail in *Section 1.4.3*).

The second molecular component, the glycan receptors, can be characterized using several approaches. At a high level, because human upper respiratory epithelia is the primary target of human adapted influenza A virus, it is essential to characterize the distribution of physiological sialylated glycan receptors on these tissues. It is well known

that the sialylated glycans on the epithelial cells of human upper respiratory tract are the receptors for influenza A HA binding and endocytosis, epithelial cells themselves possess a broad array of structurally diverse and complex glycans. Hence it is challenging to access and elucidate the structures of glycan motifs, which are the receptors for influenza A virus HA. One approach that has been employed to probe the distribution of glycan receptors is to perform staining of relevant tissue sections with fluorescently labeled plant lectins. Two plant lectins that are frequently used are *Sambucus nigra* agglutinin or SNA-I (binds specifically to Neu5Ac α 2-6Gal/GalNAc motif [47] and *Maackia amurensis* lectin or MAL-II (binds specifically to α 2-3 glycans) to identify the distribution of α 2-3 and α 2-6 glycan [48, 49]. Co-staining of SNA-I with another lectin, Jacalin, which binds to the O-linked glycans (GalNAc-Ser/Thr), provides information on the distribution of α 2-6 glycans in the context of O-linked glycans. More recently, co-staining of Jacalin with recombinant HA has shown that the HA from human adapted influenza A viruses show significant co-staining with jacalin [48] indicating their preference for α 2-6 O-linked glycans. Studies like these using lectin matrix provide insight into the cellular tropism of the virus and hence help specifically in identifying hallmarks of these human adapted viruses.

Bridging the lectin staining of relevant tissue sections with glycan profiling of representative cell lines enables deciphering the finer structural details of glycans. Various analytical methods such as matrix-assisted laser desorption ionization (MALDI) mass spectrometry (MS) and MS/MS (to fragment glycans) can be used for characterizing glycans extracted from relevant cell lines [105, 106]. Other techniques have also been employed, including capillary high-performance liquid chromatography, liquid chromatography MS, and nuclear magnetic resonance [107, 108]. Recently lectin staining of human respiratory tract tissue section (explained above) interfaced with glycan profiling of representative human upper epithelial cells enable characterize the glycan receptors for influenza A viruses [48].

The molecular and structural aspects of HA-glycan interaction can be identified using conformational analysis of HA-glycan co-crystal structures. This provides a

meaningful sequence-to-structure correlation for HA and also enables identification of distinct topologies adopted by α 2-3 and α 2-6 glycan receptors in the context of its interaction with HA [48, 109]. Analysis of the various crystal structures indicated that a highly conserved set of amino acids Tyr98, Ser/Thr136, Trp153, His183, Leu/Ile194 (numbered based on H3 HA) across different HA subtypes are involved in anchoring the sialic acid. It was also established that the specificity of HA to either α 2-3 or α 2-6 is governed by an extended range of interactions within the glycan-binding site – not only with the sialic acid, but also with the glycosidic oxygen atom and monosaccharides beyond sialic acid [48, 66]. The ensemble of conformations sampled by the α 2-3 and α 2-6 glycan receptors upon their interaction with HA was given a shape-based topological description. In the case of α 2-3 glycans, the conformations sampled by Neu5Ac α 2-3Gal linkage (keeping the Neu5Ac anchored) and the sugars beyond this linkage (at the reducing end) span a region on the receptor-binding surface of HA that resembles a “cone” (**Figure 1.14**). The assembly of these conformations is therefore described by the term *cone-like* topology.

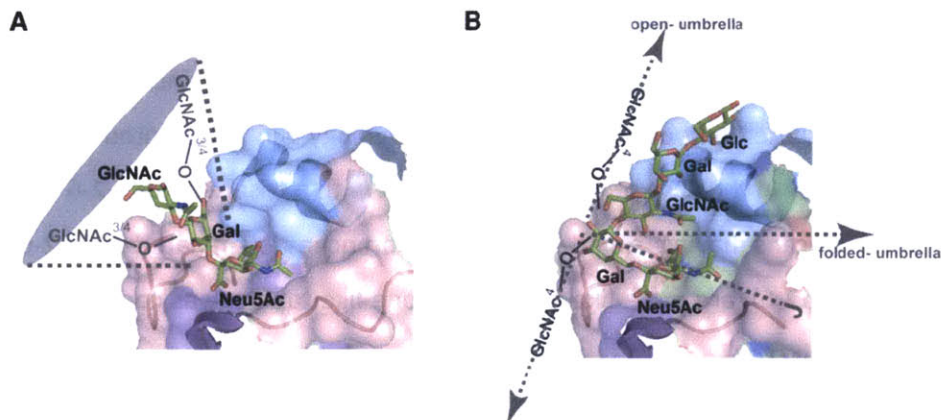


Figure 1.14 Glycan topology influences HA-glycan interaction. Interactions of HA with *cone-like* topology (A) is characteristic of avian HA binding to α 2-3 and short α 2-6 glycans (such as multiantennary N-linked glycans with single lactosamine branches terminated with α 2-6). In contrast to *cone-like* topology, interactions of HA with *umbrella-like* topology (B) is characteristic of human HA binding to long α 2-6 glycans (such as polylactosamine branch terminated with α 2-6)

When contrasted with the Neu5Ac α 2-3Gal linkage, the presence of C6-C5 bond within the Neu5Ac α 2-6Gal linkage provides additional conformational flexibility. The different conformations sampled by Neu5Ac α 2-6Gal linkage (keeping Neu5Ac anchored) and the sugars beyond this linkage (at the reducing end) this span a wider region on the HA binding surface. One part of this wider region is similar to the cone-like surface and the other part resembles a space that is readily described by the opening of an umbrella from a fully folded to a fully open form. Hence in contrast to the cone-like topology, the set of conformations sampled by α 2-6 glycans is described using the term *umbrella-like* topology (**Figure 1.14**). In this case, the stem of the umbrella is occupied by the Neu5Ac α 2-6Gal motif and the spokes of the umbrella (the flexible part) are occupied by the sugars at the reducing end of Gal.

In case of the glycans adopting cone-like topology, the majority of the interactions with the HA are made by a trisaccharide α 2-3 (Neu5Ac α 2-3Gal β 1-3/4GlcNAc-) or α 2-6 (Neu5Ac α 2-6Gal β 1-4GlcNAc-) motif. However, the glycan conformations that adopt umbrella-like topology are longer than a trisaccharide (at least 4 sugars and make substantial contacts with the receptor-binding site on HA. For instance, umbrella-like topology is adopted by poly lactosamine branches terminated by α 2-6 linked Neu5Ac (long α 2-6). The cone-like topology can be adopted by both α 2-6 and α 2-3 glycans. In the case of α 2-6 glycans those with a trisaccharide α 2-6 motif such as N-linked glycans having single lactosamine branches terminated by α 2-6 linked Neu5Ac (short α 2-6), are more likely to adopt cone-like topology as compared with the long α 2-6 branch.

Hence by looking at several HA-glycan co-crystal structures and by applying a topology-based description of glycan receptors, it was identified that the umbrella-like topology was characteristic of long α 2-6 motifs which interact with human adapted H1, H2 and H3 HAs and the cone-like topology was characteristic of α 2-3 glycans interacting with avian HA [2, 48, 95]. Because the avian HA glycan binding pocket can accommodate glycans which can adopt cone-like topology, it is highly likely that the short α 2-6 glycans can also bind to avian HA.

For biochemical characterization of HA-glycan interaction, it is important to have an assay that can quantify relative binding affinity of HA for a particular glycan receptor, while also capturing the multivalent HA-glycan interaction. As mentioned earlier, glycan array platform has emerged as a very important tool for assessing HA-glycan interaction (Section 1.5.4). In most of the earlier studies that focused on screening different HAs on the glycan arrays, the binding of HA to specific glycan motif was designated as a single point “on” or “off”. This designation though potentially is useful to screen for HA binding specificity to a particular glycan motif, the assay misses the context of the interaction and relative biological importance of the interaction. Moreover, since these assays are performed at a single saturating concentration of HA, it may overestimate the binding of HA to the glycan motifs to which otherwise HA would show no or less binding at a lower concentration. Taking into account these limitations, more recently biochemical assays have been developed to screen HA-glycan interactions over a range of HA concentrations [110]. Assays like these take into account the spacing of glycan motifs in an array platform and the spatial arrangement of glycan binding sites. In this approach, binding of HA to various glycan receptors is analyzed over a range of HA concentrations to measure approach to saturation by taking into account avidity and cooperativity effects. Further in order to specifically enhance the multivalency in the HA-glycan interactions, the recombinant HA is precomplexed with the primary and secondary antibody in a molar ratio of 4:2:1 [81]. The identical arrangement of 4 trimeric HA protein in the precomplex fixes the avidity effects. In fact, Srinivasan *et al* showed that incorporating the multivalency in HA-glycan interaction significantly enhances the glycan binding signals. For instance, there was at least an 8-fold increase in binding of SC18 HA to 6'SLNLN when HA was precomplexed with primary and secondary antibodies in a molar ratio of 4:2:1 (**Figure 1.15**).

Moreover, because the affinity of HA for its glycan ligand is low (mM range) [74], the use of such complexes has proved highly advantageous as increasing the valency by precomplexing enable obtaining detectable binding signals and also would require only small amount of protein. Using this assay, the HA-glycan receptor binding strength can

be quantified by estimating an apparent binding constant K_d' , which can be calculated by fitting the data (using the Hill equation) obtained by analyzing dose-dependent binding of HA to representative avian and human receptors. The Hill equation is defined as follows:

$$\log\left(\frac{y}{1-y}\right) = n * \log([HA]) - \log(K_d')$$

where “y” is the fractional saturation (average binding signal/maximum observed binding signal) and “n” is the cooperativity associated with HA-glycan interaction.

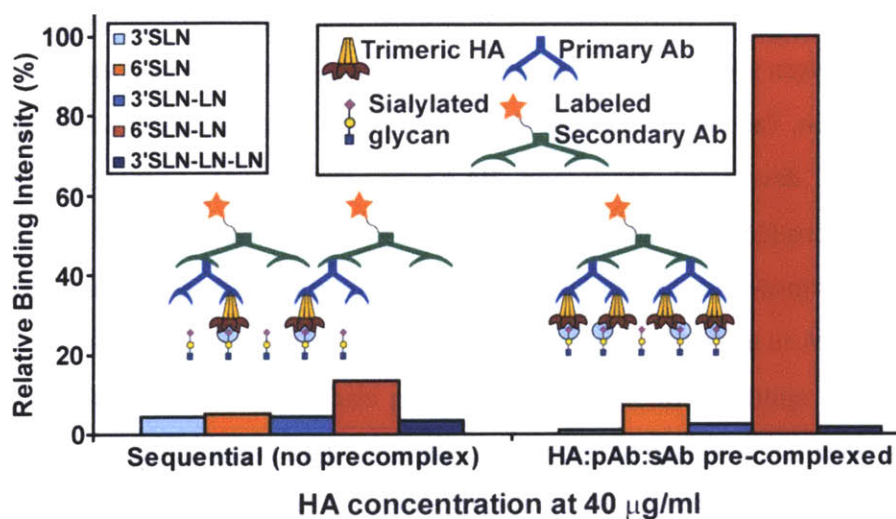


Figure 1.15 Glycan array assay to capture multivalent HA-glycan interactions. Shown is a comparison of binding signals between sequential binding assay and precomplexation of HA units with primary and secondary antibodies. Sequential assay favors the formation of HA:primary antibody:secondary antibody in 1:1:1 molar ratio as compared to 4:2:1 when HA is precomplexed with primary and secondary antibodies before adding to the glycans.

Figure adapted from Srinivasan *et al* (2008) PNAS

These assays have permitted quantification of the relative binding affinity of HA to different glycan motifs. This biochemical assay also takes into account the

multivalency associated with HA-glycan interaction. HA is pre-complexed with primary and secondary antibody before adding to the glycans on the array. In fact it has been established that the differences in the binding affinities of HA to glycan receptor is amplified by precomplexing HA with the antibodies to increase multivalency [110].

Using such quantitative assays, it has been demonstrated that the human-adapted HAs share a high binding affinity to α 2-6 glycans (particularly those that have multiple lactosamine repeats). Moreover, with the ability to express recombinant HA in insect cells [110], it is possible to test the effect of amino acid substitution mutations on the receptor binding property of HA. This can be used to monitor the evolution of the virus into a more human-adapted virus. Also, the recombinant HA can be used as a lectin to stain relevant respiratory tissue sections in order to understand the cellular and tissue tropism of the HA.

Finally, it is important to correlate these biochemical, molecular and structural aspects of HA-glycan interaction to their biological relevance in the viral pathogenesis. Ferrets have been used as a reliable animal model to study flu pathogenesis as they display symptoms similar to humans upon influenza A infection as mentioned in Section 1.6.

One of the important aspects defining the virulence of influenza A viral infection is its ability to cause human-to-human airborne respiratory droplet transmission. Both airborne respiratory droplet transmission and contact transmission of the virus can be easily studied in ferrets. For studying respiratory droplet transmission in ferrets, the infected ferret (inoculated with the virus) and the naïve ferret are housed in separate cages but share a common perforated wall (**Figure 1.16**). The onset of infection in the naïve ferret by respiratory droplet (due to sneezing by the inoculated ferret) is monitored and efficiency of viral transmission is then scored. This also depends on the number of contact ferrets that are infected by the inoculated ferret by airborne transmission. Most of the human adapted influenza A viruses show efficient respiratory droplet transmission in ferrets [67]. The 2009 H1N1 influenza A virus shows inefficient transmission in both humans and in ferrets [98, 111, 112]. In order to monitor the

contact transmission, both the inoculated and the naïve ferrets are housed together in the same cage (without a perforated wall) and share common food and other paraphernalia. Infection in the naïve ferret is then monitored. The clinical signs that are monitored to assess the pathogenicity of the virus (and the ensuing infection of the naïve ferret by the infected ferret) are sneezing, weight loss, virus shedding in the nasal washes and histopathological examination of relevant tissues and organs to assess the tropism (and systemic infection).

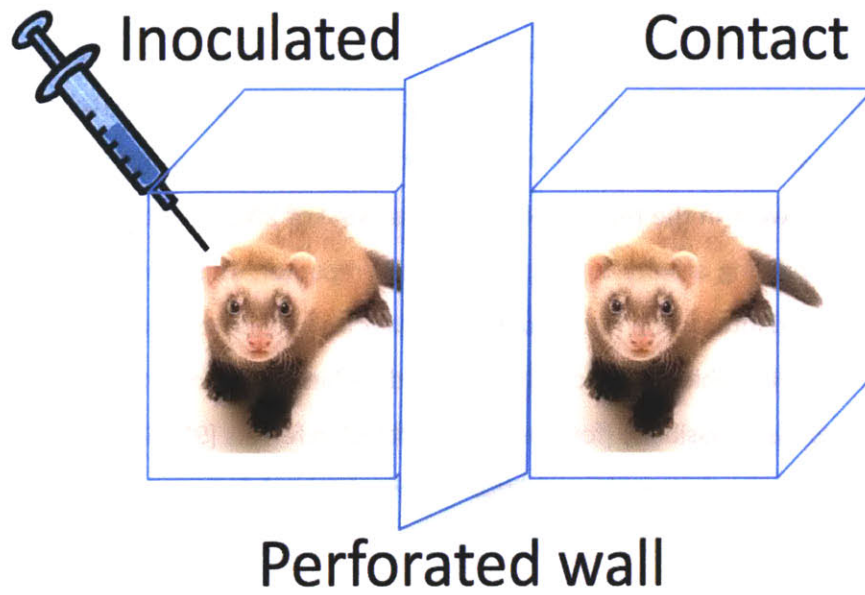
Recently, using the approach of interfacing various tools mentioned above, the biochemical rationale for the inefficient transmissibility of NY18 (D225G mutant of SC18) (**Table 1**) (a mixed α 2-3/ α 2-6 binder) in contrast to efficient respiratory droplet transmission of TX91 (which is also a mixed α 2-3/ α 2-6 binder) was established [110]. These were compared to that of the HA from a prototypic 1918 H1N1 pandemic virus, A/South Carolina/1/1918 or SC18, which has a strong α 2-6 glycan receptor binding preference and transmits efficiently in ferrets through airborne respiratory droplets. Analysis of the molecular HA-glycan contacts showed subtle changes resulting from the single amino acid variation between SC18 and NY18. The effect of these changes on their glycan receptor binding was amplified by multivalency, resulting in quantitative differences in their binding affinity to α 2-6 glycan receptor which adopts umbrella-like topology (or long α 2-6) upon its binding with HA. Furthermore, these differences in their binding affinities to the long α 2-6 glycans was also reflected in the markedly distinct binding pattern of recombinant SC18 and NY18 HA to the physiological glycan receptors present in human upper respiratory tissues. Thus the dramatic lower binding affinity of NY18 HA to long α 2-6 glycan receptor, as against a mixed α 2-3/ α 2-6 binding correlated with its lower transmission efficiency in ferrets. Moreover, TX91 HA had an increased binding affinity to long α 2-6 glycan receptor (although it is also a mixed α 2-3/ α 2-6 binder) in contrast to NY18, which correlated with its increased respiratory droplet transmission in ferrets.

Similar approach was extended to understand the glycan receptor binding property and transmissibility of the 2009 H1N1 swine origin influenza A virus [98, 99]

[Chapter 4]. It was demonstrated that the 2009 H1N1 influenza A virus HA has a lower binding affinity to long α 2-6 linked glycan (as compared to seasonal and pandemic virus), which correlated with its inefficient transmissibility in ferrets and humans. Further, by comparing the molecular HA-glycan interaction of 2009 H1N1 HA with that of seasonal and pandemic H1N1 HA, it was shown that a mismatched amino acid interaction network in the receptor-binding site (RBS) of 2009 H1N1 HA was responsible for its lower binding affinity to long α 2-6 glycan receptor. This was validated by fixing this mismatched interaction (by introducing either a single or triple mutation) in the RBS of 2009 H1N1 HA, which significantly improved its binding affinity to long α 2-6 glycans and hence its transmissibility (for the single mutant) in ferrets [99] [Chapter 4].

In summary, integration of information obtained from complementary set of approaches is important to correlate an important molecular interaction to its relevant biological function. Insight gained from aforementioned multifaceted approach for understanding HA-glycan interaction can be extended to identifying alternative antiviral strategies to combat influenza A infection as explained in Chapter 6. Such a multifaceted approach can also be extended to gaining insights into other protein-glycan interactions that impinge on other biological functions and whose functional significance is not yet fully understood.

A



B

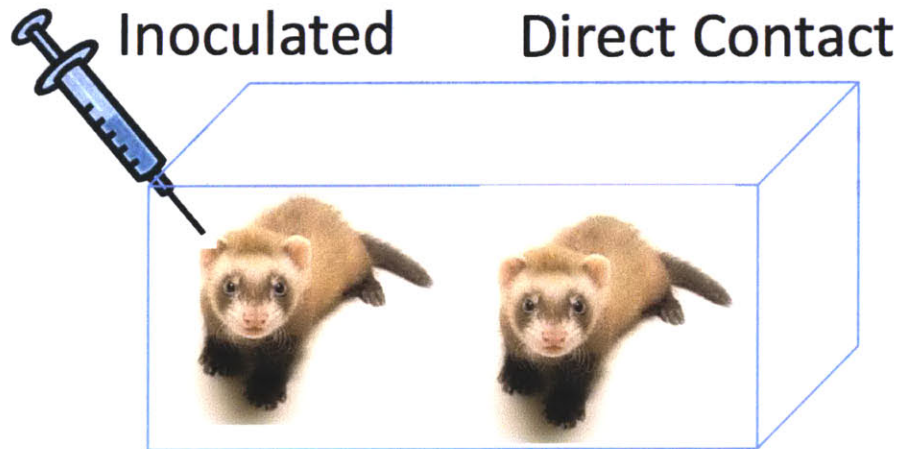


Figure 1.16 Transmission experiments in ferrets. Shown are the (A) Respiratory droplet transmission and (B) Direct contact transmission experiments. In (A) the naïve ferret is placed in the cage adjacent to the inoculated ferret but share a common perforated wall. In (B) the naïve ferret is placed in the same cage as that of the inoculated ferrets and share common water and food.

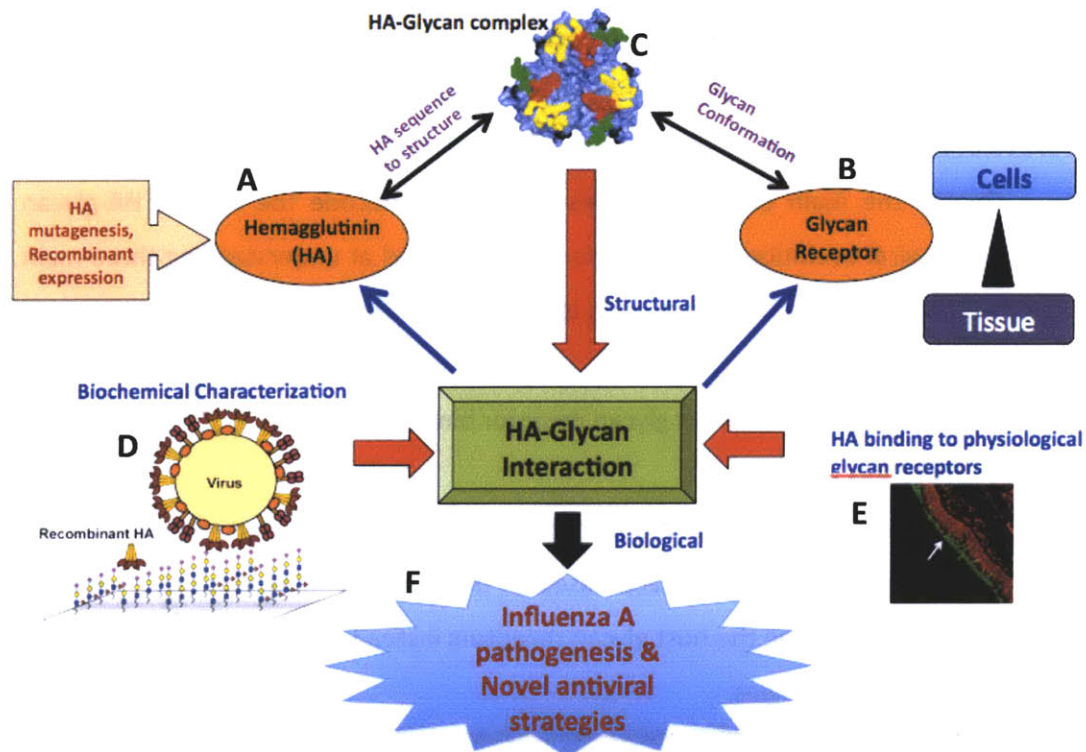


Figure 1.17 A multifaceted approach to understanding HA-glycan interaction to correlate it with its biological function. Understanding (A) HA and (B) glycans, the two molecular components involved in HA-glycan interaction, the first critical step in influenza A virus infection. (A) Identifying signatures in HA protein sequences from different host can enable identification of host-specific HA sequence to decipher its avian, human or swine origin. (B) Glycan receptors for influenza A HA can be delineated using a combination of lectin staining of relevant tissue sections and zooming in further using analytical tools for finer structural characterization of glycans extracted from relevant cell lines (C) Understanding the molecular structural aspects of HA-glycan interactions by analyzing HA-glycan crystal structures. Such an analysis can enable identification of distinct topologies adopted by glycans when they interact with HA. Similarly the amino acid interaction network involved in making contacts with the glycan receptor can also be identified. (D) The biochemical specificity of HA-glycan interaction can be characterized by performing a dose-dependent glycan array analysis with either recombinant HA or whole viruses. The array platform is designed to incorporate target glycan structures, which are predominantly expressed in upper respiratory tract (this data is obtained from B). (E) Staining of relevant tissue sections from the human respiratory tract with recombinant HA can enable probing the distribution of glycan receptors for influenza A HA. (F) The comprehensive knowledge obtained on the key determinants of HA-glycan interactions from A-E provides a much better handle to correlate it with its biological function in host adaptation and viral pathogenesis

1.8 *Thesis Outline and Specific Aims*

With the aforementioned approaches and techniques, this thesis aims to understand the multifaceted role of influenza A virus HA-glycan interaction going from viral evolution to development of new antiviral strategies to combat the infection.

Overall the main objective of this thesis is to decode the role of HA-glycan interaction in viral evolution. Towards this thesis is aimed at understanding three main factors that contribute to host adaptation leading to viral evolution:

- Antigenic drift
- HA glycosylation and its role in glycan receptor binding
- Host adaptation

Also this thesis aims to understand distribution of physiological glycan receptors for HA in ferrets and human respiratory tract. Based on this understanding, this thesis explores the possibility of targeting the host glycan receptors instead of the viral components as alternate anti-viral strategies.

SPECIFIC AIM 1: Understanding influenza A virus hemagglutinin (HA) in the context of its interaction with its glycan receptors

- a. Glycan receptor avidity of the virus and its effect on driving the antigenic drift of the virus
- b. Site-specific glycosylation of HA and its effect on glycan receptor binding
- c. Correlating HA-glycan receptor binding affinity to evolution of human host adaptation of 2009 swine origin influenza A virus

SPECIFIC AIM 2: Targeting glycan receptors of influenza A HA to combat viral infection

- a. Comparing distribution of glycan receptors in respiratory tract of model organism (Ferret) and humans
- b. Plant lectins as promising tools to specifically target glycan receptors of influenza A virus

Chapter 2. Hemagglutinin Receptor Binding Avidity Drives Influenza A Virus Antigenic Drift

Summary

In order to evade the host neutralizing antibody response, influenza A virus acquires antigenic drift mutations on its hemagglutinin (HA). This chapter reports our analysis understand this phenomenon, in order to gain insight into viral evolution. Based on this analysis it was found that repeated passaging of a representative virus (A/Puerto rico/8/34 or PR8) in immunized mice selected for mutants with single amino acid changes on its HA. No changes were observed when the virus was passaged in non-immune mice, indicating that the changes observed on HA were due to the neutralizing antibody pressure. The point mutations observed on HA increased its binding avidity to cell surface glycan receptors. Passaging these high binding avidity mutants in naïve mice, but not immune mice, selected for additional hemagglutinin mutations that decreased cellular receptor binding avidity. Analyzing a panel of monoclonal antibody hemagglutinin escape mutants revealed a positive correlation between binding avidity and escape from polyclonal antibodies. Hence this study highlights a yet another mechanism by which influenza A viruses evolve. In summary, in response to variation in neutralizing antibody pressure between individuals, influenza A virus evolves by adjusting binding avidity via amino acid substitutions throughout the hemagglutinin globular domain, many of which simultaneously alter antigenicity.

2.1 Introduction

Currently licensed seasonal influenza vaccines are designed to protect humans from the prevailing strains of human influenza A lineages H1N1 and H3N2 and of influenza B virus. These vaccines' principal target is the most abundant viral surface antigen, hemagglutinin (HA). Immunization against this sialic acid receptor-binding glycoprotein typically elicits neutralizing antibodies, which may act by blocking the attachment of the virus to host-cell receptors or by interfering with HA-mediated viral fusion [113, 114]. The annually determined trivalent influenza vaccines are standardized on the basis of the content of their HA components. Neuraminidase (NA), the other major surface protein and determinant of serotype, is not standardized in current vaccines, meaning that the amount is likely to vary from batch to batch. Antibodies against NA do not block infection, but they can inhibit the enzymatic activity of NA [115]. Therefore, immunization against NA can decrease viral replication in the lungs and reduce disease severity upon subsequent challenge [115, 116]. Although HA and NA are both highly immunogenic, intact influenza virions reportedly induce a humoral response skewed toward HA because of antigenic competition [117]. However, immunization with a commercial trivalent subvirion vaccine in which the HA and NA components are dissociated increases NA-specific antibody titers in humans [118].

Approximately 20% of the world's population is infected by influenza A each year, resulting in significant mortality and morbidity [119]. The high incidence of influenza cases is attributable to the ability of the influenza virus to escape immunity induced by prior infection or vaccination. This escape is potentiated by the accumulation of mutations in the surface glycoproteins, hemagglutinin (HA), and to a lesser extent neuraminidase (NA), which confer antigenic change to the virus. This happens due to the acquisition of "antigenic drift" mutations specifically in the globular head domain of its HA which serve as the antigenic epitopes for the neutralizing antibodies. Antigenic drift mutations are also attributed to the error-prone reverse transcriptase encoded by the viral genome. Hence one of the challenges with the vaccines against influenza A viruses is that they need to be updated annually.

The survival of human influenza A viruses in nature in the presence of a relatively high herd immunity due to prior infection or immunization has been attributed to the immunological instability of these agents [120]. The partially immune hosts provide a selective environment for the emergence of antigenic variants capable of resisting neutralization by specific antibodies [120]. This hypothesis, first advanced by Taylor *et al* (1949) [121], found support by the work of Archetti and Horsfall [122] who demonstrated the occurrence of antigenic changes during serial passage of influenza A viruses in fertile eggs in the presence of neutralizing antibodies to a related strain. This has been further established in murine model by serial passage of a mouse-adapted influenza A virus (A/Puerto rico/8/34 or PR8) in the lungs of mice previously vaccinated with formalin-inactivated homologous virus [120]. In this model it was established that antigenic variants evolve in this process only in vaccinated mice.

Previously, Yewdell *et al* (1986) have studied the effect of antibody response in viral evolution [123]. They have shown that PR8 grown in allantois-on-shell cultures in the presence of antibodies directed against antigenic epitopes on HA (Section 2.2) led to the emergence of variants. Sequencing of vRNA from these variants revealed that each of the variants differed from the parental virus by a single amino acid alteration in its HA1 subunit. Moreover, two of these changes were close to the receptor-binding site (RBS) on HA1 subunit and the third was near the trimer interface. It was hence proposed that these mutations might alter the receptor binding by HA. Hence the main goal of this study is to understand how influenza A viruses escape polyclonal antibodies given that the frequency of variants with simultaneous multiple point mutations is exceedingly low [124]. Also the effect of the single point mutations on HA1 subunit of mouse-adapted PR8 (after serially passaging in an immune and non-immune murine model) in glycan receptor binding by HA was investigated. We collaborated with Professor Jonathan Yewdell who identified escape mutants when influenza A virus was passaged in immune mice. We provided a structural and a biochemical rationale for their ability to escape neutralizing antibody response providing an alternate new mechanism for the emergence of escape mutants.

2.2 Antigenic structure of A/PR/8/34 or PR8 HA (H1 subtype)

As explained in Chapter 1, hemagglutinin or HA is a trimeric glycoprotein which is enzymatically cleaved into the amino-terminal HA1 (molecular weight 46kDa) and carboxyl-terminal HA2 (m.wt. 27kDa) polypeptides. As elucidated from HA crystal structures [125-127], HA monomer forms two distinct domains: a distal domain of globular shape, which is made up exclusively by the major portion of the HA1 polypeptide, and a proximal fibrous stem-like structure, which anchors the HA into the viral lipid envelope and is made up by the HA2 and part of the HA1 polypeptides.

Several different approaches have been employed to characterize the antigenic structure of the HA molecule. One of the approaches was to generate a panel of monoclonal anti-HA hybridoma antibodies and to use them to select mutants of the influenza A/PR/8/34 or PR8 virus expressing antigenically altered HA molecules [128, 129]. These mutants, which escape neutralization by the monoclonal antibody can then be expanded in a host system that supports virus replication. Based on this an operational antigenic map of the HA molecule was constructed by comparative antigenic analysis of the mutant viruses with the monoclonal antibodies. The observation that individual mutations concomitantly modify certain epitopes provided an operational basis for the construction of an epitope map. Thus an antigenic analysis of 34 antigenically unique PR8 virus mutants with 58 monoclonal anti-HA antibodies permitted assembling the mutant viruses into four antigenic groups viz. Sa, Sb, Ca and Cb [128] (**Figure 2.1**) Several additional anti-HA monoclonal antibodies have been used to map antigenic sites on HA [129]. Following section describes the 4 antigenic regions on PR8 HA.

2.2.1 Antigenic sites Sa and Sb

These sites are defined by the residues in the upper part of the globular head of the HA1 subunit (**Figure 2.1**). Antigenic analysis divides this region into two operationally distinct areas, identified here as sites Sa and Sb, which are, however, closely linked and cannot accommodate the simultaneous binding of antibodies to each

site [130]. Site Sa comprises the “front” of this region as viewed in **Figure 2.1**, including residues 128 and 129 and residues 158, 160 and 162 to 167 (excluding 164). The Sa site extends down through a region of β structure on the opposite side of the HA monomer to the proposed receptor binding site (Wilson et al., 1981), and in the trimer comes close to the monomer-monomer interface. The site occupies a position relatively near the receptor-binding site of the adjacent monomer when the trimer is assembled (**Figure 2.1**).

The antigenic site Sb occupies the “back” of the head region as viewed in **Figure 2.1**, comprising the external residues 192, 193 and 196 of a region of α helix, residue 198, and residues 156 and 159. These residues are along the upper edge of a pocket containing the receptor-binding site. Residues 156 and 159 lie in the same region of polypeptide chain as residues 158 and 160 of site Sa. Indeed, it is this polypeptide loop (containing residues 156-160) that separates the operationally distinct antigenic sites Sa and Sb, and residues which lie along this loop map, into one site or the other according to whether they are front-facing (residues 158 and 160, site Sa) or back-facing (residues 156 and 159, site Sb.)

2.2.2 *Antigenic sites Ca (Ca₁, Ca₂) and Cb*

Analysis of the location on the HA monomer of the residues that delineate antigenic subsites Ca₁, and Ca₂ shows two widely separated clusters of changed residues. Subsite Ca₁, contains external residues 169, 173, 207 and 240. The location of antigenic subsite Ca₂ is indicated by mutations in two loops that contain residues 140, 143 and 145 and residues 224 and 225. These loops are close to each other in the three-dimensional structure of the HA monomer, but lie on the opposite side of the monomer to those mapped as belonging to the related subsite Ca₁. However, these two subsites come into close proximity when the trimer is assembled, presenting a cleft which spans the monomer-monomer boundary and which is operationally defined as the antigenic site Ca (**Figure 2.1**).

The fourth antigenic site, Cb, defines a region near the bottom of the globular head of HA1, distinct from the Ca cleft, as indicated by mutations at residues 78 to 83 (excluding residue 80) and residue 122. The location of this site is consistent with previous analyses by competition binding of antibodies to sites Cb and Sa, which proved these sites to be topologically distinct [130].

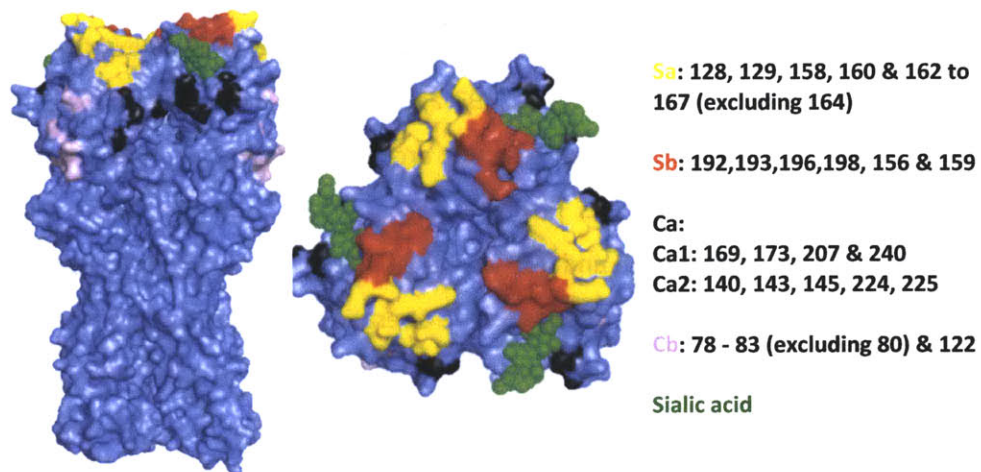


Figure 2.1 Antigenic sites on A/PR/8/34 (PR8) HA. PR8 has four non-overlapping antigenic sites. Each of the sites are indicated in various colors. Indicated on the right are the amino acids that make up each of the antigenic sites

Yellow – Sa; Red – Sb; Black – Ca; Pink – Cb; Green – Sialic acid

2.3 Receptor binding avidity and its role in driving antigenic drift

The next few sections provide proof-of-concept leading to identification of a new mechanism by which antigenic drift in influenza A virus is driven by the receptor binding avidity of its HA.

2.3.1 *In vivo* passaging of mouse-adapted A/PR/8/34 in immunized mice selects for single mutants in HA

To better understand how antigenic drift occurs in human populations, classical experiments modeling drift in outbred Swiss mice was revisited as explained in Section

2.1 [120]. Three separate infectious stocks of the mouse-adapted strain A/Puerto Rico/8/34 (H1N1) (PR8) were generated in MDCK cells using reverse genetics. Each stock was serially passaged in naïve mice or mice immunized with inactivated virus. Mice were infected intranasally with virus prepared from lung homogenates (Figure 2.2).

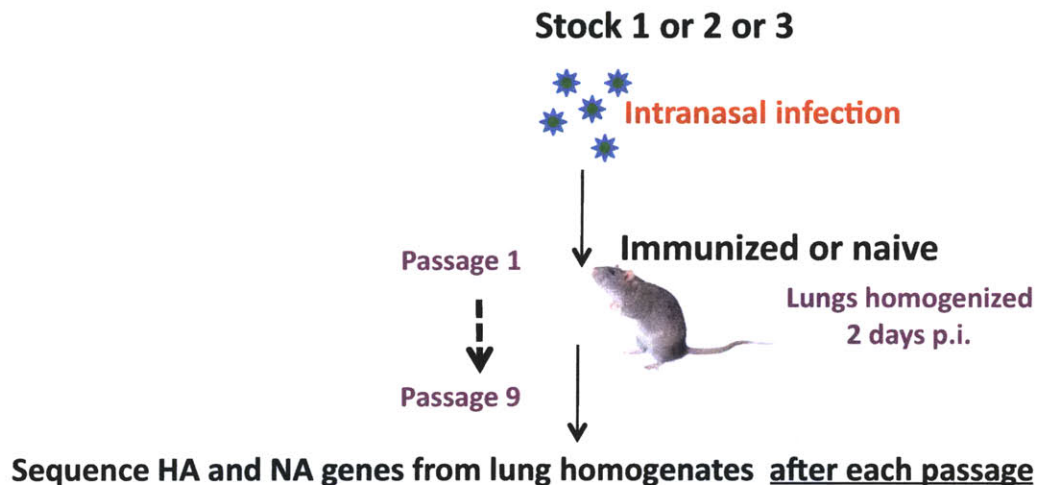


Figure 2.2 Scheme for *in vivo* passaging of PR8 in mice. The virus was passaged upto 9 times in naïve or in immunized mice to identify escape mutants. The virus obtained from the lung homogenate was subsequently used to inoculate (i.n.) the naïve mice and so on.

After nine passages, HA gene sequencing revealed no detectable mutations in viruses passaged in naïve mice (Figure 2.3). By contrast, each lineage from vaccinated mice contained a predominant population with a different single amino acid substitution: residue 158 (E to K, lineage I), 246 (E to G, lineage II), or 156 (E to K, lineage III). Residue 158 is located at the interface of the Sa/Sb antigenic sites, residue 156 is in the Sb site, and residue 246 is located outside the defined epitopes [129] (Figure 2.4). E158K, initially detected in lineage I following passage 2, predominated by passage 3. In lineage II, E246G abruptly emerged during passage 3. In lineage III, E158K and E156K co-dominated from passage 2-7, with E156K predominating following passage 8. None the lineages exhibited changes in the neuraminidase (NA) gene. Lack of any changes in NA could be attributed to a poor neutralizing response against NA as compared to HA due to low density of NA compared to HA.

	<u>HA</u>	<u>NA</u>
PR8 (stock 1) $\xrightarrow{\text{passaged 9x in vaccinated mice}}$	E158K	no change
PR8 (stock 1) $\xrightarrow{\text{passaged 9x in naive mice}}$	no change	no change
PR8 (stock 2) $\xrightarrow{\text{passaged 9x in vaccinated mice}}$	E246G	no change
PR8 (stock 2) $\xrightarrow{\text{passaged 9x in naive mice}}$	no change	no change
PR8 (stock 3) $\xrightarrow{\text{passaged 9x in vaccinated mice}}$	E156K	no change
PR8 (stock 3) $\xrightarrow{\text{passaged 9x in naive mice}}$	no change	no change

Figure 2.3 *In vivo* passaging of PR8 in vaccinated mice selects for single mutants in HA. HA and NA genes were sequences in lung homogenates from three independent PR8 stocks serially passaged in vaccinated and naïve Swiss mice. Note that mutants were selected only in vaccinated mice. Also, no mutations were identified in NA gene.

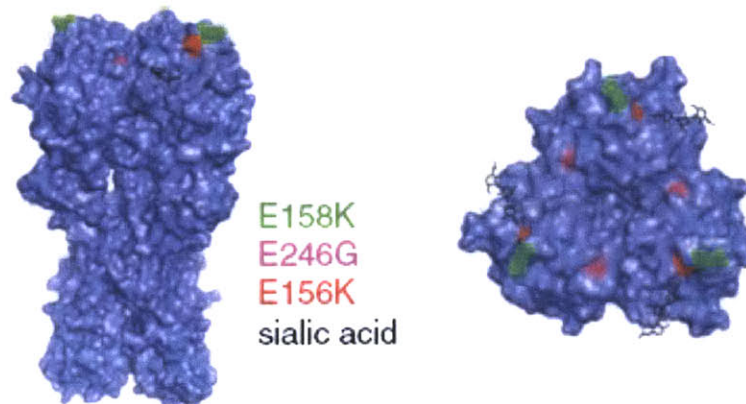


Figure 2.4 Location of amino acid mutations in *in vivo* selected influenza A viruses

2.3.2 *Single HA mutants escape antibody response*

Next it was important to evaluate if the single HA mutants identified by serial passaging in immunized mice were indeed escape mutants that have evolved to invade the neutralizing antibody response in immunized mice. Hence the mutants' ability to escape antibody responses was measured by hemagglutination inhibition (HAI) and virus neutralization assays using immune serum pooled from 45 PR8-vaccinated mice. Each mutant escaped antibody responses in these ternary (virus, antibody & cell) assays (**Figure 2.5A and B**), despite demonstrating only minor (E156K, E158K) or no (E246G) decreases in anti-HA antibody binding (**Figure 2.5C**). More precise antigenic analysis

using ELISA confirmed that the amino acid substitutions had limited effects on individual monoclonal antibody binding . E156K modified Sb antigenicity, but had no effect on the other sites. E158K altered binding of a subset of Sa- and Sb- specific monoclonal antibodies. Notably, just one of 16 monoclonal antibodies tested exhibited (slightly) altered binding to E246G, consistent with the observation that the substitution resides outside defined antigenic sites [129]. Hence it was clear that the single HA mutants were indeed escape mutants with minimal changes in antigenicity.

2.3.3 *Escape mutants acquire increased binding avidity to host glycan receptors*

It was intriguing to identify escape mutants with minimal changes in their antigenicity. This is a deviation from the popular mechanism of viral evasion of the host antibody response wherein the viral acquires mutations on its surface proteins to prevent antibody binding to its epitope. Hence the hypothesis whether the point mutations on HA increase the binding avidity of HA to host glycan receptors and hence enable evasion of the neutralizing antibody response (although the antibody can bind to these mutants) was validated.

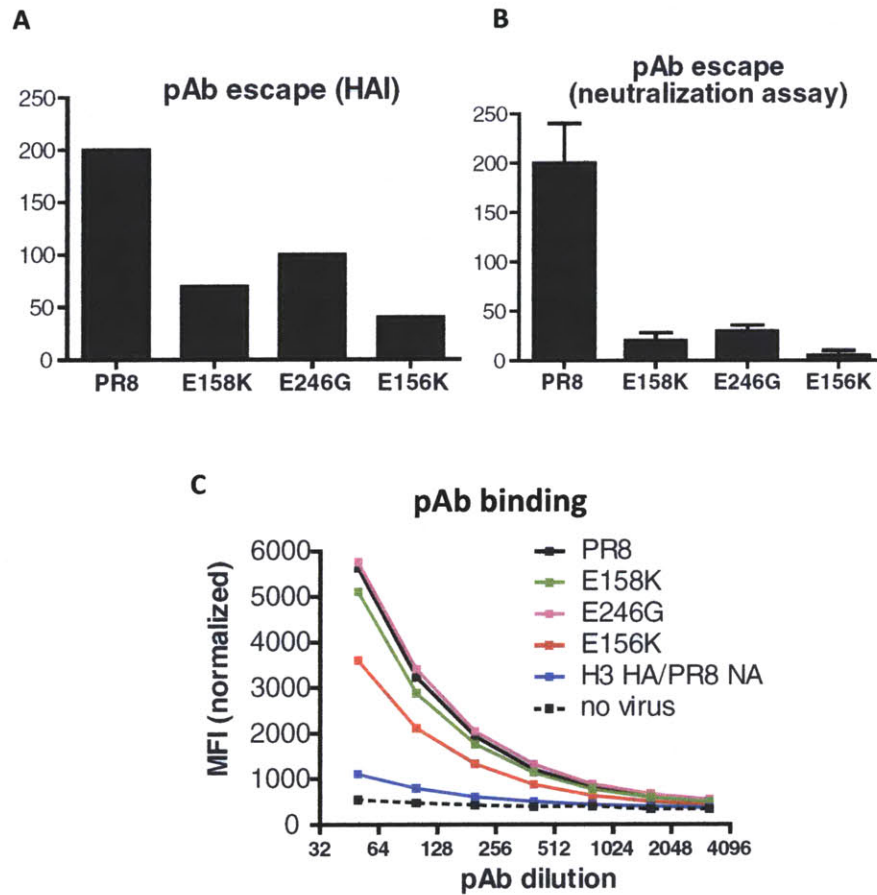


Figure 2.5 Single HA mutants escape antibody response. PR8 and mutant viruses were tested for escape from polyclonal antibodies to PR8 by (A) hemagglutination inhibition assay (HAI) with turkey RBCs or by (B) virus neutralization assays with MDCK cells. Data are expressed as inverse concentration of serum and are representative of three (HAI) or two (virus neutralization) experiments. Data are shown as mean \pm SEM (C) polyclonal antibody binding to HA was assessed by flow cytometry after addition of different dilutions of polyclonal antibody to L929 cells infected with the indicated virus followed by the addition of anti-mouse FITC. Shown is the mean fluorescent intensity (MFI) after normalizing HA expression based on the binding of a mixture of Ca monoclonal antibodies or a NA specific monoclonal antibody. Negative control used for the experiment is H3 HA/PR8 NA infected cells.

2.3.3.1 Quantitative dose-dependent glycan array analysis of mutant viruses to monitor changes in receptor binding avidity

With the advent of glycan array technology, it offers a handle to quantitatively assess the receptor binding affinity and avidity of HA using either recombinant HA or whole viruses. Glycan array platform, containing 5 different glycan motifs (Chapter 1) was used to assess the glycan binding avidities of mutant viruses and compared it with wild-type virus (**Figure 2.6**). In contrast to the wild-type virus, all the three mutants displayed increased binding avidities to both the α 2-3 and α 2-6 sialylated glycan receptors.

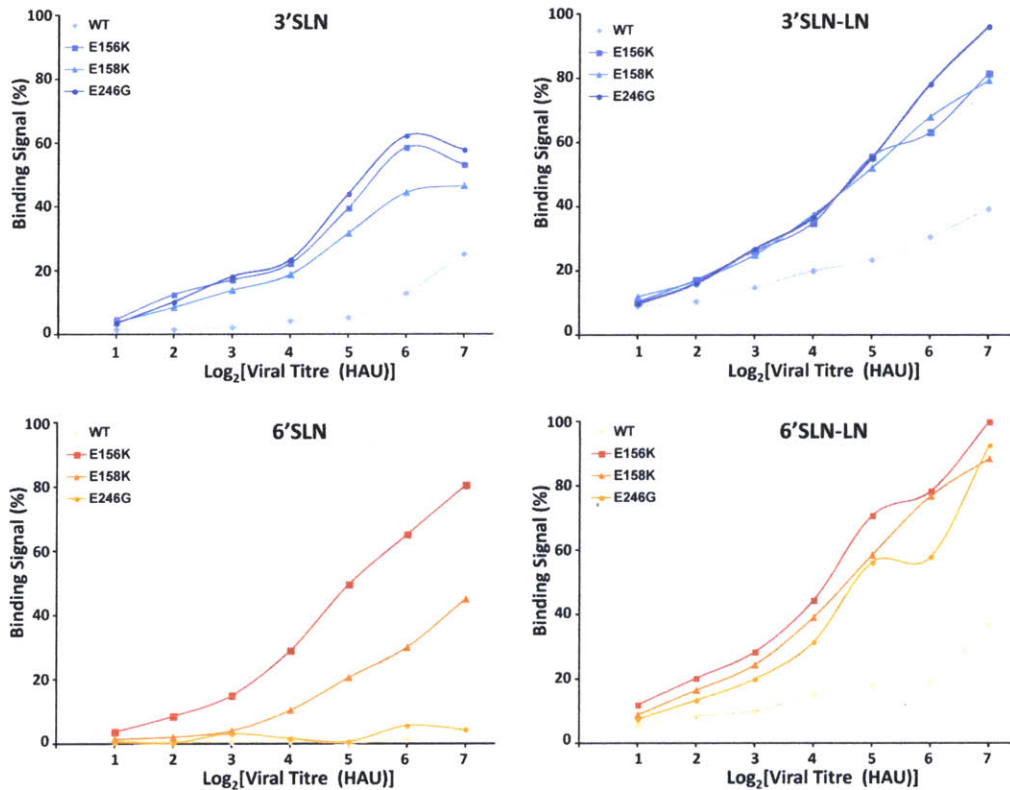


Figure 2.6 Glycan binding avidities of escape mutants. Shown are the glycan binding avidities of the three escape mutants (E156K, E158K and E246G) to the four glycan receptors (3'SLN, 3'SLN-LN, 6'SLN, and 6'SLN-LN). The binding avidities of the mutants were compared to that of the wild-type PR8 virus. Note the increased binding avidities of the mutants to the glycan receptors as compared to the wild-type virus.

2.3.4 Further passaging of mutants in immunized and non-immunized mice

Further passaging *in vivo* selected virus populations in mice (vaccinated with homologous inactivated virus e.g., E156K virus passaged in E156K-vaccinated mice), with novel amino acid substitutions distant from the receptor binding site, often distant from defined neutralizing epitopes, were detected. Substitutions that enhanced receptor binding enhanced polyclonal HAI antibody escape.

Optimizing viral fitness requires balancing host cell receptor binding of input virus with release of progeny virus. Strikingly, *in vivo* passaging of mutants in naïve mice selected mutants with reduced cellular receptor binding avidity. Mutations selected by naïve mouse passage decreased polyclonal HAI antibody escape. E158K- and E246G-derived mutants were inhibited at similar levels as *wt* PR8, demonstrating the central role of cellular receptor binding in E158K and E246G single point mutants escape from polyclonal antibodies (see also **Figure 2.5C**). E156K viruses with secondary mutations acquired in naïve mice, still escaped *wt*-specific polyclonal antibodies better than *wt* virus, despite a return to *wt* binding avidity, demonstrating that E156K alteration of Sb antigenicity contributes to immune escape.

Despite the absence of antibody selection, some secondary mutations selected in naïve mice modified HA antigenicity. A227T, located near the sialic acid-binding site, reduced binding of the Sa-specific antibody, IC5-2A7. R220G reduced binding of the Sa-specific antibody, H2-6A1. Thus, antigenic drift can be a by-product of Darwinian selection for mutations that optimize host cell receptor binding during influenza virus transmission between immune (increased receptor binding) and naïve individuals (decreased receptor binding).

To demonstrate an independent role for cellular receptor binding avidity in polyclonal antibody mediated evolution, mice were co-infected with *wt* PR8 and AM6, an absorptive mutant with a substitution (P186S) in the receptor binding site that does not modify antigenicity [123, 131]. AM6 was rapidly selected in vaccinated but not naïve mice. Next, mice were co-infected with E246G virus (minor antigenic change/high receptor binding) and E246G/A227T (greater antigenic change/low receptor binding).

Vaccinated mice selected E246G while naïve mice selected E246G/A227T, confirming the critical role of binding avidity in antibody-driven viral evolution.

To extend the drift model, E156K/R220G was passaged in mice given a high vaccine dose to generate severe antibody selection pressure. This resulted in the evolution of E156K/R220G/I244T (no selection occurred in naïve mice). I244T, located in the Sa/Ca interface, increased cellular receptor binding, and as predicted, increased polyclonal HAI antibody escape to levels exhibited by the E156K progenitor. Thus, during these passages between naïve and immune individuals, influenza A virus exhibited three cellular receptor binding avidity changes that were completely concordant with immune pressure. All of these changes were accompanied by amino acid substitutions that reduced the binding of different monoclonal antibodies.

2.4 Discussion and Significance of this study

The ramifications of this study are two-fold. *First*, this study leads to a new hypothesis for antigenic drift (**Figure 2.7**). Immune individuals select single point mutants with increased receptor binding avidity and under optimal circumstances (for the virus), diminished antigenicity. This presents with an alternate new mechanism for the emergence of escape mutants wherein influenza A virus evades neutralizing antibody response by acquiring antigenic drift mutations which increase its binding avidity to host glycan receptors. In this process there is no change in the antigenicity. The antibody can bind to the mutant HAs but because of an increased binding avidity of HA to glycan receptors than to the antibody, the virus escapes neutralization by the antibody. Substitutions modifying receptor binding cover all four antigenic sites. Several of these substitutions that enhance receptor binding, increase HA positive charge. Since virions possess ~ 900 HA monomers [132], increased positive charge may enhance cellular receptor binding by increasing charge attraction with negatively charged cell surfaces [133]. Retrospective analysis supports a relationship between H3 HA charge and receptor binding [134]. Using molecular modeling of HA with LSTc (α 2-6 glycan), the effect of these mutations at amino acid position 156, 158 and 246 on receptor binding

of HA was analyzed. Structural analysis showed that the distance between mutated amino acid side chain (at 156, 158 and 246) and the terminal sialic acid in LSTc is reduced indicating that the glycan receptor is more tightly held in the RBS of these mutant HAs (**Figure 2.8**).

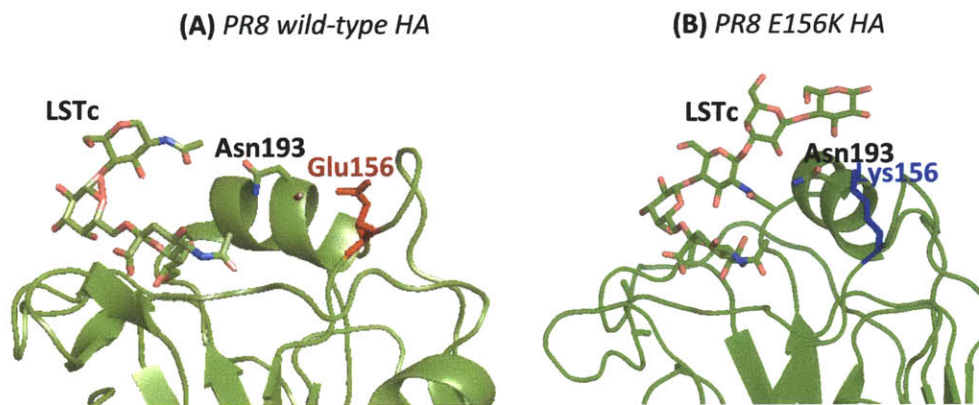


Figure 2.8 Structural modeling of wild-type and mutant (E156K) PR8 HA with LSTc. As seen from the molecular model of PR8 wt HA (A), Glu156 interacts with Asn193, which in turn interacts with the glycan receptor (LSTc). In the mutant Glu156Lys HA (B), this interaction between Lys and Asn193 is further stabilized due to the longer side chain of Lys as compared to Glu at 156. This could potentially explain the increased binding affinity of the mutant to the glycan receptors as compared to the wild-type.

Second, by our study also provides insight into the effect of passaging virus between immune and naïve population (**Figure 2.9**). Transmission to a non-immune individual leads to selection of mutants with decreased receptor binding. Since binding avidity altering-substitutions exist throughout the globular domain, they frequently modify antigenicity, even when this is not a selecting factor. Repeating the cycle, results in constant modulation of binding avidity along with steady alterations in antigenicity, even in the absence of antibody selection. Our model posits that cellular receptor binding alone exerts selection pressure for a substantial fraction of substitutions in defined antigenic regions, explaining the fixation of 30% of mutations in the globular domain outside defined antigenic regions [135].

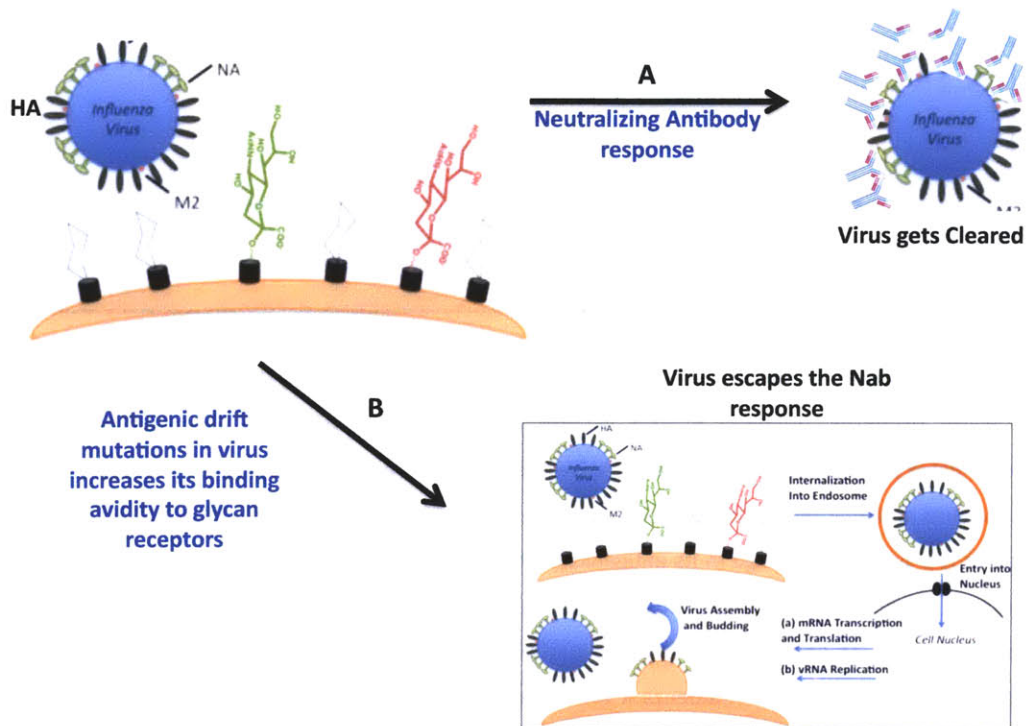


Figure 2.7 A new mechanism to evade host immune response by influenza A viruses. (a) In a naïve individual in response to a viral infection, host neutralizing antibodies (usually against HA) clears the virus. To evade this antibody response, the virus acquires antigenic drift mutations in HA, that prevents binding of the antibody to HA (b) in a immunized individual, in response to neutralizing antibody response, the virus acquires antigenic drift mutations on HA that does not change HA antigenicity but increases the binding avidity of HA to host glycan receptors. Hence even if the antibody is able to bind HA, due to an increase in the avidity effects between HA and host glycan receptors, the virus escapes antibody response and hence active infection cycle of the virus still continues.

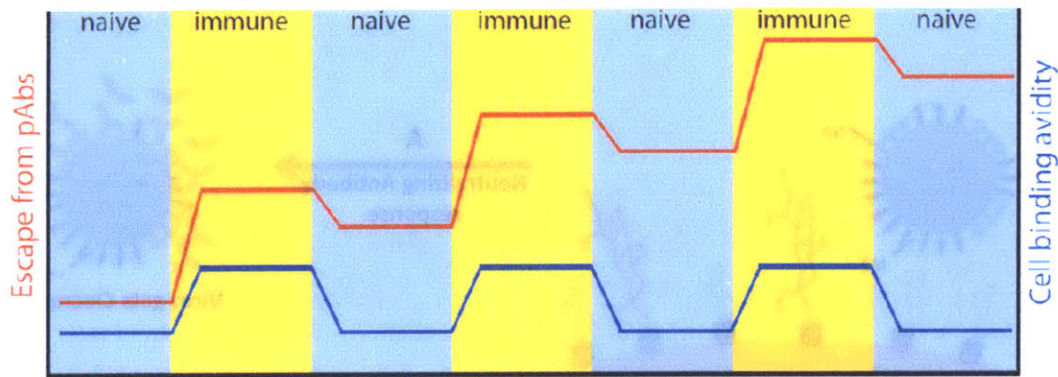


Figure 2.9 New model of antigenic drift in influenza A virus. By modulating the binding avidity of HA to host glycan receptors, influenza A virus escapes neutralizing antibody response when it transmits between naïve and immune individuals. In naïve individuals, to escape the host immune response, the virus acquires antigenic drift mutations on its HA such that there is not much change in the binding avidity but there is a significant change in its antigenicity. On the contrary, in immune individuals, to evade the neutralizing antibody response, the virus acquires mutations on its HA such that it has minimal change to the antigenicity of HA and increases its binding avidity to host glycan receptors. Hence naïve population contributes to antigenic drift in influenza A viruses and hence it is important to reduce the proportion of naïve population by vaccination.

The properties of recent human isolates are consistent with this model. A/Panama/2007/99, the 2003-2004 vaccine strain, did not match the circulating A/Fujian/411/02 strain by HAI assays. This difference was attributed to two amino acid substitutions [136]. Remarkably, one substitution is at residue 156, which in this study was identified as playing a critical dual role in Sb antigenicity/receptor binding avidity, while the other is at residue 155, which is immediately adjacent to the sialic acid binding site, and also located in the Sb site. During the antigenic evolution of H3N2 viruses from 1968 to 2003, a limited number of amino acids (in one case, a single N to K substitution increasing positive charge) dictate HAI escape from polyclonal sera [137].

This model complements recent work emphasizing the importance of HA receptor specificity in influenza virus species and organ tropism [138]. Receptor specificity and affinity are intimately related physiochemically, as demonstrated by our observation that each of the first generation absorptive mutants (E156K, E158K, E246G) demonstrates a unique avidity profile against the panel of sialylated oligosaccharides

(Figure 2.6). Thus, alterations in the viral receptor avidity, which correlates with the varied influenza virus phenotypes, can be exclusively attributed to changes in the HA-glycan receptor binding specificity. In our model, antigenic drift is accelerated by sequential passage of influenza A virus between immune and non-immune individuals, which in the human population, are nearly all children. Therefore, decreasing the naïve population size by increasing pediatric influenza A virus vaccination rates will likely retard antigenic drift and temporally extend the effectiveness of influenza vaccines. It should be noted that change in binding avidity of HA could tip-off the balance between viral binding and release from the host cell. Hence it was speculated that though the virus escapes the neutralizing antibody response in immune population, a constant increase in binding avidity may reduce viral fitness leading to a subsequent loss of the virus circulation from the human population. Hence monitoring binding avidity of circulating viral isolates may facilitate the accurate prediction of mutants with epidemic potential.

2.5 Published manuscript

Scott E. Hensley, Suman R. Das, Adam L. Bailey, Loren M. Schmidt, Heather D. Hickman, **Akila Jayaraman**, Karthik Viswanathan, Rahul Raman, Ram Sasisekharan, Jack R. Bennink, Jonathan W. Yewdell “Hemagglutinin Receptor Binding Avidity Drives Influenza A Virus Antigenic Drift” *Science* (2009); **326**; 734-736

Specific contribution made by this thesis towards this publication: One of the critical information needed for the study was to validate our hypothesis that receptor binding avidity does drive antigenic drift of influenza A viruses. Hence the single HA mutants were tested on our glycan array platform containing representative glycans of varying lengths and terminal sialic acid linkages (Section 2.3.3 and **Figure 2.6**). This provided quantitative comparison of binding avidities of mutants and wild-type PR8 viruses to various glycan motifs. This hence helped validate our hypothesis linking receptor binding avidity in driving antigenic drift. This study also provided a structural rationale for the increased receptor binding avidities observed with the mutant viruses based on understanding the local effects of the mutations at 156, 158 and 246 on the glycan binding of HA.

Chapter 3. Site-specific N-glycosylation of influenza A

HA: Implication in Glycan Receptor Binding

Summary

Influenza A HA acquire new N-glycosylation sites (by antigenic drift mutations) on its HA to evade the host neutralizing antibody response. Not much is known about the effect of these N-glycans on the glycan receptor binding properties of HA. This chapter reports our analysis of the role conserved N-glycosylation on HA and its influence on its glycan receptor binding properties. Panel of HAs were analyzed to identify conserved N-glycosylation sites on HA that could potentially impact the glycan receptor binding properties owing to their location close to the RBS of HA. One such glycosylation site on H1 HA is at the amino acid position 91. A series of deletion mutants (with the N-glycosylation sequon deleted) were generated on representative 1918 influenza A HAs: A/South Carolina/18 or SC18 (strict long α 2-6 binder), A/New York/1/18 or NY18 (mixed α 2-3/ α 2-6 binder) and A/avian/1/18 or AV18 (strict α 2-3 binder). These recombinant mutant HAs were analyzed on glycan array platform. It was noticed that there was a minimal change in the glycan receptor binding properties of mutant AV18 HA but a substantial reduction in the binding affinity of SC18 to long α 2-6 glycans. It was interesting to note that there was a complete loss of glycan binding specificity and affinity of mutant NY18 HA. Such an analysis brings into light yet another factor that can affect the receptor binding of HA and hence the pathogenicity of the virus.

3.1 Introduction

As mentioned in Chapter 1, influenza A HA play a critical role in viral entry and membrane fusion events in the viral life cycle. HA is a homotrimeric transmembrane protein with an ectodomain consisting of a globular head and a stem region (**Figure 1.7**). The globular head of HA comprises two domains: the RBD, an ~148 amino acid domain that includes the sialic acid – binding site, and the vestigial esterase domain, a smaller 75-residue region just below the RBD. Like other cellular glycoproteins, HA is synthesized on membrane-bound ribosomes and translocated into the lumen of the ER, where signal peptide cleavage and core glycosylation occur. During its intracellular transport, HA undergoes extensive posttranslational modifications, including trimerization, fatty acid acylation, trimming and processing of the N-linked glycans, and proteolytic cleavage into the disulfide-bound HA1 and HA2 subunits [139].

N-glycans are added to the asparagine amine group in the glycosylation sequon: Asn – Xaa – Ser/Thr. The amino acid sequence of the HA and hence the location of its N-linked oligosaccharides are determined by the viral genome, which is replicated by an RNA-dependent RNA polymerase encoded in the virus. This enzyme lacks editing functions so mutations in all of the viral genes occur at a high frequency. The composition and structure of the oligosaccharides put onto the HA at the various sites is determined by their position on the protein and by the array of biosynthetic and trimming enzymes provided by the cell. Thus, the plasticity of the viral genome and the host specificity of the glycosylation machinery can, together, create virus populations that are more heterogeneous in structure and function than those that would be developed by either process alone. This diversity is considered to be responsible for the survival of these viruses in a variety of biological niches.

The HA appears to have regions that must be glycosylated, others that must be free of oligosaccharides, and still others in which glycosylation may be either advantageous or detrimental to survival of the virus. Glycosylation sites at certain positions on the HA of influenza A viruses isolated from various animals and humans are highly conserved and therefore appear to be essential for the formation or maintenance

(or both) [140]. Currently isolated human H1 and H3 strains have a total of 7-9 glycosylation sites per HA subunit (21-27/trimer) as shown in **Figure 3.1**. Based on several studies, one can expect most of these sites to be glycosylated. The virus circulating in the human population are therefore largely enclosed in carbohydrate, the exact composition of which depends on the cells from which the virus has come and on constraints generated by the secondary and tertiary structure of the HA.

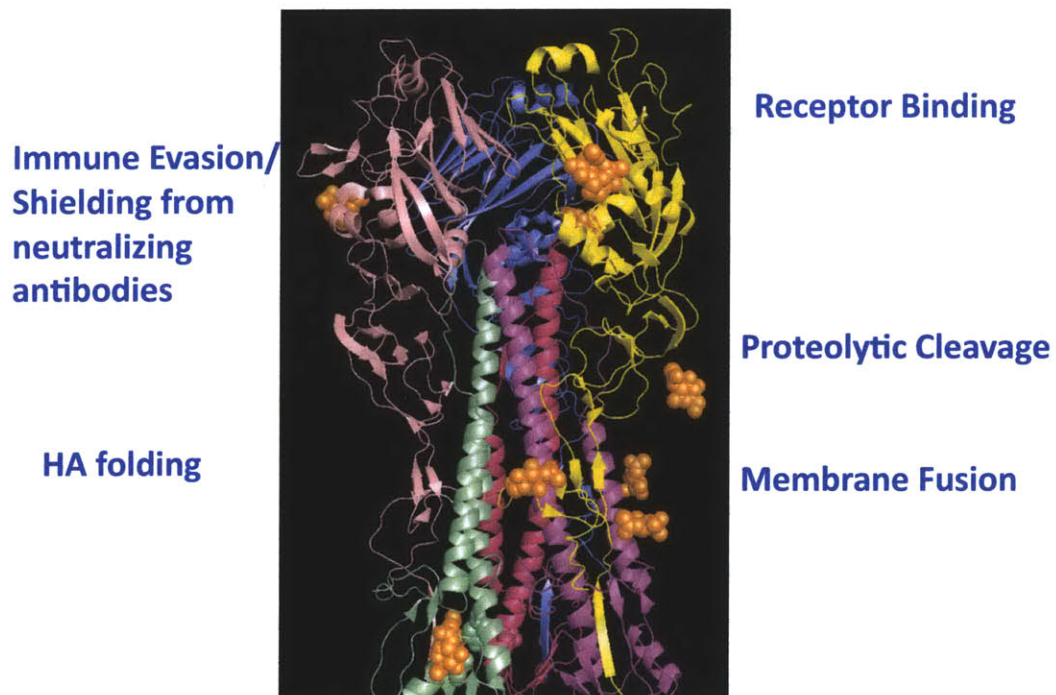


Figure 3.1 Functional roles of influenza A HA glycosylation. The glycosylation in the globular head domain are implicated in immune evasion. The ones in the stem region are implicated in membrane fusion and modulation of proteolytic cleavage of HA. The exact role of HA glycosylation in its receptor binding is not fully understood. The N-glycosylations are represented in stick and ball representation in *orange*. The HA1 and HA2 in each monomer is represented in different colors.

Among different types of influenza A viruses, there is extensive variation in the glycosylation sites of the head region, whereas the stem oligosaccharides are more conserved. The glycans in both these regions impinge on the functional properties of HA. The N-glycans in the stem region (**Figure 3.1**) maintain the HA protein in the

metastable form and are required for the fusion activity [141, 142]. Also the conserved N-glycans in the stem region are needed for replication of the virus and for the formation of replication-competent influenza A viruses [141]. Loss of these conserved N-glycans further decreased the pH stability of HA. Glycans in the globular head of HA, which are the main targets of the neutralizing antibody have emerged to interfere with the antibody recognition (**Figure 3.1**). These glycans block binding of antibodies by steric hindrance. The glycans at the conserved positions on HA have been shown to promote and stabilize a conformation compatible with the intracellular transport of HA and that they enhance trimerization and/or folding rates of HA protein [139]. Apart from being recognized by the antibodies, the glycans on the globular head also act as an important target for recognition and destruction of virus by innate immune proteins of the collectin family [143]. Loss of these glycans was shown to be associated with resistance to collectins and increased virulence in mice. Apart from the functional significance of HA glycosylation, the gross number and location of glycans on HA is known to be important for HA folding and association with calnexin and calreticulin [144].

Little is known about the effect of conserved N-glycans on the glycan receptor binding properties of HA. Effect of structure and composition of all the N-glycans on HA's activity including its structure and receptor binding was studied by Wang *et al* (2009) [145]. Wang *et al* showed that truncation of the N-glycan structures on HA had effects on glycan binding specificities and affinities of HA. But if this effect is due to the removal of a site-specific glycosylation or due to the removal of the entire N-glycan on HA remains to be elucidated. Another study has also evaluated the overall effect of host-dependent glycosylation (egg-adapted or MDCK propagated) of HA on its receptor binding properties [146]. MDCK-grown viruses were shown to bind substantially more weak than their egg-grown counterpart to the receptors of the avian origin (α 2-3 glycans). More recently, the effect of glycosylation at 158 (not conserved in all H5) of H5 HA was known to play an important role in determining the glycan receptor binding specificity of HA [147]. Wang *et al* [148] showed that truncation of the N-glycan structures on a H5N1 HA increases α 2,3 glycan receptor binding affinities, supporting

the notion that N-glycans of HA play a role in receptor binding. Moreover the loss of a specific N-glycosylation site at position 158 in some of the H5N1 clade has been associated with a potential to bind to human-like receptors [148].

Hence based on the aforementioned, this study is motivated by the need to fully understand the structure, composition and functional significance of conserved N-glycans in the globular head domain near the RBS of HA. Hence in this study, HAs from H1, H2, and H3 subtypes were analyzed to identify conserved glycosylation sites near the RBS of HA. In this study, deletion mutation analysis of the conserved N-glycosylation sequon was performed and their influence on glycan receptor-binding of HA was explored. Due to the challenges with the expression of H2, and H3 mutants, the data presented here are for three representative H1 HAs from the 1918 pandemic. The analyses presented here show that the conserved glycosylation site in H1 HA impinges on the human receptor binding and minimal avian receptor binding of HA. Studies like these could shed light on the plausible role of these conserved N-glycan sequons in determining tissue tropism and species barrier of the influenza A virus through their effects on the HA-glycan receptor interactions.

3.2 Identification of a new role for the N-glycan on the head domain HA

In this study we began our analyses by using a combination of structural modeling and alignment tools to identify conserved glycosylation sites in H1, H2 and H3 HA subtypes. The role of the identified N-glycan in the receptor binding property of HA was then biochemically validated.

3.2.1 Identification of conserved glycosylation site in H1 HA

A panel of H1 HAs (avian and human-adapted) were aligned by clustalW to identify conserved N-glycan sequon that is glycosylated (**Figure 3.2**).

```

humanA/SC/1/18          -----MEARLLVLLCAFAATNADTTCIGYHANNSTPTVDTVLEK 40
SwineA/Sw/Iowa/15/30   -----MKAILLVLLCAFAATNADTLCIGYHANNSTPTVDTVLEK 40
AvianA/Dk/Alberta/35/76 -----MEAKLFVLPCTPTVVKADTTCVGYHANNSTPTVDTVLEK 40

```

```

Aviana/Dk/NY/15024/96      QKQKGIKSTKMEAKLFLVLFCTFTVLKADTICVGYHANNSTDTVDTVLEK 50
humanA/TX/36/91           -----MKAKLLVLLCAFTATYADTICIGYHANNSTDTVDTVLEK 40
humanA/NewCaledonia/20/99 -----MKAKLLVLLCTFTATYADTICIGYHANNSTDTVDTVLEK 40
humanA/PR/8/34            -----MKANLLVLLSALAADADTICIGYHANNSTDTVDTVLEK 40
                               *:*:*:*:*:..:..:..  *:*:*:*:*:*****

humanA/SC/1/18             VTVTHSVNLLLEDHSHGKLCRLKGIAPLQLGKCNIAAGWLLGNPECDLLLTA 90
SwineA/Sw/Iowa/15/30      VTVTHSVNLLLEDHSHGKLCRLGGIAPLQLGKCNIAAGXLLGNPECDLLLTV 90
Aviana/Dk/Alberta/35/76   VTVTHSVNLLLEDHSHGKLCSLNGIAPLQLGKCNVAGWLLGNPECDLLLTA 90
Aviana/Dk/NY/15024/96     VTVTHSVNLLLEDHSHGKLCSLNGIAPLQLGKCNVAGWLLGNPECDLLLTA 100
humanA/TX/36/91           VTVTHSVNLLLEDHSHGKLCRLKGIAPLQLGNCVAGWLLGNPKCESLFSK 90
humanA/NewCaledonia/20/99 VTVTHSVNLLLEDHSHGKLCRLKGIAPLQLGNCVAGWLLGNPECELLISK 90
humanA/PR/8/34            VTVTHSVNLLLEDHSHGKLCRLKGIAPLQLGKCNIAAGWLLGNPECDPLLPV 90
                               ***** * * * * * * * * * * * * * * * * * * * * * * * * * * * * * * * *

humanA/SC/1/18             SWSYIVETSNSNGTCYPGDFIDYEELREQLSSVSSFEKFEIFPKTSSW 140
SwineA/Sw/Iowa/15/30      SWSYIVETSNSDNGTCYPGDFIDYEELREQLSSVSSFEKFEIFPKTSSW 140
Aviana/Dk/Alberta/35/76   NSWSYIETSNSNGTCYPGEFIDYEELREQLSSISSFEKFEIFPKASSW 140
Aviana/Dk/NY/15024/96     NSWSYIETSNSNGTCYPGEFIDYEELREQLSSVSSFEKFEIFPKANSW 150
humanA/TX/36/91           ESWSYIAETPNPENGTCYPGYFADYEELREQLSSVSSFERFEIFPKESSW 140
humanA/NewCaledonia/20/99 ESWSYIVETPNPENGTCYPGYFADYEELREQLSSVSSFERFEIFPKESSW 140
humanA/PR/8/34            RWSYIVETPNSENGTCYPGDFIDYEELREQLSSVSSFERFEIFPKESSW 140
                               ***** * * * * * * * * * * * * * * * * * * * * * * * * * * * * * * * *

                               130 loop
humanA/SC/1/18             PNHETTKGVTAACSYPGASSFYRNLWLTGKGSYPKLSKSYVNNKGEV 190
SwineA/Sw/Iowa/15/30      PNHETTRGVTAACPYPGASSFYRNLWLVKKENSYPKLSKSYVNNKGEV 190
Aviana/Dk/Alberta/35/76   PNHETTKGVTAACSYPGASSFYRNLWLTGKGSYPKLSKSYVNNKGEV 190
Aviana/Dk/NY/15024/96     PNHETTKGVTAACSYPGASSFYRNLWLTGKGSYPKLSKSYVNNKGEV 200
humanA/TX/36/91           PNHETTKGVTTSCSHNGKSSFYRNLWLTGKGLYPNVSKSYVNNKEV 190
humanA/NewCaledonia/20/99 PNHETVT-GVSASCSHNGKSSFYRNLWLTGKGLYPNVSKSYVNNKEV 189
humanA/PR/8/34            PNHNNTN-GVTAACSHEGKSSFYRNLWLTGEGSPKLNKSYVNNKGEV 189
                               *** .. * * * * * * * * * * * * * * * * * * * * * * * * * * * * * * * *

                               190 helix
humanA/SC/1/18             LVLWGVHHPPTGTDQSLYQONADAYVSVGSSKYNRRFTPEIARPKVRDQ 240
SwineA/Sw/Iowa/15/30      LVLWGVHHPPTSTDQSLYQONADAYVSVGSSKYDRRFTPEIARPKVRGQ 240
Aviana/Dk/Alberta/35/76   LVLWGVHHPPTVSEQSLYQONADAYVSVGSSKYNRRFPEIARPEVRGQ 240
Aviana/Dk/NY/15024/96     LVLWGVHHPPTTSEQSLYQONTDAYVSVGSSKYNRRFTPEIARPKVRGQ 250
humanA/TX/36/91           LVLWGVHHPNSIGDQRAIYHTENAYVSVVSSHYSRRFTPEIAKRPKVRDQ 240
humanA/NewCaledonia/20/99 LVLWGVHHPNIPGNQALYHTENAYVSVVSSHYSRRFTPEIAKRPKVRDQ 239
humanA/PR/8/34            LVLWGIHHPNSKEQQNIYQENAYVSVVTSNYNRRFTPEIARPKVRDQ 239
                               *****:***** .. * * * * * * * * * * * * * * * * * * * * * * * * * * * * * * * *

                               220 loop
humanA/SC/1/18             AGRMNYWTLLPEPGDTITFEATGNLIAPWYAFALNRGSGSIIITSDAPVH 290
SwineA/Sw/Iowa/15/30      AGRMNYWTLLPEPGDTITFEATGNLVAPRYAFALNRGSESIIITSDAPVH 290
Aviana/Dk/Alberta/35/76   AGRMNYWTLLDQGDITITFEATGNLIAPWYAFALNKGSDSGIITSDAPVH 290
Aviana/Dk/NY/15024/96     AGRMNYWTLLDQGDITITFEATGNLIAPWYAFALNKGSDSGIITSDAPVH 300
humanA/TX/36/91           EGRINYWTLLPEPGDTIIFEANGNLIAPWYAFALSRGFGSGIITSNAPMD 290
humanA/NewCaledonia/20/99 EGRINYWTLLPEPGDTIIFEANGNLIAPWYAFALSRGFGSGIITSNAPMD 289
humanA/PR/8/34            AGRMNYWTLLKPGDITIIFEANGNLIAPMYAFALSRGFGSGIITSNAPMH 289
                               *:*:*:*:*:..:..:..  *:*:*:*:*:*****

humanA/SC/1/18             DCNTKCQTPHGAINSSLFPQNIHPVTIGCEPKYVRSTKLRMATGLRNIPS 340
SwineA/Sw/Iowa/15/30      DCNTKCQTPHGAINSSLFPQNIHPVTIGCEPKYVSTKLRMVTGLRNIPS 340
Aviana/Dk/Alberta/35/76   NCDTRCQTPHGAINSSLFPQNVHPITIGCEPKYVSTKLRMATGLRNIPS 340
Aviana/Dk/NY/15024/96     NCDTRCQTPHGAINSSLFPQNVHPITIGCEPKYIKSTKLRMATGLRNIPS 350
humanA/TX/36/91           ECDAKCQTPQGAINSSLFPQNVHPVTIGCEPKYVRSTKLRMVTGLRNIPS 340
humanA/NewCaledonia/20/99 ECDAKCQTPQGAINSSLFPQNVHPVTIGCEPKYVRSKLRMVTGLRNIPS 339
humanA/PR/8/34            ECNTKCQTPLGAINSSLFPQNIHPVTIGCEPKYVRSKLRMVTGLRNTPS 339
                               *:*:*:*:*:..:..:..  *:*:*:*:*:*****

humanA/SC/1/18             IQSRGLFGAIAAGFIEGGWTGMIDGWYGYHHQNEQGSYAADQKSTQNAID 390
SwineA/Sw/Iowa/15/30      IQSRGLFGAIAAGFIEGGWTGLIDGWYGYHHQNGQGSYAADQKSTQNAID 390
Aviana/Dk/Alberta/35/76   IQSRGLFGAIAAGFIEGGWTGMIDGWYGYHHQNEQGSYAADQKSTQNAID 390
Aviana/Dk/NY/15024/96     IQSRGLFGAIAAGFIEGGWTGMIDGWYGYHHQNEQGSYAADQKSTQNAID 400
humanA/TX/36/91           IQSRGLFGAIAAGFIEGGWTGMIDGWYGYHHQNEQGSYAADQKSTQNAIN 390
humanA/NewCaledonia/20/99 IQSRGLFGAIAAGFIEGGWTGMVDGWYGYHHQNEQGSYAADQKSTQNAIN 389
humanA/PR/8/34            IQSRGLFGAIAAGFIEGGWTGMIDGWYGYHHQNEQGSYAADQKSTQNAIN 389
                               *****:*****:***** *****

humanA/SC/1/18             GITNKVNSVIEKMNTQFTAVGKEFNLERRIENLNKKVDDGFLDIWTYNA 440
SwineA/Sw/Iowa/15/30      GITNKVNSVIEKMNTQFTVVGKEFNLERRIENLNKKVDDGFLDVWTYNA 440
Aviana/Dk/Alberta/35/76   GITSKVNSVIEKMNTQFTAVGKEFNLERRIENLNKKVDDGFLDVWTYNA 440

```

```

AvianA/Dk/NY/15024/96      GITNKVNSVIEKMNTQFTAVGKEFNLERRIENLNKKVDDGFLDVWITYNA 450
humanA/TX/36/91           GITNKVNSVIEKMNTQFTAVGKEFNLERRMENLNKKVDDGFLDIWITYNA 440
humanA/NewCaledonia/20/99 GITNKVNSVIEKMNTQFTAVGKEFNLERRMENLNKKVDDGFLDIWITYNA 439
humanA/PR/8/34            GITNKVNTVIEKMNIQFTAVGKEFNKLEKRMENLNKKVDDGFLDIWITYNA 439
***.***:***** ***.*****:*.*:*:*****:*****:*****

humanA/SC/1/18            ELLVLEENERTLDFHDSNVRNLYEKVKSQLKNNAKEIGNGCFEFYHKCDD 490
SwineA/Sw/Iowa/15/30     EMLVLEENERTLDFHDSNVKNLYEKARSQLRNNAKEIGNGCFEFYHKCDD 490
AvianA/Dk/Alberta/35/76  ELLVLEENERTLDFHDSNVRNLYEKVKSQLRNNAKEIGNGCFEFYHKCDD 490
AvianA/Dk/NY/15024/96   ELLVLEENERTLDFHDSNVRILYEVKRSQLRNNAKELGNGCFEFYHKCDD 500
humanA/TX/36/91         ELLVLEENERTLDFHDSNVKNLYEKVKSQLKNNAKEIGNGCFEFYHKCDD 490
humanA/NewCaledonia/20/99 ELLVLEENERTLDFHDSNVKNLYEKVKSQLKNNAKEIGNGCFEFYHKCDD 489
humanA/PR/8/34          ELLVLEENERTLDFHDSNVKNLYEKVKSQLKNNAKEIGNGCFEFYHKCDD 489
*:***** *****: *****:***:*****:*****:*****:

humanA/SC/1/18            ACMESVRNGTYDYPKYSEESKLNREEIDGVKLESMGVYQILAIYSTVASS 540
SwineA/Sw/Iowa/15/30     ACMESVRNGTYDYPKYSEESKLNREEIDGVKLESMVMVYQILAIYSTVASS 540
AvianA/Dk/Alberta/35/76  ECMESVKNGTYPKYSEESKLNREEIDGVKLESMGVYQILAIYSTVASS 540
AvianA/Dk/NY/15024/96   ECMESVKNGTYPKYSEESKLNREEIDGVKLESMGVYQILAIYSTVASS 550
humanA/TX/36/91         ECMESVKNGTYPKYSEESKLNREKIDGVKLESMGVYQILAIYSTVASS 540
humanA/NewCaledonia/20/99 ECMESVKNGTYPKYSEESKLNREKIDGVKLESMGVYQILAIYSTVASS 539
humanA/PR/8/34          ECMESVRNGTYDYPKYSEESKLNREKIDGVKLESMGIYQILAIYSTVASS 539
*****:***** ***** :***** :***** *****

humanA/SC/1/18            LVLLVSLGAI SFWMC SNGSLQCRICI----- 566
SwineA/Sw/Iowa/15/30     LVLLVSLGAI SFWMC SNGSLQCRICI----- 566
AvianA/Dk/Alberta/35/76  LVLLVSWGAI SFWMC SNGSLQCRICI----- 566
AvianA/Dk/NY/15024/96   LVLLVSLGAI SFWMC SNGSLQCRICI-SLNFKMYGKTPFL 590
humanA/TX/36/91         LVLLVSLGAI SFWMC SNGSLQCRICI----- 566
humanA/NewCaledonia/20/99 LVLLVSLGAI SFWMC SNGSLQCRICI----- 565
humanA/PR/8/34          LVLLVSLGAI SFWMC SNGSLQCRICI----- 565
***** *****

```

Figure 3.2 H1 HA ClustalW alignment. The N-glycosylation sites are marked **green**. The N-glycosylation site possibly involved in interaction with the receptor is marked **red**. The receptor binding subdomains are marked grey. Conserved N-glycosylation sequons in the stem region are marked **pink**.

The conserved N-glycosylation sequons in the stem region were identified by aligning the HA sequences (**Figure 3.2**). The N-glycans in these conserved sequons are known to play an important role in the membrane fusion activity of HA (Section 1.4.2). The sequence alignment also revealed that the seasonal strains are heavily glycosylated on the top of the HA head unlike the pandemic strains which are not glycosylated at this region. Most of the seasonal strains have acquired multiple glycosylation sequons in the head region to evade the host neutralizing response as shown in **Table 3.1** [149].

Based on this analysis N-glycan sequon NGT at position 91-93, in the side of the head domain, was hypothesized to affect the receptor binding property of H1 HAs (**Figure 3.3**). A/PR/8/34 or PR8 is different as it lacks this N-glycan sequon at 91. Most of the H1 seasonal strains from 1933 till 1939 lacked this N-glycosylation sequon and later the sequon re-emerged after 1939. This glycosylation sequon however has been conserved in other seasonal and pandemic strains [149] as shown in **Table 3.1**.

Time period	Stem		Side of head		Top of head			Side of head		Stem	
1918	28	40		104					304	498	557
1933	28		73		142 [†]		179 ^{**}	286	304	498	557
1934-1939	28	40				144 ^{**}		286	304	498	557
1940-1948	28	40		104	144 [†]		179 [†]	286	304	498	557
1949-1957	28	40		90	104	144 [†]	172 [†] 177 [†]	286	304	498	557
1977-1985	28	40		104		144 [†]	177 [†]	286	304	498	557
1986-2008	28	40	71	104	142 [†]		177 [†]	286	304	498	557
2009-present	28	40		104					304	498	557

*Glycosylations on the top of the head.

†Glycosylations predicted in >30% of HA sequences.

Table 3.1 Evolution of H1N1 glycosylations. The conserved glycosylation at 104 (SC18 numbering) represent the N91, which was analyzed in the study. This site was lost in seasonal strains circulating between 1933-1939 but re-emerged after this period. The glycans in the top of the head and in the stem region are implicated in immune evasion and membrane fusion respectively.

The table was adapted from Wei *et al* (2010).

Based on the structural modeling of a representative H1 HA (A/South Carolina/1/18 or SC18), it was hypothesized that N-glycan at 91aa could potentially stabilize the 220-loop (one of the 5 loops involved in glycan binding as explained in chapter 5) that in turn would enable glycan receptor binding by HA. In order to validate this hypothesis, a single mutant lacking the N-glycan sequon at 91 in the representative H1N1 SC18 HA (a strict long α 2-6 binder) was recombinantly expressed. To further understand the role of this sequon in receptor binding, the mutants were also generated in the avian HA (AV18) (Asp190Glu/Asp225Gly mutant of SC18 and a strict α 2-3 binder) and in NY18 (Asp225Gly mutant of SC18 and a mixed α 2-3/ α 2-6 binder). These mutants were recombinantly expressed and biochemically analyzed to elucidate the effect of N-glycan at position 91 in α 2-3 and/or α 2-6 glycan receptor binding of HA.

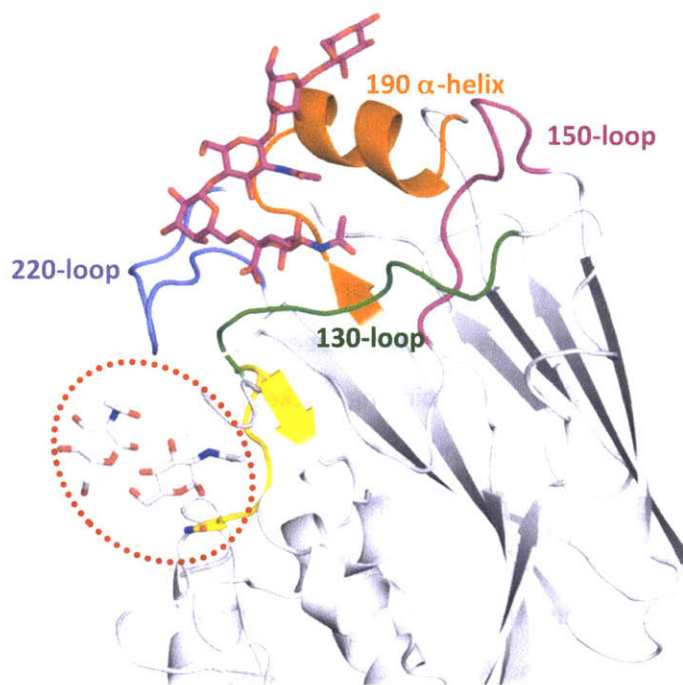


Figure 3.3 Structure of 1918-Human H1 HA. The figure shows the loops and helix in the receptor-binding site of HA. The critical N-glycosylation site on the NGT sequence is shown as red dotted circle. As seen in the figure the N-glycosylation at the NGT site (91-93 amino acids) may play an important role in the 220-loop (shown in blue) stabilization.

Only the HA monomer is shown in the figure.

3.2.2 Effect of removal of N-glycan at 91 on the receptor binding property of H1 HA

Addition of N-glycan at amino acid position 91 (Asn) was disrupted by introducing Thr93Ala point mutation by site-directed mutagenesis. This disrupted the sequon from NGT to NGA, thus preventing glycosylation at this site. The mutant HAs were recombinantly expressed in insect cells. The glycan binding specificity and affinity of the mutant HAs were characterized by performing a dose-dependent glycan array analysis. The data obtained was compared with that of their wild-type HA counterpart.

Glycan array analysis of AV18T93A mutant HA indicated no change in its glycan binding specificity and affinity. Similar to the wild-type HA, AV18T93A showed strict binding preference to α 2-3 glycans with minimal to no binding to α 2-6 glycans. This

shows that the loss of N-glycan at 91 had no effect on the binding of avian glycan receptor binding of HA (**Figure 3.4A**). Arg224 in the 220 loop makes ionic interactions with the GlcNAc in the N-glycan at N91 (**Figure 3.4B**). This interaction is important for stabilization of the 220-loop. Hence it can be assumed that knocking the glycosylation could destabilize the 220-loop leading to the loss of glycan receptor binding by AV18 HA. But a closer examination of the receptor-binding site (RBS) of AV18 indicates that the binding pocket is tighter due to the presence of Gln226 and Glu190 (**Figure 3.4B**). Moreover the interaction of the binding pocket in AV18 HA is only with the first two sugars in the reducing end (terminal sialic acid and penultimate galactose). Hence no change in the glycan receptor binding affinity and specificity of AV18T93A can be explained by the “tightness” of the receptor-binding pocket of AV18 HA.

On the other hand the RBS of SC18 HA is more open (**Figure 3.5B**). This is due to the presence of Asp190 and Asp225 (compared to avian), which makes critical contacts with the human receptor. The short chain length at 190 (Asp instead of Glu) contributes to the “openness” of the binding pocket. Hence it was predicted that the destabilization of the 220-loop due to the loss of glycan at N91 (GlcNAc in N-glycan makes contact with Arg224 in the 220-loop) would have more pronounced effect on the receptor binding property of SC18 HA. Consistent with the predictions, there was a significant reduction in the binding affinity of SC18T93A (**fold reduction to mention**) when compared to that of the wild-type SC18 HA (**Figure 3.5A**). There was no change in the binding specificity of SC18 T93A (binding was seen only to 6'SLNLN).

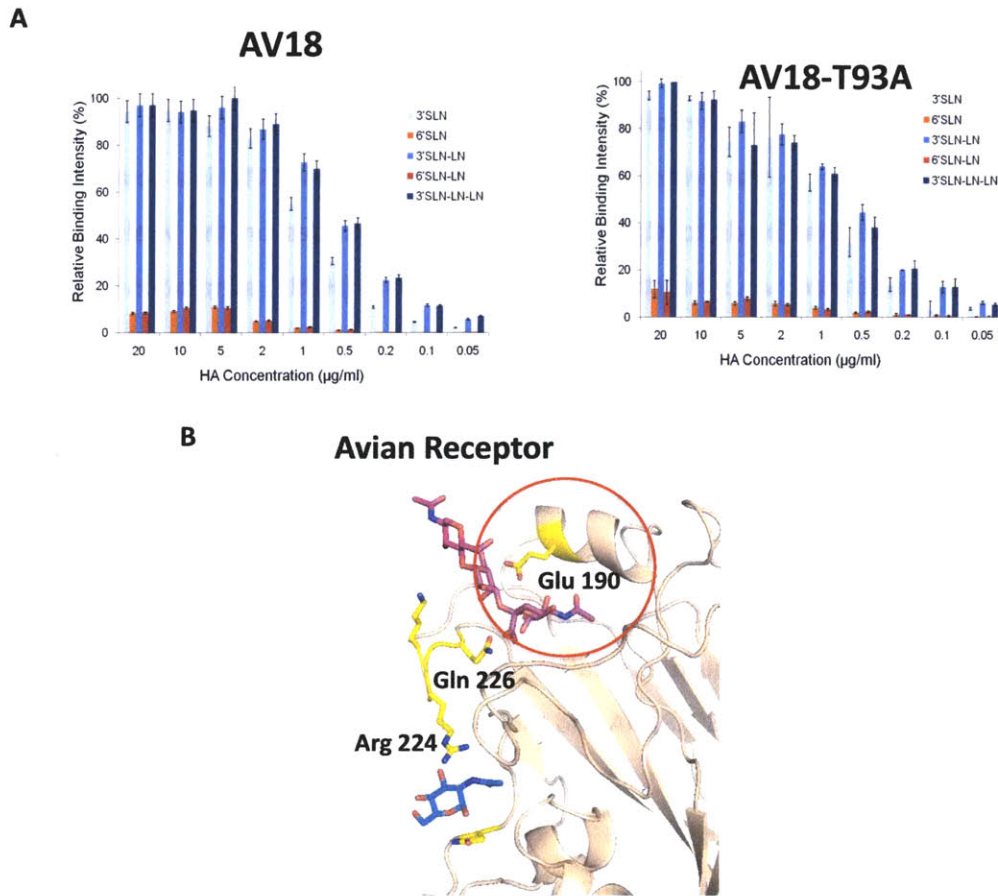


Figure 3.4 Effect of T93A mutation on AV18 receptor binding. Recombinant AV18 T93A HA was analyzed on glycan array platform and its binding property was compared to that of the wild-type AV18 (A). There was no change in the receptor binding property of AV18 T93A. This can be explained on the basis of the receptor-binding pocket of AV18 HA (B). Arg224 in the 220-loop interact with GlcNAc of N-glycan at 91. Destabilization of 220-loop due to loss of N-glycan at 91 has minimal effect of receptor binding property of AV18 T93A due to the tightness of the binding pocket conferred by Glu 190 and Gln 226.

In case of NY18 T93A HA, it was interesting to see that there was a complete loss of glycan receptor binding specificity and affinity as compared to that of NY18 wild-type HA, a mixed α 2-3/ α 2-6 binder (**Figure 3.6A**). This can be structurally explained on the basis of its RBS, which is between an avian (e.g. AV18) and a human (e.g. SC18) influenza A viruses (**Figure 3.6B**). Arg224 makes critical contacts with GlcNAc of the N-glycan at

91. In the absence of 225Asp, the de-stabilization of the 220-loop due to the loss of N-glycan at 91, has even more of a pronounced effect than that of SC18 T93A HA.

Loss of N-glycan is physiologically relevant given the emergence of Asn91Asp mutants in response to cyanovirin resistance [150]. Cyanovirin (CVN) is a small peptide (101 amino acid) that binds to high-mannose oligosaccharides on the viral HA (HA1) subunit and neutralizes virus infectivity [151]. During virus (H1N1) adaptation to mice in the absence of CVN treatment, the virus becomes resistant to CVN (CVN-MR) as did the virus passaged in cell culture in the presence of CVN (CVN-R) [150]. The CVN-R viruses possess a single amino acid mutation Asn91Asp of HA1 leading to the abrogation of the N-glycan sequon at 91-93. CVN-MR viruses on the other hand are double mutants possessing either Asp225Gly/Asn91Asp or Asp225Gly/Asn63Ser. Moreover the double mutant was lethal and highly pathogenic in mice. Hence given the significance of Asn91, in CVN resistance and in mouse adaptation, Asn91Asp mutagenesis was carried out in NY18 (Asp225Gly mutant of SC18) HA and the recombinant HA was characterized for its glycan receptor binding property using the dose-dependent glycan array analysis. NY18 N91D mutant showed a complete loss of glycan binding specificity and affinity (**Figure 3.7**). This promiscuous receptor binding of the mutant perhaps would have contributed to lethality in mice similar to the Asp225Gly mutant of A/California/04/09 (Chapter 4).

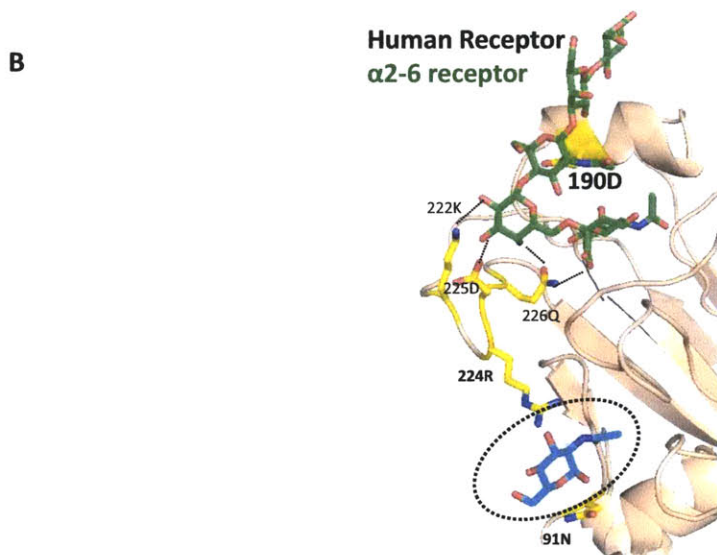
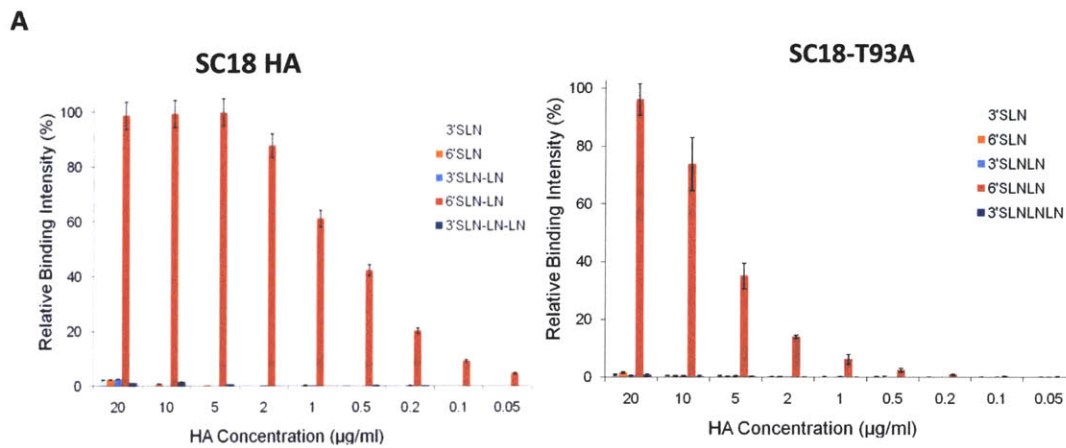


Figure 3.5 Effect of T93A mutation on SC18 receptor binding. Recombinant SC18 T93A HA was analyzed on glycan array platform and its binding property was compared to that of the wild-type SC18 (**A**). There was significant reduction in the binding affinity to 6'SLNLN as compared to the wild-type SC18. There was no change in the receptor-binding specificity of SC18 T93A. This can be explained on the basis of the receptor-binding pocket of SC18 HA (**B**). Arg224 in the 220-loop interact with GlcNAc of N-glycan at 91. Destabilization of 220-loop due to loss of N-glycan at 91 has a significant effect in the receptor binding affinity of SC18 T93A due to the “open-ness” of the binding pocket conferred by Asp 190 unlike AV18, which has Glu 190.

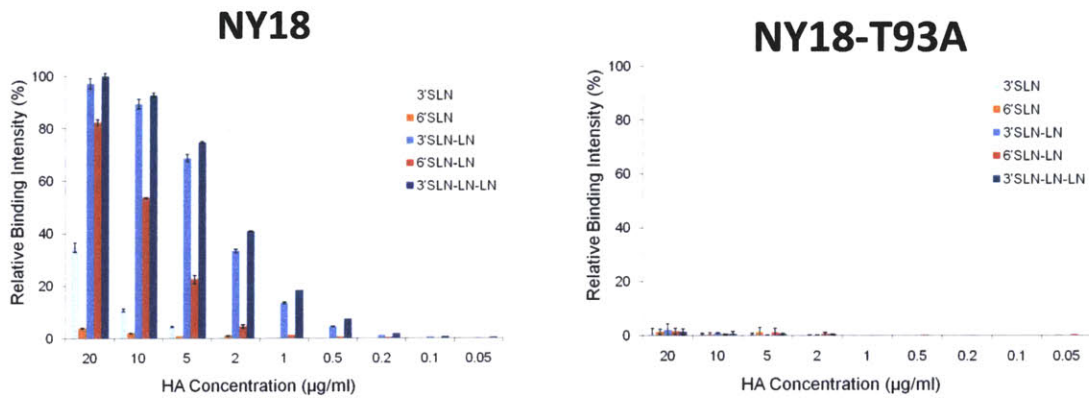
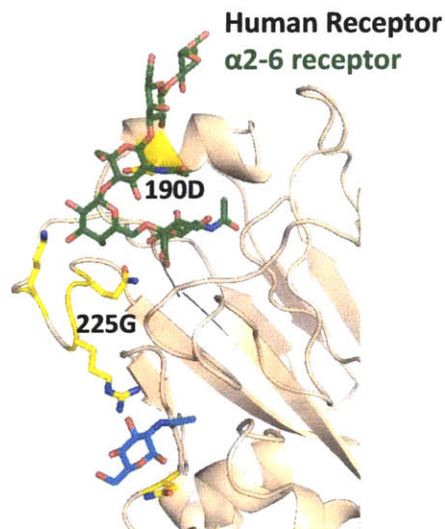
A**B**

Figure 3.6 Effect of T93A mutation on NY18 receptor binding. Recombinant NY18 T93A HA was analyzed on glycan array platform and its binding property was compared to that of the wild-type NY18 (**A**). There was a complete loss of receptor binding affinity and specificity of NY18 T93A as compared to the wild-type NY18. This can be explained on the basis of the receptor-binding pocket of NY18 HA (**B**). Arg224 in the 220-loop interact with GlcNAc of N-glycan at 91. Destabilization of 220-loop due to loss of N-glycan at 91 has a significant effect in the receptor binding affinity of NY18 T93A due to the binding pocket being between an avian and human HAs due to the presence of Asp225Gly and Glu190Asp.

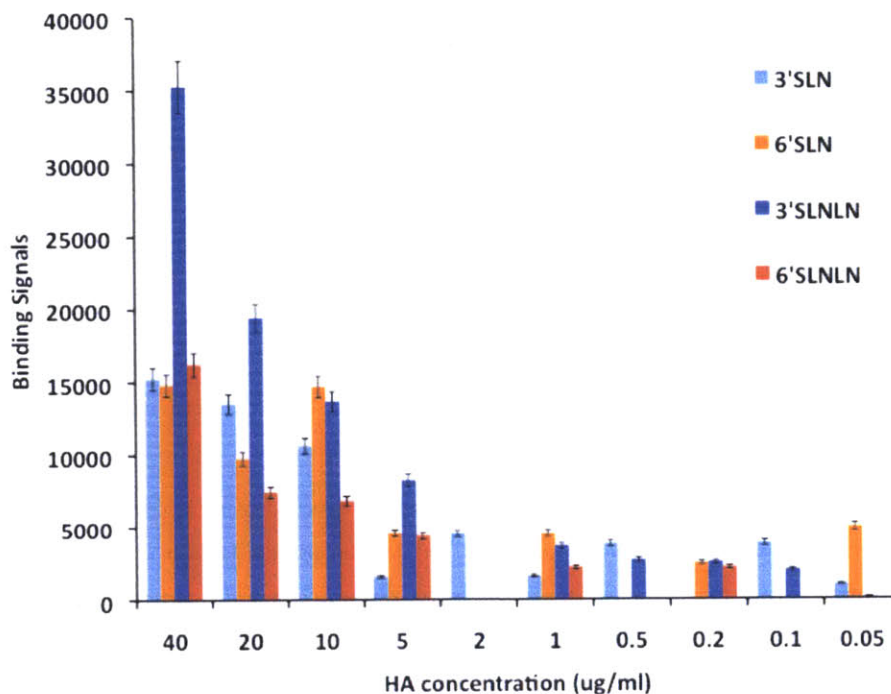


Figure 3.7 Effect of N91D mutation on AV18 receptor binding. Recombinant NY18 N91D HA was analyzed on glycan array platform. There was a complete loss of receptor binding affinity and specificity of NY18 N91D as compared to the wild-type NY18 (**Figure 3.16A**). The loss of receptor binding combined with a promiscuous binding by NY18N91D could have accounted for lethality in mouse similar to the D225G mutants of 2009 H1N1 pandemic virus (Chapter 4). The binding signals presented in the figure are the actual (and not the relative) binding signals to indicate the low non-specific binding of the HA (close to the background).

3.2.3 Circular dichroism analysis of T93A mutant H1 HAs

N-glycosylation is known to play an important role in folding and maintaining the 3-dimensional structural stability of proteins. In order to make sure that knocking-out of the glycosylation at position 91 did not affect the 3-dimensional structure of the protein, circular dichroism (CD) analysis of the T93A mutant proteins was performed. The spectra generated for the mutant proteins were compared with that of the wild-type HAs. The CD spectra of all the mutant proteins were generated between 190nm and 280nm to identify changes in the secondary structure of protein if any. All the

mutants had identical secondary structure as that of their wild-type counterparts as indicated by their CD spectra (**Figure 3.8**).

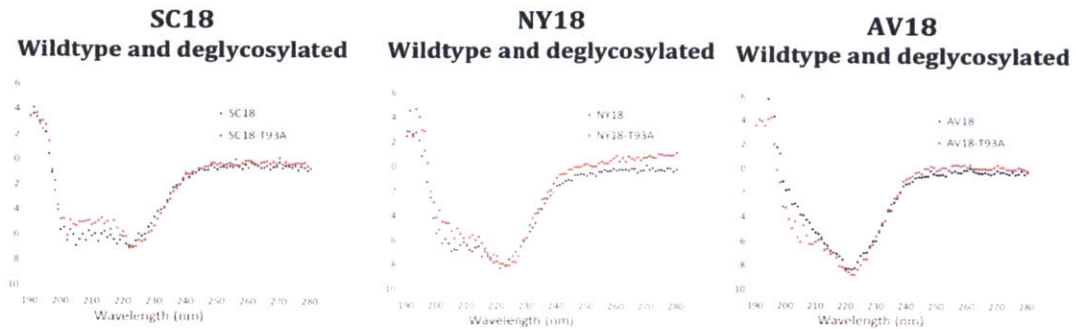


Figure 3.8 Circular Dichroism analysis of wild-type and mutant HAs. CD spectra were obtained between 190 and 280nm. The wild type (shown in *color*) and the mutant protein (shown in *color*) have similar secondary structure indicating that the de-glycosylation did not affect the structure of the mutant protein.

3.2.4 Glycosylation analysis of H2 and H3 HAs

H3 HAs have acquired several N-glycan sequon in the globular head domain by antigenic drift mutations [152]. H2 on the other hand was lost from circulation in human population and now currently circulates in birds. Hence there is not much change in the N-glycosylation sequon in H2 HA [152]. In the course of viral evolution, some of the N-glycan sequons were conserved.

Similar to the glycosylation analysis for H1 HA, identification of conserved N-glycans was performed for H2 and H3 HAs. HA sequences from representative influenza A viruses of H2 and H3 subtypes were aligned by ClustalW (**Figure 3.9 and 3.10**). In both H2 (Asn169) and H3 (Asn165), the glycosylation in one monomer influences glycan receptor binding of the adjacent monomer in HA trimer (**Figure 3.11**). In H2 HA the glycosylation site is in the interface of trimerization. Hence expression of a representative mutant H2 HA; A/Alb/6/58 or Alb58 lacking this conserved glycosylation site, Alb58 T171A was challenging as trimerization of HA was affected though HA monomers were seen to be expressed. Hence it was concluded that apart from our speculated role of the glycosylation site at Asn169 in receptor binding property of H2

HA, it also plays an important role in maintaining the structural integrity of trimeric H2 HA.

Molecular dynamic simulations to understand HA-glycan interaction in a representative H3 HA have shown that the N-glycan at Asn165 in one monomer directly with the sialic acid receptor bound by the adjacent monomer [153]. This correlated with our molecular modeling analysis of a representative H3 HA, A/Aichi/68 (**Figure 3.11**). This is in contrast to H1 HAs, where the N-glycan at 91 interacts with the 220-loop (within the same monomer), which in turn interacts with the glycan receptor (Section 3.2.2). Previously Srinivasan *et al* and Tumpey *et al* showed biochemically that mutating residues in the 220-loop affects receptor-binding affinity of HA and hence its transmissibility in ferrets [67, 110]. Given the importance of 220-loop in the receptor binding property of HA, in this study in H1 HA (in contrast to H2 and H3 HAs), one of the other factors that could impinge on the stability of this 220-loop was identified. Moreover the challenges associated with the expression of mutant H2 and H3 HAs further prompted the analysis of H1 HAs and the role of its conserved N-glycan in its receptor binding property.

```

humanA/Albany/57      MAIIYLILLFTAVRGDQICIGYHANS165TEKVDTILERNV166IVTHAMDILEKTHNGKLC167 60
humanA/Ann            MAIIYLILLFTAVRGDQICIGYHANS165TEKVDTILERNV166IVTHAKDILEKTHNGKLC167 60
humanA/E1             MAIIYLILLFTAVRGDQICIGYHANS165TEKVDTILERNV166IVTHAKDILEKTHNGKLC167 60
A/Albany/6/58        MAIIYLILLFTAVRGDQICIGYHANS165TEKVDTILERNV166IVTHAKDILEKTHNGKLC167 60
Aviana/Ck/PA/04      MAIIYLILLFTAVRGDQICIGYHS165TEKVDTILERNV166IVTHAQDILEKTHNGKLC167 60
*****:*****:*****:*****:*****:*****:*****:*****:*****

humanA/Albany/57      GIPPLELGDCSIAGWLLGNPECDRLLSVPEWSYIMEKENPRDGLCYPGSFNDYEELK118 120
humanA/Ann            GIPPLELGDCSIAGWLLGNPECDRLLSVPEWSYIMEKENPRNGLCYPGNFNDYEELK118 120
humanA/E1             GIPPLELGDCSIAGWLLGNPECDRLLSVPEWSYIMEKENPRDGLCYPGSFNDYEELK118 120
A/Albany/6/58        GIPPLELGDCSIAGWLLGNPECDRLLSVPEWSYIMEKENPRDGLCYPGSFNDYEELK118 120
Aviana/Ck/PA/04      GIPPLELGDCSIAGWLLGNPECDRL118LVPEWSYIIEKENPRNGLCYPGSFN119YEELK120 120
*****:*****:*****:*****:*****:*****:*****:*****

                                130 loop
humanA/Albany/57      SSVKHF130EKVKILPKDRW131TQHTTTGGS132RACAVSG133NP134SFFRN135MVWLTEKGS136NPVAKGS137Y138 180
humanA/Ann            SSVKHF130EKVKILPKDRW131TQHTTTGGS132QACAVSG133NP134SFFRN135MVWLTEKES136NPVAKGS137Y138 180
humanA/E1             SSVKHF130EKVKILPKDRW131TQHTTTGGS132RACAVSG133NP134SFFRN135MVWLTEKGS136NPVAKGS137Y138 180
A/Albany/6/58        SSVKHF130EKVKILPKDRW131TQHTTTGGS132RACAVSG133NP134SFFRN135MVWLTKKGS136NPVAKGS137Y138 180
Aviana/Ck/PA/04      SSVRH130FEKVKILARNR131W132TQHTTPGGS133QACAIYGG134PSFFRN135MVWLTKKGS136NPV137ARG138SY139 180
***:*****:*****:*****:*****:*****:*****:*****

                                183      190 helix      220 loop
humanA/Albany/57      TS183GEQMLIIWGV184HP185IDETE186QRTLY187QNVGTYVSVGT188STLNKRSTPEIAT189RPKV190NGLGGR191M 240
humanA/Ann            TS183GEQMLIIWGV184HP185IDETE186QRTLY187QNVGTYVSVGT188STLNKRSTPEIAT189RPKV190NGLGSR191M 240
humanA/E1             TS183GEQMLIIWGV184HP185NDETE186QRTLY187QNVGTYVSVGT188STLNKRSTPEIAT189RPKV190NQGGR191M 240
A/Albany/6/58        TS183GEQMLIIWGV184HP185NDETE186QRTLY187QNVGTYVSVGT188STLNKRSTPDIAT189RPKV190NGLGSR191M 240
Aviana/Ck/PA/04      TS183GEQMLIIWGI184HP185NDETE186Q187RALY188QNVGTYVSVGT189SKLNKR190SVEIAT191RPKV192NQGGR193M 240
*****:*****:*****:*****:*****:*****:*****:*****

```

```

humanA/Albany/57      EFSWTLDMWDTINFESTGNLIAPEYGFKISKRGSSGIMKTEGTLENCETKCQTPLGAIK 300
humanA/Ann            EFSWTLDMWDTITFESTGNLIAPEYGFKISKRGSSGIMKTEGTLENCETKCQTPLGAI 300
humanA/EI            EFSWTLDMWDTINFESTGYLIAPEYGFKISKRGSSGIMKTEGTLENCETKCQTPLGAI 300
A/Albany/6/58       EFSWTLDMWDTINFESTGNLIAPEYGFKISKRGSSGIMKTEGTLENCETKCQTPLGAI 300
AvianA/Ck/PA/04     EFSWTLDMWDTINFESTGNLIAPEYGFKISKRGSSGIMKTEGTLENCETKCQTPLGAI 300
*****:*** **_.***** *****:*** *****:
humanA/Albany/57      TLLPFHNVHPLTIGECPKYVKSEKLVLATGLRNVQIES----- 339
humanA/Ann            TLLPFHNVHPLTIGECPKYVKSEKLVLATGLRNVQIES----- 339
humanA/EI            TLLPFHNVHPLTIGECPKYVKSEKLVLATGLRNVQIES----- 339
A/Albany/6/58       TLLPFHNVHPLTIGECPKYVKSEKLVLATGLRNVQIESRGLFGAIAGFIEGGWQGMVDG 360
AvianA/Ck/PA/04     TLLPFHNIHPLTIGECPKYVKSKRLVLATGLRNVQIESRGLFGAIAGFIEGGWQGMVDG 360
*****:*****:*****:*****:
humanA/Albany/57      -----
humanA/Ann            -----
humanA/EI            -----
A/Albany/6/58       WYGYHHSNDQSGSYAADKESTQKAFDGITNRVNSVIEKMNTQFEAVGKEFSNLERLENL 420
AvianA/Ck/PA/04     WYGYHHSNDQSGSYAADKESTQKADIGIINKVNSVIEKMNTQFEAVGKEFNNLEKLENL 420
humanA/Albany/57      -----
humanA/Ann            -----
humanA/EI            -----
A/Albany/6/58       NKKMEDGFLDVWVTYNAELLVLMENERTLDFHDSNVKNLYDKVKMQLRDNVKELGNGCFEF 480
AvianA/Ck/PA/04     NKKMEDGFLDVWVTYNAELLVLMENERTLDFHDSNVKNLYDKVVMQLRDNVKELGNGCFEF 480
humanA/Albany/57      -----
humanA/Ann            -----
humanA/EI            -----
A/Albany/6/58       YPKCDECMNSVKNGTYDYPKYEEESKLNREIKGVKLSMGMVYQILAIYATVAGSLSLA 540
AvianA/Ck/PA/04     YHKCDECMNSVKNGTYDYPKYEEESKLNREIKGVKLSMGMVYQILAIYATVAGSLSLA 540
humanA/Albany/57      -----
humanA/Ann            -----
humanA/EI            -----
A/Albany/6/58       IMMAGISFWMCSNGSLQCRICI 562
AvianA/Ck/PA/04     IMIAGIFLWMCSNGSLQCRICI 562

```

Figure 3.9 H2 HA ClustalW alignment. The N-glycosylation sites are marked green. The N-glycosylation site possibly involved in interaction with the receptor is marked red. The receptor binding subdomains are marked grey.

```

HumanA/Moscow/10/99    MKTIIALSIIICLVFAQKLPNDNSTATLCLGHHAVPNGILVKTTITNDQI 50
HumanA/Wyoming/3/03   MKTIIALSIIICLVFVSQKLPNDNSTATLCLGHHAVPNGIIVKTTITNDQI 50
HumanA/Phillipines/2/82 MKTIIALSIIICLVFAQNLPGNDNSTATLCLGHHAVPNGILVKTTITNDQI 50
HumanA/Aichi/2/68     MKTIIALSIIICLVFALGQDLPNDNSTATLCLGHHAVPNGILVKTTITDDQI 50
AvianA/Dk/Ukraine/63  MKTVIALSIIICLVTFGQDLPNDNSTATLCLGHHAVPNGIIVKTTITDDQI 50
*****:*** **_.***** *****:*** *****:
HumanA/Moscow/10/99    EVTNAIELVQSSSTGRICDSPHQILDGENCTLIDALLGDPHCDGPFQNKWE 100
HumanA/Wyoming/3/03   EVTNAIELVQSSSTGGICDSPHQILDGENCTLIDALLGDPQCDGPFQNKWK 100
HumanA/Phillipines/2/82 EVTNAIELVQSSSTGRICDSPHRILDGKCTLIDALLGDPHCDGPFQNEKW 100
HumanA/Aichi/2/68     EVTNAIELVQSSSTGKICNNPHRILDGIDCTLIDALLGDPHCDVFPQNETW 100
AvianA/Dk/Ukraine/63  EVTNAIELVQSSSTGKICNNPHRILDGRAC TLIDALLGDPHCDVFPQNETW 100
*****:*** **_.***** *****:*** *****:
                                130 loop
HumanA/Moscow/10/99    DLFVERSKAYSNCYPYDVPDYASLRSLVASSGTLEFNNEFNWGVAVQNG 150
HumanA/Wyoming/3/03   DLFVERSKAYSNCYPYDVPDYASLRSLVASSGTLEFNNEFNWAGVTQNG 150
HumanA/Phillipines/2/82 DLFVERSKAFSNCYPYDVPDYASLRSLVASSGTLEF INEGFNWGVTVQSG 150
HumanA/Aichi/2/68     DLFVERSKAFSNCYPYDVPDYASLRSLVASSGTLEFITEGFTTWTGVTQNG 150
AvianA/Dk/Ukraine/63  DLFVERSNAFSNCYPYDIPDYASLRSLVASSGTLEFITEGFTTWTGVTQNG 150
*****:*** **_.***** *****:*** *****:
                                183

```

HumanA/Moscow/10/99	SSSSCKRRS	IKSFFSRLNWLHQLKYRYPALNV	MPNNDKFDKLYIWGV	HH	200
HumanA/Wyoming/3/03	SSACKRRS	IKSFFSRLNWLHLKYKYPALNV	MPNNEKFDKLYIWGV	HH	200
HumanA/Phillipines/2/82	GSYTCKRGS	IKSFFSRLNWLVESESKYPVLNV	MPNNGKFDKLYIWGI	HH	200
HumanA/Aichi/2/68	GSNACKRGP	SGSFFSRLNWLTKSGSTYPVLNV	MPNNDNFDKLYIWGI	HH	200
AvianA/Dk/Ukraine/63	GSSACKRGP	ANGSFFSRLNWLTKSESAYPVLNV	MPNNDNFDKLYIWGV	HH	200
	*	:***	..*****	.	**..*****
		190 helix	220 loop		
HumanA/Moscow/10/99	PSTDS	DQTS	SLY	QASGRVT	VSTKRSQ
HumanA/Wyoming/3/03	PVTDS	DQIS	LYA	QASGRIT	VSTKRSQ
HumanA/Phillipines/2/82	PSTDKE	QTNLY	IRASGRVT	VSTKRSQ	TVIPNIGSRP
HumanA/Aichi/2/68	PSTNQ	EQTSLY	VQASGRVT	VSTRRSQ	TIIPNIGSRP
AvianA/Dk/Ukraine/63	PSTNQ	EQTNLY	VQASGRVT	VSTRRSQ	TIIPNIGSRP
	*	:.:*	**	:***:***:***:***	** *..*****
HumanA/Moscow/10/99	TIVKPGD	ILLIN	STGNLI	IAPRGY	FKIRSGKSS
HumanA/Wyoming/3/03	TIVKPGD	ILLIN	STGNLI	IAPRGY	FKIRSGKSS
HumanA/Phillipines/2/82	TIVKPGD	ILLIN	STGNLI	IAPRGY	FKIRSGKSS
HumanA/Aichi/2/68	TIVKPGD	VLVINS	NGNLI	IAPRGY	FKMRTGKSS
AvianA/Dk/Ukraine/63	TIVKPGD	VLVINS	NGNLI	IAPRGY	FKMRTGKSS
	*****	:*	:***	:*****	:*****
HumanA/Moscow/10/99	NGSIP	NDKPFQ	NVNRI	TYGAC	PRYVKQ
HumanA/Wyoming/3/03	NGSIP	NDKPFQ	NVNRI	TYGAC	PRYVKQ
HumanA/Phillipines/2/82	NGSIP	NDKPFQ	VNKNIT	TYGAC	PRYVKQ
HumanA/Aichi/2/68	NGSIP	NDKPFQ	VNKNIT	TYGAC	PKYVKQ
AvianA/Dk/Ukraine/63	NGSIP	NDKPFQ	VNKNIT	TYGAC	PKYVKQ
	*****	:*****	:*****	:*****	:*****
HumanA/Moscow/10/99	IAGFI	ENGWEG	MMDGWY	GFRHQ	NSEGTG
HumanA/Wyoming/3/03	IAGFI	ENGWEG	MVDGWY	GFRHQ	NSEGTG
HumanA/Phillipines/2/82	IAGFI	ENGWEG	MIDGWY	GFRHQ	NSEGTG
HumanA/Aichi/2/68	IAGFI	ENGWEG	MIDGWY	GFRHQ	NSEGTG
AvianA/Dk/Ukraine/63	IAGFI	ENGWEG	MIDGWY	GFRHQ	NSEGTG
	*****	:*****	:*****	:*****	:*****
HumanA/Moscow/10/99	IEKTNE	KFHQIE	KEFSE	VEGRI	QDLEKY
HumanA/Wyoming/3/03	IGKTNE	KFHQIE	KEFSE	VEGRI	QDLEKY
HumanA/Phillipines/2/82	IEKTNE	KFHQIE	KEFSE	VEGRI	QDLEKY
HumanA/Aichi/2/68	IEKTNE	KFHQIE	KEFSE	VEGRI	QDLEKY
AvianA/Dk/Ukraine/63	IEKTNE	KFHQIE	KEFSE	VEGRI	QDLEKY
	*	*****	*****	*****	*****
HumanA/Moscow/10/99	HTIDL	TDSEMN	KLFER	TRKQL	RENAED
HumanA/Wyoming/3/03	HTIDL	TDSEMN	KLFER	TRKQL	RENAED
HumanA/Phillipines/2/82	HTIDL	TDSEMN	KLFER	TRKQL	RENAED
HumanA/Aichi/2/68	HTIDL	TDSEMN	KLFER	TRRQL	RENAE
AvianA/Dk/Ukraine/63	HTIDL	TDSEMN	KLFER	TRRQL	RENAE
	*****	:*****	:*****	:*****	:*****
HumanA/Moscow/10/99	TYDHD	VYRDE	ALN	NRFQI	KGVEL
HumanA/Wyoming/3/03	TYDHD	VYRDE	ALN	NRFQI	KGVEL
HumanA/Phillipines/2/82	TYDHD	VYRDE	ALN	NRFQI	KGVEL
HumanA/Aichi/2/68	TYDHD	VYRDE	ALN	NRFQI	KGVEL
AvianA/Dk/Ukraine/63	TYDHD	IYRDE	ALN	NRFQI	KGVEL
	*****	:*****	:*****	:*****	:*****
HumanA/Moscow/10/99	IMWAC	QKGN	IRCN	ICI	566
HumanA/Wyoming/3/03	IMWAC	QKGN	IRCN	ICI	566
HumanA/Phillipines/2/82	IMWAC	QKGN	IRCN	ICI	566
HumanA/Aichi/2/68	IMWAC	QKGN	IRCN	ICI	566
AvianA/Dk/Ukraine/63	IMWAC	QKGN	IRCN	ICI	566
	*****	:*****	:*****	:*****	:*****

Figure 3.10 H3 HA ClustalW alignment. The N-glycosylation sites are marked green. The N-glycosylation site possibly involved in interaction with the receptor is marked red. The receptor binding subdomains are marked grey. Conserved N-glycosylation sequons in the stem region are marked pink.

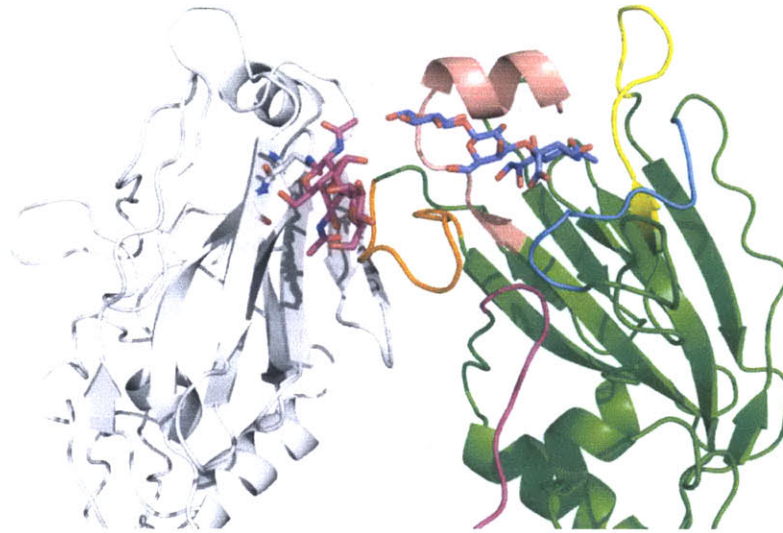


Figure 3.11. Structure of a representative H3 HA (1963-Avian/Duck/Ukraine). Note: two monomers are shown. The glycan ligand is shown as blue stick. The key glycosylation site on NVT (165 -167 amino acids) is shown as magenta stick. It is quite interesting to note that the N-glycosylation site on one of the receptor subdomain stabilizes the glycan binding on the other subdomain in the H1 trimer.

3.3 Discussion and Significance of this study

Glycosylation in influenza A virus hemagglutinin (HA) has evolved as part of the antigenic drift mutations. Except for in H2, which is not in circulation in human population, there has been an increase in the number of N-glycan sequons in the globular head domain of HA. The globular head domain is the prime target of the host antibody response. The glycans in the globular head domain have hence evolved to block binding of neutralizing antibodies. There are a few N-glycan sequons that have been preserved during the course of viral evolution. The ones in the stem region of HA have been well studied and have been implicated in fusion activity of HA. The role of gross glycosylations in the globular head domain has been implicated in replication of virus. Moreover the global effect of HA glycosylation in HA receptor binding was studied by Wang *et al.* However not much is know about the role of conserved N-glycan in the receptor binding property of HA.

In this study the effect of a conserved N-glycosylation sequon, Asn91, in the receptor binding property of H1 HA was systematically studied using a combination of molecular modeling and biochemical assay. It was interesting to identify the role of the N-glycan at N91 only in human glycan receptor binding but not in avian receptor binding. This has been previously suggested by molecular dynamic simulation studies [153]. Glycosylation site at Asn91 along with Asp225Gly mutation of HA has previously been implicated in cyanovirin resistance and in mouse adaptation. Hence it was further crucial to delineate the functional significance of Asn91 (and also in combination with asp225gly) given its physiological relevance.

Such a systematic study is important for understanding molecular evolution of influenza A viruses and also to identify factors that can potentially contribute to the receptor binding property of the virus. This is crucial as glycan receptor binding impinges on the host, tissue and cellular tropism of the virus that can contribute to viral pathogenesis. Such an approach can also enable effective surveillance of evolution of a virulent influenza A virus strains.

Chapter 4. Correlating Glycan Receptor Binding of the Pandemic 2009 H1N1 HA to Viral Transmissibility

Summary

This chapter reports our analysis of the transmissibility and pathogenicity of 2009 pandemic H1N1 virus. Our study showed that the virus has inefficient transmissibility in ferrets as compared to seasonal and pandemic strains. Previously Srinivasan et al (2008) had correlated the transmission efficiency of influenza A viruses to the human receptor binding affinity of its HA. Hence the binding specificity and affinity of a representative 2009 pandemic H1N1 virus: A/California/04/09 or CA04/09 HA to human receptors was characterized using the glycan array platform. This showed that the CA04/09 HA has lower binding affinity to human receptor (6'SLNLN) as compared to the pandemic and seasonal viruses and that this could potentially account for its lower transmission efficiency. Further, to understand the lower human glycan receptor binding affinity, the receptor binding site (RBS) of the HA was compared with that of the seasonal and pandemic influenza A HA. It was hypothesized that the destabilization of interaction network at 186, 189 and could account for its lower receptor binding affinity. In order to validate this, the mismatched interaction was fixed by making it fully ionic (CA04/09Mut1) or fully hydrophobic (CA04/09Mut2). Glycan array analysis of these two mutants showed that fixing the mismatch indeed improved the human receptor binding affinity. Next the transmission experiments with CA04/09Mut1 in ferrets showed that it had improved transmission efficiency compared to the wild type virus. This study provides an alternate strategy for surveillance of influenza A viruses into a more transmissible and pathogenic strain. This study has led to two publications in Science (Maines T et al 2009) and Plos One (Jayaraman A et al, 2011)

4.1 Introduction

The Year 2009 witnessed the first pandemic of the century due to the emergence of the novel swine-origin H1N1 influenza A virus (**Table 4.1**). In response to the emergence and the global spread, on June 11th, 2009, World Health Organization declared it as a pandemic. Phylogenetic analysis of these viruses showed that these viruses resulted from the reassortment of North American H3N2 and H1N2 swine viruses (avian/human/swine “triple” reassortant viruses) with Eurasian avian-like swine viruses (**Figure 4.1**) [154]. As a result these viruses possess PB2 and PA genes of North American avian virus origin, a PB1 gene of human H3N2 virus origin, HA (H1), NP and NS genes of classical swine virus origin and NA (N1) and M genes of Eurasian avian-like swine virus origin. Owing to a decline in the number of cases of 2009 H1N1 viral infection in 2010, the WHO declared the end of the 2009 H1N1 pandemic in early August 2010 [155]. As of August 2010, there are more than 600,000 laboratory confirmed cases of 2009 H1N1 infection and over 18,449 deaths in more than 214 countries as reported by the WHO [156]. Although most confirmed cases have occurred among individuals with uncomplicated, febrile, upper respiratory tract illnesses with symptoms similar to seasonal influenza, there have been over 180 deaths and approximately 40% of infected individuals have experienced symptoms that include gastrointestinal distress and vomiting, which is higher than that reported for seasonal influenza.

The factors that lead to the generation of pandemic viruses are complex and poorly understood, however the ability of a novel influenza virus to transmit efficiently through the air via respiratory droplets appears to be a critical property of pandemic influenza strains [157]. Thus, knowing the inherent virulence and transmissibility of the 2009 A(H1N1) viruses, relative to seasonal influenza viruses, is important to inform appropriate public health responses. We have therefore characterized the virulence and transmissibility of influenza viruses of various subtypes in the ferret (*Mustela putorius furo*) model, which appears to recapitulate not only human disease severity but also

efficient transmission of seasonal (H1N1 and H3N2) influenza viruses and the poor transmission of avian (H5 and H7) influenza viruses [89, 158-160]. Previously our group has shown a strong correlation between the glycan receptor binding affinity of HA to the transmissibility of influenza A virus [110]. Hence the glycan receptor binding specificity and affinity of the viral HA to human receptors was characterized. Building on this receptor-binding site (RBS) of a representative 2009 pandemic H1N1 virus: *A/California/04/09* or *CA04/09* was compared to that of the seasonal and pandemic H1N1 influenza A HA. The key differences in the RBS of *CA04/09* HA were identified which provided a structural rationale for the observed glycan receptor binding affinity and transmissibility of the 2009 H1N1 virus in ferrets. Further, this hypothesis was validated by engineering the RBS of 2009 H1N1 HA to make it similar to the RBS of seasonal and pandemic HAs. The receptor binding property of these engineered HAs were characterized and tested for their transmissibility in ferrets.

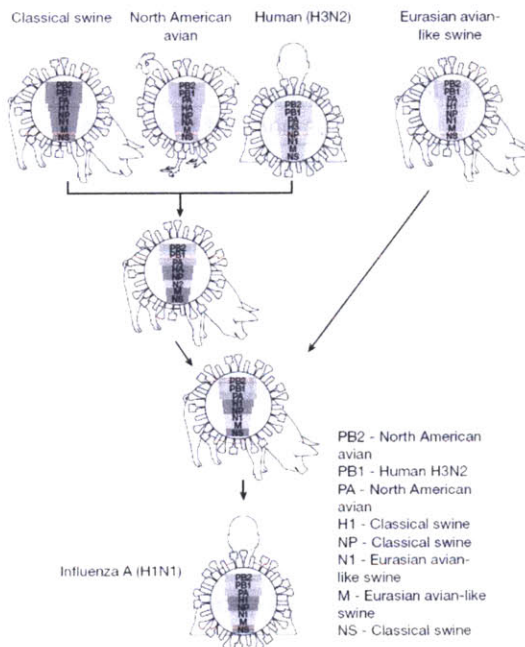


Figure 4.1 Genesis of 2009 H1N1 swine flu virus. In the late 1990s, reassortment between human H3N2, North American avian, and classical swine viruses resulted in triple reassortant H3N2 and H1N2 swine viruses that have since circulated in North American pig populations. A triple reassortant swine virus reassorted with a Eurasian avian-like swine virus, resulting in the S-OIVs that are now circulating in humans.

Figure adapted from Kawaoka *et al* (2009)

Table 4.1 Timeline of Swine flu Outbreak

Date	Event
<i>Mid-February</i>	Outbreak of respiratory illness in La Gloria, Veracruz, Mexico
<i>12 April 2009</i>	Mexican public health authorities report outbreak in Veracruz to the PAHO
<i>15 April 2009</i>	CDC identifies Swine-origin influenza A virus (H1N1) in the specimen of a boy from San Diego, California
<i>21 April 2009</i>	CDC alerts doctors to a new strain of swine-origin influenza A virus
<i>24 April 2009</i>	WHO issues disease outbreak notice
<i>27 April 2009</i>	WHO raises pandemic alert from phase 3 to 4 due to global spread and human-to-human transmission
<i>29 April 2009</i>	WHO raises the pandemic alert from phase 4 to 5
<i>21 May 2009</i>	41 countries report infection and deaths due to the H1N1 virus
<i>June 2009</i>	First case of tamiflu resistance
<i>11 June 2009</i>	WHO raises pandemic alert to Phase 6
<i>October 2009</i>	US declares national emergency and calls for more swine flu vaccine production
<i>November 2009</i>	Emergence of Asp225 variants in Norway and Ukraine
<i>December 2009</i>	Reduction in flu related deaths and infection but above epidemic threshold
<i>January 2010</i>	Reduction in flu related deaths and infection but below epidemic threshold
<i>April 2010</i>	Isolated flu activity in various parts of the world
<i>August 2010</i>	WHO declares that the H1N1 pandemic is over and it is declared as a seasonal strain

4.2 Pathogenicity and Transmissibility of 2009 H1N1 influenza A viruses

We tested the pathogenesis and transmissibility of three 2009 A (H1N1) viruses (isolated from nasopharyngeal swabs) and compared with a representative seasonal H1N1 virus, A/Brisbane/59/2007 (Brisbane/07; H1N1) [160]. A/California/04/2009 (CA/04) virus was isolated from a pediatric patient with uncomplicated, upper respiratory tract illness; A/Mexico/4482/2009 (MX/4482) virus was isolated from a 29-year-old female patient with severe respiratory disease; and Texas/15/2009 (TX/15) virus was isolated from a pediatric patient with fatal respiratory illness. To date, 2009 A (H1N1) viruses exhibit high genome sequence identity (99.9%) and lack previously identified molecular markers of influenza A virus virulence or transmissibility [154]. Alignments of the

deduced amino acid sequences between the three viruses revealed a few differences. These were observed in the polymerase (PA), hemagglutinin (HA), nucleoprotein (NP), and non-structural proteins NS1 and NS2 (**Table 4.2**). Viruses were propagated in Madin-Darby canine kidney cells (MDCK) or embryonated hen's eggs (14). For respiratory droplet transmission experiments, three animals were inoculated intranasally (i.n.) with 10^6 PFU (plaque forming units) of virus (14). Approximately 24 hours later, inoculated-contact animal pairs were established by placing a naïve ferret in each of three adjacent cages with perforated side walls, allowing exchange of respiratory droplets without direct or indirect contact (**Figure 1.16**) [158]. Direct contact transmission experiments were performed similarly except naïve ferrets were placed in the same cage as each of the inoculated ferrets where they shared a common food and water source. Transmission was assessed by titration of infectious virus in nasal washes and detection of virus specific antibodies in convalescent sera [158]. Inoculated and contact animals were monitored for clinical signs over a 14 day period using previously described methods [158]. Three additional inoculated ferrets from each virus-infected group were euthanized on day 3 post-inoculation (p.i.) for assessment of virologic parameters [27].

4.2.1 Pathogenesis of 2009 H1N1 influenza A viruses in ferrets

Ferrets inoculated with CA/04 virus showed no overt clinical signs but displayed mild signs of inactivity (relative inactivity index (RII) = 1.0). TX/15 or MX/4482 virus infection resulted in more pronounced clinical features including a slight increase in RII (1.2). Significantly greater weight loss was observed with all of the 2009 A(H1N1) viruses than that with the seasonal influenza virus, Brisbane/07 ($P < 0.05$; **Table 4.2**). One ferret infected by direct contact transmission from a TX/15-inoculated ferret was euthanized at 10 days p.i. due to excessive weight loss and three MX/4482-inoculated ferrets were euthanized before the end of the experimental period due to severe lethargy or excessive weight loss (**Table 4.2**). Ferrets inoculated with either of the 2009 A(H1N1) virus isolates had elevated body temperatures (peak mean change in body temperature

ranging from 2.0 to 3.2°C over baseline) and shed high peak mean titers of infectious virus in nasal washes as early as day 1 p.i. ($10^{7.1-7.7}$ PFU/ml) (Supplementary Figures 1 & 2), that were sustained at titers of $\geq 10^{4.4}$ PFU/ml for 5 days p.i. The 2009 A(H1N1) virus shedding showed similar kinetics to Brisbane/07 virus, which was also sustained for 5 days in ferrets at titers of $\geq 10^{4.7}$ PFU/ml. In contrast to Brisbane/07, CA/04, TX/15 and MX/4482 viruses were detected in the lower respiratory tract at high titers ($10^{5.8-6.0}$ PFU/g lung tissue) and the intestinal tract. For the latter, viral titers were detected in rectal swabs or tissue samples collected throughout the intestinal tract (Table 4.2, Figure 4.2). There was no evidence of viremia or infectious virus in the brain, kidney, liver and spleen tissues with any of the viruses tested (Figure 4.3).

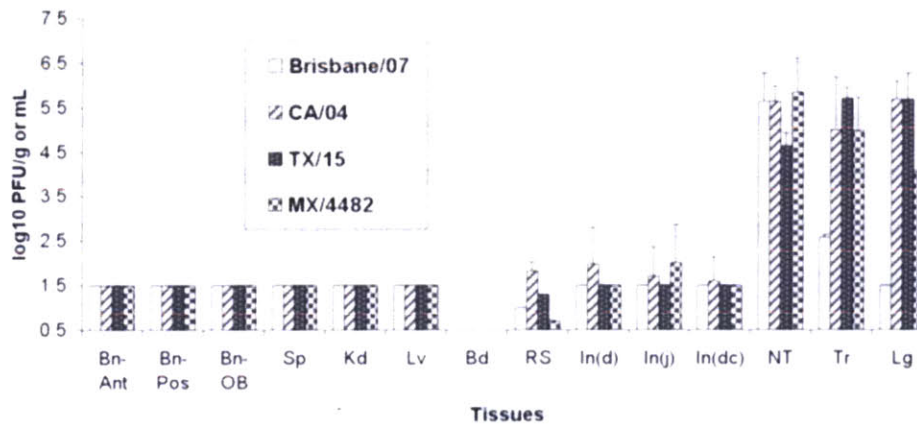


Figure 4.2 Detection of H1N1 virus in ferret tissues. Three ferrets were intranasally inoculated with 10^6 PFU of virus and three days later tissues were collected and virus titers were determined. Bn-Ant, anterior brain; Bn-Pos, posterior brain; Bn-OB, olfactory bulb; Sp, spleen; Kd, kidneys; Lv, liver; Bd, whole blood; RS, rectal swab; In(d), duodenum; In(j), jeuno-ileal loop; In(dc), descending colon; NT, nasal turbinates; Tr, trachea; Lg, lung. Mean virus titers are expressed as PFU/g for all tissues except Bd, RS and NT which are expressed as PFU/mL. Mean virus titers of RS samples are based on the mean of positive samples only. All isolation attempts without recovery of virus were given a value of $1.5 \log_{10}$ PFU/g or mL for all tissues except those tested without dilution (Bd and RS) which were given a value of $0.5 \log_{10}$ PFU/mL.

Table 4.2: Replication and transmission of novel 2009 and seasonal H1N1 viruses in ferrets.

Virus	Inoculated Animals					DC Contact Animals ^a		RD Contact Animals ^a	
	Weight Loss (%) ^b	Sneezing ^c	Lethality ^d	Lung (peak titer) ^e	Intestinal Tract ^f	Virus Detection	Seroconversion ^g	Virus Detection	Seroconversion ^g
A/California/04/2009	6/6 (10.3)	2/6	0/6	3/3 (5.8)	5/9 (2.3)	3/3	3/3	2/3	2/3
A/Texas/15/2009	6/6 (9.1)	1/6	0/6	3/3 (6.0)	1/9 (1.3)	3/3	3/3	2/3	2/3
A/Mexico/4482/2009	6/6 (17.5)	3/6	3/6	2/3 (4.1)	2/9 (2.7)	3/3 ^h	3/3	2/3 ^h	2/3
A/Brisbane/59/2007	6/6 (4.9)	6/6	0/6	0/3	0/9	3/3	3/3	3/3	3/3

^a DC, direct contact; RD, respiratory droplet.

^b The percentage mean maximum weight loss observed during the first 10 days post-inoculation.

^c Number of animals in which sneezing was observed during the first 10 days post-inoculation.

^d Number of animals euthanized before the end of the 14 day experimental period due to reaching a clinical end point.

^e Virus titers are expressed as mean log₁₀ peak PFU/mL or PFU/gram of tissue.

^f Virus titers in intestinal tissue or rectal swabs are expressed as the mean log₁₀ peak PFU/ml for the positive samples.

^g HI antibody titers ranged from 640 to 1280 and were determined using homologous virus and serum collected at least 17 days post contact.

^h Virus was detected in intestinal tract as well as nasal wash for 1 of 3 DC and 2 of 3 RD contact animals.

4.2.2 Transmission of 2009 H1N1 influenza A viruses in ferrets

To assess the transmission efficiency of the virus, viral shedding in nasal washes, detection of neutralizing antibody in the convalescent sera and the onset of clinical symptoms in the contact ferrets (housed in adjacent cage with perforated walls) are monitored [67]. The number of contact ferrets infected by the inoculated ferrets also determines the transmission efficiency of the virus. Previously, Tumpey *et al.*, showed that seasonal and pandemic influenza A viruses transmit efficiently via respiratory droplets from inoculated to contact ferrets (all the 3 contact ferrets were infected by the inoculated ferrets). A similar approach was used to test the transmission efficiency of 2009 H1N1 influenza A viruses.

Consistent with the experimental transmission data obtained with contemporary human H1N1 and H3N2 viruses [27, 67, 158, 161], the seasonal influenza H1N1 (Brisbane/07) virus efficiently transmitted via direct contact and respiratory droplets to all of the contact ferrets which shed virus as early as day 1 post-contact (p.c.) (**Figures 4.3 & 4.4**). Direct contact transmission was observed between all animal pairs for CA/04, TX/15 and MX/4482 viruses; infectious virus was recovered from nasal washes and seroconversion was detected in all contact animals (**Table 4.2 and Figure 4.4**). However, the 2009 A(H1N1) viruses did not spread by respiratory droplet to every contact ferret and transmission was delayed by five or more days post exposure in two of six infected ferret pairs (**Figure 4.3**). Respiratory droplet transmission of 2009 A(H1N1) viruses was significantly reduced compared to respiratory droplet transmission of the seasonal influenza virus ($P \leq 0.01$; **Table 4.2**). Sneezing was frequently observed in Brisbane/07-inoculated ferrets but was rarely observed in the CA/04-, TX/15- or MX4482-inoculated ferrets during the study period, similar to the infrequent sneezing observed in ferrets infected with avian influenza viruses [158]. Collectively, these findings demonstrate that 2009 A(H1N1) viruses elicited elevated respiratory disease relative to seasonal H1N1 viruses in ferrets, yet despite efficient direct contact transmission, the viruses exhibited less efficient respiratory droplet transmission, compared with contemporary seasonal human influenza viruses [27, 158].

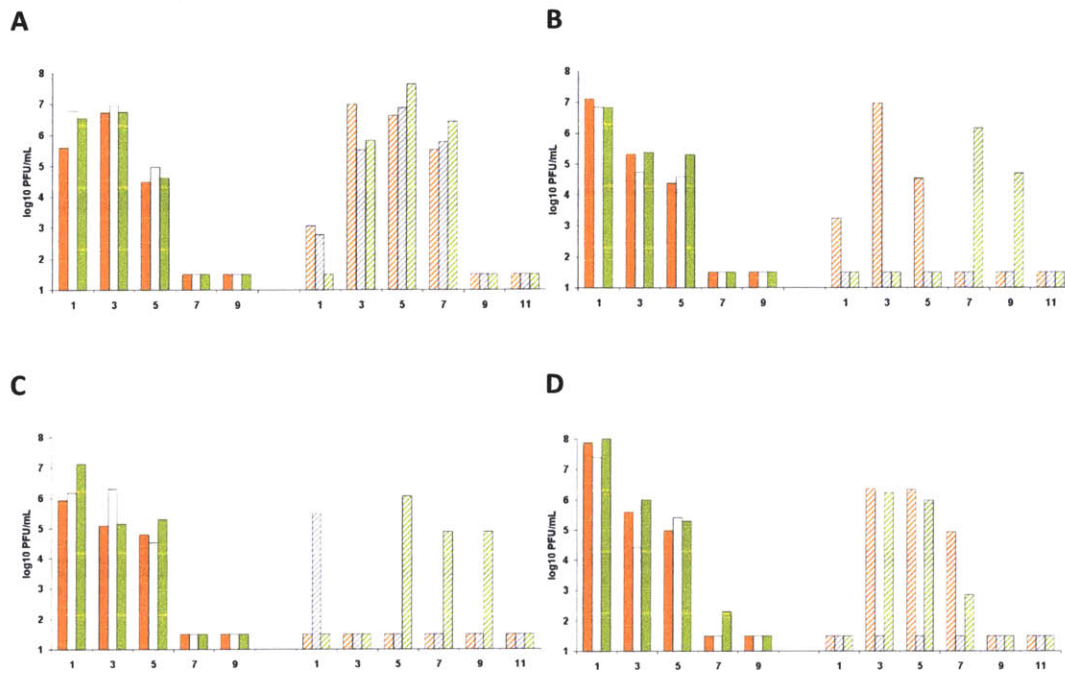


Figure 4.3. Respiratory droplet transmissibility of H1N1 influenza viruses. Three ferrets were intranasally inoculated with 10^6 PFU of Brisbane/07 (A), CA/04 (B), TX/15 (C) or MX/4482 (D) virus. A naïve ferret was placed in an adjoining cage to each inoculated ferret and viral shedding in nasal washes was assessed every other day for the inoculated (left) and contact (right) ferrets. Results from individual ferrets are presented. Solid and striped bars of the same color represent a ferret pair housed in adjoining cages. Limit of detection is $1.5 \log_{10}$ PFU/mL.

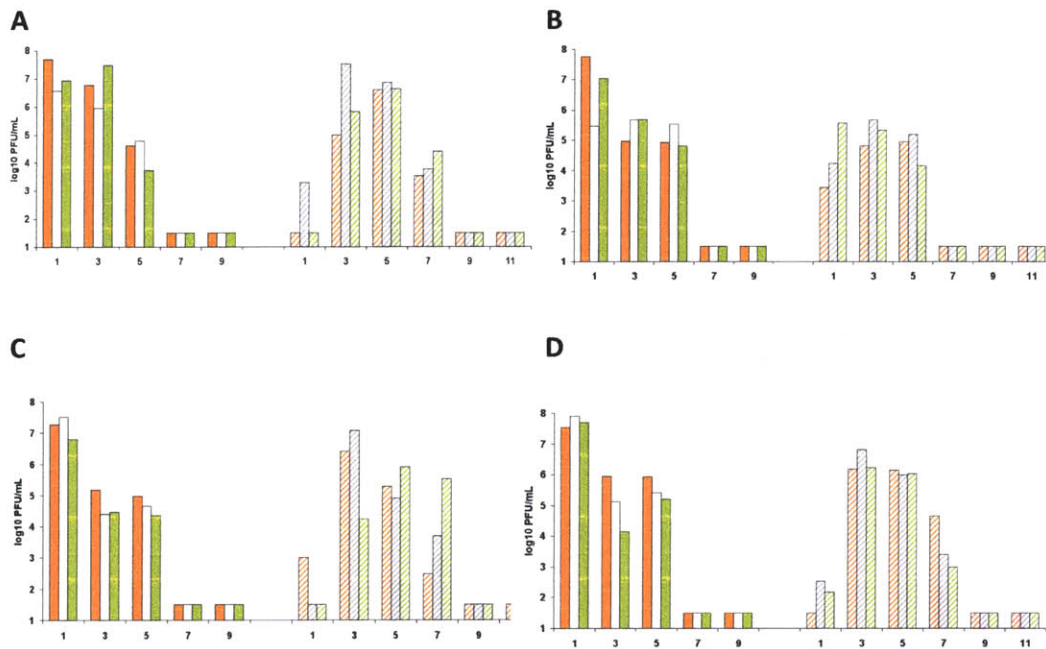


Figure 4.4. Direct contact transmissibility of H1N1 influenza viruses. Three ferrets were intranasally inoculated with 10^6 PFU of Brisbane/07 (A), CA/04 (B), TX/15 (C) or MX/4482 (D) virus. A naïve ferret was housed in the same cage with each inoculated ferret and viral shedding in nasal washes was assessed every other day for the inoculated (left) and contact (right) ferrets. Results from individual ferrets are presented. Solid and striped bars of the same color represent a ferret pair housed together. Limit of detection is $1.5 \log_{10}$ PFU/mL.

4.3 Glycan receptor binding property of 2009 H1N1 influenza A viruses

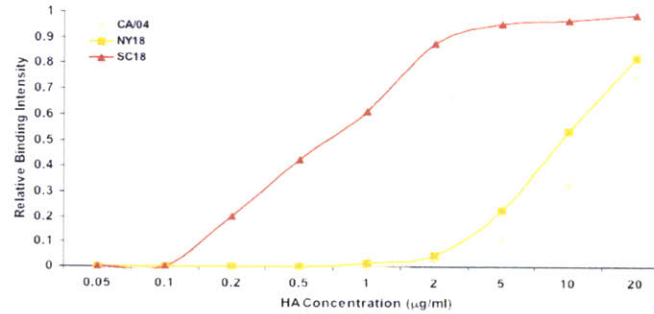
4.3.1 Biochemical characterization of glycan receptor binding property of 2009 H1N1 influenza A viruses

As mentioned earlier, one of the critical determinants of the viral transmission is its HA (Chapter 1). HA mediates binding of the virus to their target cells by binding to specific sialylated glycan receptors. Increased binding affinity and specificity of human-adapted influenza A HA to human receptors (long α 2-6 sialylated glycans which adopt *umbrella-like* topology) was shown to correlate with increased transmission efficiency of the virus in ferrets and humans [110]. Hence to understand the glycan receptor binding property of 2009 H1N1 HA, glycan array analysis of the HA and whole viruses was

performed using the glycan array platform (Chapter 1). Soluble HA from the representative 2009 H1N1 virus *A/California/04/09* or *CA04/09* was recombinantly expressed and purified in Sf9 insect cells. Whole viruses were generated using reverse genetics by using eight-plasmid system [101].

A quantitative dose-dependent glycan array analysis with HA (pre-complexed with primary and secondary antibody) was performed. The array platform comprised of 5 glycans: 3'SLN, 6'SLN, 3'SLNLN, 6'SLNLN and 3'SLNLN (LN corresponds to lactosamine (Gal β 1-4GlcNAc) and 3'SLN and 6'SLN respectively correspond to Neu5Ac α 2-3 and Neu5Ac α 2-6 linked to LN). *CA04/09* HA exhibited a dose-dependent binding to only a single α 2-6 glycan (6'SLNLN) and no observable binding to any α 2-3 glycans (**Figure 4.5A**). While the binding specificity of *CA04/09* HA is similar to that of HA from the 1918 pandemic influenza A virus (*A/South Carolina/1/1918*; or SC18 **Figure 4.5B**), the binding affinity of *CA/04* HA is however considerably lower than that of SC18 HA (**Figures 4.6A**). We also performed glycan array analysis with *CA04/09* whole virus (generated by reverse genetics). *CA04/09* virus showed a strict α 2-6 binding specificity (although 6'SLN binding was also seen in contrast to 6'SLNLN binding specificity of the HA) and no α 2-3 binding was seen. The 6'SLN binding seen with the whole viruses can be attributed to the increased multivalency of HA on viruses than the pre-complexed HA and hence an amplification of binding signals can be seen with whole viruses (**Figure 4.7**).

A

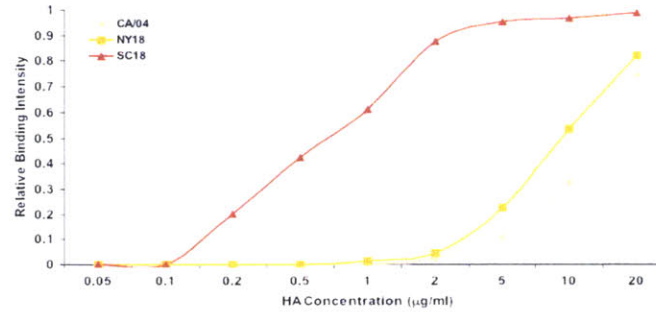


B

Virus	Inoculated Ferrets Number with characteristic/total number			Respiratory Droplet Contact Ferrets Number with characteristic /total number	Respiratory droplet transmission
	Sneezing	Weight loss (%) ^a	Nasal Wash	Virus Detection in nasal wash (Peak/dpc) ^b	
SC18	3/3	3/3 (11.7)	3/3	3/3 (7.5/1,1,1)	Efficient
NY18	0/3	3/3 (18.9)	3/3	1/3 (3.8/3)	Inefficient
CA/04	2/6	6/6 (9.1)	6/6	2/3 (6.7/2,8)	Inefficient

Figure 4.6. Correlation between α 2-6 binding affinity and respiratory droplet ferret transmission of H1N1. Shown on the *top* is the binding curve comparing α 2-6 binding (to 6'SLN-LN in the direct receptor binding assay) of SC18, NY18 (a single amino acid HA variant of SC18) and CA/04 HA . Shown in the *bottom* is a table showing clinical symptoms, virus replication, transmissibility among ferrets inoculated with the H1N1 viruses. Note that the substantially lower α 2-6 binding affinity of NY18 and CA/04 HA as compared to SC18 HA correlates with their transmission efficiency.

A



B

Virus	Inoculated Ferrets Number with characteristic/total number			Respiratory Droplet Contact Ferrets Number with characteristic /total number	Respiratory droplet transmission
	Sneezing	Weight loss (%) ^a	Nasal Wash	Virus Detection in nasal wash (Peak/dpc) ^b	
SC18	3/3	3/3 (11.7)	3/3	3/3 (7.5/1,1,1)	Efficient
NY18	0/3	3/3 (18.9)	3/3	1/3 (3.8/3)	Inefficient
CA/04	2/6	6/6 (9.1)	6/6	2/3 (6.7/2,8)	Inefficient

Figure 4.6. Correlation between α 2-6 binding affinity and respiratory droplet ferret transmission of H1N1. Shown on the top is the binding curve comparing α 2-6 binding (to 6'SLN-LN in the direct receptor binding assay) of SC18, NY18 (a single amino acid HA variant of SC18) and CA/04 HA. Shown in the bottom is a table showing clinical symptoms, virus replication, transmissibility among ferrets inoculated with the H1N1 viruses. Note that the substantially lower α 2-6 binding affinity of NY18 and CA/04 HA as compared to SC18 HA correlates with their transmission efficiency.

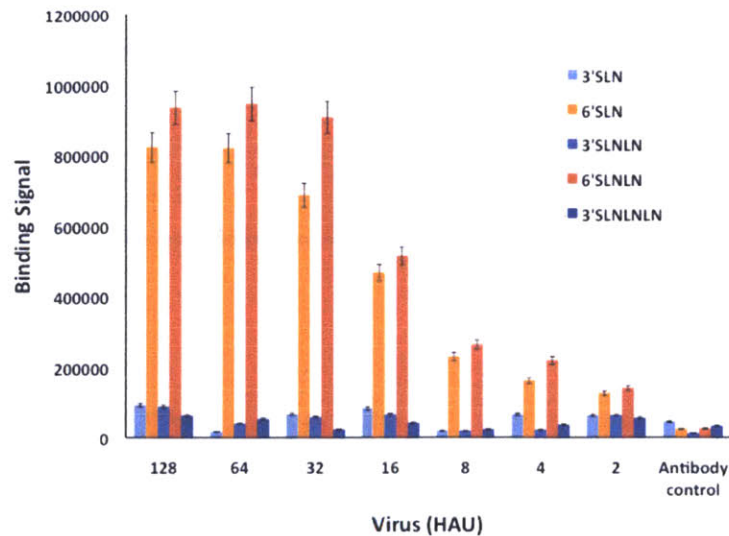


Figure 4.7 Glycan array analysis with the wild-type CA04/09 virus (generated by reverse genetics). The wild-type virus showed a strict binding preference to α 2-6 glycans. In contrast to the HA (Figure 4.6), the whole virus showed binding to 6'SLN glycans as well, this can be attributed to the increased multivalency of the virus as compared to the recombinant HA.

Nevertheless, it can be concluded that one of the factors that contribute to the lower transmission efficiency of the 2009 H1N1 influenza A viruses is their reduced binding affinity to the human receptors. In order to corroborate this binding specificity of CA04/09 on the glycan array to the binding of the HA to physiological glycan receptors, the recombinant HA was used to stain human tracheal and alveolar tissue sections. Previously, increased binding affinity to human receptors has been correlated to extensive staining of goblet cells and in some cases to ciliated cells and apical surface as well [41, 48, 162]. In accordance with that, CA04/09 HA showed less extensive staining of the goblet cells and the apical surface of the tracheal epithelium (Figure 4.8A). Human deep lung comprising of the alveolus is known to predominantly express α 2-3 glycans. CA04/09 HA did not show any α 2-3 binding on the glycan array, and hence as expected there was minimal to no staining of the alveolus (Figure 4.8B). The sialic acid binding specificity of CA04/09 HA was tested using *Sialidase A* treatment of tissues prior to staining with HA (Figure 4.9).

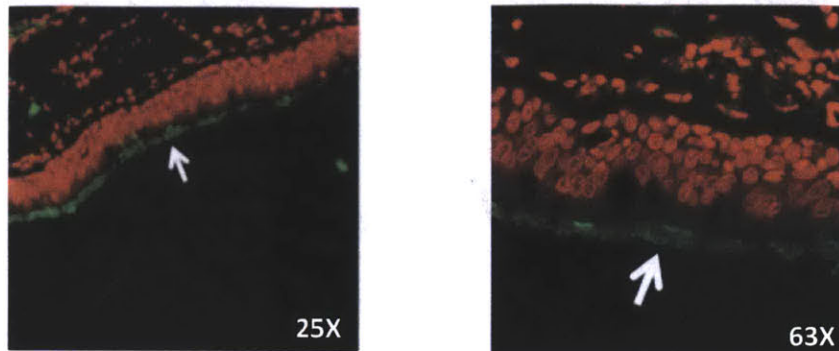
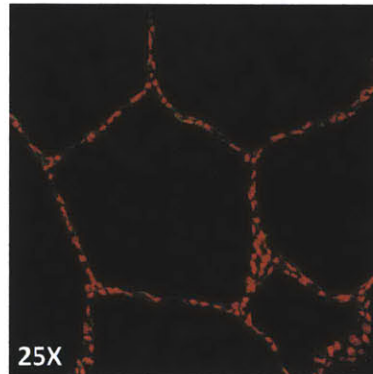
A**CA04/09HA/PI****B**

Figure 4.8 Human respiratory tract tissue binding of CA04/09 HA. Shown in **(A)** is the binding of CA04/09 HA at 20 μ g/ml concentration to apical surface (*white arrow*) of human tracheal tissue sections (green as against propidium iodide staining in red). Note the binding of HA to the apical surface of tracheal tissue which is known to predominantly express α 2-6 sialylated glycans (Chandrasekharan *et al.*), Shown in **(B)** is the minimal binding of HA at 20 μ g/ml concentration to the alveolar tissue section. The binding of the recombinantly expressed HA to the human tissues was carried out as described previously (Chandrasekharan *et al.*) by precomplexing HA: primary antibody:secondary antibody in the molar ratio of 4:2:1 to enhance multivalent presentation of HA.

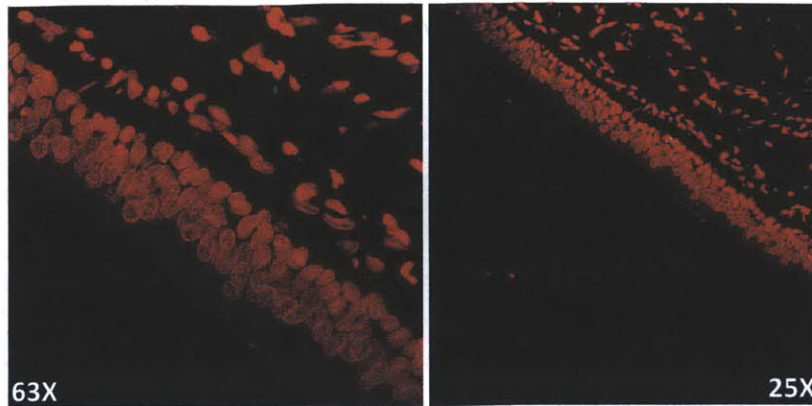


Figure 4.9 Sialic acid specificity of CA04/09 HA The sialic acid specific binding of HA to the tracheal tissue section was confirmed by the minimal binding of HA to the tissue section pre-treated with 0.2 U of Sialidase A (recombinantly expressed in *Arthrobacter ureafaciens*). The binding of the recombinantly expressed HA to the human tissues was carried out as described previously (Chandrasekharan *et al.*) by precomplexing HA: primary antibody:secondary antibody in the molar ratio of 4:2:1 to enhance multivalent presentation of HA.

4.3.2 Biochemical characterization of glycan binding properties of natural variants of 2009 H1N1 virus

Since the emergence of CA/04 in March-April 2009, there has been an evolution of the natural variants of the virus that have acquired mutations in the HA. Notably, Asp225 (H3 HA numbering) has mutated into Glu or Asn or Gly in the more recent 2009 H1N1 strains. The Asp225->Gly and Asp225->Asn variants were derived directly from clinical specimens of patients with severe infection [163]. The Asp225Gly was isolated from the deeper lung regions in three of the fatal cases in Ukraine [164]. Asp225 is a hallmark residue of human-adapted H1N1 HAs and has been shown to play a critical role in the $\alpha 2 \rightarrow 6$ glycan-binding specificity of these HAs [67] (Figure 4.10).

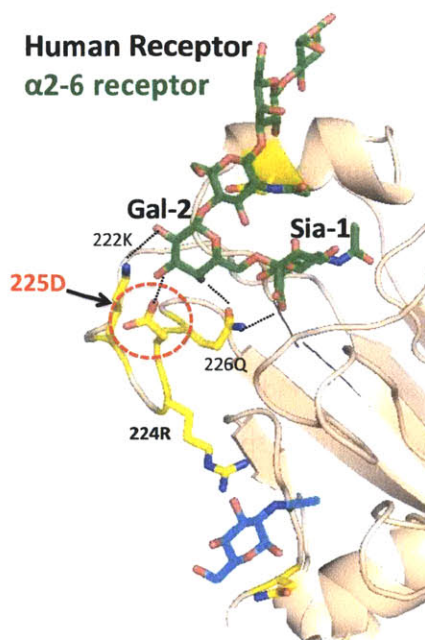


Figure 4.10 Role of Asp225 in human receptor binding of HA. Shown is a molecular model of H1 HA with human receptor. Aspartate at 225, is part of the 220-loop, and makes critical contacts with Gal-2 of the human receptor. The recent isolates of 2009 H1N1 have mutated Asp225 to either Asn, Glu or Gly. Asp225 is highlighted in *red* dotted circle.

Hence in order to understand the effect of the D225 mutations, the natural variants that acquired the Asp225→Glu (CA04M3), Asp225→Asn (CA04M4) and Asp225→Gly (CA04M5) mutations were also designed on CA/04 HA and a dose-dependent glycan array analysis was performed (Figure 4.11). Our analysis showed that the binding specificity to the representative human receptor (6'SLN-LN) was the same between the Asp225→Glu (CA04M3) and Asp225→Asn (CA04M4) mutants, consistent with the previous study [165]. However there were differences in their human receptor binding strengths where CA04M4 ($K_d' \sim 0.7$ nanomolar (nM)) > CA04 ($K_d' \sim 1$ nM) >> CA04M3 ($K_d' \sim 7$ nM). The Asp225→Gly (CA04M5) mutant, on the other hand, showed dramatically reduced dose-dependent binding to human receptors and bound to avian receptors as well (Figure 4.11). The binding of CA04M5 mutant to representative avian receptors is in agreement with the previous studies [165]. Taken together, none of the

mutants with the natural amino acid substitutions at the 225 position show substantially improved human receptor binding strength over the *WT* HA. More recently, the Asp225→Gly mutation has been analyzed to understand its cellular tropism, as this mutant is associated with causing a more severe and a fatal disease [166]. The 225Gly mutant infected a higher proportion of ciliated cells in cultures of human airway epithelium than did viruses with 225Asp or 225Glu, which mainly targeted non-ciliated goblet cells. This converges with our glycan array data, where 225Asp and 225Glu mutants showed highly specific binding to long α 2-6 glycans (6'SLNLN). Hence a more promiscuous α 2-3 and α 2-6 binding specificity of 225Gly (*CA04M5*) might contribute to exacerbation of disease.

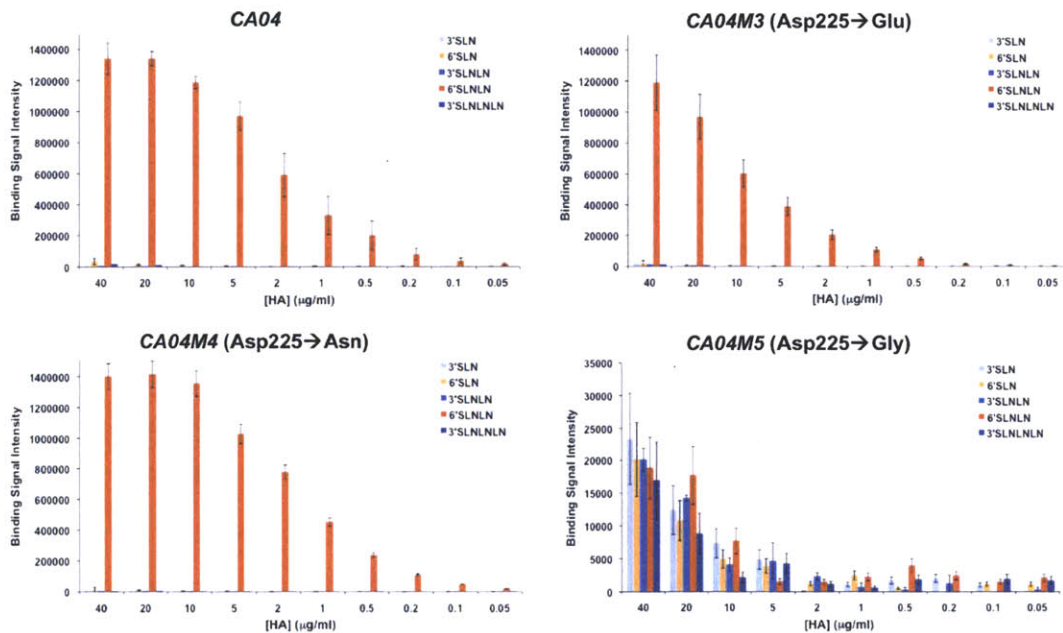


Figure 4.11 Dose dependent glycan array analysis of natural variants of 2009 H1N1 virus. The three natural variants: Asp225Glu or CA04M3, Asp225Asn or CA04M4 and Asp225Gly or CA04M5 were expressed in insect cells and analyzed on the glycan array. There was a complete loss of glycan binding specificity and affinity for CA04M5 and this could account for its pathogenicity. Shown are the promiscuous binding of CA04M5 to α 2-3 and α 2-6 glycans. The binding signals seen for CA04M5 are closer to the background binding signals. For comparison the binding data off CA04wt HA is also shown.

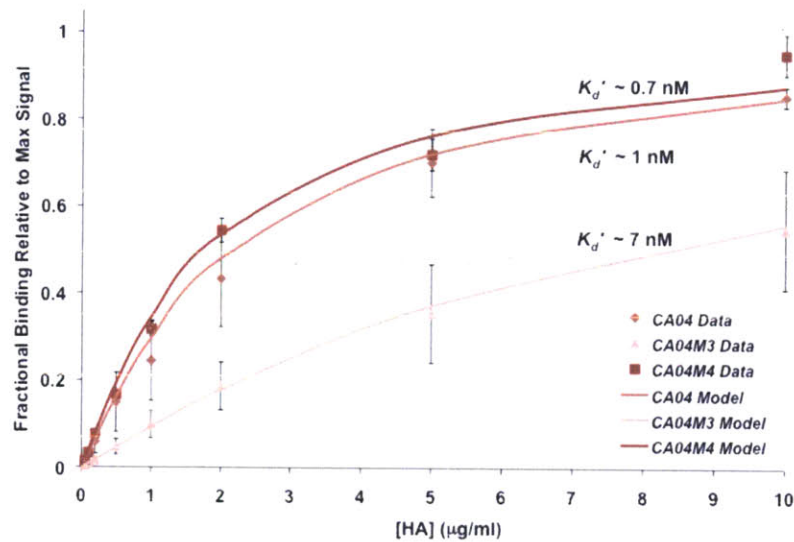


Figure 4.12 6'SLNLN binding curves for the natural variants of the 2009 H1N1 virus. CA04M4 (Asp225Asn) had increased binding affinity to 6'SLNLN as compared to the wild-type. CA04M3 (Asp225Glu) had significantly reduced affinity to 6'SLNLN. This indicates that the amino acid chain length at position 225 and not the charge governs the receptor binding property of the HA. Note that since CA04M5 (Asp225Gly) displayed a complete loss of receptor binding affinity and specificity, its binding curve is not shown.

4.3.3 Fixing the mismatched interaction in the RBS of CA04/09 HA

Two strategies were employed (based on the comparison of the RBS of pandemic and a seasonal influenza A virus HA, **Table 4.3, Figure 4.13**) to correct the mismatched combination of residues in the RBS of CA04/09 HA (**Figure 4.14A**) as mentioned in Section 4.3.1. *First* strategy was to generate a single mutant; Ile219→Lys (CA04/09mut1) that would generate a stable ionic interaction between Lys219 and Glu227. To confirm this analysis a homology-based structural of CA04/09mut1 HA in complex with human receptor was constructed (**Figure 4.14B**). Based on this model it was observed that Lys219 and Glu227 are positioned to make ionic contacts that would facilitate the stabilization of interaction network involving residues 186, 187, 189 and 190. The *second* strategy was to make this interaction network hydrophobic. This would involve three amino acid changes, Ser186→Pro / Ala189→Thr / Glu227→Ala

(*CA04mut2*) (**Figure 4.14C**) that would make the interactions hydrophobic similar to that observed in the RBS of SC18 HA (**Figure 4.14D**). It was hypothesized that fixing this mismatched interaction would improve the binding affinity of the HA and hence improve its transmissibility in ferret model.

4.3.3.1 Biochemical characterization using glycan array analysis:

To test the aforementioned hypothesis, recombinant soluble *CA04mut1* and *CA04mut2* were expressed in insect cells and their respective glycan receptor binding affinity and specificity was characterized by analyzing them (in their pre-complexed state) using the dose-dependent glycan array analysis (**Figure 4.15**). A dose-dependent binding of HA to representative human and avian receptors on a biotin-streptavidin based glycan array platform permitted quantification of binding affinity using an apparent binding constant K_d' [110]. The parameter K_d' was calculated by fitting the binding data (over a range of HA concentrations) using the Hill equation for multivalent binding [110].

Table 4.3 Glycan binding residues of H1N1 HAs

H1N1 Strains	Cluster 1				Cluster 2				Cluster 3			Cluster 4				Cluster 5						
	136	138	226	137	153	155	194	183	145	222	225	190	189	187	186	219	227	192	193	156	159	196
Solls_3_06	S	S	Q	A	W	T	L	H	S	K	D	D	G	N	P	K	E	R	A	G	G	H
Bris_59_07	S	S	Q	A	W	T	L	H	S	K	D	D	G	N	P	K	E	K	A	G	G	H
NewCal_20_99	S	S	Q	A	W	T	L	H	S	K	D	N	G	N	P	K	E	R	A	G	G	H
TX_36_91	T	S	Q	T	W	T	I	H	S	K	D	D	R	N	S	K	E	R	A	E	G	H
SC18	T	A	Q	A	W	T	L	H	S	K	D	D	T	T	P	A	A	Q	S	K	S	Q
TX/15	T	A	Q	A	W	V	L	H	K	K	D	D	A	T	S	I	E	Q	S	K	N	Q
Mex_4482_09	T	A	Q	A	W	V	L	H	K	K	D	D	A	T	S	I	E	Q	S	K	N	Q
CA/04	T	A	Q	A	W	V	L	H	K	K	D	D	A	T	S	I	E	Q	S	K	N	Q
	Neu5Ac-1								Gal-2			GlcNAc-3				Gal-4, Glc-5, ...						

The residues are organized into network forming clusters. The sugar unit (numbered as shown in Figure 3), which makes contact with the clusters, is shown in the last row. The unique amino acids in 2009 H1N1 HAs are highlighted in *red*. The key for the virus strains Solls_3_06 (A/Solomon Islands/3/06); Bris_59_07 (A/Brisbane/59/07); NewCal_20_99 (A/New Caledonia/20/99); Mex_4482_09 (A/Mexico/4482/09).

```

CA04/09      MKAILVLLYTFATANADTLCIGYHANNSTDVDTVLEKNVTVTHSVNLLLEDKHNGKLC
A/SC/1/18   MEARLLVLLCAFAATNADTICIGYHANNSTDVDTVLEKNVTVTHSVNLLLEDSHNGKLC
A/Brisbane/59/07 MKVKLLVLLCTFTATYADTICIGYHANNSTDVDTVLEKNVTVTHSVNLLLENSHNGKLC
*:.*:*** :*:: **:*:*****:*****:*****:*****:*****

CA04/09      LRGVAPLHLGKCNIAGWILGNPECESLSTASSWSYIVETPSSDNGTCYPGDFIDYEELRE
A/SC/1/18   LKGIAPLQLGKCNIAGWLLGNPECDLLLTASSWSYIVETSNSENGTCTYPGDFIDYEELRE
A/Brisbane/59/07 LKGIAPLQLGNCVAGWILGNPECELLISKEWSYIVEKPNPENGTCTYPGHFADYEELRE
*:.*:***:*:*:*:***:*****: * : .*****.....*****.* *****

CA04/09      QLSSVSSFERFEIFPKTSSWPNHDSNKGVTACPHAGAKSFYKNLIWLVKKNSYPKLSK
A/SC/1/18   QLSSVSSFEKFEIFPKTSSWPNHETTKGVTACSYAGASSFYRNLLWLTKKSSYPKLSK
A/Brisbane/59/07 QLSSVSSFERFEIFPKESWPNHVT-VVSACSHNGESSFYRNLLWLTKNGLYPNLSK
*****:***** ***** . **:*:*:* * .***:***:*. *.. **:*:***

CA04/09      186 190 219 225
A/SC/1/18   SYINDKGKEVLVLWGVIHHPSTSAQQSLYQNADTYVFGSSRYSKFKPEIAIRPKVRDQ
A/Brisbane/59/07 SYVNNKGKEVLVLWGVHHPPTGTQQSLYQNADAYVSVGSSKYNRRFTPEIAARPKVRDQ
SYANNKEKEVLVLWGVHHPNIGQKALYHTENAYVSVVSSHYSRKFTPEIAKRPKVRDQ
** *:* *****:***. **:*:*:. :** * **:*:*. * .*** *****

CA04/09      227
A/SC/1/18   EGRMNYWTLVEPGDKITFEATGNLVVPRYAFAMERNAGSGIISDTPVHDCNTTCQTPK
A/Brisbane/59/07 AGRMNYWTLLEPGDTITFEATGNLIAPWYAFALNRGSGGIITSDAPVHDCNTKQTPH
EGRINYWTLLEPGDTIIFEANGNLIAPRYAFALSRGFGSGIINSNAPMDKCDKQTPQ
**:*:*****:*****.* ***.***:.* *****:*. ***** *:: :. :. :. :. *****

CA04/09      GAINSSLPFQNIHPITIGKCPKYVKSTKLRLATGLRNIPSIQSR
A/SC/1/18   GAINSSLPFQNIHPVTIGKCPKYVRSTKLRLATGLRNIPSIQSR
A/Brisbane/59/07 GAINSSLPFQNVHPVTIGKCPKYVRSKLRMTGLRNIPSIQSR
****:*:*****:***:***:*****:***:***:*****:*****

```

Figure 4.13 ClustalW Sequence alignment of CA04/09, SC18 and Bris07 HAs. Only the HA1 part of the HA comprising of the RBS is shown. The hallmark Asp190 and Asp225 residues are highlighted in green. Residue positions highlighted in gray represent the residues involved in positioning Asp190. Residue positions 219 and 227 are highlighted in yellow to indicate the mismatched combination of residues in CA04/09 HA.

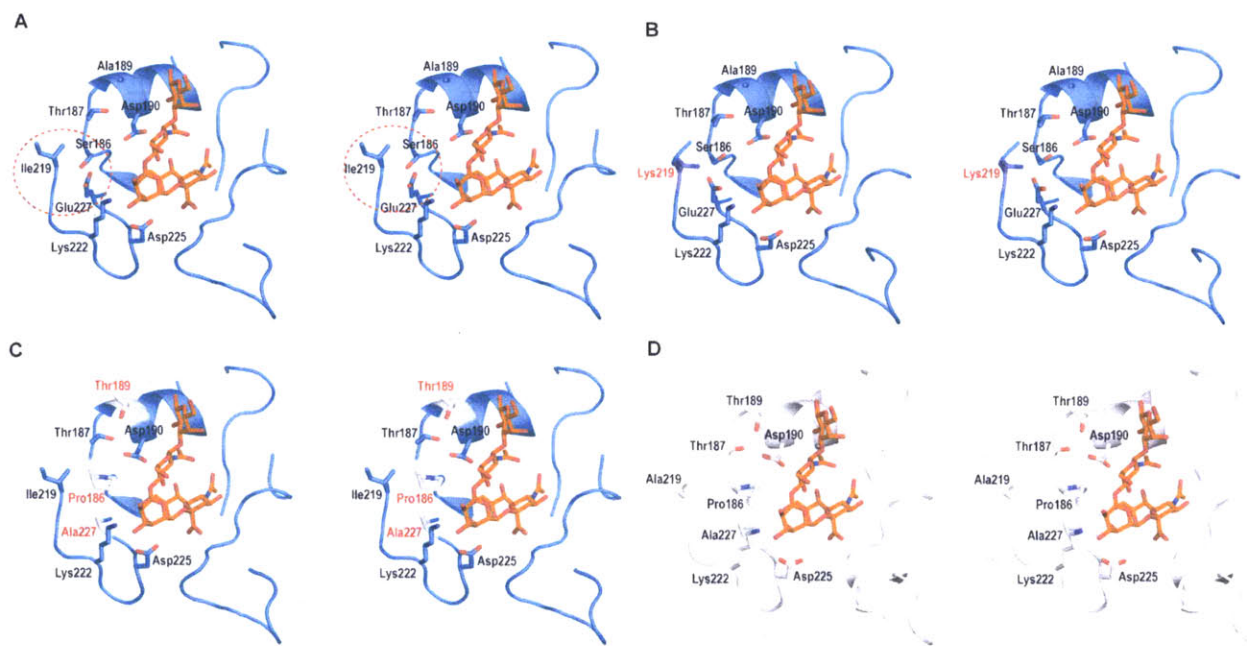


Figure 4.14 Fixing the mismatched interaction in RBS of *CA04* HA. **A**, Structural complex of RBS of *CA04* HA with human receptor (mismatched Ile219 – Glu227 contacts highlighted in *red* circle). **B**, RBS of *CA04M1* complexed with human receptor where Lys219 (highlighted in *red*) makes ionic contacts with Glu227. **C**, RBS of *CA04M2* complexed with the human receptor. **D**, RBS of *SC18* HA complexed with human receptor. The hydrophobic interactions between Ile219, Pro186 and Ala227 and interactions between Ser187, Thr189 and Asp190 in RBS of *CA04M2* HA are similar to that between analogous residues in *SC18* HA. The structural complexes are shown in stereo with RBS represented as a cartoon schematic with side chains of key amino acids. The substituted amino acids are labeled *red*. Stick representation of human receptor is shown with carbon atoms in *orange*.

CA04mut1 and *CA04mut2* showed specific binding to both the representative human receptors (6'SLN and 6'SLN-LN) on the array (only minimal binding signals to avian receptors were observed at the higher concentrations of 20-40 μ g/ml) (**Figure 4.15**). To compare the binding affinity of *CA04/09*, *CA04/09mut1* and *CA04/09mut2* HAs to a representative human receptor, the binding constant K_d' was calculated from the 6'SLN-LN binding curves (**Figure 4.16**). The binding strength of *CA04/09mut1* ($K_d' \sim 50$ picomolar (pM)) and *CA04/09mut2* ($K_d' \sim 6$ pM) to 6'SLN-LN is significantly higher than that of *CA04/09* HA ($K_d' \sim 1.5$ nM), and the natural variants at the 225 position. The human receptor-binding affinities of *CA04/09mut1* and *CA04/09mut2* HAs quantified using K_d' is in the same range (picomolar) as that of *SC18* HA ($K_d' \sim 6$ pM). Therefore fixing the mismatched combination of residues in the RBS of 2009 H1N1 HA substantially increases its human receptor-binding affinity. We also verified that the dose-dependent binding profile of recombinant *CA04/09mut1* HA was consistent with that of the whole virus harboring the Ile219 \rightarrow Lys HA mutation on our glycan array platform (**Figure 4.18**).

4.3.3.2 Binding of *CA04/09mut1* and *CA04/09mut2* HAs to human tracheal tissue sections

Human upper respiratory tissues are the primary targets for infection by human-adapted influenza A viruses for efficient viral transmission by respiratory droplets [48, 110]. The tracheal tissue section, a representative human upper respiratory tissue, has been shown to predominantly express $\alpha 2 \rightarrow 6$ sialylated glycan receptors in the ciliated and non-ciliated (goblet) cells in the apical surface of the pseudostratified epithelium [39, 41, 48, 49, 167]. In contrast, the human alveolus, a representative deep lung tissue, has been shown to predominantly express $\alpha 2 \rightarrow 3$ sialylated glycan receptors [38, 48, 138, 167]. The binding of *CA04/09*, *CA04/09mut1* and *CA04/09mut2* HAs to physiological glycan receptors was assessed by staining human tracheal and alveolar tissue sections with these HAs. Consistent with their minimal $\alpha 2 \rightarrow 3$ glycan receptor-binding on the array, no visible alveolar staining was observed with these HAs (data not shown). On the other hand, *CA04/09*, *CA04/09mut1* and *CA04/09mut2* HAs stained the

apical surface of the human tracheal epithelium (**Figure 4.15**) consistent with their human receptor-binding on the array. Furthermore, *CA04/09mut1* and *CA04/09mut2* HAs showed more intense tracheal staining and goblet cell staining (**Figure 4.17**) in comparison with *CA04/09* HA, which correlated with the broader human receptor specificity [binding to both 6'SLN and 6'SLN-LN] and increased human receptor affinity of the mutant HA on the glycan array. The sialic acid specific binding of HAs to the tracheal tissue sections was confirmed by loss of staining upon pre-treatment of the tissue sections with Sialidase A (from *Arthrobacter ureafaciens*), an enzyme that cleaves terminal sialic acid from both avian and human receptors.

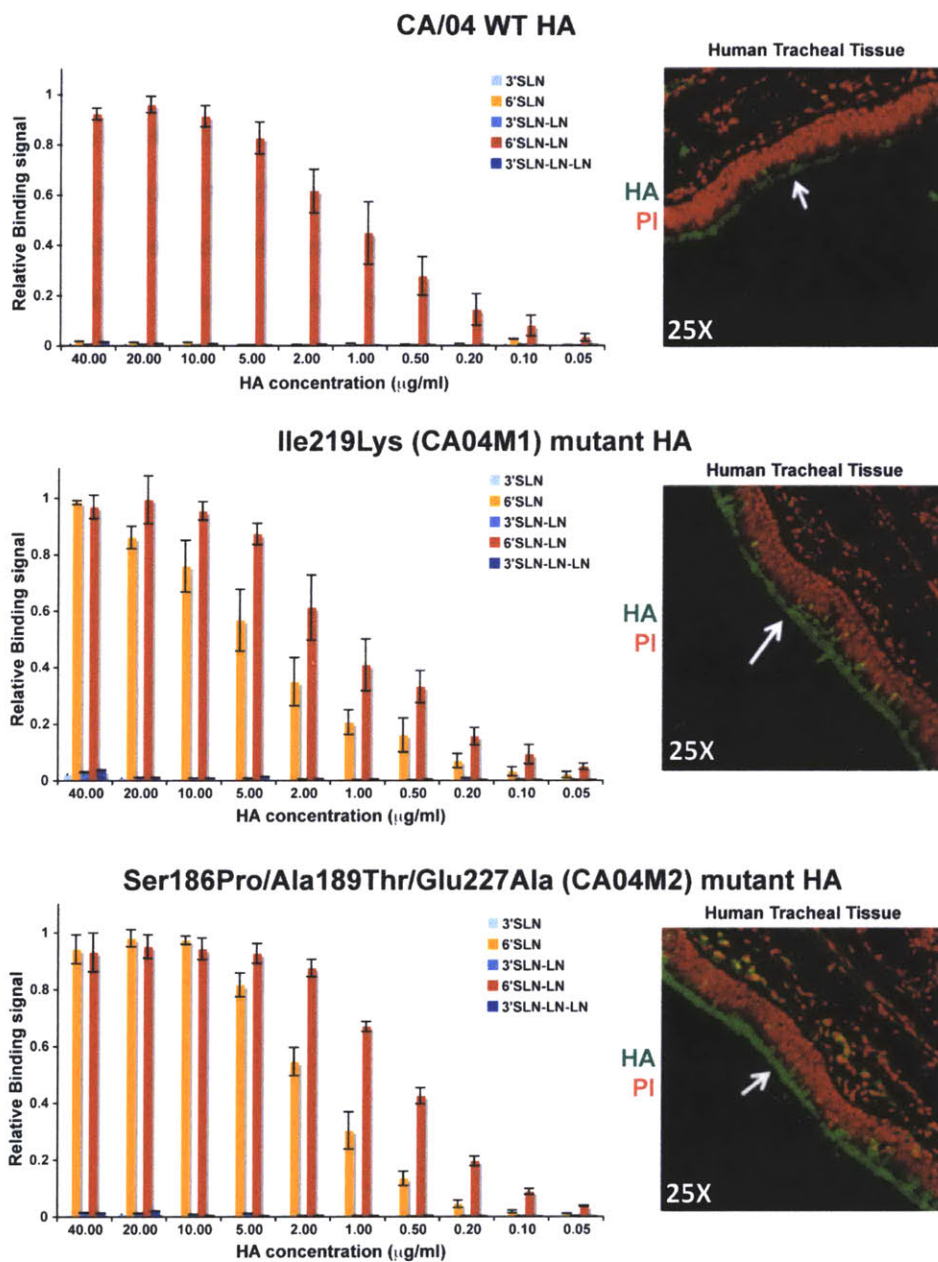


Figure 4.15 Results from dose-dependent direct glycan-receptor binding assay (on the left) and human tracheal tissue binding assay (on the right). LN: $\rightarrow 3\text{Gal}\beta 1 \rightarrow 4\text{GlcNAc}\beta 1 \rightarrow$; 3'SLN and 6'SLN: $\text{Neu5Ac}\alpha 2 \rightarrow 3$ and $\text{Neu5Ac}\alpha 2 \rightarrow 6$ linked to LN respectively. Binding signals normalized to maximum observed value. HA staining (green) of the apical surface (white arrow) is shown against propidium iodide staining of cell nuclei (red). The images were captured at 25X magnification.

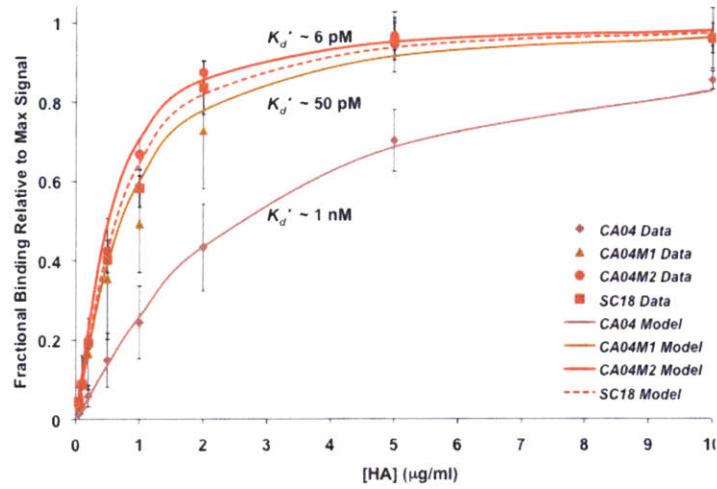


Figure 4.16 Binding curves of mutant and wild-type HAs to 6'SLNLN. Binding curves of CA04, CA04M1, CA04M2 and SC18 HAs to 6'SLN-LN. The experimental data (disconnected markers indicated using "Data") is shown along with the theoretical binding curve (line indicated using "Model"). The K_d' of SC18 HA is around 6pM (in the same range as that of CA04M2 HA) and hence is indicated using the same label.

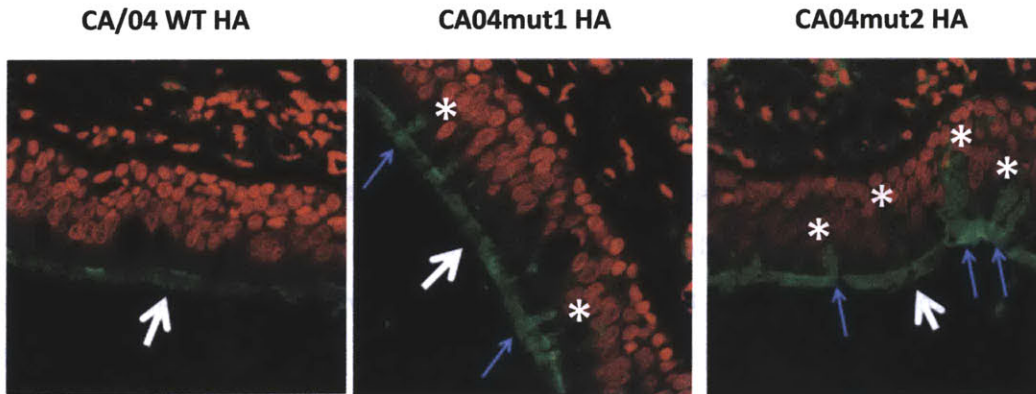


Figure 4.17 Human tracheal Goblet cell staining by wild-type and mutant HAs. The mutants (CA04mut1 and CA04mut2) show extensive staining of the apical surface and goblet cells in the human tracheal epithelium. The images were captured at 63X magnification. The goblet cell staining is marked with a star (*)

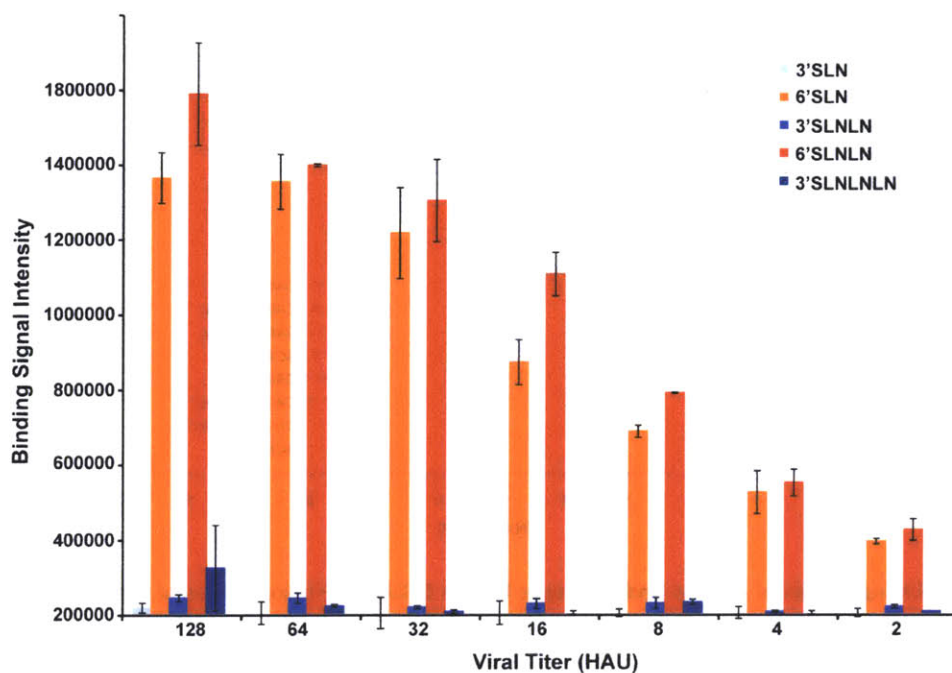


Figure 4.18 Dose-dependent direct glycan array analysis of *rgCA04/09 HA Ile219Lys* mutant virus. The binding profile of this virus is consistent with that of the recombinant *CA04/09mut1* HA shown in Figure 4.15.

4.3.3.3 Transmissibility of a reverse genetics wild-type and mutant *CA04/09* virus in ferrets.

The Ile219Lys mutation (*CA04/09mut1*) lies in the mutational “hot-spot” of HA and involves a single base pair change. Hence the probability of such a mutant to emerge is quite high as compared to the triple mutant (*CA04/09mut2*). Since *CA04/09mut1* HA showed increased binding affinity to human receptor, it was hypothesized that this would have efficient air-borne transmissibility in case such a virus with this single mutation were to evolve. Hence transmission studies were carried out in ferrets using *CA04/09* virus (generated by reverse genetics) harboring Ile219Lys mutation in its HA. For respiratory droplet transmission experiments, three ferrets were inoculated intranasally (i.n.) with 10^6 PFU (plaque forming units) of virus. Approximately 24 hours later, inoculated-contact animal pairs were established by placing a naïve ferret in each of three adjacent cages with perforated sidewalls, allowing exchange of respiratory

droplets without direct or indirect contact [98]. Inoculated and contact animals were monitored for clinical signs over a 16-day period and transmission was assessed by titration of infectious virus in nasal washes and confirmed by the detection of virus specific antibodies in convalescent sera. Ferrets inoculated with the *CA04/09* (*rgCA04/09*) virus, created by reverse genetics, showed no substantial clinical signs and only displayed transient weight loss during the first week of infection (**Table 4.4**). Ferrets inoculated with *rgCA04/09* virus shed high peak mean titers of infectious virus in nasal washes as early as day 1 p.i. ($10^{6.1-6.9}$ PFU/ml), that were sustained at titers of $\geq 10^{2.9}$ PFU/ml for 7 days p.i. The *rgCA04/09* virus shedding showed similar kinetics to mutant virus harboring the Ile219→Lys amino acid mutation in HA, which was sustained for 5 days in ferrets at titers of $\geq 10^{4.3}$ PFU/ml. Consistent with the experimental transmission data obtained with wild type *CA04/09* H1N1 virus [98], *rgCA04/09* virus did not spread by respiratory droplet to every contact ferret and transmission was delayed by five days post exposure in one of two contact ferrets (**Figure 4.20**). Seroconversion confirmed the virus shedding data of 2/3 transmission events (**Table 4.4**). The reduced respiratory droplet transmission suggests that additional virus adaptation in mammals may be required to reach the high-transmissible phenotypes observed with seasonal H1N1 or the 1918 pandemic virus [67, 98]. Mutation of the HA at amino acid position 219 (Ile219→Lys) resulted in a virus (*rgCA04/09 HA Ile219Lys*) that efficiently transmitted via respiratory droplets to all of the contact ferrets which shed virus by day 3 post-contact (p.c.) (**Figure 4.19**). Despite the differences in transmissibility of the parental *rgCA04/09* virus and the *rgCA04/09 HA Ile219Lys* mutant virus, similar virus replication kinetics, and comparable levels of fever induction and weight loss in ferrets were observed with both viruses (**Table 4.4**). This pattern of transmission suggests that a lysine at HA position 219 enhances transmission of the 2009 H1N1 virus through the air.

Table 4.4 Replication and transmission of CA04/09 Ile219->Lys HA mutant virus in ferrets

Virus	Inoculated Animals				RD Contact Animals ^a			
	Weight Loss (%) ^c	Virus in nasal wash ^d	Sneezing ^e	Sero-conversion ^f	Weight Loss (%) ^c	Virus in nasal wash ^d	Sneezing ^e	Sero-conversion ^f
<i>rgCA04/09 HA Ile219Lys^b</i>	13.1	3/3 (6.4)	1/3	3/3 (640-1280)	8.5	3/3 (6.9)	1/3	3/3 (640-1280)
<i>rgCA04/09</i>	8.0	3/3 (6.6)	2/3	3/3 (640-1280)	7.1	2/3 (5.5)	1/3	2/3 (80-160)

^a RD, respiratory droplet

^b This experiment was performed using virus that was obtained from plaque purification and grown in MDCK cells.

^c The percentage mean maximum weight loss observed during the first 10 days post-inoculation.

^d Number of animals positive for infectious virus. Virus titers are expressed as mean log₁₀ peak PFU/mL

^e Number of animals in which sneezing was observed during the first 10 days after inoculation (sneezing was infrequent for all infected animals tested)

^f Hemagglutination inhibition (HI) assay was performed with homologous virus and turkey red blood cells. No. of positive animals and HI range indicated.

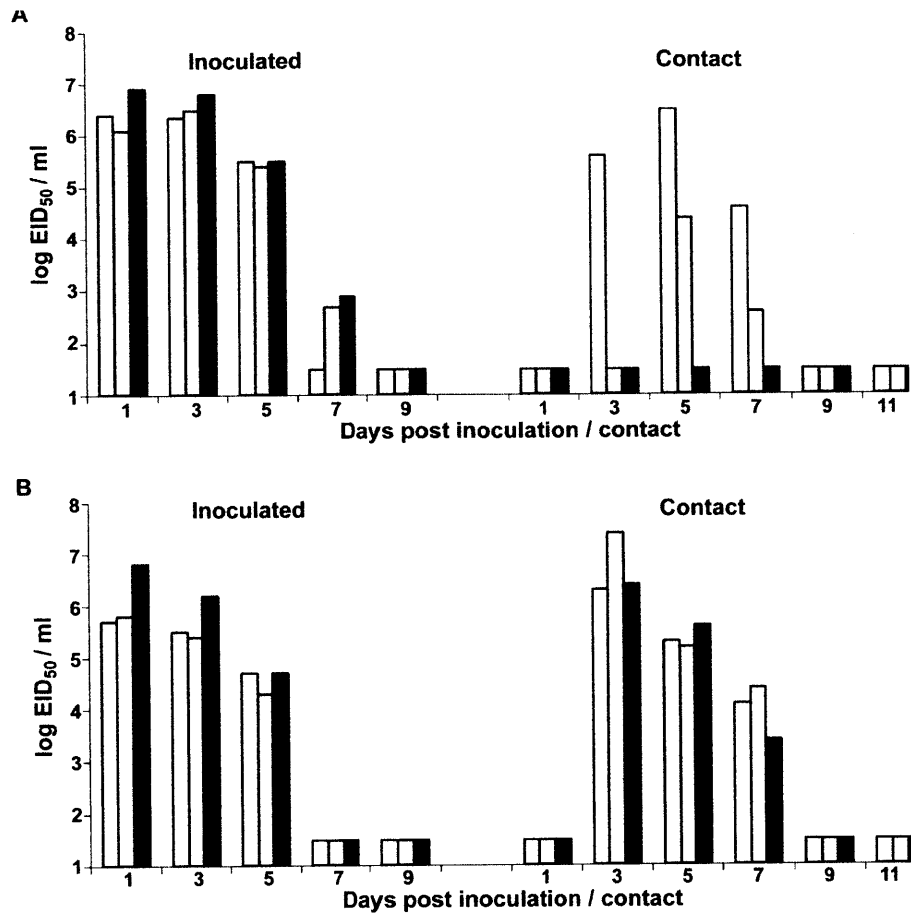


Figure 4.19 Respiratory droplet transmissibility of *rgCA04/09* and *rgCA04/09 HA Ile219Lys* mutant virus. Three ferrets were intranasally inoculated with 10^6 PFU of *rgCA04/09* (A) or *rgCA04/09 HA Ile219Lys* mutant virus (B). A naïve ferret was placed in an adjoining cage to each inoculated ferret and viral shedding in nasal washes was assessed every other day for the inoculated (left) and contact (right) ferrets. Results from individual ferrets are presented. Limit of detection is 10 PFU/mL.

4.4 Discussion and Significance of this study:

The emergence of the 2009 H1N1 virus created a global health concern given that it was a novel strain of influenza A resulting from reassortment of gene segments derived from avian, human and swine viruses. Although the 2009 H1N1 influenza A virus was declared as a pandemic, the epidemiological studies [111, 112, 168] [combined with our ferret transmission studies] showed that the virus had inefficient transmissibility as compared to other pandemic and seasonal strains. Average secondary attack rates amongst household contacts (comprising of 2-4 members) were ~13% in contrast to pandemic and seasonal influenza A viruses, which is greater than 40% [112]. We have in the current study, correlated this lower transmission efficiency of 2009 H1N1 virus to its lower binding affinity to human receptors as compared to seasonal and pandemic influenza A viruses. Currently the 2009 H1N1 virus circulates as a seasonal strain causing dispersed infection worldwide. A representative 2009 H1N1 strain, A/California/04/09 (CA04/09), was chosen for trivalent seasonal flu vaccine in 2010.

In the study presented here the receptor-binding site (RBS) of CA04/09 HA was also analyzed to gain insight into the amino acid interaction network that account for its lower receptor binding affinity. Based on this analysis and after comparing with the RBS of seasonal and pandemic influenza A HA, it was demonstrated that a single (Ile219→Lys or CA04/09mut2) amino acid change in the RBS of the HA, stabilizes the ionic molecular interaction network involving residues 219, 227 and 186 in the RBS of 2009 H1N1 HA that in turn substantially increases its human receptor affinity in comparison with wild-type HA. We also designed and tested another mutant form of CA04/09 HA involving three mutations (Ser186→Pro / Ala189→Thr / Glu227→Ala) to make this interaction network hydrophobic (similar to that in SC18 HA) and showed that this mutant (CA04/09mut2) HA had substantially higher affinity than wild-type HA. The findings presented here emphasize the importance of using a quantitative dose-dependent binding assay with recombinant HA in order to correlate biochemical glycan-binding affinity with molecular HA-glycan interactions. The increased human receptor affinity of the mutant HA (CA04/09mut1) correlated with efficient airborne transmission

of a virus that harbored this HA mutation in ferrets compared with inefficient transmission of the wild-type *rgCA04/09* virus. These results highlight two important aspects of understanding evolution of 2009 H1N1 virus. First, the inter-amino acid interaction network in the RBS plays a key role in governing human receptor binding affinity of HA. Second, the ferret transmission results demonstrate that the quantitative human receptor-binding affinity of HA is one of the key factors that govern human host adaptation of the virus for efficient human-to-human transmission.

It has been estimated that around 59% of United States population has some immunity to the 2009 H1N1 virus either due to pre-existing immunity, through vaccination, or due to the infection with the pandemic virus [169]. Recent surveillance data has shown that genetic variants of the 2009 H1N1 virus, carrying mutations in HA, have already begun to dominate the later part of 2010 in Singapore, New Zealand and Australia [170]. Although these mutations were found to be in the antigenic sites of HA, the strains carrying these mutations were not antigenically different from *CA04/09* (no significant differences in hemagglutination inhibition titers using ferret anti-sera raised to these viruses). Previous studies using another H1N1 strain (*A/Puerto Rico/8/34*) have shown that in order to escape polyclonal neutralizing antibody challenge, this virus acquires mutations in its HA that increased glycan receptor-binding affinity [171]. Given that the 219 position is a part of the antigenic loop and that a single amino acid mutation in 219 increases human receptor-binding affinity, this mutation may occur as a part of antigenic drift in the currently circulating 2009 H1N1 strains. Moreover, the Ile219->Lys mutation requires a single nucleotide change, which also increases the probability of such a mutation to occur. In summary, our study provides a systematic approach to monitor the evolution of HA mutations in the currently circulating 2009 H1N1 viruses that would potentially result in strains with higher human receptor-binding affinity and human-to-human transmissibility.

4.5 **Published Manuscripts:**

1. Maines TR, **Jayaraman A**, Belser JA, Wadford DA, Pappas C, Zeng H, Gustin KM, Pearce MB, Viswanathan K, Shriver ZH, Raman R, Cox NJ, Sasisekharan R, Katz JM, Tumpey TM. "Transmission and pathogenesis of swine-origin 2009 A(H1N1) influenza viruses in ferrets and mice". *Science* (2009); **325**(5939):484-7

Specific contribution made by this thesis towards this publication: Biochemical characterization of the glycan receptor binding property of the 2009 H1N1 HA was provided to correlate it with the viral transmissibility in ferrets. Further a structural analysis and HA sequence comparison of the 2009 H1N1 HA with other pandemic and seasonal HAs was done. This led to the identification of amino acid interaction network in the RBS of 2009 H1N1 HA that led to its lower receptor binding affinity. This was then validated in the following publication #2

2. **Akila Jayaraman**, Claudia Pappas, Rahul Raman, Jessica A. Belser, Karthik Viswanathan, Zachary Shriver, Terrence M. Tumpey, and Ram Sasisekharan "A single base pair change in 2009 H1N1 hemagglutinin increases human receptor affinity and leads to efficient airborne viral transmission in ferrets". *Plos One* (2011) 6(3): e17616. doi:10.1371/journal.pone.0017616

Chapter 5. Decoding the Distribution of Glycan Receptors for Human-Adapted Influenza A Viruses in Ferret Respiratory Tract

Summary

Ferrets are widely used as animal models for studying influenza A viral pathogenesis and transmissibility. Though ferrets exhibit similar clinical symptoms of influenza A infection as that observed in humans, the viral tropism is different between ferrets and humans. Human-adapted influenza A viruses primarily target the upper respiratory tract in humans, while in ferrets, both upper and lower respiratory tract are targets. Viral tropism is governed by the distribution of host sialylated glycan receptors, which are recognized by influenza A virus hemagglutinin (HA). Although detailed structural characterization of glycan receptors in human upper respiratory tract was done previously, much less is known about the distribution of glycan receptors in the ferret respiratory tract. In this study, a panel of plant lectins and recombinant HAs were used to stain ferret trachea (which represents the upper respiratory tract) and lung hilar region (which represents the lower respiratory tract). The sialylated glycan receptors recognized by human-adapted HAs are predominantly distributed in submucosal gland of lung hilar region as a part of O-linked glycans. Such a study has implications in understanding influenza A viral pathogenesis in ferrets and also in employing ferrets as animal models for developing therapeutic strategies against influenza.

5.1 Introduction

An important determinant of influenza A virus pathogenesis is the tropism of virus in terms of the specific tissues and cell types that it infects in different host species. The host tissue or cell tropism of the virus was investigated previously using *in vitro* pattern of viral adherence (PVA) to tissues from humans and other model animal systems or staining of fixed *ex vivo* tissue sections with viruses [39]. These studies demonstrated that human-adapted influenza viruses such as H1N1 and H3N2 subtypes specifically bind to human upper respiratory tissues (tracheal/bronchial), whereas avian-adapted viruses such as H5N1 bind to human deep-lung and gastrointestinal tract and avian respiratory tissues [39, 40].

Ferrets are widely used as an animal model for understanding influenza A viral pathogenesis and transmission. Unlike the mouse, human influenza A viruses infect the ferret without the requirement for prior host adaptation. Ferrets exhibit clinical signs (sneezing, fever and nasal discharge), pathogenesis, and immunity similar to humans upon influenza A infection [100]. Furthermore, ferrets show respiratory droplet transmission of viruses that have adapted to human host but not avian-adapted viruses [67, 158]. However, the tissue and cellular tropism of human-adapted viruses is different between ferrets and humans. In humans, viral binding and infection is observed predominantly in the upper respiratory tract [167], whereas in ferrets, it is observed in lower respiratory tract (specifically in the hilar regions and not as much in the alveolar regions) [20, 172, 173].

One of the important factors governing the tissue or cellular tropism of the virus is the specific binding of its surface glycoprotein hemagglutinin (or HA) to sialylated glycan receptors (complex glycans terminated by sialic acid) on the host cell surface [2, 174]. Human-adapted influenza A viruses preferentially bind to $\alpha 2 \rightarrow 6$ sialylated glycan receptors (or human receptors) wherein the terminal sialic acid is $\alpha 2 \rightarrow 6$ -linked to the penultimate galactose (Neu5Ac $\alpha 2 \rightarrow 6$ Gal). On the other hand, avian-adapted viruses bind preferentially to $\alpha 2 \rightarrow 3$ sialylated glycan receptors (or avian receptors) wherein the terminal sialic acid is $\alpha 2 \rightarrow 3$ -linked to the penultimate galactose (Neu5Ac $\alpha 2 \rightarrow 3$ Gal) [43,

82, 175]. The distribution of sialylated glycan receptors in cells and tissues of different species has been investigated by histological staining with plant lectins such as *Sambucus nigra* agglutinin (SNA) and *Maackia amurensis* lectin (MAL) [49]. The glycan-binding specificity of these plant lectins were defined traditionally based on their binding to a specific terminal sialic acid linkage, for example, SNA bound to $\alpha 2 \rightarrow 6$ -sialylated glycans and MAL bound to $\alpha 2 \rightarrow 3$ -sialylated glycans.

The advancements in the chemical and chemoenzymatic synthesis of glycans have led to development of microarray platforms comprising of hundreds of diverse glycan structures and structural motifs displayed on various surfaces [81, 84]. Screening the binding of plant lectins and HA on these glycan microarray platforms have permitted the elaboration of their glycan binding specificities going beyond the terminal sugars such as sialic acid linkage [84]. This expanded knowledge on glycan-binding specificities improves the use of these lectins and/or HAs in tissue staining experiments to obtain more detailed information on glycan structural motifs present on different tissues. Given the importance of ferrets as widely used animal models for influenza infection, in this study, the glycan structural motifs distributed in the trachea and hilar region (primary sites of influenza A virus infection) of the ferret respiratory tract was systematically characterized (**Figure 5.1**). This study has important implications in better understanding the tropism of influenza A viruses in the established ferret animal model that in turn provides a better understanding of the viral pathogenesis.

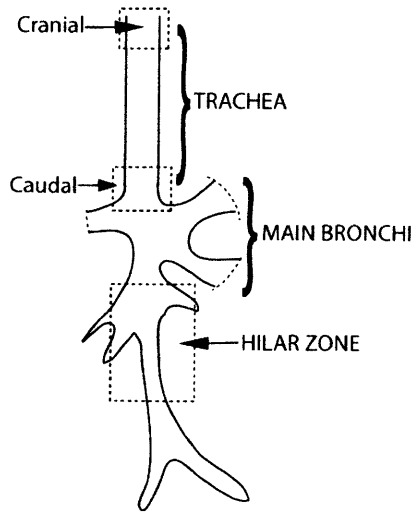


Figure 5.1 Regions of ferret respiratory tract analyzed in the study. Ferret trachea can be separated into a cranial region (upper trachea) and a caudal region (lower trachea). Hilar region represents the lower respiratory tract of ferret. The respiratory system of ferrets is adapted to its burrowing nature. The long trachea and the larger diameter airways in ferrets result in a much lower pulmonary and central airway resistance than other lab animals

5.2 Lectins as tools to probe the distribution of glycan receptors in ferret respiratory tract

The lectins used in this study and their glycan binding specificities are summarized in **Table 5.1**. In order to characterize the $\alpha 2 \rightarrow 6$ sialylated glycan receptors, SNA, and recombinant HAs of two prototypic human-adapted pandemic virus strains from the 1918 H1N1 pandemic, A/South Carolina/1/1918 (or SC18), and from 1957-58 H2N2 pandemic, A/Albany/6/58 (or Alb58) were used in this study. MAL was used to characterize $\alpha 2 \rightarrow 3$ sialylated glycan receptors. As observed earlier, human-adapted viruses showed predominant binding to non-ciliated (including goblet cells) cells in the upper respiratory tract [110]. Goblet cells are known to predominantly express O-linked glycans as a part of mucins [176, 177]. Jacalin, which has high specificity to Tn antigen (GalNAc-O-Ser/Thr) predominantly found as part of O-linked glycans in mucins, was used to delineate the goblet cell regions in the tissue section. These lectins and recombinant HAs were used individually or in a multiplexed fashion (co-staining) to stain different regions of the ferret respiratory tract that are known to be infected by human-adapted influenza A viruses. The extent of lectin staining of various cell types in the different tissue sections was visually scored and is summarized in **Table 5.2**. Based on this staining pattern, a detailed picture of the distribution of sialylated glycan structural

motifs going beyond terminal sialic acid linkage was obtained. This glycan receptor distribution observed in ferrets were further compared with that observed in the human upper respiratory tract.

Table 5.1 Lectins and their glycan binding specificities

<i>Lectins</i>	<i>Glycan motifs recognized</i>
SNA-I	
MAL-II	
Jacalin	
SNA-I/Jacalin co-staining	
SC18 HA (H1) from the 1918 pandemic	
Alb58 HA (H2) from the 1958 pandemic	

Nomenclature for the cartoon representation of distinct glycan motifs recognized by the lectins used in this study is as follows

●: Galactose ■: N-Acetyl Glucosamine ◆: N-Acetyl Neuraminic Acid ●: Mannose ■: N-Acetyl Galactosamine

5.2.1 Hematoxylin and Eosin staining of Ferret Respiratory Tract tissue sections

Paraffinized tissue sections (0.5u thickness) were stained with hematoxylin and eosin to identify distinct cell types and compare it with that of human respiratory tract. Tracheal tissue sections (cranial and caudal) and ferret lung hilar region were analyzed (**Figure 5.2**). Both ciliated and non-ciliated goblet cells (which store mucins that are heavily O-glycosylated) were identified in all the three regions. However, the regions

differed in the proportion of goblet cell distribution. The cranial region had very few goblet cells (identified as unstained non-ciliated cells) as compared to the caudal region. On the contrary, goblet cells formed a major fraction of the epithelium in the lung hilar region. Human trachea has more goblet cells than ferret trachea.

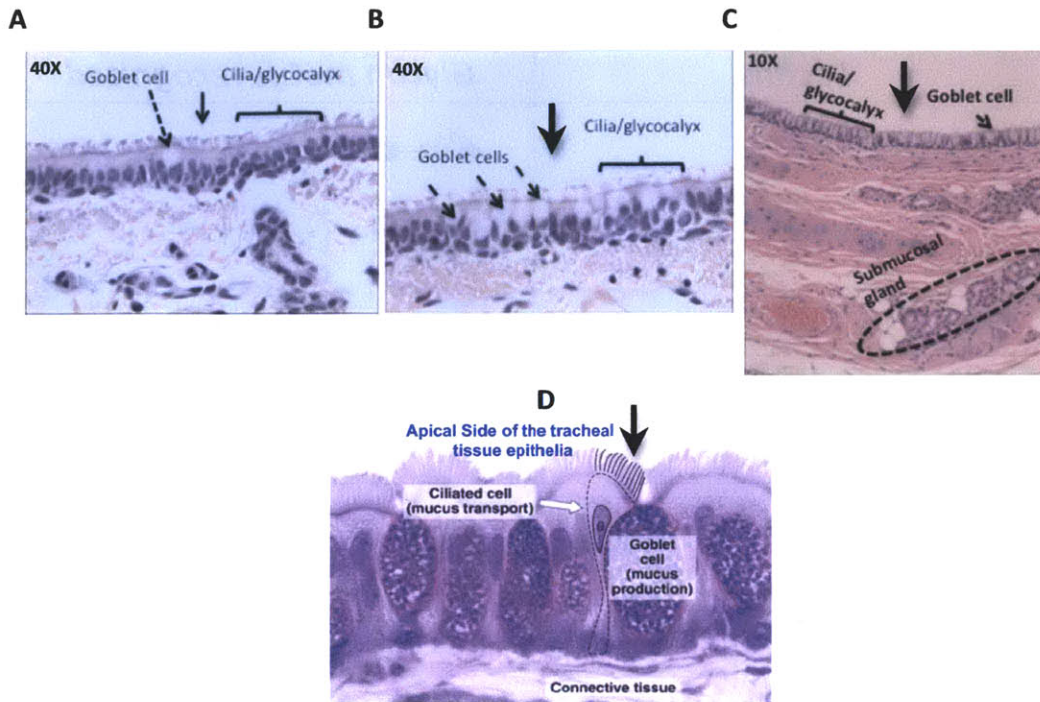


Figure 5.2 H & E stained images of tissue sections. Ferret Cranial (A), Caudal (B), Hilar region (C) and human Trachea (D) were stained with hematoxylin and eosin to identify major subcellular types and their distribution. As seen from the images, the lung hilar region which represents the lower respiratory tract, in ferret, seems to have more goblet cells than the ferret trachea (upper respiratory tract), a feature distinct from human respiratory tract wherein abundant goblet cells are found in trachea (upper respiratory tract) than in deep lung (lower respiratory tract). The apical surface is marked with a *black* arrow.

5.2.2 O-linked glycans in ferret respiratory tract

Jacalin was used to probe the distribution of O-linked glycans in ferret respiratory tract and in human trachea (Figure 5.3). All the goblet cells and submucosal glands that express soluble and membrane-bound mucins showed staining with Jacalin (Figure 5.3). All the goblet cells in the human trachea also showed intense staining with Jacalin. As was shown in H & E staining of the tissue sections, the ferret trachea cranial

region had goblet cells that were sparsely distributed as compared to the caudal region. The ferret lung hilar region had abundant goblet cells as highlighted by jacalin staining. Staining intensity in these cells was scored (**Table 5.2**).

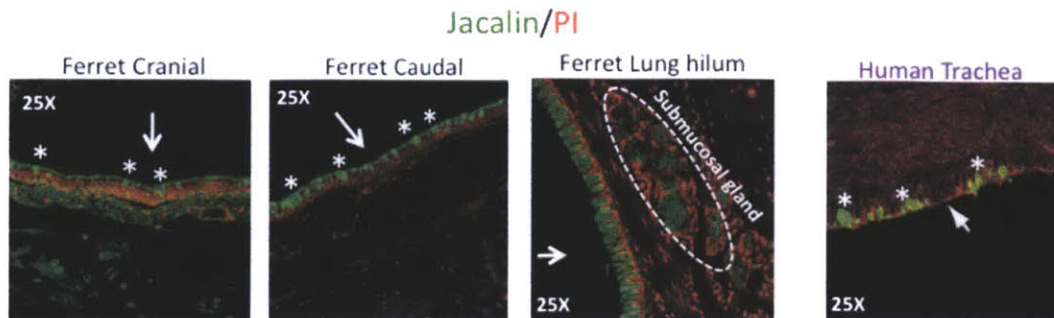


Figure 5.3 O-linked glycan distribution in ferret respiratory tract. FITC-labeled Jacalin (green), a plant lectin having specificity to Tn antigen was used to stain ferret cranial, caudal, lung hilar regions and human trachea. Jacalin stained the goblet cells, and the submucosal glands in all the three regions of ferret respiratory tract. In human trachea only the goblet cells were intensely stained with jacalin. The nuclei were stained with PI (red). The images were captured at 25X magnification. The apical surface is marked with a white arrow. The goblet cell staining is marked with a star (*).

5.2.3 O-linked $\alpha 2 \rightarrow 6$ glycan receptor distribution in ferret respiratory tract

Fluorescently labeled SNA-I was used to stain the tissue sections as mentioned above (**Figure 5.4**) to probe the distribution of $\alpha 2 \rightarrow 6$ glycans. Glycocalyx in the apical side of both cranial and caudal regions and the submucosal gland in ferret trachea showed significant staining with SNA-I. There was no staining of the goblet cells which suggests minimal expression of $\alpha 2 \rightarrow 6$ glycan motifs that are a part of mucin-type O-linked glycans typically found on goblet cells. In contrast to the ferret tracheal glycan receptor distribution, ferret lung hilar region showed significant SNA-I staining of goblet cells in the bronchial epithelium and of submucosal glands. This is also in contrast to human deep lung region that has predominant expression of $\alpha 2 \rightarrow 3$ glycans and not $\alpha 2 \rightarrow 6$ glycans [48, 49] In order to probe distribution of $\alpha 2 \rightarrow 6$ O-linked glycan in ferret respiratory tract, a combination of Jacalin and SNA-I was used to co-stain ferret trachea and lung hilar region (**Figure 5.5**). There was minimal to no co-staining of goblet cells in

ferret trachea (co-staining is identified by *yellow* staining pattern). There was significant co-staining of submucosal glands in ferret trachea. On the contrary, in the ferret lung hilar region, the submucosal glands and a fraction of goblets cells showed significant co-staining. This staining pattern indicates predominant distribution of $\alpha 2 \rightarrow 6$ sialylated glycan motifs as a part of cell surface mucin-type O-linked glycans in the hilar region as compared to the tracheal region of the ferrets. The tracheal staining pattern in ferrets is in contrast to human trachea wherein there is extensive co-staining of SNA-I and Jacalin in goblet cell regions [48]. The staining pattern in human trachea indicates substantial expression of $\alpha 2 \rightarrow 6$ sialylated glycan motifs as a part of mucin-type O-linked glycans in the goblet cell regions [48].

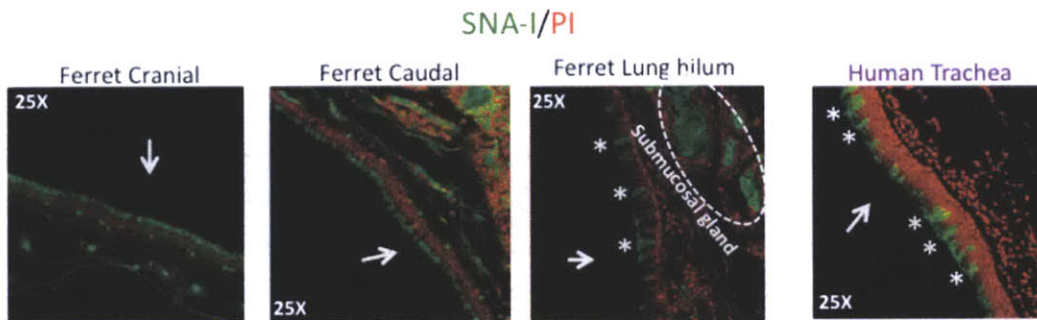


Figure 5.4 $\alpha 2$ -6 linked glycan distribution in ferret respiratory tract. FITC-labeled SNA-I (*green*) was used to stain ferret cranial, caudal, lung hilar region and human trachea. As seen from the images, SNA-I did not stain any of the goblet cells (in comparison to human trachea) in the ferret trachea although some of the goblet cells in the lung hilar region were stained by SNA-I. Submucosal glands and glycocalyx in both the trachea and lung hilar region showed significant staining with SNA-I. The nuclei were stained with PI (*red*). The images were captured at 25X magnification. Goblet cells staining is marked with a star (*). The apical surface is marked with a *white* arrow.

5.2.4 $\alpha 2$ -3 glycan receptor distribution in ferret respiratory tract

Maackia amurensis agglutinin (MAL-II) was used to probe $\alpha 2$ -3 glycan receptor distribution in ferret respiratory tract (**Figure 5.6**). There was no staining of the ciliated or non-ciliated cells in the tracheal cranial epithelium. Although there was staining of the underlying connective tissue. In the caudal region, there were a very small proportion of goblet cells (~1%) that showed faint staining with MAL II, indicating some expression of O-linked $\alpha 2$ -3 glycans. The underlying connective tissue was also

extensively stained with MAL-II. In contrast to the ferret trachea, there is no expression of α 2-3 linked glycans in the ferret lung hilar as indicated by a complete lack of staining of both ciliated and non-ciliated cells in the epithelium and in the underlying connective tissue and submucosal glands (**Figure 5.6**). The staining intensity was scored as shown in **Table 5.2**.

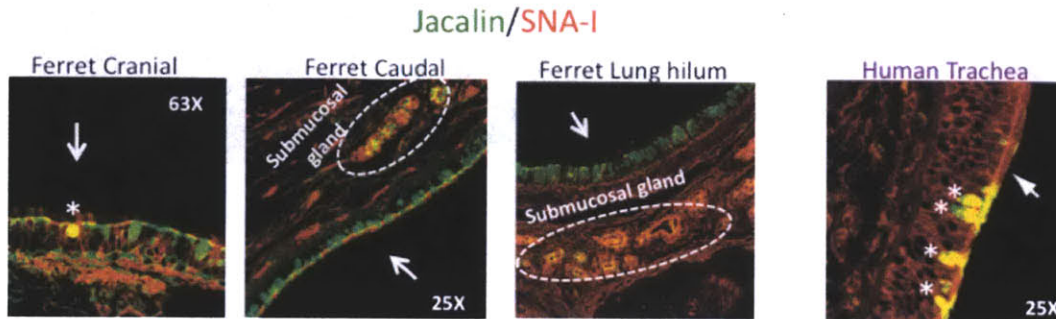


Figure 5.5 O-linked α 2-6 glycan distribution in ferret respiratory tract. Co-staining with FITC-labeled Jacalin (*green*) and SNA-I tagged to a 546nm fluorophore (*red*) was done to probe O-linked α 2-6 glycans in ferret cranial, caudal, lung hilar regions and in human trachea. Co-staining is seen as *yellow* color due to the overlap of *green* (Jacalin) and *red* (SNA) fluorophores. As seen from the images, although some co-staining was seen in the goblet cells in ferret lung hilar region, significant co-staining was seen in the submucosal glands. Submucosal gland co-staining was also seen in ferret trachea. This co-staining pattern is in contrast to human trachea wherein significant co-staining is seen in the goblet cells rather than in submucosal glands. The nuclei were stained with PI (*red*). The regions that show co-staining are marked with a star (*). The apical surface is marked with a *white* arrow.

MAL-II/PI (25X magnification)

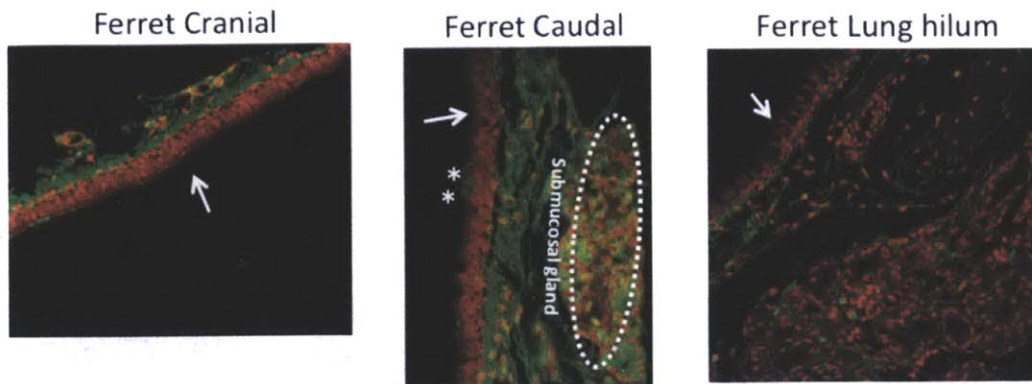


Figure 5.6 α 2-3 linked glycan distribution in ferret respiratory tract. MAL-II lectin (green) was used to stain ferret cranial, caudal and lung hilar regions. As seen from the images, MAL-II stained the submucosal glands, the underlying mucosa and some goblet cells (in the caudal region marked with broken arrow) in ferret trachea. There was no staining of the lung hilar region indicating an absence of α 2-3 sialylated glycans. The nuclei were stained with PI (red). The images were captured at 25X magnification. The apical surface is marked with a white arrow.

5.2.5 Tropism of human influenza A HA and distribution of their glycan receptors in ferret respiratory tract

It has been shown that human-adapted HAs from the pandemic viruses such as SC18 and Alb58 bind with high affinity to glycans having Neu5Ac α 2 \rightarrow 6-linked to longer oligosaccharide motifs (> trisaccharide) such as polylactosamine terminating in α 2 \rightarrow 6-linked sialic acid (6'SLN-LN) [95, 110]. Moreover, both these viruses from the 1918 and the 1958 pandemic have been shown to transmit efficiently via respiratory droplet in ferrets [67, 95]. SC18 HA shows highly specific binding to 6'SLN-LN and minimal binding to α 2 \rightarrow 3 sialylated glycans. On the other hand, Alb58 HA has a broader binding specificity to α 2 \rightarrow 6 sialylated glycans including both short α 2 \rightarrow 6 oligosaccharide such as 6'SLN and the longer 6'SLN-LN. In addition Alb58 HA also shows observable binding to α 2 \rightarrow 3 sialylated glycans albeit at a much lower affinity than that to α 2 \rightarrow 6 sialylated glycans [95]. Recombinant HAs have been used to stain human tracheal and alveolar tissue sections to probe the distribution of glycan receptors for human-adapted

influenza A viruses [48, 95, 98]. Therefore using these recombinant HAs to stain the ferret tracheal regions provides additional details on distribution of short and long $\alpha 2 \rightarrow 6$ oligosaccharide motifs.

SC18 HA showed predominant staining of submucosal glands in both ferret trachea and deep lung (**Figure 5.8**). It was interesting to note that SC18 HA did not stain goblet cells (which were stained by SNA-I) in lung hilar region. This indicates that $\alpha 2 \rightarrow 6$ sialylated glycans comprising of longer oligosaccharide motifs are more extensively distributed in the sub-mucosal glands in comparison with the goblet cells in the hilar region. On the other hand, due to a broader glycan binding specificity of Alb58 HA, it stained the glycocalyx and the underlying submucosal glands in ferret trachea (**Figure 5.7**). Alb58 HA also stained the goblet cells (similar to SNA-I) and the submucosal glands in the lung hilar region.

Furthermore, a characteristic staining pattern of human-adapted HAs such as SC18 and Alb58 is substantial binding to goblet cell regions of human tracheal tissue [95, 110] (**Figure 5.7**). Hence predominant binding to the $\alpha 2$ -6 glycan motifs is seen in the context of O-linked glycans. In order to correlate this in ferret respiratory tract, ferret tracheal and lung hilar tissue sections were co-stained with a representative HA (Alb58) and jacalin (**Figure 5.9**). Predominant co-staining was seen in the submucosal glands in ferret trachea (**Figure 5.11**) and lung hilum. Some co-staining was seen in the goblet cells in the tissue sections analyzed. This could also be due to the binding of O-linked $\alpha 2$ -3 sialylated glycan motifs in the goblet cells by Alb58 HA. Further staining with MAL-II lectin also indicated some expression of $\alpha 2$ -3 O-linked glycans (**Figure 5.6**). Hence it is the co-staining pattern indicates a predominant distribution of O-linked $\alpha 2$ -6 glycans (recognized by human influenza HAs) in submucosal glands of ferret respiratory tract. The restricted staining of submucosal glands by SC18 HA further corroborates this.

In order to verify the sialic acid binding specificity of lectins used in this study, the tissue sections were treated with *Sialidase A* prior to staining with the lectins. *Sialidase A* is an endonuclease that broadly cleaves terminal sialic acids (both $\alpha 2 \rightarrow 3$ and $\alpha 2 \rightarrow 6$). All the plant lectins and HAs used in this study showed a complete loss of

staining upon *Sialidase A* treatment of ferret tissue sections (**Figure 5.10**). However, in case of human trachea, the goblet cell staining by SNA-I is still retained upon *Sialidase A* treatment although there is a complete loss of SNA-I staining of the glycocalyx and also HA staining of both goblet cell region and glycocalyx on the apical surface. SNA-I has a broader $\alpha 2 \rightarrow 6$ sialylated glycan-binding specificity in that it binds to both Neu5Ac $\alpha 2 \rightarrow 6$ Gal(or GalNAc) $\beta 1 \rightarrow$ terminal motif in N- and O-linked glycans and Neu5Ac $\alpha 2 \rightarrow 6$ GalNAc $\alpha 1 \rightarrow$ O-Ser/Thr (sialyl-Tn-antigen) motif in O-linked glycans. On the other hand human-adapted HAs recognize at least a trisaccharide Neu5Ac $\alpha 2 \rightarrow 6$ Gal $\beta 1 \rightarrow 4$ GlcNAc $\beta 1 \rightarrow$ motif. This could perhaps explain the differences in loss of staining to human tracheal tissue by SNA-I and HAs after sialidase treatment.

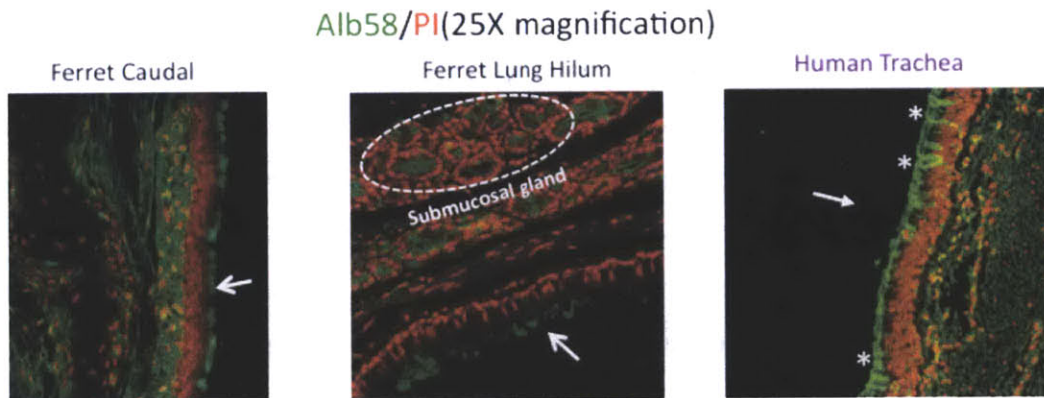


Figure 5.7 Glycan receptor distribution for recombinant Alb58 (H2) HA. Recombinant Alb58 HA (expressed in insect cells) was used to stain ferret trachea (shown is the caudal region), lung hilar and human tracheal regions. As seen from the images, Alb58 HA stained the submucosal glands, the underlying mucosa and some goblet cells in the caudal. This staining pattern is contrast to that in human trachea wherein all the goblet cells, submucosal glands and the glycocalyx are stained extensively with Alb58 HA. The nuclei were stained with PI (*red*). The significant goblet cell staining of Alb58 HA of human trachea as compared to ferret respiratory tract is in accordance with predominant expression of O-linked $\alpha 2$ -6 sialic acid in human tracheal goblet cells as compared to that in ferret respiratory tract (**Figure 5.4**). The images were captured at 25X magnification. The apical surface is marked with a *white* arrow.

SC18/PI(25X magnification)

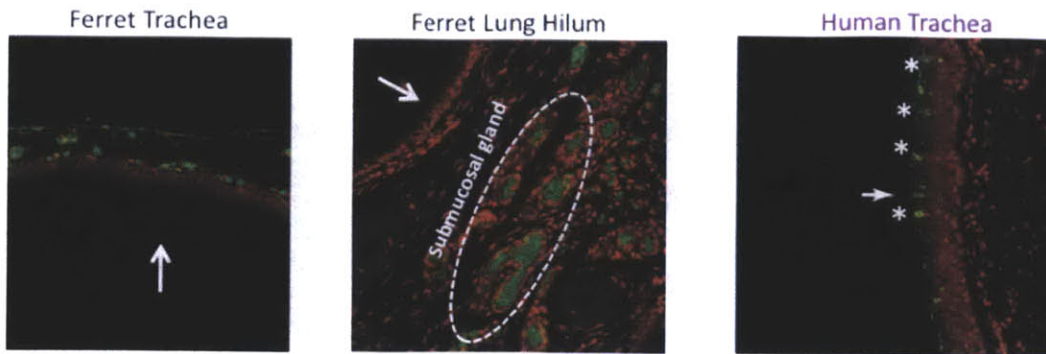


Figure 5.8 Glycan receptor distribution for recombinant SC18 (H1) HA. Recombinant SC18 HA (expressed in insect cells) was used to stain ferret trachea, lung hilar region and human trachea. As seen from the images, SC18 HA stained only the submucosal glands in the ferret lung hilar region. This restricted binding pattern of SC18 HA can be attributed to its stringent binding specificity to long α 2-6 linked (6'SLNLN) glycans. This restricted staining in human trachea is seen only in the goblet cells and not in submucosal gland. The nuclei were stained with PI (red). The goblet cell and submucosal gland staining is marked with a star (*). The images were captured in 25X magnification. The apical surface is marked with a *white* arrow.

Jacalin/Alb58(25X magnification)

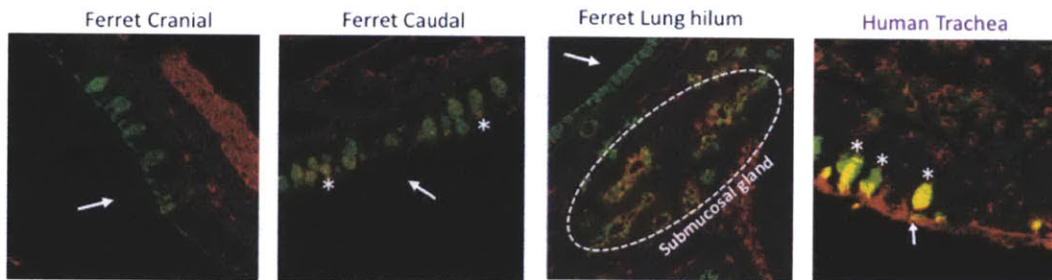
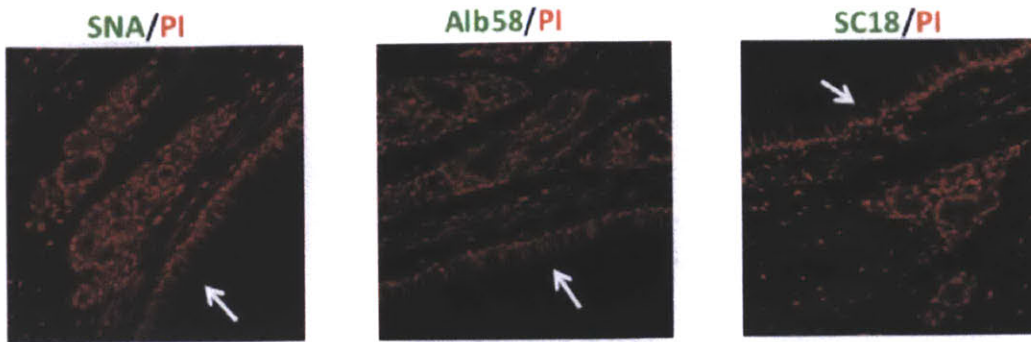


Figure 5.9 Co-staining of recombinant Alb58 (H2) HA with Jacalin. Ferret cranial (A) caudal (B) lung hilar region (C) were co-stained with 10 μ g/ml of Jacalin (FITC labeled) and 20 μ g/ml of recombinant Alb58 HA. The intensity of co-staining (*yellow*) was scored as shown in the table above. As seen from the images, co-staining was predominantly seen in the submucosal glands of ferret trachea and lung hilar region (A, B and C). Some co-staining was also seen in the goblet cells of trachea and lung hilar region. This staining pattern is in contrast to human trachea (D) wherein co-staining is predominantly seen in goblet cells. The goblet cell and submucosal gland staining is marked with a star (*). The images were captured in 25X magnification. The apical surface is marked with a *white* arrow.

A (Ferret Lung Hilar region)



B *Sialidase A* + SNA-I/PI (human trachea)

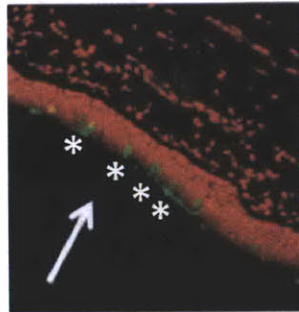


Figure 5.10 Sialic acid binding specificity of lectins. *Sialidase A* from *Arthrobacter ureafaciens* was used to cleave all the sialic acids from the relevant tissue sections (shown is that for the ferret lung hilar region) prior to staining with **(A)** SNA-I, Alb58 HA and SC18 HA (green). There was a complete loss of staining upon *Sialidase A* treatment. This was compared with the staining pattern of **(B)** SNA-I of human trachea, where the goblet cell staining was retained upon *Sialidase A* treatment. There was a complete loss of SC18 and Alb58 HA staining of human trachea upon *Sialidase A* treatment (data not shown). The goblet cell staining in human trachea (after *Sialidase A* treatment) is marked with a star (*). The images were captured in 25X magnification. The apical surface is marked with a white arrow.

Jacalin/Alb58 HA

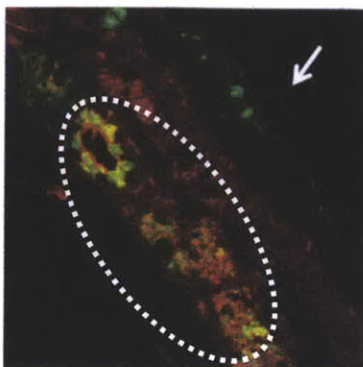


Figure 5.11 Submucosal gland co-staining with Jacalin and Alb58 HA. Submucosal glands in the ferret trachea showed extensive co-staining with Jacalin and Alb58 HA. The co-staining is indicated by a *yellow* staining pattern. The submucosal glands are marked by *white* dotted circle. The images were captured in 25X magnification. The apical surface is marked with a *white* arrow.

5.3 Discussion and significance of this study:

Ferrets are widely used as an animal model for understanding influenza A viral pathogenesis and transmission. Although ferrets exhibit similar clinical manifestation as that of humans upon influenza A infection, there seems to be a difference in viral tropism between ferrets and humans. Upper respiratory tract is the primary site of influenza A infection in humans. Apart from upper respiratory tract, involvement of lower respiratory tract (lung hilar region) is also reported in ferrets. Viral tropism impinges on the viral pathogenesis and hence understanding former is crucial. Viral tropism is determined by distribution of influenza A glycan receptors, which are recognized by the viral hemagglutinin (HA) to gain entry into the epithelial barrier. In this study a panel of plant lectins and recombinant HAs were used to probe the distribution of glycan receptors for influenza A HA (**Figure 5.12**). As can be seen from this analysis, there are differences in the glycan receptor distribution between human and ferret respiratory tract. SNA-I lectin staining showed that α 2-6 glycans are predominantly found in the glycocalyx and submucosal glands in both ferret trachea and lung hilar region. Some of the goblet cells in the lung hilar region also showed staining

with SNA-I. Of these the long α 2-6 glycans, which are the main receptors for human-adapted influenza A HA are predominantly found in the submucosal glands in both ferret trachea and lung hilar region (**Figure 5.9**). This correlates with earlier reports of viral antigens being predominantly found in the submucosal glands in ferret trachea and lung hilar region upon infection with human influenza A virus [178]. It is interesting to note that though glycan receptors for human influenza A viruses are differentially distributed in humans and ferret, they are predominantly expressed in the context of O-linked glycans in either goblet cells (in humans) or in submucosal glands (in ferrets). Binding to these mucin secreting cells could potentially might promote respiratory droplet mediated transmission of the virus and hence contribute to viral pathogenesis. This further demands for studies evaluating the role of mucins in influenza A infection. The recent findings on increased expression of this Tn antigen (in the context of mucin secreting cells) upon virus infection due to goblet cell and/or acinar gland neoplasia was shown [179]. This highlights yet another aspect of influenza A virus infection, though its exact role in viral pathogenesis has to be elucidated.

MAL-II lectin staining of ferret tissues showed that that there are no α 2-3 sialylated glycans found in the ferret lung hilar region. This is in contrast to humans, wherein α 2-3 glycans are predominantly expressed in deep lung region. This warrants the need to assess ferret as a model system especially to study avian influenza A virus (e.g. H5N1) pathogenesis. This is because, the viral tropism (determined by glycan receptor distribution), impinges on the route of transmission and pathogenesis. Hence varying sites of infection (in humans and ferrets), can make it challenging to correlate viral pathogenesis of avian influenza A viruses in ferrets to that in humans.

In summary, using a panel of lectins, the glycan receptor distribution for influenza A HA in ferret respiratory tract was systematically characterized (**Figure 5.9**). Also the staining intensity of lectins in specific cell types was visually scored (**Table 5.2**). Such an approach is needed to understand viral pathogenesis in ferrets in order to truly correlate it with that in humans. Moreover, it is important to have a thorough understanding of glycan receptor distribution for improving anti-influenza drug delivery

strategies for especially those drugs, which target glycan receptors such as DAS181, a sialidase fusion protein that cleaves off the sialic acid and hence prevents viral entry [180].

Table 5.2 Visual scoring of lectin staining intensity of various cell types in ferret upper (trachea) and lower (lung hilar region) tract

Lectins used	Trachea			Lung Hilar		
	<i>Glycocalyx</i>	<i>Goblet cells</i>	<i>Submucosal glands</i>	<i>Glycocalyx</i>	<i>Goblet cells</i>	<i>Submucosal glands</i>
SNA I	++	-	++	+	+	++
MAL II	-	+/-	++	-	-	-
Jacalin	++	++	++	-	++	++
SNA/Jacalin co-staining	-	-	++	-	+	++
A/Albany/6/58 (Alb58) HA	++	-	++	+	+	++
A/South Carolina/1/18 (SC18) HA	-	-	++	-	-	++
Alb58 HA/Jacalin co-staining	-	+	++	-	+	++

- No staining
- + Moderate staining
- +/- Only few cells stained (<10%)
- ++ Extensive staining

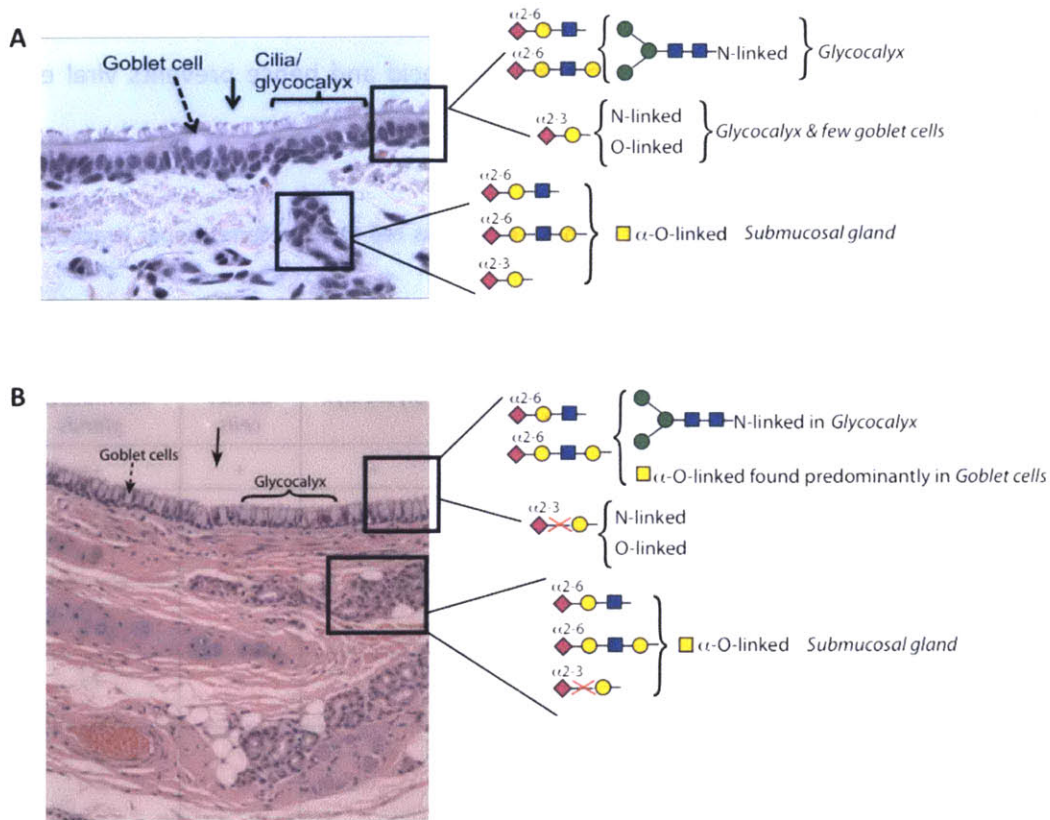


Figure 5.12 Mapping of glycan receptor distribution in ferret respiratory tract. The figure shown above highlights the glycan receptor distribution in ferret trachea **(A)** and in lung hilar region **(B)**. Note that predominant α 2-6 glycan receptors recognized by human influenza A viruses are found in the submucosal glands of trachea and lung hilum. Further, unlike human lower respiratory tract, there is minimal to no α 2-3 sialylated glycan receptor expression in the lung hilar region of ferret. Except for differences in the number of goblet cells in ferret cranial and caudal region, there were no significant differences in the glycan receptor expression. The apical surface is marked with a *black* arrow.

Chapter 6. Targeting Glycan Receptors of Influenza A virus: A Viable Alternative Strategy

Summary

One of the major challenges with the currently available anti-viral therapeutics is the evolution of drug resistant strains. Also the vaccine against flu has to be updated annually due to emergence of new strains of viruses by antigenic drift. In essence any antiviral strategy targeting the viral components can lead to evolution of drug resistant strains. This chapter reports our strategy of targeting the host glycan receptors instead of the viral components. Two specific plant lectins; SNA-I and PSL, which have binding specificity to α 2-6 sialylated glycans (6'SLN and 6'SLNLN), which are predominantly recognized by human influenza A viruses on the host cell surface, were chosen to target glycan receptors. Unlike SNA-I, PSL was easily expressed in E.coli based expression system and hence PSL was chosen for the study. The glycan-binding domain of PSL lectin (designated as rPSL-N) was recombinantly expressed. This domain by itself displayed stability and retained the glycan binding specificity as that of the native lectin which was validated using a combination of homology-based structural modeling of rPSL-N – trisaccharide motif complex and a dose-dependent glycan array binding assay. While native PSL was highly cytotoxic, rPSL-N was not cytotoxic even at the highest concentration tested. rPSL-N was able to effectively inhibit infection of MDCK cells by representative H3N2 and H1N1 influenza A viruses. Here our study provides an alternate viable strategy to combat influenza infection using rPSL-N that can block viral infection by its high affinity binding to the sialylated glycan receptors of human-adapted influenza A virus HA.

6.1 Introduction

Annually the seasonal influenza epidemic results in about three to five million cases of severe illness [181]. Illnesses result in hospitalizations and deaths mainly among high-risk groups (the very young, elderly or chronically ill). The current anti-viral strategies against influenza A virus includes an annual formulation of influenza A vaccine and other small molecule anti-viral drugs. The following section describes these anti-viral strategies in detail.

6.1.1 Vaccines to prevent influenza A infection

Vaccines against influenza have been around for 50 years. The results of challenge studies indicated that immunity is induced by the host responses to the virus hemagglutinin (HA) and to neuraminidase (NA). Antibody against HA is the most important component in the protection against influenza viruses. Due to a lower density of NA in comparison to HA, the host antibody response is more skewed towards HA [182]. The annual trivalent influenza A vaccine comprises of a combination of A/H3N2, A/H1N1 (seasonal) and influenza B viruses. Though vaccination has been successful in reducing human cost of influenza virus infection, antigenic drift and complete genetic reassortments periodically result in new viral strains, which require vaccines to be constantly updated.

6.1.2 Therapeutic strategies to combat influenza A infection

There are currently two classes of therapeutic agents against influenza A viruses: the M2 channel blockers (adamantanes) and neuraminidase inhibitors or NAIs (oseltamivir and zanamivir) [7]. Both of these are described in detail in the following section.

6.1.2.1 M2 channel blockers (adamantanes)

Amantidine and rimantidine are M2 channel blockers that are only effective against influenza A, because only A strain of viruses have M2 ion channel proteins. Both these adamantane class of drugs blocks M2 channel protein that is implicated in viral uncoating.

Amantidine has been shown to have both therapeutic and prophylactic effects. The compound confers 70% protection against influenza A when given prophylactically. Amantidine can occasionally induce mild neurological symptoms such as insomnia, loss of concentration and mental disorientation. The therapeutic and prophylactic activity of amantidine is now generally accepted and numerous analogues of this compound have been prepared. Prophylaxis with 200mg of amantidine per day for 5 to 6 weeks or for the duration of the influenza A outbreak is not recommended for all persons. However, elderly persons with chronic underlying disease, institutionalized persons, staff and patients in hospital, close contacts of an index case, and patients who cannot receive influenza A vaccine due to sensitivity to egg protein may benefit from prophylaxis. Amantidine can also be used for therapy of uncomplicated influenza A infections. The recommended dose is 200mg for 5 days.

Rimantidine may be used in place of amantidine for prophylaxis and the treatment of uncomplicated influenza A infections. Rimantidine is similar to amantidine but has fewer side effects. It is approved by the FDA for the treatment and prophylaxis of influenza A infection in persons one year or older. It should be used for uncomplicated influenza A infections only since it is thought to be less effective than amantidine. Amantidine and rimantidine resistant viruses are readily generated in the laboratory. Resistance has been linked to changes in the M2 protein. To date, the emergence of resistant influenza A has been documented primarily in young children undergoing therapy with rimantidine. The resistant viruses had been transmitted and caused influenza. The universal susceptibility of all types of naturally occurring influenza A isolated from man and animals suggests that resistance will be found only in individuals treated with the drug.

6.1.2.2 Neuraminidase inhibitors (NAI)

The rational approach to drug design has led to the design of several potent inhibitors of influenza neuraminidase. Zanamivir was the first neuraminidase inhibitor available for clinical use and is effective against both influenza A and B. Because of its poor bioavailability, zanamivir must be administered by inhalation. Zanamivir had been shown to be effective and devoid of significant side effects in clinical trials. It is now approved by the FDA for use as treatment for influenza A and B in persons 12 years or older but not for prophylaxis.

Oseltamivir is another neuraminidase inhibitor but unlike zanamivir, it can be given orally. Like zanamivir, it had been shown to be effective and devoid of significant side effects in clinical trials. It is approved by the FDA for use as treatment for influenza A and B in persons 18 years or older. It is also approved for prophylaxis in persons 13 years or older. Lack of side effects with neuraminidase inhibitors makes them particularly an attractive drug against influenza.

Apart from the aforementioned therapeutic agents, there are drugs designed against other viral components such as ribavirin, which inhibits viral RNA polymerase. Ribavirin was found to have inherent cytotoxicity and hence is not used currently [183]. With the recent identification of host factors necessary for viral replication [184], research is underway to target some of these host factors such as receptor tyrosine kinase. Drug targets against these demand more analysis to evaluate their specificity and hence cytotoxicity. Moreover any drug that targets viral components can potentially lead to an emergence of drug resistant viral strains. Therefore the search continues for effective broad-spectrum therapeutic agents for influenza A virus. Targeting the glycan receptors of influenza A virus instead presents an attractive alternate therapeutic strategy to counter viral infection. Moreover, such a strategy is less likely to induce drug resistance given that a change in specificity to the target glycan receptors would alter host tissue tropism of the virus or a loss of replicative efficiency of the virus in the human upper respiratory tract.

6.1.3 *Plant lectins as tools to target host glycan receptor*

As mentioned in chapter 1 of this thesis, the viral coat glycoprotein, hemagglutinin (HA), is a lectin, which recognizes specific sialylated glycan receptors on the surface of host cell and mediates attachment, viral entry and membrane fusion events [14, 54]. Specifically the HA of human-adapted influenza A viruses recognize $\alpha 2 \rightarrow 6$ sialylated glycan receptors, i.e. glycans terminated by N-acetyl neuraminic acid (Neu5Ac) linked $\alpha 2 \rightarrow 6$ to galactose (Neu5Ac $\alpha 2 \rightarrow 3$ Gal), expressed on the human upper respiratory epithelia [41]. On the other hand HA of avian influenza A viruses recognize $\alpha 2 \rightarrow 3$ sialylated glycan receptors (Neu5Ac $\alpha 2 \rightarrow 3$ Gal) expressed both on the gut and respiratory epithelia of birds [40, 49].

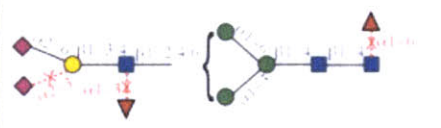
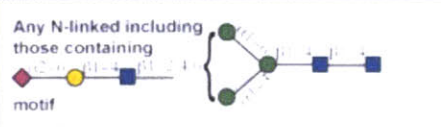

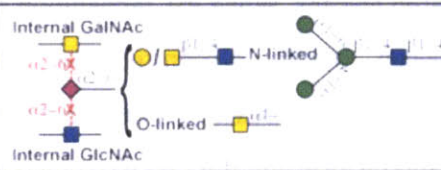
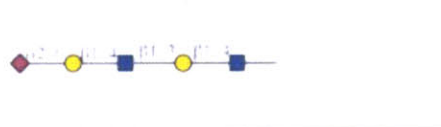
Plant lectins that recognize human receptors for influenza A viruses. The data mining method described by Srinivasan *et al* (2008) was used to determine binding classifiers or rules in terms of glycan structural motifs that govern binding of each lectin to the glycan array. Motifs that have a detrimental effect on binding are shown in *red* dotted line with *red* 'X'. Calsepa, Morniga and SaIT show binding to $\alpha 2 \rightarrow 6$ sialylated glycans in the context of the trimannosyl-core and hence they also bind to several non-sialylated N-linked glycans. On the other hand PSL and SNA-I bind exclusively to $\alpha 2 \rightarrow 6$ sialylated glycans. While PSL recognition requires a trisaccharide motif (common feature of glycan motifs recognized by human-adapted HA), SNA-I also recognizes Neu5Ac $\alpha 2 \rightarrow 6$ GalNAc $\alpha 1 \rightarrow$ motif in O-linked glycans. The glycan array data can be accessed by inserting the CFG ID (shown in first column) at the end of the following URL: http://www.functionalglycomics.org/glycomics/HServlet?operation=view&sideMenu=n_o&psId=. Based on this analysis, we hypothesized that the glycan-binding domain of SNA-I and PSL could potentially be used to target host glycan receptors to combat influenza A infection.

6.2 *Sambucus nigra agglutinin I or SNA-I to target host glycan receptor*

In 1984 SNA-I was isolated from the elder (*Sambucus nigra*) bark by affinity chromatography on fetuin-agarose [185, 186]. The lectin was found to be rich in

asparagine/aspartic acid, glutamine/glutamic acid, valine and leucine. SNA-I belongs to the family of type II ribosome-inactivating protein (RIP) containing an A-chain or RNA *N-glycosylase* domain which binds to one specific adenosine of the large ribosomal RNA and catalyzes the endohydrolysis of the N-glycosidic bond, whereas the B-chain comprises a typical glycan binding or a lectin domain [187].

Table 6.1 Rationale for Selection of SNA-I and PSL to target the glycan receptors of Influenza A virus

Protein	Binding Classifiers
<i>Calystedia sepium</i> lectin (<i>Calsepa</i>) CFG ID: <i>primscreen_3428</i>	
<i>Morus nigra</i> lectin (<i>Morniga</i>) CFG ID: <i>primscreen_3431</i> <i>Orystata satvia</i> lectin (<i>SaIT</i>) CFG ID: <i>primscreen_3424</i>	Any N-linked including those containing motif 
<i>Polyporus squamosus</i> lectin (<i>PSL</i>) CFG ID: <i>primscreen_2825</i>	
<i>Sambucus nigra</i> agglutinin (<i>SNA-I</i>) CFG ID: <i>primscreen_2794</i>	Internal GalNAc  Internal GlcNAc
<i>A/South Carolina/1/18</i> HA (Human H1N1) CFG ID: <i>primscreen_PA_v1_262_12072005</i> <i>A/Moscow/10/99</i> HA (Human H3N2) CFG ID: <i>primscreen_PA_v1_260_12072005</i>	

●: Galactose ■: N-Acetyl Glucosamine ◆: N-Acetyl Neuraminic Acid ●: Mannose ■: N-Acetyl Galactosamine

6.2.1 Molecular structure of SNA-I

SNA-I specifically binds to the disaccharide motif Neu5Ac α 2-6Gal/GalNAc [47, 186, 188]. SDS-PAGE of reduced and iodoacetylated SNA-I has demonstrated that it is composed of two different polypeptides, namely an A chain of 33kDa and a B chain of 35kDa (**Figure 6.1A**). Molecular cloning and sequence analysis demonstrated that the B chains consist of six randomly arrayed subdomains (1α , 1β , 1γ , 2α , 2β , 2γ) of approximately 40 amino acid residues. The domain 1 and 2 adopt a characteristic β -trefoil fold reported for carbohydrate binding domains of toxins such as ricin which is a type 2 ribosome inactivating protein (RIP) [186, 188]. Only subdomains 1α , and 2γ possess a functional carbohydrate-binding site where 1α is a low affinity glycan binding site whereas 2γ is a high affinity glycan binding site (**Figure 6.1B**) [189].

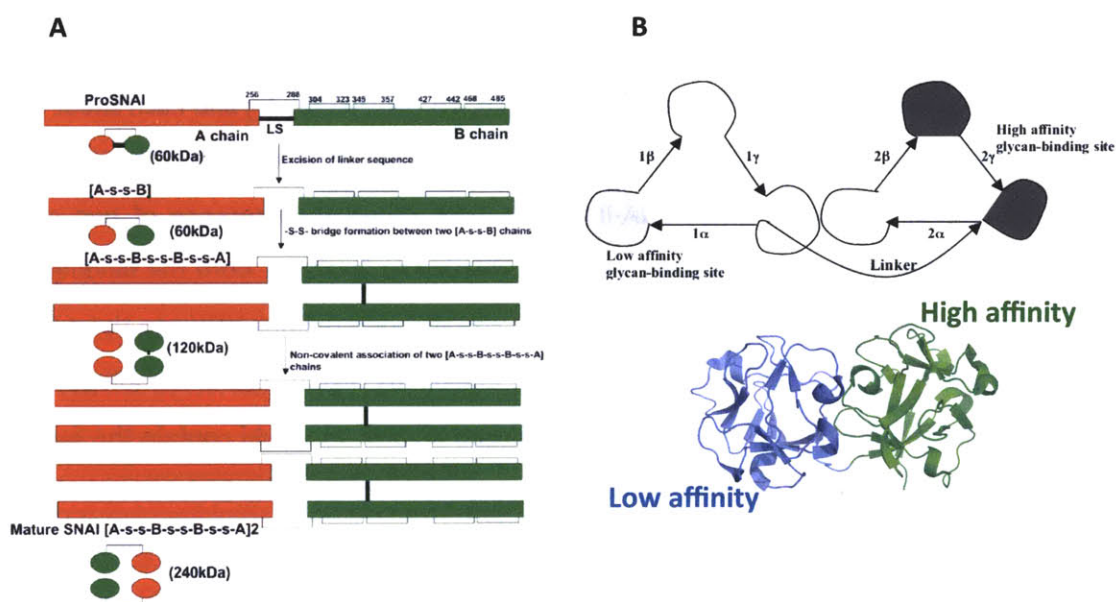


Figure 6.1 (A) Molecular structure of SNA-I Schematic representation of molecular structure of the mature lectin. Shown are the key steps involved in the generation of mature lectin from SNA-I precursor. **(B)** Schematic representation of the β -trefoil structure of the B chain (generated by homology modeling). Shown are the high affinity and a low affinity glycan binding sites. Shown in the *top* is the cartoon representation of the molecular model of the B chain shown *below*.

6.2.2 Homology modeling of SNA-I

Given that there are no X-ray crystal structures of SNA-I, homology based structural model of its lectin domain was generated. The co-crystal structure of SNA-II (the lectin domain or B chain) in complex with lactose (PDB ID: 3CA4) [190] was chosen as the template. The homology-based structural model was obtained using the SWISS-MODEL web-based homology modeling tools (<http://swissmodel.expasy.org/>) (**Figure 6.1B**). The use of co-crystal structures as templates facilitated the identification of the glycan-binding sites and docking of α 2-6 oligosaccharide motifs into the putative glycan binding sites helped in analyzing the molecular contacts between the lectin and the glycan motif.

Based on the homology modeling, details on various aspects of structural features of the lectin domain were obtained. First, the lectin domain of SNA-I adopts a ricin-B chain like fold comprising of two β -trefoil scaffolds connected by a linker. Second, each scaffold has three antiparallel β sheets (1α , 1β , 1γ , 2α , 2β , 2γ) and each sheet has 4 β -strands (A, B, C and D) connected by loop regions (**Figure 6.1B**). The co-crystal structure of lectin domain of SNA-II with lactose shows the presence of two glycan binding sites, one in the 1α sheet and the other in the 2γ sheet. Both the binding sites are constituted by two antiparallel β strands and the loop regions between them, - 1α C-loop- 1α D-loop- and 2γ C-loop- 2γ D-loop-. The analogous regions in the homology model of the lectin domain of SNA-I (constructed based on SNA-II) would contain the putative glycan binding sites. Indeed, site-directed mutagenesis studies with SNA-I have indicated the presence of a high affinity binding site in the 2γ and a relatively lower affinity binding site in the 1α sheet [189].

6.2.3 Characterizing the glycan binding properties of native SNA-I

As mentioned earlier, SNA-I has specificity to α 2-6 sialylated glycans. Not much is known about its specificity beyond its linkage specificity. Hence even before we designed engineered constructs based on SNA-I, it was imperative to understand its glycan binding specificity beyond its linkage specificity. Hence SNA-I was analyzed on the

glycan array platform to quantitatively and qualitatively characterize its binding affinity and binding specificity. Further, SNA-I (labeled with fluorescein isothiocyanate designated as SNA-FITC) was used to stain human tracheal tissue sections to understand its glycan binding specificity in the context of N- and O- linked glycans.

A dose-dependent glycan array analysis was performed with SNA-FITC. The analysis showed a highly specific binding of SNA-I to α 2-6 glycans (6'SLN and 6'SLNLN). No binding to α 2-3 glycans was noticed (**Figure 6.2**). The binding affinity to the α 2-6 glycans was calculated by fitting in the Hill's equation and was found to be in the sub-picomolar range. Staining of human tracheal tissue section revealed that SNA-I stained α 2-6 glycans in the context of both N- and O- linked glycans (**Figure 6.3A**). SNA-I stained the apical surface or the glycocalyx (that has a predominant expression of N-linked glycans) and stained the non-ciliated goblet cells (which have a predominant expression of mucin-like O-linked glycans). Staining of O-linked glycans was further validated by co-staining SNA-I with Jacalin (a lectin that binds to Tn antigen predominantly found in O-linked glycans) (**Figure 6.3A**). *Sialidase A* pre-treatment of human tracheal tissues prior to SNA I staining caused loss of binding to the apical surface of the ciliated epithelial cells (predominantly express N-linked glycans) but not to the goblet cells (**Figure 6.3B**). This pattern is consistent with the ability of SNA I to bind to the additional disaccharide Neu5Ac α 2 \rightarrow 6GalNAc α 1 \rightarrow motif in O-linked glycans.

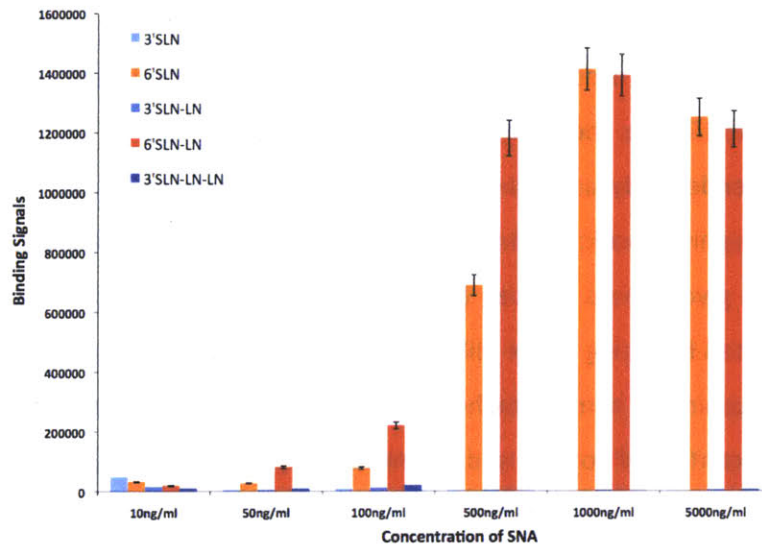
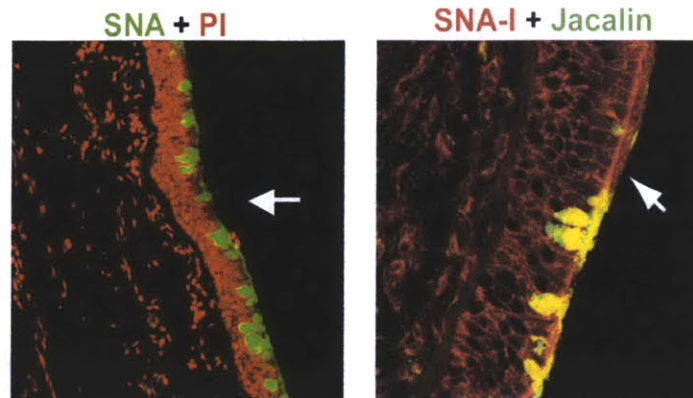


Figure 6.2 Glycan binding specificity of SNA-I. Glycan binding specificity of SNA-I was characterized by performing dose-dependent glycan array analysis. SNA-I has highly specific binding to α 2-6 glycan. Binding affinity of SNA-I to 6'SLN was calculated by linearized Hill's plot. The binding affinity was in the sub-picomolar range for both 6'SLN and 6'SLNLN.

A



B

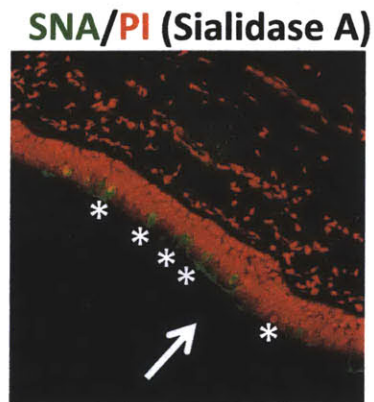


Figure 6.3 Cellular tropism of SNA-I. FITC labeled SNA-I (*green*) was used to stain paraffinized human tracheal tissue sections. SNA-I showed specific binding to the apical surface of the tracheal epithelium. Both the glycocalyx and the non-ciliated goblet cells were stained by SNA-I (**A**). Goblet cell staining by SNA-I was confirmed by co-staining tissue sections with both SNA-I and Jacalin (a lectin that binds to mucin O-linked glycans in goblet cells). Co-staining is seen as *yellow* staining of the goblet cells (**A**). *Sialidase A* (from *Arthrobacter ureafaciens*) treatment of human tracheal tissue prior to staining with SNA leads to loss of apical surface staining but some goblet cell staining is retained. Nuclei was counterstained with propidium iodide (*red*). The images were captured at 25X magnification. The goblet cell staining is marked with a star (*). The apical surface is marked with a *white* arrow.

6.2.4 Engineering SNA-I to target glycan receptors

The effect of the observed spatial distribution of the two glycan binding sites across two β -trefoil scaffolds on the glycan binding affinity of SNA-I is unclear. Therefore multiple constructs with different spatial arrangements of the glycan binding sites were constructed (**Figure 6.4**) and evaluated for their glycan binding properties to determine the best candidates for targeting the HA-glycan interactions (**Figure 6.5**). The basis for generation of these constructs was to generate the smallest possible protein scaffold that can retain the glycan binding properties viz., specificity and affinity as that of the native SNA-I.

- I. The 2α - 2β - 2γ C-terminal single β -trefoil scaffold that comprises of the putative high affinity glycan-binding site (~121 amino acids)
- II. Construct that has only the 2γ antiparallel β -sheet (42 amino acids) – it is anticipated that this single antiparallel β sheet would likely self-associate into a dimer or trimer given that it is derived from the β -trefoil scaffold comprising of a hydrophobic core.

Strategy 1: 121aa sequence of SNA-I B-chain

2α B loop 2α C 2α D 2β A 2β B 2β C 2β D
 TFFIV GYKQM **C**LRN GENN FVWLE **D**CVLNRVQQ EWAL YGDG TIRV NSNRSL **C**VTS EDHEP**S**DL**I** VILK

 2γ A 2γ B 2γ C 2γ D 2α A
CEGSGNQ **R**WVF NTNG **T**ISN PNAKL **L**M**V** **A**QRDVSLR**K** **I**L**L****V** RPT**G****N****P****N****Q** **Q**WITT

Strategy 2: 42aa sequence of SNA-I B chain

2γ A . . . 2γ B 2γ C 2γ D
RWVF NTNG **T**ISN PNAKL **L**M**V** **A**QRDVSLR**K** **I**L**L****V** RPT**G****N****P****N****Q**

Figure 6.4 Strategies adopted for engineering SNA-I B chain. In strategy 1 (*top*), the entire β -trefoil scaffold comprising the high affinity glycan binding site was retained. In strategy 2 (*bottom*), only the 2γ sheet of β -trefoil scaffold (high-affinity glycan binding site) was chosen. **Key:** **X** – residue within β -strand; **X** – side-chain facing inside of β -trefoil core; **C** – cysteine involved in di-sulfide linkage; **X** - residue involved in contacts with Neu5Ac α 2-6Gal-

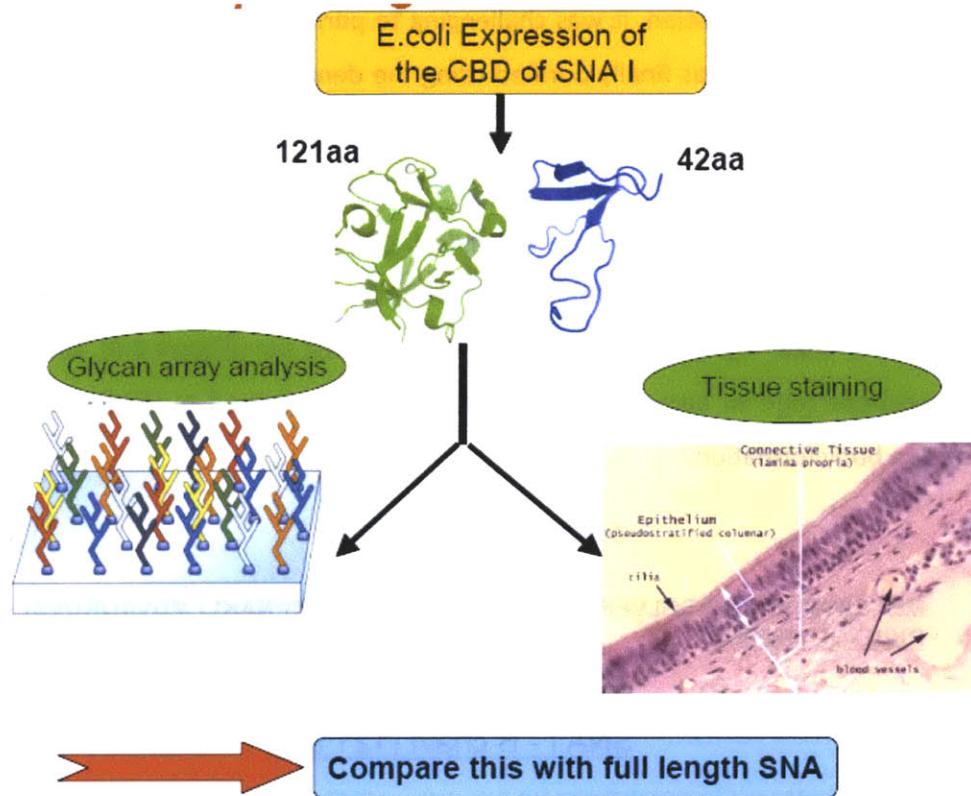


Figure 6.5 Strategies to engineer SNA-I to target host glycan receptors for human influenza A viruses. In the first strategy the high affinity glycan-binding site present in the 2α - 2β - 2γ C-terminal single β -trefoil scaffold (121aa) was cloned and expressed in *E. coli*. In the second strategy, 2γ antiparallel β -sheet, which has the high affinity glycan binding site (42aa), was cloned and expressed in *E. coli*. Functionality of both these protein constructs were tested using the glycan array analysis and by staining of human tracheal sections. This was compared to that of native SNA-I to check the functional similarity between the native and engineered SNA-I constructs.

6.2.5 Functional characterization of the receptor binding properties of the engineered constructs of SNA-I

Both the constructs were cloned into pET15b vector and expressed in *E. coli* as a N-terminal his-tagged protein. With both the constructs, expression was challenging as they were found in the insoluble fraction as inclusion bodies. Both the 42aa and 121aa inclusion bodies were solubilized using 6M guanidium hydrochloride to denature the

protein. Finally the protein was purified and re-folded using reducing concentrations of 6M urea in FPLC purification. It was challenging to purify the 121aa construct this way but the 42aa peptide was finally purified using the denaturing and renaturing protocol (**Figure 6.7**). The 42aa peptide was tested for its functionality using the glycan array platform (Chapter 1) and by staining of the relevant respiratory tract tissue sections. The formation of inclusion bodies was attributed to misfolding of the protein due to bacterial expression. Both 121aa and 42aa proteins were found to have 2 and 1 key glycosylation sites respectively around the glycan binding site ((**Figure 6.6**). Lack of these glycosylations (due to bacterial expression) could have caused misfolding and hence inclusion body formation.

42 peptide sequence

METGSSHHHHHSSGLVPRGSHMETRWVFNT*NGTISN***PNAKLLMDVAQRDVSL**
RKIILYRPTGNPNQ

SNA I - B chain (121 aa)

MGSSHHHHHHSSGLVPRGSHMTFIVGYKQMCLRENGENNFVWLEDCVLNRVQ
QEWALYGDGTIRVNS*NRSLCVTSEDHEPSDLIVILKCEGSGNQRWVFNT***NGTISN**
PNAKLLMDVAQRDVSL*RKIILYRPTGNPNQQWITT*

Figure 6.6 N-glycosylation sites on 42aa and 121aa protein constructs. The Asn residue that is glycosylated is marked in *red*. The Asn-Xaa-Thr glycosylation sequon is marked in *blue*. The lectin domain of both the protein constructs is marked in *green*.

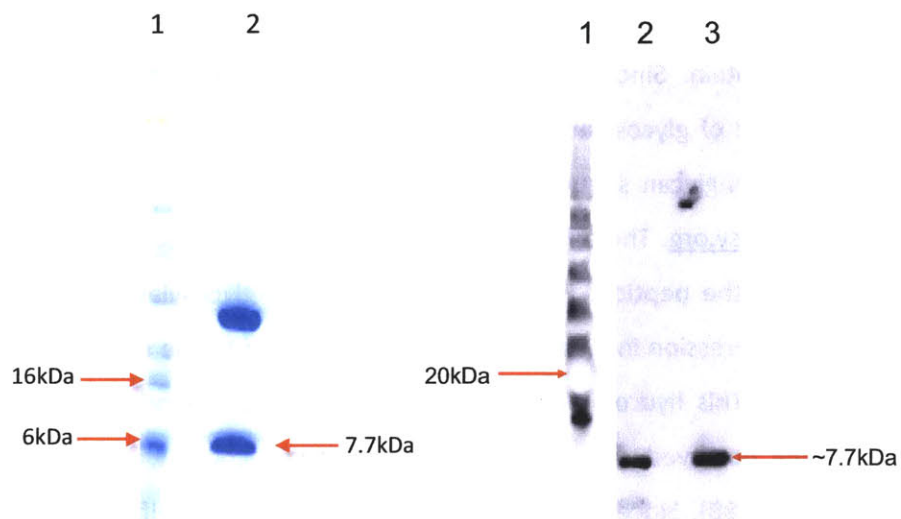


Figure 6.7 Purification of 42aa SNA-I construct. 42aa protein was expressed as an N-terminal his-tagged protein in *E.coli* and purified using Fast Performance Liquid Chromatography (FPLC) using Ni²⁺ column using a combination of denaturation and renaturation procedure (refer to Materials and Methods section). The protein was concentrated using a 3K MWCO centrifugation filter and buffer exchanged with 1X PBS (pH 7.4). The concentrated protein was run on SDS-PAGE and stained by coomassie blue as shown in the *left* above. The protein was also validated by western blotting, using anti-His antibody (shown in the *right* above). The protein was seen as a 7.7kDa protein. Note: in the coomassie blue staining a non-specific protein (as it did not light-up in western blotting as seen in the image on the *right*) was also seen which was purified along with the 42aa protein (seen on top of the 42aa protein in the image on the *left*).

Key: For the image on the left: Lane 1 – See blue plus 2 protein marker; Lane 2 – concentrated 42aa protein

For the image on the right: Lane 1 – magic marker; Lane 2 & 3: 42aa protein from two different batches.

A quantitative dose-dependent glycan array analysis was performed using various concentrations (in pmoles) of the peptide (**Figure 6.8A**). The peptide showed binding to all the glycans (α 2-3 and α 2-6). Negative control (without glycans but with the peptide) also showed binding to the well (**Figure 6.8A**). This was attributed to the hydrophobicity of the peptide Hence though the peptide was being purified it was not

folded properly and all the hydrophobic sites were exposed leading to the non-specific binding or “stickiness” of the peptide. Lack of glycosylation can contribute to the misfolding of the protein. Since the peptide was expressed in *E.coli* there it was hypothesized that lack of glycosylation could contribute to misfolding of the peptide. Putative numbers of N-glycan sequons in the peptide were analyzed using NetNGlyc program in www.expasy.org. The analysis revealed the presence of several putative N-glycosylation sites in the peptide. Hence the lack of the N-glycosylation sites in the peptide (due to its expression in *E.coli*) could have contributed to the misfolding of the peptide (**Figure 6.6**). This hydrophobicity leading to non-specific binding of the 42aa peptide was further observed when human tracheal tissue sections were stained with the peptide (**Figure 6.8B**). Since the 42aa protein is expected to self-associate, 42aa peptide by itself may exhibit multivalency. Hence dose-dependent tissue staining experiments were done without pre-complexing the protein with primary and secondary antibodies. Highly non-specific binding of the human tracheal tissue section was seen (**Figure 6.8B**). There was non-specific staining of the apical surface and the underlying connective tissue with the peptide. This further validated the misfolding and the ensuing non-specific binding seen with the peptide on the glycan array platform.

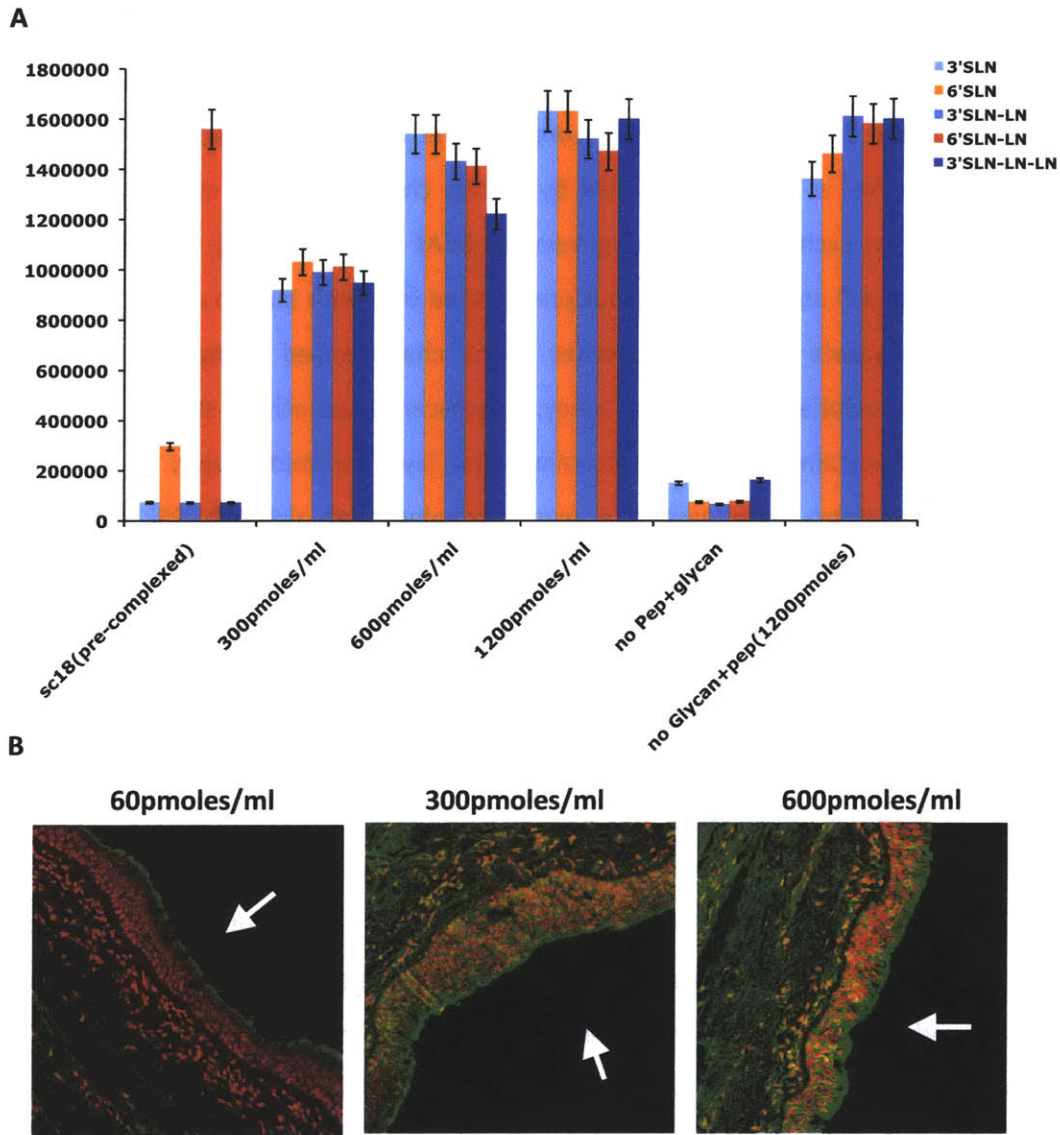


Figure 6.8 Functional characterization of 42aa peptide. A dose-dependent glycan array analysis (**A**) and staining of the human tracheal tissue sections (**B**) with the 42aa peptide was performed to characterize the glycan binding properties of the peptide. The peptide showed a highly non-specific binding to the glycans on the glycan array (**A**) and on the human trachea (**B**). The glycan array data (**A**) is representative of data sets obtained from n=3 experiments. The images were captured at 25X magnification. The apical surface is marked with a *white arrow*.

6.3 Lectin from the mushroom *Polyporus squamosus* (PSL) to target host glycan receptor

Lectin from the fruiting body (carpophores) of the mushroom *Polyporus squamosus* (termed hereafter as PSL) was purified by affinity chromatography on β -D-galactosyl-Synsorb and ion exchange chromatography on DEAE Sephacel [191]. PSL agglutinated human A, B, and O and rabbit RBCs but precipitated only with human α_2 -macroglobulin [191]. Carbohydrate binding properties were characterized using four different approaches: precipitation inhibition assay, fluorescence quenching studies, glycolipid binding by lectin staining on high-performance thin layer chromatography. Based on the results obtained by these assays, it was concluded that although PSL binds β -D-galactosides, it has an extended carbohydrate-binding site that exhibits highest specificity and affinity towards non-reducing terminal Neu5Ac α 2-6Gal β 1-4Glc/GlcNAc (2000-fold stronger than towards galactose) [191].

6.3.1 Molecular structure of PSL

Upon gel filtration chromatography, the purified lectin was eluted as a single, symmetric peak at an elution volume corresponding to an apparent molecular mass of 52-kDa. Upon SDS-polyacrylamide gel electrophoresis, with or without β -mercaptoethanol, PSL gave a single band with an apparent mass of 28kDa [191]. This indicated that the native PSL lectin, is composed of two identical 28-kDa subunits (as a homodimer) associated by non-covalent bonds.

6.3.2 Homology modeling of PSL

Since there is no X-ray crystal structure of PSL, a homology based structural model of PSL was generated (**Figure 6.9B**). PSL shares the highest protein sequence identity to mushroom lectin, *Marasmius oreades* agglutinin [MOA] [192], whose crystal structure has been solved. Homology-based structural model of PSL using the crystal structure of MOA showed that PSL comprises of C-terminal and N-terminal domain

(**Figure 6.9B**). The C-terminal domain has been implicated in facilitating oligomerization and providing structural stability [192]. The N-terminus of PSL on the other hand appears to adopt the anti-parallel β -trefoil scaffold with three tandemly repeated homologous β -sheet subdomains (α , β and γ) all of which have the conserved (Q/N)/XW motif, which is a common feature of the ricin B-chain lectin domains (**Figure 6.9A**). Studies have indicated that β and γ subdomains comprise the glycan binding sites [191, 192]. The functional role of the C-terminal domain in both PSL and MOA apart from oligomerization remains unknown due to the unique structural fold adopted by this domain, which has not been observed thus far in any other protein. Our approach was to remove the C-terminal oligomerization domain and retain the N-terminal lectin domain and it was hypothesized that the N-terminal by itself should retain the glycan binding properties of the full length PSL. Previously, Goldstein *et al* had cloned and expressed PSL and its forms in *E.coli*. Hence PSL's glycan binding domain was cloned (designated as *rPSL-N*) and expressed in *E.coli* as a N-terminal his-tagged protein (**Figure 6.10A**). Unlike SNA, there were no challenges in the expression and purification of *rPSL-N*. The protein was confirmed by western blot analysis with anti-His antibody (**Figure 6.10B**). This functionality of the protein was then assessed by performing a quantitative dose-dependent glycan array analysis and by staining human tracheal tissue sections with *rPSL-N*.

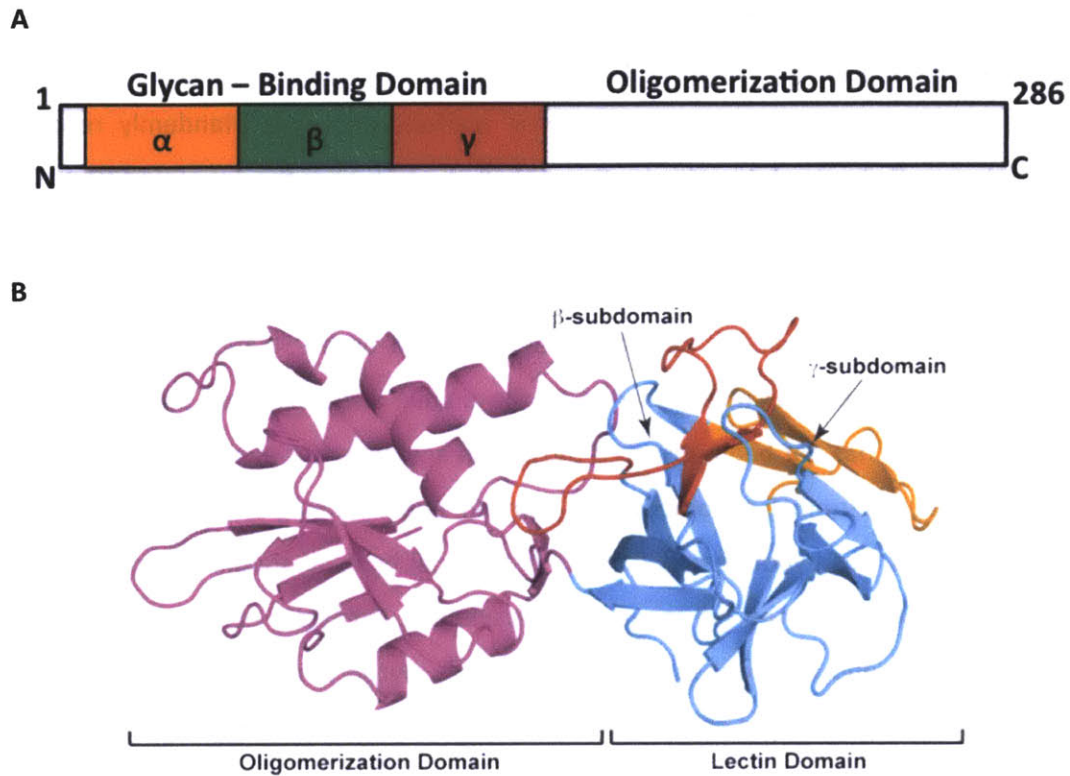


Figure 6.9 Molecular structure of PSL and homology modeling of PSL. PSL has a N-terminal glycan binding domain and a C-terminal oligomerization domain (**A & B**). The N-terminal lectin domain adopts an antiparallel β -trefoil fold a common feature of ricin B-chain lectin domain. The exact function of the C-terminal domain beyond oligomerization and stabilization of the protein structure is not clearly known. Structure of PSL lectin, which was generated by homology modeling using MOA lectin as template. Based on the MOA crystal structure (co-crystallized with glycan motif), each of the β - and γ - subdomains comprises of distinct binding sites for the $\alpha 2 \rightarrow 6$ trisaccharide motif.

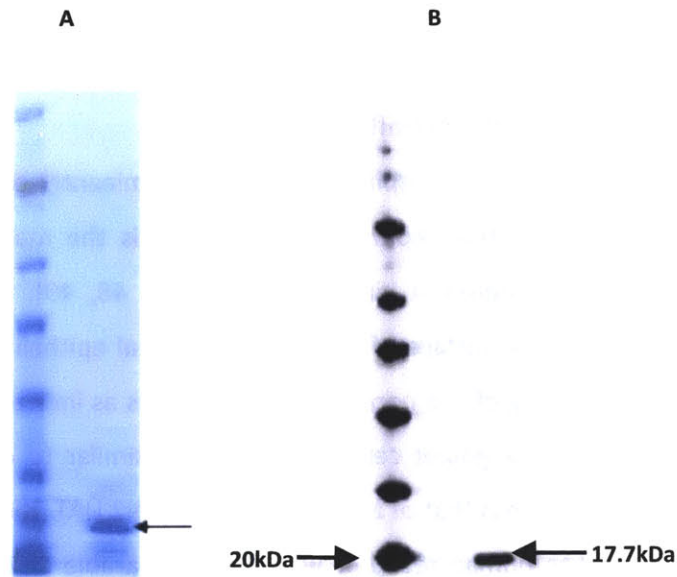


Figure 6.10 Purification of *rPSL-N*. The protein was expressed as a N-terminal his-tagged protein and purified by Nickel column affinity chromatography (A). The protein was purified as a 17.7kDa protein, which was validated by western blot analysis (B).

6.3.3 *rPSL-N* binds to the glycan receptors targeted by human-adapted influenza A viruses

In order to characterize the glycan binding specificity of *rPSL-N*, a quantitative dose-dependent glycan array analysis [110] was performed with the purified *rPSL-N* protein. The glycan array platform was composed of both α 2-3 and α 2-6 sialylated glycans (Chapter 1). *rPSL-N* showed a dose-dependent binding to representative α 2 \rightarrow 6 sialylated glycan receptors (6'SLN and 6'SLNLN) of human-adapted influenza A viruses (**Figure 6.11A**). This binding to α 2 \rightarrow 6 glycans was comparable to that of the full length PSL (**Figure 6.11B**) indicating that the *rPSL-N* is able to retain the glycan-receptor binding properties of PSL even in the absence of the oligomerization C-terminal domain. In all the glycan array analysis in order to capture the multivalent *rPSL-N*-glycan receptor interaction, *rPSL-N* was pre-complexed with primary and secondary antibodies before adding to the glycans. An apparent binding constant (K_d') of *rPSL-N* for the 6'SLN-LN and 6'SLN glycans was calculated using Hill's equation. The K_d' value (sub picomolar range) for *rPSL-N* was in the same range as that calculated for binding of HA from human-

adapted pandemic H1N1 (A/South Carolina/1/1918) and H2N2 (A/Albany/2/58) influenza viruses [95, 110] indicating that *rPSL-N* binds with high-affinity to the glycan receptors of human-adapted influenza virus HA.

The human upper respiratory tract predominantly expresses $\alpha 2 \rightarrow 6$ sialylated glycan receptors on their epithelial surface and is the main target for infection by human-adapted influenza A viruses [40, 41, 43, 48, 49]. *rPSL-N* showed extensive staining of the apical surface of the human tracheal epithelium (**Figure 6.12A**). *rPSL-N* also showed staining of the non-ciliated goblet cells as indicated by its co-staining with Jacalin, a marker for goblet cells (**Figure 6.13A**) similar to other human adapted HA (**Figure 6.13B**, shown is that of a representative H3N2 HA). The apparent binding affinity (K_d') of *rPSL-N* to human receptor was also comparable to that of the pandemic HAs (**Figure 6.13C**). *rPSL-N* did not show any staining of the human deep lung and alveolus (**Figure 6.12D**) which are known to express $\alpha 2 \rightarrow 3$ sialylated glycan receptors [48]. The binding pattern of *rPSL-N* to the human respiratory tissues is consistent with the observed specificity on the glycan array. This binding pattern of *rPSL-N* to human tracheal epithelium was comparable to that of the full length PSL lectin which also showed sialic-acid specific binding to the apical surface and the non-ciliated goblet cells of the human tracheal epithelium (**Figure 6.12B**).

The binding of *rPSL-N* to both ciliated and goblet cells in the tracheal epithelium points to the expression of the $\alpha 2 \rightarrow 6$ trisaccharide (Neu5Ac $\alpha 2 \rightarrow 6$ Gal $\beta 1 \rightarrow 4$ GlcNAc $\beta 1 \rightarrow$) as a terminal motif on both N-linked (ciliated) and O-linked (goblet cells) glycoconjugates. The specific binding of *rPSL-N* to this trisaccharide motif in the human upper respiratory tissues was confirmed by pretreatment of the tissue sections with *Sialidase A*. This enzyme cleaves terminal sialic acid that is either $\alpha 2 \rightarrow 6$ or $\alpha 2 \rightarrow 3$ linked to a penultimate lactosamine (Gal $\beta 1 \rightarrow 4$ GlcNAc). There was a complete loss of *rPSL-N* staining of the human tracheal epithelium upon *Sialidase A* pre-treatment of the trachea (**Figure 6.12C**) in contrast to the SNA-I staining pattern after *Sialidase A* treatment (**Figure 6.3C**) Also the tracheal-tissue binding of *rPSL-N* was compared with that of SNA-I (which shows predominantly

staining of the apical surface of human tracheal epithelium; Section 6.2). This highlighted the broader specificity of SNA-I in that it binds to both the $\alpha 2 \rightarrow 6$ trisaccharide motif recognized by PSL as well as disaccharide motifs such as Neu5Ac $\alpha 2 \rightarrow 6$ linked to core GalNAc structure of O-linked glycoconjugates (Neu5Ac $\alpha 2 \rightarrow 6$ GalNAc $\alpha 1 \rightarrow$).

Human respiratory tissue binding pattern of *rPSL-N* was further compared with that of hemagglutinin from human-adapted influenza A viruses analyzed in previous studies [48, 95]. The binding pattern was very similar wherein the HAs also show specific binding to ciliated and non-ciliated cells of the human tracheal epithelium and no binding to the alveolus. Moreover *Sialidase A* pre-treatment of the tracheal section completely abolishes binding of HA similar to what is observed for *rPSL-N*. Together, these results indicate that *rPSL-N* specifically binds to the glycan receptors targeted by human-adapted influenza A viruses.

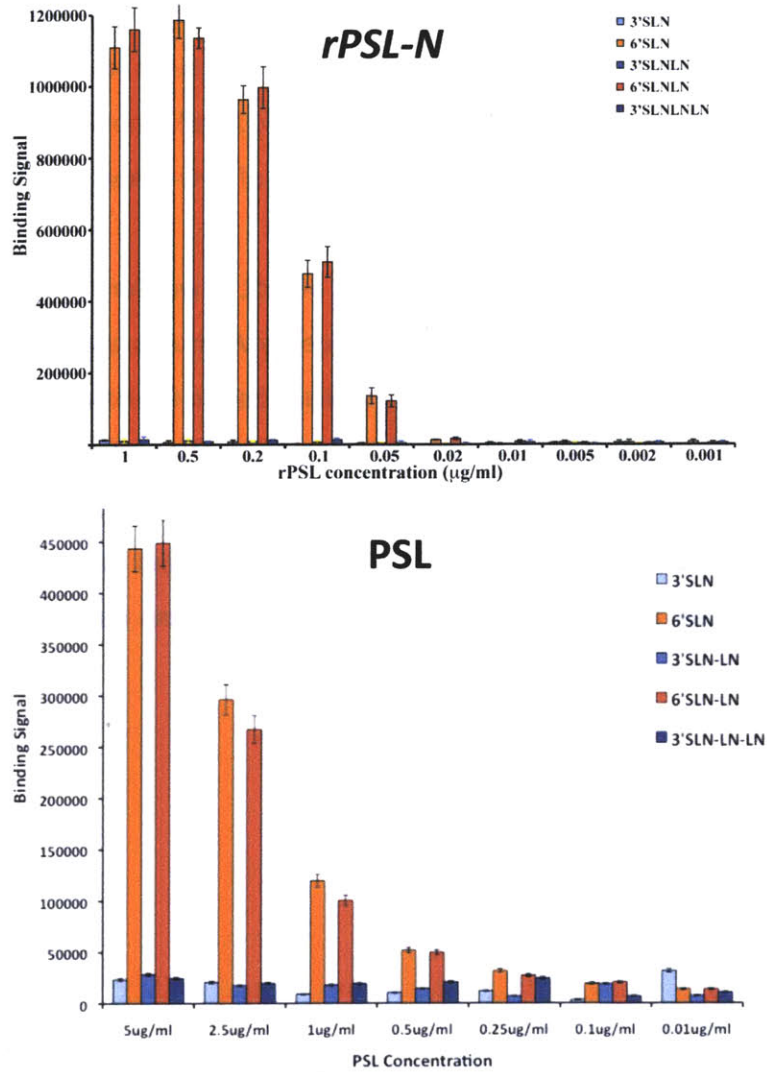


Figure 6.11 Glycan binding specificity of *rPSL-N* and native PSL. A quantitative dose-dependent glycan array analysis was performed with *rPSL-N* by pre-complexing it with primary and secondary antibodies (*top*). For comparison, the assay was also performed with the native PSL (*bottom*, EY labs) without pre-complexation. Similar to native PSL, *rPSL-N* showed highly specific binding to α 2-6 sialylated glycans (6'SLN and 6'SLN-LN). The affinity of *rPSL-N* was higher than the native PSL.

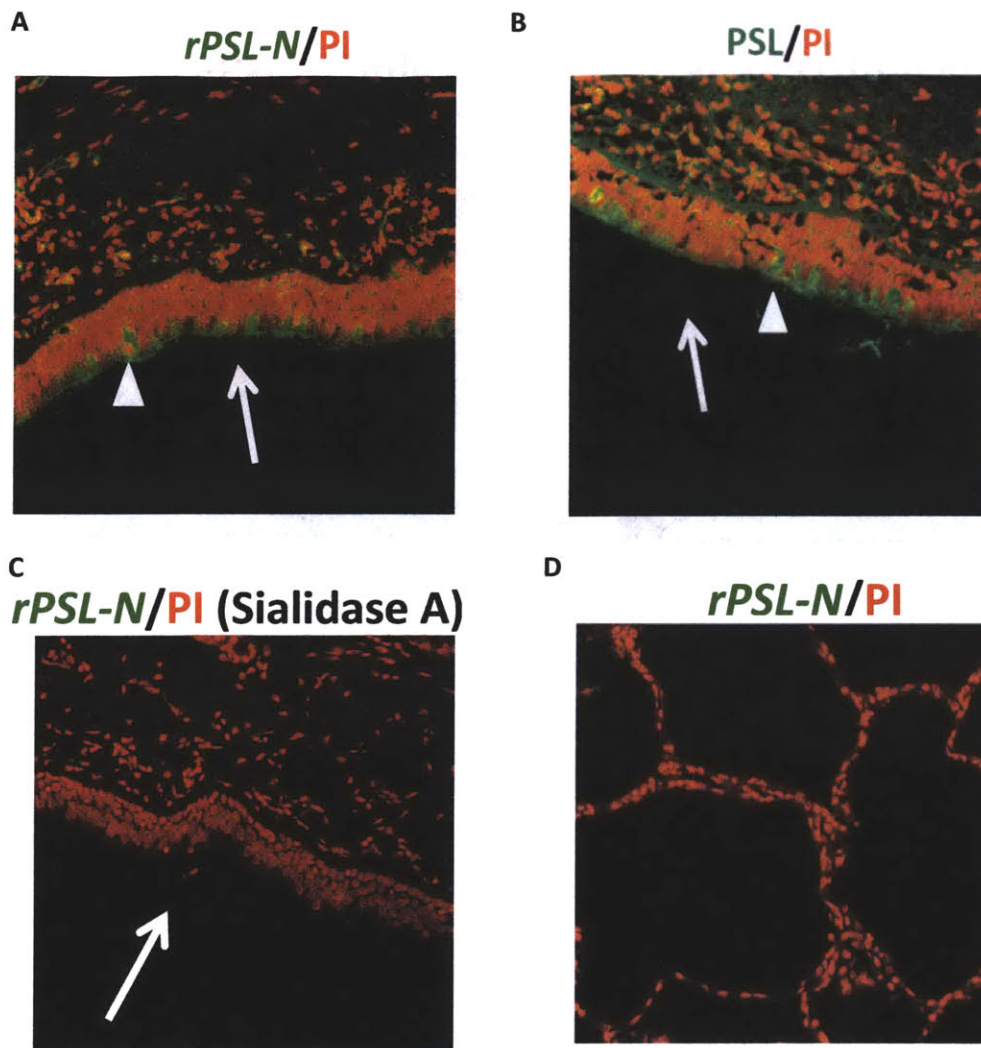


Figure 6.12 Cellular tropism of *rPSL-N*. Confocal image (25X) of paraffinized human tracheal tissue with 20µg/ml of *rPSL-N* (green) pre-complexed with primary and secondary antibody (labeled with 488 fluorophore). *rPSL-N* stained the apical surface of the tracheal epithelium and the non-ciliated goblet cells (marked with an arrowhead) (A). This staining pattern was very similar to that of the native PSL (B). *Sialidase A* treatment of human tracheal tissue section prior to staining with *rPSL-N* led a complete loss of tracheal epithelium staining indicating sialic acid specific binding of *rPSL-N* to glycan receptors (C). *rPSL-N* did not stain human lung alveolus (D). The apical surface is marked with a solid arrow. The nuclei are counterstained by propidium iodide (red). The nucleus was counterstained by propidium iodide (red). The apical surface is marked with solid white arrow.

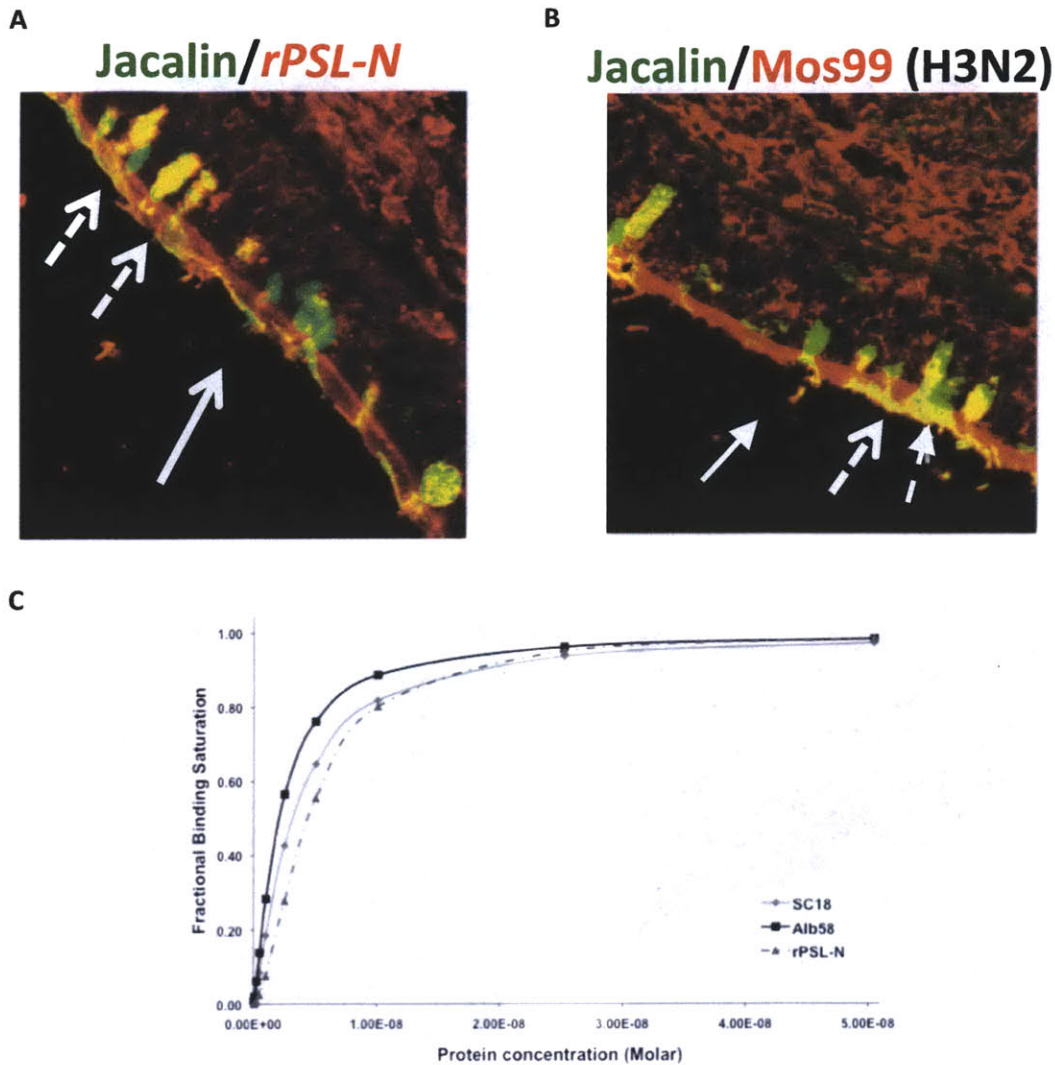


Figure 6.13 *rPSL-N* binds to the glycan receptors targeted by human influenza A viruses. Similar to the HAs from human adapted influenza A viruses (**B**), *rPSL-N* shows co-staining of the goblet cells with Jacalin (**A**) and a complete loss of staining upon Sialidase A treatment (**Figure 6.12**). This is in contrast to SNA wherein the goblet cell staining is seen even after Sialidase A treatment (**Figure 6.3**) indicating that *rPSL-N* more specifically targets glycan motifs recognized by human-adapted influenza A HAs. Shown in **B** is the confocal image of staining of human tracheal sections with Jacalin and recombinant HA from a representative H3N2 pandemic influenza A virus Moscow 99. The co-staining is indicated by a yellow staining pattern of the goblet cells. The images were captured at 63X magnification. The apical surface of the tracheal epithelium is indicated by a bold white arrow. The co-staining of the goblet cells is indicated by a broken white arrow. Shown in (**C**) is the binding affinity of *rPSL-N* to human receptors and it is comparable to that of pandemic virus HAs (SC18 and Alb58).

6.3.4 Inhibition of influenza A virus infection by *rPSL-N*

To determine the anti-viral effect of *rPSL-N* against influenza A infection, MDCK cells (which are known to express both α 2-3 and α 2-6 sialylated glycans [193]) were incubated with different concentrations of *rPSL-N* for 2h prior to infection with representative influenza A viruses. The presence of α 2-6 glycan receptors in MDCK cells were further confirmed by staining with SNA-I lectin (**Figure 6.14B**). Two specific viral strains were chosen for this analysis. The first strain, A/Victoria/3/75 or Vic75, belongs to the H3N2 subtype and binds specifically to α 2 \rightarrow 6 sialylated glycans on the glycan array (data obtained from functionalglycomics.org [194]). The second strain, A/Puerto Rico/8/34 or PR8, belongs to the H1N1 subtype and shows a mixed binding to both α 2 \rightarrow 3 and α 2 \rightarrow 6 sialylated glycans on the glycan array [171]. Therefore these representative strains span different human-adapted influenza A virus subtypes as well as have varying specificities to α 2 \rightarrow 6 sialylated glycans. The assay is schematically represented in (**Figure 6.14A**).

After 48h of incubation, viral RNA was extracted and the change in viral titer was quantified by real time PCR analysis of the conserved viral matrix gene (M) [195]. The reduction in viral RNA was estimated by comparing the viral RNA titer quantified from untreated MDCK cells (**Figure 6.15**). A 10-fold dilution of vRNA was made to generate standard curve for absolute quantification (**Figure 6.16**). IC_{50} was calculated as the concentration of *rPSL-N* at which there is a 50% reduction in the viral RNA as compared to the control untreated cells. The results showed that there was a dose-dependent reduction in viral RNA as compared to the untreated cells (**Figure 6.15A**). The IC_{50} of *rPSL-N* for inhibiting Vic75 infection was found to be \sim 2.5 μ g/ml which corresponds to 140nM to 280nM of *rPSL-N* (**Figure 6.15B**). On the other hand, IC_{50} of *rPSL-N* for inhibiting PR8 infection was 4-fold higher (\sim 10 μ g/ml) (**Figure 6.15B**). This observation further demonstrates that *rPSL-N* specifically competes with the binding of viral hemagglutinin to α 2 \rightarrow 6 sialylated glycan receptors on the MDCK cells. Further, the specificity of *rPSL-N* was validated against avian H5N1 virus. There was no inhibition of

H5N1 infection. These results also highlight the ability of *rPSL-N* to inhibit infection of human adapted influenza A viruses across different subtypes.

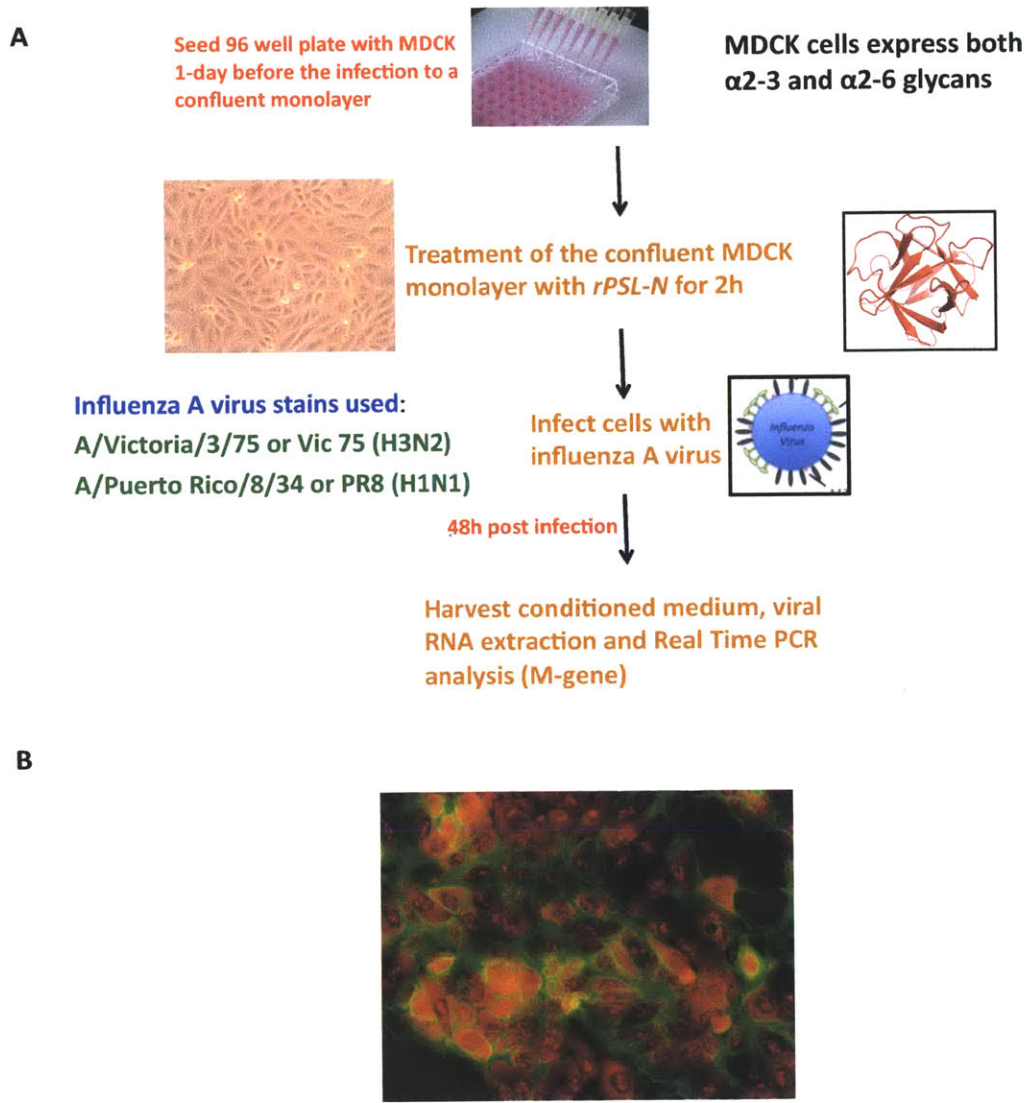
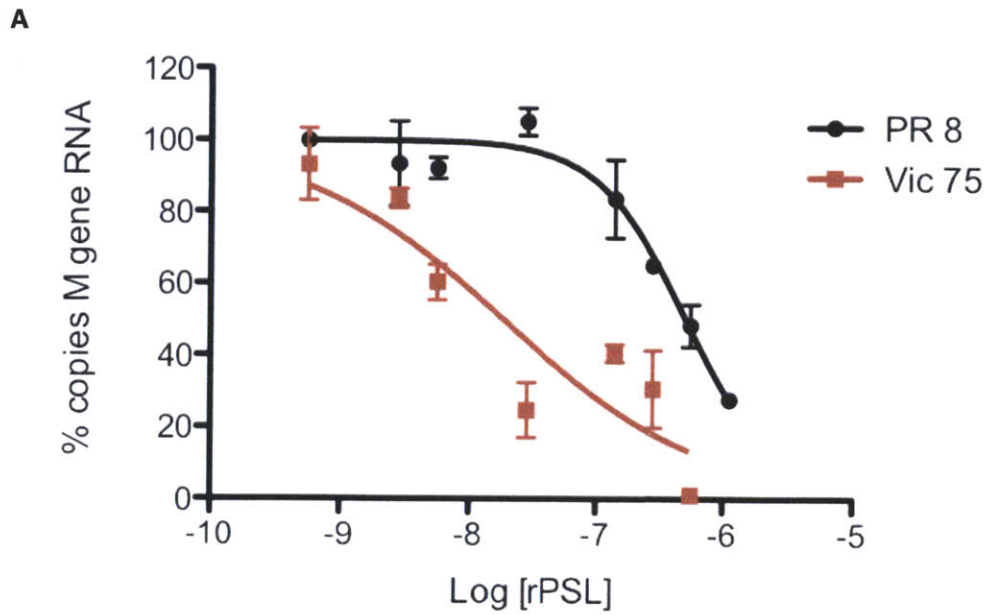


Figure 6.14 Experimental design for *rPSL-N* inhibition of influenza A infection. Madin-Darby Canine Kidney Cells (MDCK) were used to test the ability of *rPSL-N* to inhibit influenza A infection. Two different human influenza A virus strains (PR8 and Vic75) were used for the assay (**A**) due to their differential glycan receptor binding properties. Viral inhibition was assessed by quantification of viral M-gene using quantitative real time PCR analysis. The presence of α 2-6 receptors on MDCK cells was validated by staining them with SNA-I (*green*) (**B**). The nuclei were stained with propidium iodide.



B

Viral Strains	IC ₅₀ (µg/ml)
<i>A/Victoria/3/75 or Vic75 (H1N1)</i>	2.5 to 5
<i>A/Puerto rico/8/34 or PR8 (H3N2)</i>	10

Figure 6.15 *rPSL-N* inhibits infection of MDCK cells by influenza A viruses. MDCK cells were treated with a range of concentrations of *rPSL-N* prior to infecting the cells with influenza A virus. Quantification of viral M-gene (**A**) showed a dose-dependent reduction in both PR8 and Vic75 expression. IC₅₀ was calculated using Graphpad Prism 5 (**B**). There was a shift in the IC₅₀ values for PR8 as compared to Vic75. This can be explained by their differential glycan binding properties (see text for details). Data is representative of n=3 experiments. The data shown here is normalized to the viral RNA quantified from the virus infected untreated MDCK cells.

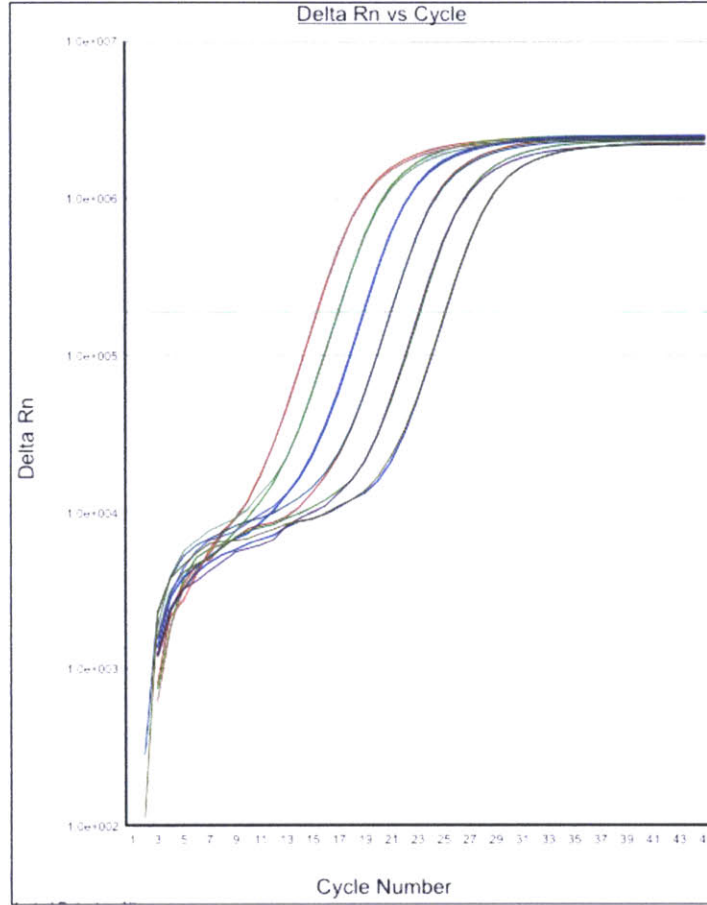


Figure 6.16 Standards for quantitative real time PCR. Shown is the amplification plot of Vic75 viral RNA standards (10-fold dilution from 10^6 to 10^1 vRNA molecules)

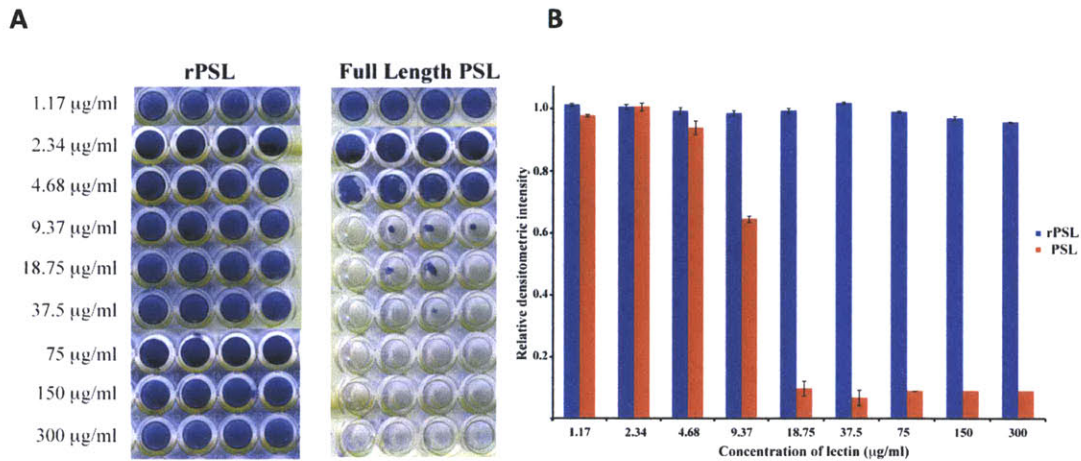


Figure 6.17 Native PSL but not *rPSL-N* is highly cytotoxic to MDCK cells. (A) Scanned image of cytotoxicity assay plate showing lectin treated MDCK cells stained with crystal violet. The image on the left shows the wells treated with *rPSL-N* and that on the right shows the wells treated with PSL. The concentrations of lectin used are shown in the left of the image. Note the loss of MDCK cell monolayer in PSL treated wells on the right as compared to the *rPSL-N* treated wells on the left. Also shown are the non-treated MDCK cells stained with crystal violet. **(B)** shows comparison of cytotoxicity between PSL and *rPSL-N*. Densitometric scanning to quantify the crystal violet staining (indicative of intact MDCK monolayer) was performed using Adobe Photoshop. Relative intensity was calculated after normalizing the crystal violet staining intensity of the drug treated cells with that of the MDCK cells not treated with the drug. There were significant cytopathic effects and loss of cell monolayer in MDCK cells treated with full length PSL at concentrations higher than 9 µg/ml **(A)**. There were no significant CPEs and loss of cell monolayer in *rPSL-N* treated wells. The data is representative of n=4.

6.3.5 *PSL and not rPSL-N is cytotoxic to MDCK cells*

Since most of the plant lectins possess inherent cytotoxicity [196, 197] cytotoxicity of PSL and *rPSL-N* were evaluated. For native PSL, MDCK cells, plated on a 96 well plate, were incubated with various lectin concentrations (from 1.17µg/ml to 300µg/ml) for 2h followed by overlaying the cells with 1X MEM media and incubation for 48h. Cytopathic effects (CPE) were monitored 24h post-incubation and at 48h post infection. Visible CPEs (several dead and non-adherent cells) were noticed in drug treated wells from ~9 µg/ml. After 48h of incubation, there was complete loss of MDCK

monolayer in PSL treated cells from $\sim 9 \mu\text{g/ml}$ as compared to the untreated cells (**Figure 6.17**).

Cytotoxicity assay with *rPSL* was performed similar to that for native PSL. After 24h and 48h of incubation, there were no visible CPEs in the *rPSL-N* treated wells. The MDCK monolayer was intact after 48h in the drug treated wells. The cells were fixed and stained with crystal violet (**Figure 6.17A**). A densitometric scanning (for both native PSL and *rPSL-N* treated wells) was done in order to assess the intensity of staining (indicative of intact monolayer) and normalized to the intensity of untreated cells (**Figure 6.17B**). Hence the cytotoxicity analysis showed that removal of the C-terminal oligomerization domain from native PSL (which is *rPSL-N*) does significantly reduce its cytotoxicity.

6.3.6 *In vivo studies with rPSL-N*

In order to test the *in vivo* efficacy of *rPSL-N*, 8 weeks old female BALB/c mice were treated with 1mg/kg of *rPSL-N* prior to infection with mouse-adapted A/California/04/09 or maCA04/09. Mice were treated with 1mg/kg of *rPSL-N* (intranasally) for 0-5 days. Control mice were treated with 1XPBS prior to infection with mouse-adapted CA04/09. Daily weight, lung titers and survival were monitored for all the 6 days. There was no significant reduction in lung viral titers ($7.68 \log_{10}\text{EID}_{50}/\text{ml}$ and $7.45 \log_{10}\text{EID}_{50}/\text{ml}$ for *rPSL-N* treated and PBS treated mice respectively). There was a marginal improvement in the survival of the *rPSL-N* treated mice (**Figure 6.18**) though the mice succumbed to the infection after Day 6.

Previously mouse-adaptation is shown to alter receptor binding specificity of the virus given the predominant $\alpha 2-3$ glycan expression in the mouse respiratory tract. Hence a dose-dependent glycan array analysis was performed with the maCA04/09 and compared with the binding data of the wild-type virus. Interestingly, there was a reduction in the $\alpha 2-6$ glycan binding affinity (**Figure 6.19**) as compared to the wild-type virus (**Figure 4.7**). Also the maCA04/09 virus showed an increased binding to $\alpha 2-3$ glycans. Given the high specificity of *rPSL-N* to $\alpha 2-6$ glycans, the $\alpha 2-3$ binding of the maCA04/09 would have negated the inhibitory effects of *rPSL-N*. Hence ferrets would be a

more appropriate model system for testing the *in vivo* effects of *rPSL-N*, as they predominantly express α 2-6 glycans in their respiratory tract.

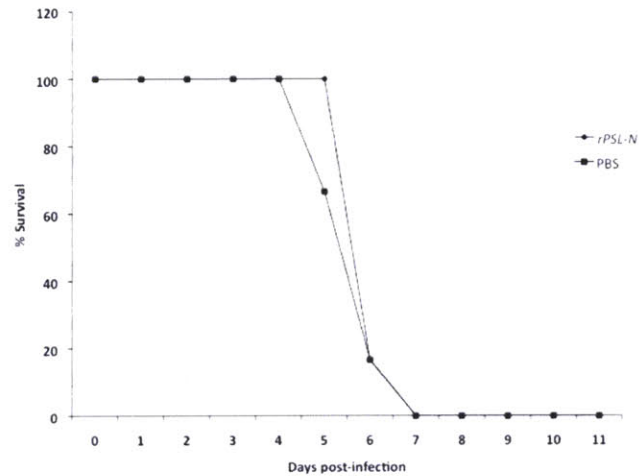


Figure 6.18 Survival curve of BALB/c mice treated with *rPSL-N*.

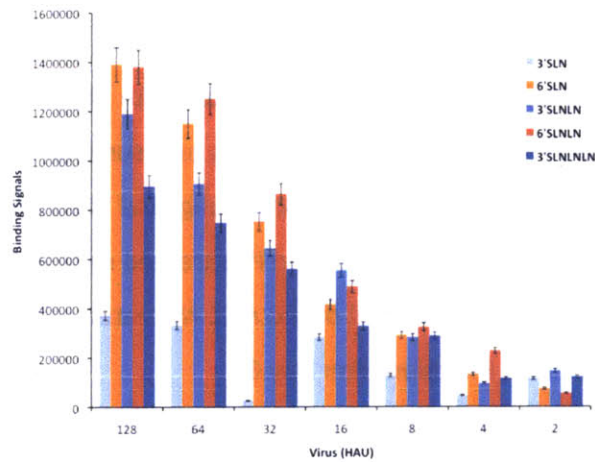


Figure 6.19 Glycan array analysis with mouse-adapted CA04/09 (ma-CA04/09) virus. Mouse adaptation of a representative 2009 H1N1 influenza A virus A/California/04/09 led to a change in the receptor binding specificity of the virus. The virus acquired α 2-3 binding preference upon mouse adaptation when compared to the wild-type virus (Figure 4.7).

6.4 Discussion and Significance of this study

One of the major challenges with current antiviral strategies for influenza A virus is the emergence of new viral strains which are resistant to these antivirals. Hence there is a need to look for alternate antiviral strategies to combat influenza A virus infection. One such strategy that has emerged recently is to generate antibodies that target the highly conserved stem region of HA that are involved in fusion of viral envelope to the host nuclear membrane [198, 199]. However, even this strategy has not resulted in an antiviral agent that broadly targets all subtypes known to have adapted to the human host such as H1N1 and H3N2.

Plant lectins have recently been shown to have antiviral properties [151, 200, 201]. For instance, cyanovirin N (CV-N) is a lectin isolated from the cyanobacterium *Nostoc ellipsosporum* that to the high-mannose residues on the viral hemagglutinin 1 (HA1) and neutralizes influenza A viral infection [151]. Though CV-N was found to be effective against several influenza A virus strains, its effectiveness was limited by the emergence of influenza A virus resistant to CV-N lectin. The CV-N resistant strains lacked the key glycosylation site specifically targeted by the lectin. Hence one of the main challenges with the anti-viral drugs targeting the virus itself is the potential emergence of drug resistant viral strains.

Influenza A virus hemagglutinin binds to specific glycans receptors on the surface of the host cell. These glycan receptors mediate viral attachment and entry process during the initial stages of the viral life cycle. Given the importance of these glycan receptors in the viral life cycle, they offer a promising alternative target for countering influenza A virus infection. Recently DAS 181, a sialidase fusion protein was found to be effective against several influenza A viral strains [180, 202, 203]. DAS 181 functions by removing terminal sialic acid from the glycan receptors for influenza A virus and thus renders the host cells ineffective from being infected by the virus. Unlike DAS 181, which cleaves all the sialic acid on the surface of the host cell, recombinant N-terminal glycan-binding domain of *Polyporus squamosus* lectin (designated *rPSL-N*) binds specifically to the glycan receptors for influenza A virus and inhibits its infection of

MDCK cells. Although the high affinity glycan binding site of PSL resides in just one of the antiparallel β -sheets (γ subdomain, a 42-mer peptide), this subdomain by itself was found to be unstable and found to have completely lost its glycan binding specificity (as mentioned in Section 6.2). On the other hand, *rPSL-N*, the minimum N-terminal domain that forms a complete β -trefoil lectin scaffold, is stable and exhibits glycan-binding properties similar to the native PSL. There is scope for additional improvement in its stability and efficacy of *rPSL-N* by various protein engineering strategies. For instance, addition of cysteine residues in the N- and C- terminus of *rPSL-N* with an intention of introducing disulfide linkage could potentially stabilize the β -trefoil fold of *rPSL-N*.

Given the unique mode of action of *rPSL-N* as compared to other anti-viral therapeutics, *rPSL-N* may offer a potential therapeutic option against influenza A infection. Targeting the host cells rather than the virus can slow down the emergence of drug-resistant viral strains. Furthermore *rPSL-N* also shows a broad-spectrum inhibitory property across H1 and H3 subtypes of influenza A viruses.

Chapter 7. Summary and Significance of this Thesis

Influenza A virus hemagglutinin (HA) binds to the cell surface sialylated glycan receptors and mediates viral entry into the host cells. The binding property of the viral HA to the host cell surface glycan receptor impinges on various aspects of the viral pathogenesis such as host adaptation and transmissibility. Hence there is a need to understand the critical HA-glycan interaction to truly correlate it with its functional significance in viral pathogenicity. Much of influenza A research has been oversimplified by studying HA only in the context of its sialic acid linkage specificity. This undermines the complexity associated with the glycan receptor. Moreover the multivalency associated with the HA-glycan interaction is also not taken into account. In this thesis, in order to address these aforementioned challenges we undertook a multifaceted approach going from understanding the two molecular components: HA and glycan receptors respectively, to converging on their biological relevance in ferret and mouse models. By interfacing complementary set of tools we were able to deduce a novel mechanism by which influenza A virus escapes host immune response by modulating the HA binding avidity to host glycan receptors. We were also able to gain insights into subtle modifications of HA such as site-specific glycosylation, and its role in determining the receptor binding property of HA. Further by using recombinant HA from a representative 2009 H1N1 influenza A virus we were able to correlate the receptor binding affinity of HA to its transmissibility in ferret model. This highlights the importance of quantifying HA binding avidity, taking into account the multivalency associated with HA-glycan interaction. Finally, by multiplexing lectin staining with enzymes we were able to understand influenza A viral tropism in ferret respiratory tract. This combined with data mining enabled us to map the gross glycan motif distribution in ferret upper and lower respiratory tract. Finally based on the understanding of viral tropism and their glycan receptor distribution, we were able to devise a novel therapeutic strategy to combat influenza A infection. We used a combination of tools

ranging from data mining analysis, glycan array analysis and human tracheal tissue staining to identify a derivative of the mushroom lectin *rPSL-N*, which targets the glycan receptors of human-adapted influenza A virus and inhibits infection by H1 and H3 viruses *in vitro*.

It is challenging to decode the functional significance of a protein-glycan interaction due to the enormous complexity associated with this interaction. The non-template driven synthesis of glycans combined with its complexity makes it challenging to analyze the active glycan motif from relevant cells or tissue sections. Lectin staining combined with mass spectrophotometry analysis enables characterization of the active glycan motifs at various molecular levels. As highlighted by this thesis, multiplexing lectin staining with glycosidases can also enable further characterization of glycan motifs. Further, since any protein-glycan interaction typically exhibits multivalency, it is important to capture this valency issue in any ELISA based assay system aimed at characterizing protein-glycan interaction. Further a dose-dependent analysis of the protein on the glycan array not only enables identifying the glycan binding specificity of the protein, but also enables characterization of binding avidities (provided multivalency is captured in the assay).

Overall the approach used in this thesis enabled us to get greater insights into the role of HA-glycan interaction in various aspects (such as antigenic drift, transmissibility and host adaptation) of influenza A virus infection (**Figure 7.1**). Such a study enabled us to identify a novel therapeutic strategy against influenza A infection. We have also provided a strategy for effective surveillance of emergence of influenza A virus into a more pathogenic strain. This thesis has hence contributed to answering the big question to possibly predict the emergence of any future pandemic outbreaks. Such an approach can be extended to understanding various protein-glycan interactions that impinge on other disease models.

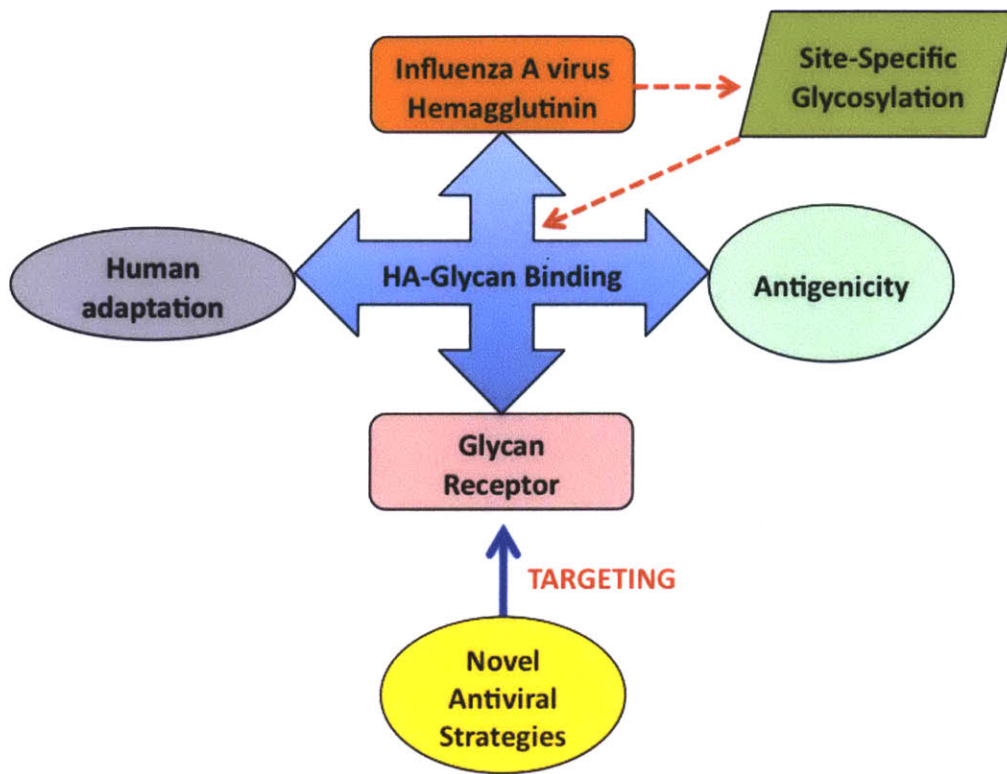


Figure 7.1 Overall summary of this thesis. This thesis has investigated the role of HA-glycan interaction in influenza A virus antigenic drift, transmissibility and host adaptation. Based this understanding, this thesis proposes a novel therapeutic strategy of targeting the host glycan receptor instead of the viral components against influenza A virus infection.

Appendix 1: Materials and Methods

A1.1 Materials and Methods for Chapter 2

Mice.

Swiss mice were purchased from Charles River and C57BL/6 and Balb/c mice were purchased from Taconic. Mice were maintained under specific pathogen-free conditions and all procedures involving mice were approved by the Animal Care and Use Committee of the National Institute of Allergy and Infectious Diseases.

Viruses.

To study antigenic drift in an animal model, it is essential to start the experiment with a virus that is completely adapted to its host. Therefore, in these experiments PR8, a mouse adapted virus was used. Several stocks of viruses were used in these experiments. 3 independent stocks of PR8 were isolated after transfecting plasmids containing the 8 PR8 gene segments into MDCK cells. These viruses were expanded only once on MDCK cells to prevent cell line adaptations. Serial passaging of these viruses began by directly infecting mice i.n. with MDCK supernatant. In other experiments, virus that has been continuously grown in 10-day old embryonated chicken eggs (CBT Farms) was passaged in the laboratory (this virus has never been grown on MDCK cells).

Vaccination.

For all vaccine stocks, allantoic fluid was treated with paraformaldehyde (1:864 dilution) for 2 days at 4°C. Mice were injected intraperitoneally with ~100-500 hemagglutination units of inactivated influenza A viruses. 10 days after vaccination, mice were retro-orbitally bled, and the erythrocytes were removed using serum-gel tubes (Sarstedt). Serum was inactivated by incubating at 56°C for 30 min and tested for anti-influenza A virus antibodies by HAI. This vaccination scheme induces primarily IgG

and IgM antibodies. To generate a large diverse pool of antibodies, serum isolated from 45 vaccinated Swiss mice was pooled.

HAI assay.

HAI titrations were performed in 96-well round plates (Corning). Sera were serially diluted 2-fold and added to 4 agglutinating doses of influenza A virus in a total volume of 200 μ l. Next, 25 μ l of a 2% (vol/vol) erythrocyte solution was added. The sera, virus, and erythrocytes were gently mixed and the assay was read out after incubating for 60 min at room temperature. Titers were recorded as the inverse of the highest antibody dilution that inhibited 4 agglutinating doses of virus.

Polyclonal antibody binding assays.

L929 cells were infected with virus for 3h, the time with maximal ratio of HA to NA expression. Serial dilutions of polyclonal antibodies were added to the cells for 30 min at 4°C. Duplicate samples were incubated with a Ca monoclonal antibody mixture or an NA antibody to normalize the amount of HA/NA expressed on the cell surface. Flow cytometry was performed, and data are expressed as normalized mean fluorescent intensity.

Serial passaging of influenza A virus.

For all *in vivo* experiments, individual mice were used for each passage. To begin the passaging experiments, mice were anesthetized with isoflurane and infected i.n. with stock virus diluted in 50 μ l PBS. Lungs were isolated 2 days after infection and homogenized. Passaging was continued by infecting a second group of mice with 50 μ l of the lung homogenate from passage #1. Lungs were again isolated 2 days after this infection and homogenized. This process continued between 6-9 passages for each experiment. For co-infection experiments using P186S and PR8 and other experiments using E246G and E246G/A227T, starting virus amounts were normalized based on infectivity on MDCK cells. The presence of virus was monitored by TCID₅₀ (lung titers of

vaccinated mice were typically between 10^4 and 10^6 TCID₅₀/mL). When infections were unsuccessful, the infection using the same lung homogenate from the previous successful infection was repeated. For vaccination experiments, mice were used 10-21 days following vaccination. Mice with lower HAI titers were used during early passages.

Monoclonal antibody binding analysis.

Influenza A viruses were diluted in PBS and added in triplicate to 96 well flat bottom microtiter plates (Thermo Electron Corp). After incubation for >15 hr at 4°C, wells were blocked with PBS-FBS. A non-saturating concentration of monoclonal antibody in the linear portion of the antibody titration curve (determined by prior titration of each monoclonal antibody stock) was added to each well and allowed to incubate for 1 hr at room temperature. After washing, anti-mouse HRP antibody (MP Biomedicals) was then added and allowed to incubate for 1 hr at room temperature. After washing, TMB substrate (KPL Biomedical) was then added and the reaction was stopped by adding HCL and the amount of HRP product was determined using a plate reader. Data (O.D.s) were graphed using matrix2png software (Pavlidis, P. and Noble W.S. (2003) Matrix2png: A Utility for Visualizing Matrix Data. Bioinformatics 19: 295-296).

Sequencing.

RNA was extracted from lung homogenate, MDCK supernatant (endpoint titrated viruses and stocks), or allantoic fluid using QiAmp viral RNA mini kit (Qiagen). cDNA was made (using a kit from Marligen), HA and NA were amplified by PCR, and sequencing was performed on an AppliedBiosystem DNA analyzer.

Dose-dependent quantitative glycan array analysis with whole viruses.

Streptavidin-coated high binding capacity 384-well plates (Pierce) were incubated overnight at 4°C with 50µl of 2.4µM biotinylated 3' SLN, 3' SLN-LN, 6' SLN or 6' SLN-LN (LN corresponds to lactosamine (Galβ1-4GlcNAc) and 3' SLN and 6' SLN

correspond respectively to Neu5Aca2-3 and Neu5Aca2-6 linked to LN). Glycans were provided by the Consortium of Functional Glycomics (www.functionalglycomics.org). 50µl virus diluted in PBS 1% (w/v) BSA (PBS-BSA) added to glycan-coated wells were incubated overnight at 4°C, and washed 3 times with PBST (PBS, 0.1% Tween-20) and three times with PBS. Wells were then blocked with PBS-BSA for 2 h at 4°C, before incubating with NA2-1C1 anti-NA mAb diluted in PBSBSA for 5 h at 4°C. After washing as above, wells were incubated with goat anti-mouse IgG HRP conjugated antibody in PBS-BSA. Wells were washed as above, and binding of secondary antibody was detected using the Amplex Red Peroxidase Assay (Invitrogen) according to the manufacturer's instructions. Appropriate negative controls were included. Assays were performed in duplicate.

In vitro neutralization assays.

Quadruplicate samples of serial dilutions of polyclonal antibody serum mixed with viruses were incubated at room temperature for 30 min, and then incubated with MDCK cells for 1 hr at 37°C. Cells were washed twice with serum-free media, and then serum-free media containing trypsin was added. Virus growth was scored 3 days later by cytopathic effect. Data are expressed as the inverse dilution of serum that caused neutralization.

A1.2 Materials and Methods for Chapter 3

Site-directed mutagenesis of HA.

Site-directed mutagenesis was carried out with the QuikChange multi site-directed mutagenesis kit (Stratagene). The primer used for mutagenesis was designed by using the web-based program, Primer3 (<http://frodo.wi.mit.edu/primer3/>) and synthesized by IDT DNA Technologies. The primer sequence used for generating T93A mutants is 5'GAA ACA TCG AAC TCA GAG AAT GGA GCA TGT TAC CCA GGA GAT TTC ATC G 3'. The primer sequence used for generating N91D mutant in NY18 HA is 5' GTA GAA ACA TCG AAC TCA GAG GAT GGA ACA TGT TAC CCA GGA GAT TTC 3'.

Cloning, baculovirus synthesis, expression and purification of HA.

Briefly, recombinant baculoviruses with wild-type or mutant HA gene respectively, were used to infect (MOI=1) suspension cultures of Sf9 cells (Invitrogen, Carlsbad, CA) cultured in BD Baculogold Max-XP SFM (BD Biosciences, San Jose, CA). The infection was monitored and the conditioned media was harvested 3-4 days post-infection. The soluble HA from the harvested conditioned media was purified (using a gradient of imidazole HCl concentration ranging from 20mM to 250mM) using Nickel affinity chromatography (HisTrap HP columns, GE Healthcare, Piscataway, NJ). Eluting fractions containing HA were pooled, concentrated and buffer exchanged into 1X PBS pH 8.0 (Gibco) using 100K MWCO spin columns (Millipore, Billerica, MA). The purified protein was quantified using BCA method (Pierce). Shown below is the purification profile for a representative HA (SC18T93A). HA in lanes 6 and 7 is marked below.

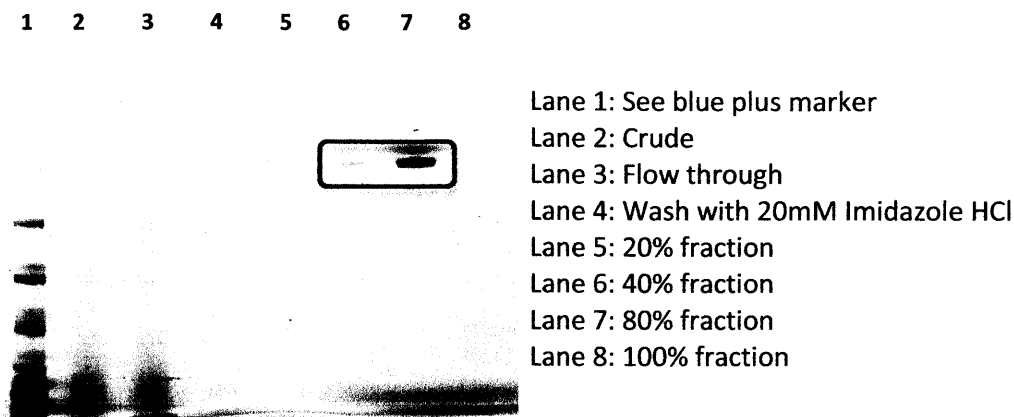


Figure A1.2 SDS-PAGE profile of recombinant HA purified by affinity chromatography

Circular dichroism analysis of mutant HAs.

Circular dichroism analysis was performed using the Aviv Model 202 Circular Dichroism spectrometer. The spectra was generated between 190 and 280nm. Identical concentration of the mutant and wild type proteins was used to avoid any differences in the spectra due to the differences in their concentration.

Dose dependent direct binding of wild-type and mutant HAs.

To investigate the multivalent HA-glycan interactions a streptavidin plate array comprising of representative biotinylated $\alpha 2 \rightarrow 3$ and $\alpha 2 \rightarrow 6$ sialylated glycans was used as described previously [110], (Table A1.2). 3'SLN, 3'SLN-LN, 3'SLN-LN-LN are representative avian receptors. 6'SLN and 6'SLN-LN are representative human receptors. The biotinylated glycans were obtained from the Consortium of Functional Glycomics through their resource request program. Streptavidin-coated High Binding Capacity 384-well plates (Pierce) were loaded to the full capacity of each well by incubating the well with 50 μ l of 2.4 μ M of biotinylated glycans overnight at 4 °C. Excess glycans were removed through extensive washing with PBS. The trimeric HA unit comprises of three HA monomers (and hence three RBS, one for each monomer). The spatial arrangement of the biotinylated glycans in the wells of the streptavidin plate

array favors binding to only one of the three HA monomers in the trimeric HA unit. Therefore in order to specifically enhance the multivalency in the HA-glycan interactions, the recombinant HA proteins were pre-complexed with the primary and secondary antibodies in the molar ratio of 4:2:1 (HA:primary:secondary). The identical arrangement of 4 trimeric HA units in the precomplex for all the HAs permit comparison between their glycan binding affinities.

A stock solution containing appropriate amounts of Histidine tagged HA protein, primary antibody (Mouse anti 6X His tag IgG, Abcam) and secondary antibody (HRP conjugated goat anti Mouse IgG Santacruz Biotechnology) in the ratio 4:2:1 and incubated on ice for 20 min. Appropriate amounts of precomplexed stock HA were diluted to 250 μ l with 1% BSA in PBS. 50 μ l of this precomplexed HA was added to each of the glycan-coated wells and incubated at room temperature for 2 hrs followed by the above wash steps. The binding signal was determined based on HRP activity using Amplex Red Peroxidase Assay (Invitrogen, CA) according to the manufacturer's instructions. The experiments were done in triplicate. Minimal binding signals were observed in the negative controls including binding of precomplexed unit to wells without glycans and binding of the antibodies alone to the wells with glycans. The binding parameters, cooperativity (n) and apparent binding constant (K_d'), for HA-glycan binding were calculated by fitting the average binding signal value (from the triplicate analysis) and the HA concentration to the linearized form of the Hill equation:

$$\log\left(\frac{y}{1-y}\right) = n * \log([HA]) - \log(K_d')$$

where y is the fractional saturation (average binding signal/maximum observed binding signal). The theoretical y values calculated using the Hill equation:

$$y = \frac{[HA]^n}{[HA]^n + K_d'}$$

(for the set of n and K_d' parameters) were plotted against the varying concentration of HA to obtain the binding curves for the representative human receptor (6'SLN-LN).

K_d' can also be calculated based on concentration of HA at half saturation.

$$K_d' = [HA_{y=0.5}]^n$$

Table A1.2 Expanded nomenclature of glycans used in the glycan array

Glycan	Expanded nomenclature
3'SLN	Neu5Ac α 2-3Gal β 1-4GlcNAc β 1-
6'SLN	Neu5Ac α 2-6Gal β 1-4GlcNAc β 1-
3'SLN-LN	Neu5Ac α 2-3Gal β 1-4GlcNAc β 1-3Gal β 1-4GlcNAc β 1-
6'SLN-LN	Neu5Ac α 2-6Gal β 1-4GlcNAc β 1-3Gal β 1-4GlcNAc β 1-
3'SLN-LN-LN	Neu5Ac α 2-3Gal β 1-4GlcNAc β 1-3Gal β 1-4GlcNAc β 1-3Gal β 1-4GlcNAc β 1-

Key: Neu5Ac: N-acetyl D-neuraminic acid; Gal: D-galactose; GlcNAc: N-acetyl D-glucosamine. α / β : anomeric configuration of the pyranose sugars. All the sugars are linked via a spacer to biotin (-Sp-LC-LC-Biotin as described in <http://www.functionalglycomics.org/static/consortium/resources/resourcecored5.shtm>

!)

A1.3 Materials and Methods for Chapter 4

Homology based structural modeling of CA04/09, CA04/09mut1 CA04/09mut2.

Using the SWISS-MODEL web-based automated homology-modeling platform (<http://swissmodel.expasy.org/>) the homology structural models of CA04/09 (**Figure 4.15A**), and CA04/09mut1 (**Figure 4.15B**) were constructed. The template structure chosen by SWISS-MODEL was that of a recently solved crystal structure of 2009 H1N1 HA (PDB ID: 3LZG). The starting pose of the HA-human receptor complex was obtained by superimposing the modeled HA structure with the co-crystal structure of 1918 H1N1 HA with human receptor (PDB ID: 2WRG). The starting structural complex was subject to energy minimization (500 steps of steepest descent followed by 500 steps of conjugate gradient). The AMBER force-field was used to assign potentials and charges. The default version of AMBER was provided with the Discover module of InsightII molecular modeling suite (Accelrys, San Diego, CA).

CA04/09mut2 HA (**Figure 4.15C**) mutant was designed to make the interaction network involving residues 186, 219 and 227 hydrophobic. Three mutations Ser186Pro, Ala189Thr and Glu227Ala in CA04/09mut2 HA make the inter-amino acid interaction network identical to that observed in SC18 HA (**Figure 4.15D**). The mutated residues are highlighted in *red*.

Cloning, baculovirus synthesis, expression and purification of HA.

Site-directed mutagenesis was carried out on CA04/09 wild-type HA backbone to generate CA04/09mut1, CA04/09mut2, CA04M3, CA04M4, and CA04M5 mutant HAs. The expression and purification of these mutant HAs were carried out as explained in **Appendix A1.2**. The proteins were validated by running them on SDS-PAGE (shown below, HAs are marked with a *black box*) and by performing Western blotting using anti-His antibody.

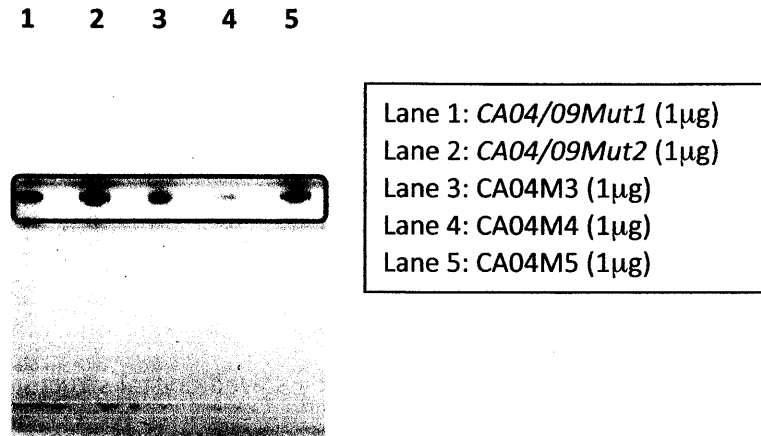


Figure A1.3 SDS-PAGE profile of mutant and wild-type recombinant HA (2009 H1N1) purified by affinity chromatography

Binding of recombinant CA04/09, CA04/09mut1 and CA04/09mut2 HAs to human tracheal tissue sections.

Paraffinized human tracheal (US Biological) tissue sections were deparaffinized, rehydrated and incubated with 1% BSA in PBS for 30 minutes to prevent non-specific binding. HA was pre-complexed with primary antibody (mouse anti 6X His tag, Abcam) and secondary antibody (Alexa fluor 488 goat anti mouse, Invitrogen) in a molar ratio of 4:2:1, respectively, for 20 minutes on ice. The tissue binding was performed over different HA concentrations by diluting the pre-complexed HA in 1% BSA-PBS. Tissue sections were then incubated with the HA-antibody complexes for 3 hours at RT. The tissue sections were counterstained by propidium iodide (Invitrogen; 1:100 in TBST). The tissue sections were mounted and then viewed under a confocal microscope (Zeiss LSM510 laser scanning confocal microscopy). In the case of sialidase pretreatment, tissue sections were incubated with 0.2 units of Sialidase A (recombinant from *Arthrobacter ureafaciens*, Prozyme) for 3 hours at 37° C prior to incubation with the proteins. This enzyme has been demonstrated to cleave the terminal Neu5Ac from both Neu5Ac α 2 \rightarrow 3Gal and Neu5Ac α 2 \rightarrow 6Gal motifs.

Dose dependent direct binding of CA04/09, CA04/09mut1, CA04/09mut2, CA04M3, CA04M4 and CA04M5 HAs.

The protocol described in **Appendix A1.2** was used to characterize the binding affinity and specificity of the mutant and wild-type recombinant HAs.

Construction of plasmids.

The eight reverse-genetics plasmids used for the rescue of recombinant influenza A/California/04/2009 (Cal/09) virus—pDZ-Cal04-PB2, pDZ-Cal04-PB1, pDZ-Cal04-PA, pDZ-Cal04-NP, pDZ-Cal04-HA, pDZ-Cal04-NA, pDZ-Cal04-M, and pDZ-Cal04-NS - were constructed by methods described previously [204, 205]. The HA plasmid pDZ-Cal04-Ile219->Lys was a derivative of the wild-type (WT) HA segment. The mutation Ile219->Lys was created by altering the position 219 codons from ATA to AAA using Stratagene QuickChange site-directed mutagenesis kit and pDZ-Cal04-HA as template.

Rescue of recombinant influenza A viruses.

The influenza A CA04/09 viruses were rescued as described previously [206]. Briefly, 293T cells were transfected with the eight pDZ-Cal04 vectors encoding each of the viral genomic RNA segments. At 12 h post transfection, the 293T cells were co-cultured with MDCK cells. The rescued viruses were further isolated by plaque purification on MDCK cells. The coding sequences of each PDZ construct and viruses generated by reverse genetics were confirmed by automated sequencing performed at the Centers for Disease Control and Prevention sequencing core facility.

Inoculation of ferrets.

The 2009 H1N1 virus animal experiments were conducted under biosafety level 3 enhanced (BSL3+) laboratory conditions. Male Fitch ferrets (Triple F Farms), 6 to 12 months of age that were serologically negative by hemagglutination inhibition (HI) assay

for currently circulating influenza viruses were used in this study. At the start of each experiment, all ferrets had body weights greater than 1.0 kg, with a range of 1.01-1.57 kg. Ferrets were housed throughout each experiment in cages within a Duo-Flo Bioclean mobile clean room (Lab Products, Inc. Seaford, DE). Baseline serum, temperature and weight measurements were obtained prior to infection. Temperatures were measured using a subcutaneous implantable temperature transponder (BioMedic Data Systems, Inc.). Ferrets were inoculated intranasally with 10^6 PFU (plaque forming units) in a 1ml volume, a dose reported to consistently infect ferrets with human or avian influenza viruses [207]. Ferrets were monitored for changes in body temperature and weight, and the presence of the following clinical signs: sneezing, lethargy, anorexia, nasal or ocular discharge, dyspnea, diarrhea, neurological dysfunction [158]. Nasal washes were collected every other day for at least 9 days post inoculation (p.i.) or contact (p.c.), analyzed [208] and titrated by standard plaque assay.

Ethics Statement.

All animal research described in this study was specifically approved by CDC's Institutional Animal care and Use Committee (IACUC). The animal research was conducted under the guidance of CDC's IACUC and in an Association for Assessment and Accreditation of Laboratory Animal Care International-accredited facility.

Transmission experiments.

For the respiratory droplet transmission experiments, ferrets were housed in adjacent transmission cages, each modified so that a side wall was replaced with a stainless-steel, perforated wall with holes 1-5 mm in diameter and spaced 3 mm apart to facilitate the transfer of respiratory droplets through the air while preventing direct contact between ferrets and indirect contact with the bedding and food of neighbouring ferrets. A total of six ferrets were used for each respiratory droplet transmission experiment [158]. Twenty-four hours after inoculation (day 1 p.i. for the inoculated ferrets and day 0 p.c. for the contact ferrets), three naive ferrets were each placed in a

cage adjacent to an inoculated ferret. To prevent inadvertent physical transmission of virus by the investigators, the contact ferrets were always handled first, and all items that came into contact with the ferrets or their bedding were decontaminated between each ferret. The use of the term “respiratory droplet transmission” throughout this report refers to transmission in the absence of direct or indirect contact and does not imply an understanding of the droplet size involved in virus spread between ferrets. The ability of each virus to undergo respiratory droplet transmission among ferrets was assessed by measuring virus titres in nasal washes from contact animals every other day for at least 11 days. HI analysis was also performed on post-exposure ferret sera collected 18-21 days p.c. using 0.5% turkey erythrocytes against homologous virus [208].

Dose dependent direct binding of rgCA04/09 Ile219Lys HA mutant virus on glycan array.

The protocol described in **Appendix A1.1** was used for the glycan array analysis with the virus. The primary antibody used was ferret anti – CA04/09 antisera; 1:500 diluted in 1X PBS + 1% BSA. The secondary antibody used was goat anti – ferret HRP conjugated antibody from Abcam; 1:500 diluted in 1X PBS + 1% BSA). The assays were done in duplicates.

A1.4 Materials and Methods for Chapter 5

Cloning, baculovirus synthesis, expression and purification of HA.

Recombinant SC18 and Alb58 HAs were expressed and purified as mentioned in **Appendix A1.2**.

Binding of hemagglutinin to ferret respiratory tissues.

Formalin fixed and paraffin embedded (5u thickness) ferret cranial and caudal tracheal tissue sections were obtained from Lovelace Respiratory Research Institute (LRRI). Formalin fixed and paraffin embedded ferret lung hilar tissue sections (5u thick) were obtained from Professor James G Fox's laboratory (Division of Comparative Medicine, Massachusetts Institute of Technology). Protocol followed for human tracheal tissue staining with HAs (**Appendix A1.3**) was followed for ferret respiratory tract tissues.

Lectin staining of ferret and human respiratory tract.

Formalin fixed and paraffin embedded ferret tracheal and lung hilar tissue sections were obtained from Lovelace Respiratory Research Institute and Division of Comparative Medicine (Massachusetts Institute of Technology) respectively. Tissue sections were deparaffinized and rehydrated. The tissue sections were incubated with 10µg/ml of lectins (SNA-I, Jacalin and MAL-II) respectively for 3 hours in dark at RT. Lectins were obtained from Vector Labs. To visualize the cell nuclei, sections were counterstained with propidium iodide (Invitrogen; 1:100 in TBST) for 20 minutes at RT. Sections were then washed, mounted and viewed under a Zeiss LSM510 laser scanning confocal microscope. For MAL-II, since the lectin was biotinylated, prior to adding the lectin, the tissue sections were incubated with streptavidin/biotin kit (Vector Labs) to block endogenous biotin for preventing non-specific staining of the tissues. For lectin co-staining experiments, Jacalin and SNA-I (10µg/ml each) was added simultaneously to the tissue sections.

A1.5 Material and Methods for Chapter 6

Structural analysis of SNA-I to identify its glycan-binding domain

The homology based structural model of SNA-I lectin domain was constructed using the co-crystal structure of SNA-II with lactose (PDB ID: 3CA4) as a template given that this template was selected by the SWISS-MODEL program. The use of this co-crystal structure as a template facilitated the identification of the glycan-binding sites (high-affinity and low-affinity) in the B chain enabling us to engineer the SNA-I B chain.

Cloning, Expression and Purification of 2 γ peptide of SNA-I

The 2 γ peptide (42aa, ~7.7kDa) gene sequence was cloned in a pET15b (in Nde I and BamH I sites). BL21star(DE3) cells (from Invitrogen, Carlsbad) was transformed with the recombinant plasmid for expression. For expression, an overnight culture (5ml) of BL21star(DE3) harboring the 2 γ peptide (in LB ampicillin) was used to inoculate a 1L LB media (containing 100 μ g/ml ampicillin). The cells were grown at 37°C till OD_{600nm} reached 0.6 to 1. The protein induction was carried out by adding 1mM IPTG (isopropyl thio β -D galactoside). The cells were grown for 16h at 25°C post-induction to avoid formation of inclusion bodies. The cells were pelleted by centrifugation at 4500rpm at 4°C for 15mins. The supernatant was discarded and the pellets were stored at -80°C.

Purification of the peptide was carried out using a denaturation/renaturation protocol. Briefly, the protein was unfolded to facilitate binding to the NI column and later refolded. The buffers used for the purification are:

- Binding/lysis buffer: 50mM NaH₂PO₄, 300mM NaCl, 5mM Imidazole HCl, 6M Guanidium hydrochloride, pH 8.0
- Wash buffer: 50mM NaH₂PO₄, 300mM NaCl, 10mM Imidazole HCl, 6M Urea, pH 8.0
- Refolding buffer: Same as Wash buffer but without 6M urea
- Elution buffer: 50mM NaH₂PO₄, 300mM NaCl, 250mM Imidazole HCl, pH 8.0

Lysate Preparation: The cells (stored in -80°C) were thawed on ice. The cells were suspended in the lysis buffer and incubated on a magnetic stirrer for 50mins at room temperature (25°C). This process should lyse the cells and unfold the protein. The lysate was then centrifuged at 4800rpm for 30mins. The supernatant was harvested and used for purification on a nickel column using FPLC (AKTA purifier from GE). For the purification, the lysate was loaded onto the nickel column followed by a wash with the binding buffer. Following this the column was washed with the wash buffer (containing 6M urea). To re-fold the protein, the column was washed with a gradient of urea concentration from 6M urea to no urea (in the re-folding buffer). Following this the protein was eluted from the column using a gradient method, which involves a gradual increase in imidazole concentration ranging from 10mM to 250mM. Fractions were collected when peaks (at OD280nm) were seen during the process of elution. The samples were analyzed on SDS PAGE and fractions containing the peptide were identified by western blotting using anti-his antibody (Abcam). The fractions containing the peptide were pooled, concentrated and buffer exchanged to 1X PBS in Vivaspin filter spin column with 500Da MWCO. Protein concentration was estimated by Bradford's method.

Structural analysis of PSL to identify its glycan-binding domain

Although the crystal structure of PSL has not been solved, based on sequence identity, it has been implicated to adopt the same fold observed in the crystal structure of *Marasmius oreades* agglutinin (MOA). In this structural fold, PSL has a single ricin-B like β -trefoil domain at the N-terminus that is composed of three homologous subdomains (α , β , and γ). Mutant constructs that have single amino acid mutations in the putative sugar-binding sites, based on the sequence alignment with the ricin B-chain, indicate that β and γ subdomains are the probable sugar binding sites [192]. The homology based structural model of PSL was constructed using the co-crystal structure of MOA with Gal α 1-3Gal β 1-4GlcNAc (PDB ID: 2IHO) as a template given that this

template was selected by the SWISS-MODEL program. The use of this co-crystal structure as a template facilitated the identification of the glycan-binding sites on PSL and docking of an α 2-6 oligosaccharide motif (Neu5Ac α 2-6Gal β 1-4GlcNAc) into the glycan binding site of the modeled PSL structure. These docking studies facilitated the identification of the β -trefoil lectin domain in PSL and also provided insights into the molecular interactions of this lectin domain with the glycan motif.

Cloning, Expression and Purification of glycan binding domain of PSL

The glycan binding domain of PSL (6-149aa) was synthesized (DNA2.0) and subcloned into *Nde I* and *BamH I* sites of pET15b vector and transformed into BL21star(DE3) *E.coli* (Invitrogen) cells. The expression of *rPSL-N* was carried out as described previously. Briefly, a 5ml overnight culture of BL21star(DE3) *E.coli* cells harboring the recombinant *rPSL-N* expression vector was grown at 37°C in Luria-Bertani (LB) medium containing 100 μ g/ml of ampicillin. The 5ml culture was added to a 1l LB medium containing 100 μ g/ml of ampicillin and incubated at 37°C shaker. The culture was induced with 1mM (final concentration) of isopropyl β -D-thiogalactoside (IPTG) after the absorbance at 600 nm reached \sim 0.6-1 and the cells were further cultured at 25°C overnight. The induced cells were harvested by centrifugation. The cells were lysed by sonication and the insoluble fraction was removed by centrifugation. The soluble *rPSL-N* from the lysate was purified using Nickel affinity chromatography (HisTrap HP columns, GE Healthcare, Piscataway, NJ). Eluting fractions containing *rPSL-N* were pooled, concentrated and buffer exchanged into 1X PBS pH 8.0 (Gibco) using 3K MWCO spin columns (Millipore, Billerica, MA). The purified protein was quantified using BCA method (Pierce).

Cytotoxicity Analysis of PSL vs. rPSL-N

MDCK cells were seeded in a 96-well plate and incubated with various lectin concentrations for 2h in 37°C, 5% CO₂ incubator. The cells were then overlaid with 1X MEM + 0.1% BSA and incubated for 48h in 37°C, 5% CO₂ incubator. Cytopathic effects

were analyzed in light microscope after 24h and 48h of incubation and compared with that of the non-treated cells. To quantitatively estimate the cytotoxicity, the cells were stained with crystal violet and densitometric scanning was performed using Adobe Photoshop. Briefly, after 48h of incubation with the drug, the media was aspirated and the cells were washed twice with 1X PBS. The cells were fixed for 15mins with 10% buffered formalin followed by washes with water. The cells were finally stained with 10% crystal violet (in 20% methanol) for 15 mins. The cells were washed with tap water and allowed the plate to dry completely before performing the densitometric scanning analysis with Photoshop. For each lectin concentration, 4 microwells were used.

Binding of recombinant rPSL-N to human tracheal and alveolar tissue sections

The protocol followed for HA staining (**Appendix A1.3**) was followed for rPSL-N staining of human tracheal tissue section. rPSL-N was precomplexed with primary (mouse anti-his monoclonal antibody) and secondary (goat anti-mouse IgG HRP) antibodies in a molar ratio of 4:2:1 before adding to the tissue sections.

Dose dependent direct binding of rPSL-N protein

The protocol followed for glycan array analysis of HA (**Appendix A1.2**) was followed. The binding parameters, cooperativity (n) and apparent binding constant (K_d') were calculated by fitting the average signal value (from the triplicate analysis) and the rPSL-N concentration to the linearized form of the Hill equation:

$$\log\left(\frac{y}{1-y}\right) = n * \log([rPSL]) - \log(K_d')$$

where y is the fractional saturation (average binding signal/maximum observed binding signal). The theoretical y values calculated using the Hill equation:

$$y = \frac{[rPSL]^n}{[rPSL]^n + K_d'}$$

(for the set of n and K_d' parameters) were plotted against the varying concentration of rPSL-N to obtain the binding curves for the representative human receptor (6'SLN-LN).

Inhibition of influenza A virus infection by rPSL-N: detection of viral RNA by quantitative real time PCR

For measuring inhibition of influenza A virus infection by *rPSL-N*, viral M-gene copy number was quantified from the *rPSL-N* treated Madin Darby Canine Kidney Cells (MDCK) cells by real time PCR analysis. Briefly, MDCK cells were seeded in a 96-well plate at a density of 2.4×10^4 cells per well and incubated overnight at 37°C in 5% CO₂. After the cells were grown to a confluent monolayer, the cells were pretreated with various *rPSL-N* dilutions for 2h in 37°C, 5% CO₂ incubator. After 2h, the pretreated cells were infected with influenza A virus (diluted in 1X MEM + 2 µg/ml of TPCK trypsin) at a multiplicity of infection (MOI) of 0.001 for 1h in 35°C, 5% CO₂ incubator. The influenza A viruses used for the assay are A/Victoria/3/75 (H3N2) [ATCC] and A/PR/8/34 (H1N1). The cells were overlaid with 1X MEM + 0.1% BSA + 2 µg/ml of TPCK trypsin and incubated in 35°C, 5% CO₂ incubator. After 48h of incubation, the media was harvested and 50 µl of the conditioned media was used for viral RNA extraction using QIAamp viral RNA mini kit (Qiagen). Quantitative real time PCR (qRT-PCR) reaction was set up as described [195] using Qiagen one-step RT-PCR kit (Qiagen). The conditions used for the PCR were: reverse transcription at 50°C for 30 mins, heat inactivation of polymerase at 94°C for 15 mins followed by two-step cycle (45 cycles) involving denaturation at 94°C for 1s and annealing/extension at 60°C for 20s. The quantitative PCR was carried out with 8 µl of viral RNA (for both standards and the samples) or water for the no template control. The standards for the qRT-PCR analysis were generated by doing serial dilution (4 times) of viral RNA extracted from influenza A virus with a known titer (from 4×10^6 to 975). Ct threshold was determined manually and the Ct values for the standards were plotted. The standards gave a good linearity ($R^2 \sim 0.99$). The assay was repeated twice and for each *rPSL-N* concentration, 8 microwells for were used. Viral RNA extracted from each of the technical replicate was then used in triplicate for the qRT-PCR analysis. Curve – fitting and IC₅₀ calculation was done using Graphpad Prism 5 software.

In vivo studies with rPSL-N

On the morning of day 0, ketamine anesthetized 8 week-old female BALB/c mice (weighing 25g) received the first intranasal treatment of *rPSL-N* (or PBS for control animals) at a concentration of 1mg/kg. 6 hours later, the mice were inoculated intranasally with 5 LD₅₀ of mouse-adapted CA04/09 virus. Following this mice were daily treated intranasally with 1mg/kg of *rPSL-N* for 5 days p.i. Totally 10 mice were treated with *rPSL-N* or with 1X PBS alone. Survival and weights were monitored for 6 mice and virus tissue titers were estimated for the rest of the 4 mice 4 days post-infection (p.i.).

Abbreviations Used

A ₆₀₀	Absorbance at 600nm
BSA	Bovine Serum Albumin
CBD	Carbohydrate Binding Domain
CDC	Centers for Disease Control
CPE	Cytopathic Effect
FDA	Food and Drug Administration
FITC	Fluorescein Isothiocyanate
FPLC	Fast Protein Liquid Chromatography
HA	Hemagglutinin
HAI	Hemagglutinin Inhibition
H & E	Hematoxylin and Eosin
HPAI	Highly Pathogenic Avian Influenza A virus
IC ₅₀	Concentration of a drug at which there is 50% reduction
K _d '	Apparent Dissociation constant
LB	Luria Bertani media
LPAI	Low Pathogenic Avian Influenza A virus
MAL-II	<i>Maackia amurensis</i> Lectin II
MDCK	Madin-Darby Canine Kidney Cells
MOA	<i>Marasmius oreades</i> Agglutinin
mRNA	messenger Ribonucleic Acid
MWCO	Molecular Weight Cut-Off
NA	Neuraminidase
NEP	Nuclear Export Protein
Neu5Ac	N-Acetyl Neuraminic acid
pAb	Polyclonal Antibody
PBS	Phosphate Buffer Saline
PFU	Plaque Forming Units

PI	Propidium Iodide
PSL	<i>Polyporus squamosus</i> Lectin
<i>rPSL-N</i>	N-terminal of PSL lectin
RBCs	Red Blood Cells
RBS	Receptor Binding Site
rg	Reverse Genetics
SDS-PAGE	Sodium Dodecyl Sulfate Polyacrylamide Gel Electrophoresis
SNA	<i>Sambucus nigra</i> Agglutinin
vRNA	Viral Ribonucleic Acid
vRNP	Viral Ribonucleoprotein
y	Fractional Saturation

Bibliography

1. Taubenberger, J. K. and Morens, D. M. (2008) The pathology of influenza virus infections. *Annu Rev Pathol* 3, 499-522.
2. Viswanathan, K., Chandrasekaran, A., Srinivasan, A., Raman, R., Sasisekharan, V., Sasisekharan, R. (2010) Glycans as receptors for influenza pathogenesis. *Glycoconj J* 27, 561-70.
3. Neumann, G. and Kawaoka, Y. (2006) Host range restriction and pathogenicity in the context of influenza pandemic. *Emerg Infect Dis* 12, 881-6.
4. McAuley, J. L., Hornung, F., Boyd, K. L., Smith, A. M., McKeon, R., Bennink, J., Yewdell, J. W., McCullers, J. A. (2007) Expression of the 1918 influenza A virus PB1-F2 enhances the pathogenesis of viral and secondary bacterial pneumonia. *Cell Host Microbe* 2, 240-9.
5. Chen, W., Calvo, P. A., Malide, D., Gibbs, J., Schubert, U., Bacik, I., Basta, S., O'Neill, R., Schickli, J., Palese, P., Henklein, P., Bennink, J. R., Yewdell, J. W. (2001) A novel influenza A virus mitochondrial protein that induces cell death. *Nat Med* 7, 1306-12.
6. Zamarin, D., Garcia-Sastre, A., Xiao, X., Wang, R., Palese, P. (2005) Influenza virus PB1-F2 protein induces cell death through mitochondrial ANT3 and VDAC1. *PLoS Pathog* 1, e4.
7. Neumann, G., Noda, T., Kawaoka, Y. (2009) Emergence and pandemic potential of swine-origin H1N1 influenza virus. *Nature* 459, 931-9.
8. Gratzl E, a. K. H. (1968) Gefluegelpest. In: *Spezielle Pathologie und Therapie der Gefluegelkrankheiten*. Ferdinand Enke Verlag., Stuttgart, Germany. 178 - 200.
9. Van Campen, H., Easterday, B. C., Hinshaw, V. S. (1989) Virulent avian influenza A viruses: their effect on avian lymphocytes and macrophages in vivo and in vitro. *J Gen Virol* 70 (Pt 11), 2887-95.
10. Van Campen, H., Easterday, B. C., Hinshaw, V. S. (1989) Destruction of lymphocytes by a virulent avian influenza A virus. *J Gen Virol* 70 (Pt 2), 467-72.
11. Kobayashi, Y. e. a. (1996) Pathological studies of chickens experimentally infected with two highly pathogenic influenza A viruses. *Avian Pathol* 25, 285-304.
12. Feldmann, A., Schafer, M. K., Garten, W., Klenk, H. D. (2000) Targeted infection of endothelial cells by avian influenza virus A/FPV/Rostock/34 (H7N1) in chicken embryos. *J Virol* 74, 8018-27.
13. Wagner, R., Matrosovich, M., Klenk, H. D. (2002) Functional balance between haemagglutinin and neuraminidase in influenza virus infections. *Rev Med Virol* 12, 159-66.
14. Gamblin, S. J. and Skehel, J. J. (2010) Influenza hemagglutinin and neuraminidase membrane glycoproteins. *J Biol Chem* 285, 28403-9.
15. Claas, E. C., Osterhaus, A. D., van Beek, R., De Jong, J. C., Rimmelzwaan, G. F., Senne, D. A., Krauss, S., Shortridge, K. F., Webster, R. G. (1998) Human influenza

- A H5N1 virus related to a highly pathogenic avian influenza virus. *Lancet* 351, 472-7.
16. Matsuoka, Y., Swayne, D. E., Thomas, C., Rameix-Welti, M. A., Naffakh, N., Warnes, C., Altholtz, M., Donis, R., Subbarao, K. (2009) Neuraminidase stalk length and additional glycosylation of the hemagglutinin influence the virulence of influenza H5N1 viruses for mice. *J Virol* 83, 4704-8.
 17. Vigerust, D. J., Ulett, K. B., Boyd, K. L., Madsen, J., Hawgood, S., McCullers, J. A. (2007) N-linked glycosylation attenuates H3N2 influenza viruses. *J Virol* 81, 8593-600.
 18. Klenk, H. D., Garten, W., Matrosovich, M. (2011) Molecular mechanisms of interspecies transmission and pathogenicity of influenza viruses: Lessons from the 2009 pandemic. *Bioessays*.
 19. Taubenberger, J. K. and Kash, J. C. (2010) Influenza virus evolution, host adaptation, and pandemic formation. *Cell Host Microbe* 7, 440-51.
 20. Watanabe, T., Watanabe, S., Shinya, K., Kim, J. H., Hatta, M., Kawaoka, Y. (2009) Viral RNA polymerase complex promotes optimal growth of 1918 virus in the lower respiratory tract of ferrets. *Proc Natl Acad Sci U S A* 106, 588-92.
 21. Hatta, M., Gao, P., Halfmann, P., Kawaoka, Y. (2001) Molecular basis for high virulence of Hong Kong H5N1 influenza A viruses. *Science* 293, 1840-2.
 22. Naffakh, N., Tomoiu, A., Rameix-Welti, M. A., van der Werf, S. (2008) Host restriction of avian influenza viruses at the level of the ribonucleoproteins. *Annu Rev Microbiol* 62, 403-24.
 23. Steel, J., Lowen, A. C., Mubareka, S., Palese, P. (2009) Transmission of influenza virus in a mammalian host is increased by PB2 amino acids 627K or 627E/701N. *PLoS Pathog* 5, e1000252.
 24. Li, Z., Chen, H., Jiao, P., Deng, G., Tian, G., Li, Y., Hoffmann, E., Webster, R. G., Matsuoka, Y., Yu, K. (2005) Molecular basis of replication of duck H5N1 influenza viruses in a mammalian mouse model. *J Virol* 79, 12058-64.
 25. Gabriel, G., Abram, M., Keiner, B., Wagner, R., Klenk, H. D., Stech, J. (2007) Differential polymerase activity in avian and mammalian cells determines host range of influenza virus. *J Virol* 81, 9601-4.
 26. Gabriel, G., Herwig, A., Klenk, H. D. (2008) Interaction of polymerase subunit PB2 and NP with importin alpha1 is a determinant of host range of influenza A virus. *PLoS Pathog* 4, e11.
 27. Van Hoeven, N., Pappas, C., Belser, J. A., Maines, T. R., Zeng, H., Garcia-Sastre, A., Sasisekharan, R., Katz, J. M., Tumpey, T. M. (2009) Human HA and polymerase subunit PB2 proteins confer transmission of an avian influenza virus through the air. *Proc Natl Acad Sci U S A*.
 28. Hale, B. G., Randall, R. E., Ortin, J., Jackson, D. (2008) The multifunctional NS1 protein of influenza A viruses. *J Gen Virol* 89, 2359-76.
 29. Palese, P., and Shaw, M. L. (2007) *Orthomyxoviridae: the viruses and their replication*. Lippincott, Williams & Wilkins, Philadelphia. 1647-1690.
 30. Seo, S. H., Hoffmann, E., Webster, R. G. (2002) Lethal H5N1 influenza viruses escape host anti-viral cytokine responses. *Nat Med* 8, 950-4.

31. Seo, S. H., Hoffmann, E., Webster, R. G. (2004) The NS1 gene of H5N1 influenza viruses circumvents the host anti-viral cytokine responses. *Virus Res* 103, 107-13.
32. Conenello, G. M., Tisoncik, J. R., Rosenzweig, E., Varga, Z. T., Palese, P., Katze, M. G. (2010) A Single N66S Mutation in the PB1-F2 Protein of Influenza A Virus Increases Virulence by Inhibiting the Early Interferon Response In Vivo. *J Virol*.
33. Conenello, G. M., Zamarin, D., Perrone, L. A., Tumpey, T., Palese, P. (2007) A single mutation in the PB1-F2 of H5N1 (HK/97) and 1918 influenza A viruses contributes to increased virulence. *PLoS Pathog* 3, 1414-21.
34. Bui, M., Wills, E. G., Helenius, A., Whittaker, G. R. (2000) Role of the influenza virus M1 protein in nuclear export of viral ribonucleoproteins. *J Virol* 74, 1781-6.
35. Rossman, J. S. and Lamb, R. A. (2009) Autophagy, apoptosis, and the influenza virus M2 protein. *Cell Host Microbe* 6, 299-300.
36. Lakadamyali, M., Rust, M. J., Zhuang, X. (2004) Endocytosis of influenza viruses. *Microbes Infect* 6, 929-36.
37. Paulson, J. C., Blixt, O., Collins, B. E. (2006) Sweet spots in functional glycomics. *Nat Chem Biol* 2, 238-48.
38. van Riel, D., Munster, V. J., de Wit, E., Rimmelzwaan, G. F., Fouchier, R. A., Osterhaus, A. D., Kuiken, T. (2006) H5N1 Virus Attachment to Lower Respiratory Tract. *Science* 312, 399.
39. van Riel, D., Munster, V. J., de Wit, E., Rimmelzwaan, G. F., Fouchier, R. A., Osterhaus, A. D., Kuiken, T. (2007) Human and Avian Influenza Viruses Target Different Cells in the Lower Respiratory Tract of Humans and Other Mammals. *Am J Pathol*.
40. van Riel, D., den Bakker, M. A., Leijten, L. M., Chutinimitkul, S., Munster, V. J., de Wit, E., Rimmelzwaan, G. F., Fouchier, R. A., Osterhaus, A. D., Kuiken, T. (2010) Seasonal and pandemic human influenza viruses attach better to human upper respiratory tract epithelium than avian influenza viruses. *Am J Pathol* 176, 1614-8.
41. Matrosovich, M. N., Matrosovich, T. Y., Gray, T., Roberts, N. A., Klenk, H. D. (2004) Human and avian influenza viruses target different cell types in cultures of human airway epithelium. *Proc Natl Acad Sci U S A* 101, 4620-4.
42. Matrosovich, M., Matrosovich, T., Uhlendorff, J., Garten, W., Klenk, H. D. (2007) Avian-virus-like receptor specificity of the hemagglutinin impedes influenza virus replication in cultures of human airway epithelium. *Virology* 361, 384-90.
43. Mansfield, K. G. (2007) Viral tropism and the pathogenesis of influenza in the Mammalian host. *Am J Pathol* 171, 1089-92.
44. Campitelli, L., Mogavero, E., De Marco, M. A., Delogu, M., Puzelli, S., Frezza, F., Facchini, M., Chiapponi, C., Foni, E., Cordioli, P., Webby, R., Barigazzi, G., Webster, R. G., Donatelli, I. (2004) Interspecies transmission of an H7N3 influenza virus from wild birds to intensively reared domestic poultry in Italy. *Virology* 323, 24-36.
45. Rohm, C., Horimoto, T., Kawaoka, Y., Suss, J., Webster, R. G. (1995) Do hemagglutinin genes of highly pathogenic avian influenza viruses constitute unique phylogenetic lineages? *Virology* 209, 664-70.

46. Webster, R. G., Bean, W. J., Gorman, O. T., Chambers, T. M., Kawaoka, Y. (1992) Evolution and ecology of influenza A viruses. *Microbiol Rev* 56, 152-79.
47. Van Damme, E. J., Roy, S., Barre, A., Citores, L., Mostafapous, K., Rouge, P., Van Leuven, F., Girbes, T., Goldstein, I. J., Peumans, W. J. (1997) Elderberry (*Sambucus nigra*) bark contains two structurally different Neu5Ac(alpha2,6)Gal/GalNAc-binding type 2 ribosome-inactivating proteins. *Eur J Biochem* 245, 648-55.
48. Chandrasekaran, A., Srinivasan, A., Raman, R., Viswanathan, K., Raguram, S., Tumpey, T. M., Sasisekharan, V., Sasisekharan, R. (2008) Glycan topology determines human adaptation of avian H5N1 virus hemagglutinin. *Nat Biotechnol* 26, 107-13.
49. Shinya, K., Ebina, M., Yamada, S., Ono, M., Kasai, N., Kawaoka, Y. (2006) Avian flu: influenza virus receptors in the human airway. *Nature* 440, 435-6.
50. Ito, T., Couceiro, J. N., Kelm, S., Baum, L. G., Krauss, S., Castrucci, M. R., Donatelli, I., Kida, H., Paulson, J. C., Webster, R. G., Kawaoka, Y. (1998) Molecular basis for the generation in pigs of influenza A viruses with pandemic potential. *J Virol* 72, 7367-73.
51. Kida, H., Ito, T., Yasuda, J., Shimizu, Y., Itakura, C., Shortridge, K. F., Kawaoka, Y., Webster, R. G. (1994) Potential for transmission of avian influenza viruses to pigs. *J Gen Virol* 75 (Pt 9), 2183-8.
52. Ludwig, S., Stitz, L., Planz, O., Van, H., Fitch, W. M., Scholtissek, C. (1995) European swine virus as a possible source for the next influenza pandemic? *Virology* 212, 555-61.
53. Scholtissek, C. (1990) Pigs as "mixing vessels" for the creation of new pandemic influenza A viruses *Med Princ Pract* 2, 65-71.
54. Skehel, J. J. and Wiley, D. C. (2000) Receptor binding and membrane fusion in virus entry: the influenza hemagglutinin. *Annu Rev Biochem* 69, 531-69.
55. Jiang, S., Li, R., Du, L., Liu, S. (2010) Roles of the hemagglutinin of influenza A virus in viral entry and development of antiviral therapeutics and vaccines. *Protein Cell* 1, 342-54.
56. Kido, H., Yokogoshi, Y., Sakai, K., Tashiro, M., Kishino, Y., Fukutomi, A., Katunuma, N. (1992) Isolation and characterization of a novel trypsin-like protease found in rat bronchiolar epithelial Clara cells. A possible activator of the viral fusion glycoprotein. *J Biol Chem* 267, 13573-9.
57. Bottcher-Friebertshauer, E., Stein, D. A., Klenk, H. D., Garten, W. (2010) Inhibition of influenza virus infection in human airway cell cultures by an antisense peptide-conjugated morpholino oligomer targeting the hemagglutinin activating protease TMPRSS2. *J Virol*.
58. Chaipan, C., Kobasa, D., Bertram, S., Glowacka, I., Steffen, I., Tsegaye, T. S., Takeda, M., Bugge, T. H., Kim, S., Park, Y., Marzi, A., Pohlmann, S. (2009) Proteolytic activation of the 1918 influenza virus hemagglutinin. *J Virol* 83, 3200-11.

59. Perdue, M. L., Garcia, M., Senne, D., Fraire, M. (1997) Virulence-associated sequence duplication at the hemagglutinin cleavage site of avian influenza viruses. *Virus Res* 49, 173-86.
60. Stieneke-Grober, A., Vey, M., Angliker, H., Shaw, E., Thomas, G., Roberts, C., Klenk, H. D., Garten, W. (1992) Influenza virus hemagglutinin with multibasic cleavage site is activated by furin, a subtilisin-like endoprotease. *EMBO J* 11, 2407-14.
61. Steinhauer, D. A. (1999) Role of hemagglutinin cleavage for the pathogenicity of influenza virus. *Virology* 258, 1-20.
62. Harrison, S. C. (2008) Viral membrane fusion. *Nat Struct Mol Biol* 15, 690-8.
63. Reed, M. L., Bridges, O. A., Seiler, P., Kim, J. K., Yen, H. L., Salomon, R., Govorkova, E. A., Webster, R. G., Russell, C. J. (2010) The pH of activation of the hemagglutinin protein regulates H5N1 influenza virus pathogenicity and transmissibility in ducks. *J Virol* 84, 1527-35.
64. Bullough, P. A., Hughson, F. M., Skehel, J. J., Wiley, D. C. (1994) Structure of influenza haemagglutinin at the pH of membrane fusion. *Nature* 371, 37-43.
65. Fleury, D., Wharton, S. A., Skehel, J. J., Knossow, M., Bizet, T. (1998) Antigen distortion allows influenza virus to escape neutralization. *Nat Struct Biol* 5, 119-23.
66. Shriver, Z., Raman, R., Viswanathan, K., Sasisekharan, R. (2009) Context-specific target definition in influenza A virus hemagglutinin-glycan receptor interactions. *Chem Biol* 16, 803-14.
67. Tumpey, T. M., Maines, T. R., Van Hoeven, N., Glaser, L., Solorzano, A., Pappas, C., Cox, N. J., Swayne, D. E., Palese, P., Katz, J. M., Garcia-Sastre, A. (2007) A two-amino acid change in the hemagglutinin of the 1918 influenza virus abolishes transmission. *Science* 315, 655-9.
68. Paulson, J. C. and Rogers, G. N. (1987) Resialylated erythrocytes for assessment of the specificity of sialyloligosaccharide binding proteins. *Methods Enzymol* 138, 162-8.
69. Connor, R. J., Kawaoka, Y., Webster, R. G., Paulson, J. C. (1994) Receptor specificity in human, avian, and equine H2 and H3 influenza virus isolates. *Virology* 205, 17-23.
70. Rogers, G. N. and Paulson, J. C. (1983) Receptor determinants of human and animal influenza virus isolates: differences in receptor specificity of the H3 hemagglutinin based on species of origin. *Virology* 127, 361-73.
71. Yang, Z. Y., Wei, C. J., Kong, W. P., Wu, L., Xu, L., Smith, D. F., Nabel, G. J. (2007) Immunization by avian H5 influenza hemagglutinin mutants with altered receptor binding specificity. *Science* 317, 825-8.
72. Carroll, S. M., Higa, H. H., Paulson, J. C. (1981) Different cell-surface receptor determinants of antigenically similar influenza virus hemagglutinins. *J Biol Chem* 256, 8357-63.
73. Gambaryan, A. S. and Matrosovich, M. N. (1992) A solid-phase enzyme-linked assay for influenza virus receptor-binding activity. *J Virol Methods* 39, 111-23.

74. Sauter, N. K., Hanson, J. E., Glick, G. D., Brown, J. H., Crowther, R. L., Park, S. J., Skehel, J. J., Wiley, D. C. (1992) Binding of influenza virus hemagglutinin to analogs of its cell-surface receptor, sialic acid: analysis by proton nuclear magnetic resonance spectroscopy and X-ray crystallography. *Biochemistry* 31, 9609-21.
75. Collins, B. E. and Paulson, J. C. (2004) Cell surface biology mediated by low affinity multivalent protein-glycan interactions. *Curr Opin Chem Biol* 8, 617-25.
76. Gambaryan, A. S., Tuzikov, A. B., Bovin, N. V., Yamnikova, S. S., Lvov, D. K., Webster, R. G., Matrosovich, M. N. (2003) Differences between influenza virus receptors on target cells of duck and chicken and receptor specificity of the 1997 H5N1 chicken and human influenza viruses from Hong Kong. *Avian Dis* 47, 1154-60.
77. Gambaryan, A. S., Tuzikov, A. B., Piskarev, V. E., Yamnikova, S. S., Lvov, D. K., Robertson, J. S., Bovin, N. V., Matrosovich, M. N. (1997) Specification of receptor-binding phenotypes of influenza virus isolates from different hosts using synthetic sialylglycopolymers: non-egg-adapted human H1 and H3 influenza A and influenza B viruses share a common high binding affinity for 6'-sialyl(N-acetyl)lactosamine. *Virology* 232, 345-50.
78. Matrosovich, M., Tuzikov, A., Bovin, N., Gambaryan, A., Klimov, A., Castrucci, M. R., Donatelli, I., Kawaoka, Y. (2000) Early alterations of the receptor-binding properties of H1, H2, and H3 avian influenza virus hemagglutinins after their introduction into mammals. *J Virol* 74, 8502-12.
79. Gambaryan, A., Yamnikova, S., Lvov, D., Tuzikov, A., Chinarev, A., Pazynina, G., Webster, R., Matrosovich, M., Bovin, N. (2005) Receptor specificity of influenza viruses from birds and mammals: new data on involvement of the inner fragments of the carbohydrate chain. *Virology* 334, 276-83.
80. Gambaryan, A., Tuzikov, A., Pazynina, G., Bovin, N., Balish, A., Klimov, A. (2006) Evolution of the receptor binding phenotype of influenza A (H5) viruses. *Virology* 344, 432-8.
81. Stevens, J., Blixt, O., Paulson, J. C., Wilson, I. A. (2006) Glycan microarray technologies: tools to survey host specificity of influenza viruses. *Nat Rev Microbiol* 4, 657-64.
82. Gambaryan, A. S., Piskarev, V. E., Yamskov, I. A., Sakharov, A. M., Tuzikov, A. B., Bovin, N. V., Nifant'ev, N. E., Matrosovich, M. N. (1995) Human influenza virus recognition of sialyloligosaccharides. *FEBS Lett* 366, 57-60.
83. Gambaryan, A. S., Tuzikov, A. B., Pazynina, G. V., Desheva, J. A., Bovin, N. V., Matrosovich, M. N., Klimov, A. I. (2008) 6-sulfo sialyl Lewis X is the common receptor determinant recognized by H5, H6, H7 and H9 influenza viruses of terrestrial poultry. *Virol J* 5, 85.
84. Blixt, O. and Razi, N. (2006) Chemoenzymatic synthesis of glycan libraries. *Methods Enzymol* 415, 137-53.
85. Blixt, O., Head, S., Mondala, T., Scanlan, C., Huflejt, M. E., Alvarez, R., Bryan, M. C., Fazio, F., Calarese, D., Stevens, J., Razi, N., Stevens, D. J., Skehel, J. J., van Die, I., Burton, D. R., Wilson, I. A., Cummings, R., Bovin, N., Wong, C. H., Paulson, J. C.

- (2004) Printed covalent glycan array for ligand profiling of diverse glycan binding proteins. *Proc Natl Acad Sci U S A* 101, 17033-8.
86. Song, X., Lasanajak, Y., Xia, B., Smith, D. F., Cummings, R. D. (2009) Fluorescent glycosylamides produced by microscale derivatization of free glycans for natural glycan microarrays. *ACS Chem Biol* 4, 741-50.
 87. Fukui, S., Feizi, T., Galustian, C., Lawson, A. M., Chai, W. (2002) Oligosaccharide microarrays for high-throughput detection and specificity assignments of carbohydrate-protein interactions. *Nat Biotechnol* 20, 1011-7.
 88. Huang, W., Ochiai, H., Zhang, X., Wang, L. X. (2008) Introducing N-glycans into natural products through a chemoenzymatic approach. *Carbohydr Res* 343, 2903-13.
 89. Belser, J. A., Blixt, O., Chen, L. M., Pappas, C., Maines, T. R., Van Hoeven, N., Donis, R., Busch, J., McBride, R., Paulson, J. C., Katz, J. M., Tumpey, T. M. (2008) Contemporary North American influenza H7 viruses possess human receptor specificity: Implications for virus transmissibility. *Proc Natl Acad Sci U S A* 105, 7558-63.
 90. Kumari, K., Gulati, S., Smith, D. F., Gulati, U., Cummings, R. D., Air, G. M. (2007) Receptor binding specificity of recent human H3N2 influenza viruses. *Virology* 4, 42.
 91. Stevens, J., Blixt, O., Tumpey, T. M., Taubenberger, J. K., Paulson, J. C., Wilson, I. A. (2006) Structure and receptor specificity of the hemagglutinin from an H5N1 influenza virus. *Science* 312, 404-10.
 92. Wan, H., Sorrell, E. M., Song, H., Hossain, M. J., Ramirez-Nieto, G., Monne, I., Stevens, J., Cattoli, G., Capua, I., Chen, L. M., Donis, R. O., Busch, J., Paulson, J. C., Brockwell, C., Webby, R., Blanco, J., Al-Natour, M. Q., Perez, D. R. (2008) Replication and transmission of H9N2 influenza viruses in ferrets: evaluation of pandemic potential. *PLoS ONE* 3, e2923.
 93. Duverger, E., Frison, N., Roche, A. C., Monsigny, M. (2003) Carbohydrate-lectin interactions assessed by surface plasmon resonance. *Biochimie* 85, 167-79.
 94. Dam, T. K., Gerken, T. A., Brewer, C. F. (2009) Thermodynamics of multivalent carbohydrate-lectin cross-linking interactions: importance of entropy in the bind and jump mechanism. *Biochemistry* 48, 3822-7.
 95. Viswanathan, K., Koh, X., Chandrasekaran, A., Pappas, C., Raman, R., Srinivasan, A., Shriver, Z., Tumpey, T. M., Sasisekharan, R. (2010) Determinants of glycan receptor specificity of H2N2 influenza A virus hemagglutinin. *PLoS One* 5, e13768.
 96. Hoffmann, E., Neumann, G., Kawaoka, Y., Hobom, G., Webster, R. G. (2000) A DNA transfection system for generation of influenza A virus from eight plasmids. *Proc Natl Acad Sci U S A* 97, 6108-13.
 97. Pleschka, S., Jaskunas, R., Engelhardt, O. G., Zurcher, T., Palese, P., Garcia-Sastre, A. (1996) A plasmid-based reverse genetics system for influenza A virus. *J Virol* 70, 4188-92.
 98. Maines, T. R., Jayaraman, A., Belser, J. A., Wadford, D. A., Pappas, C., Zeng, H., Gustin, K. M., Pearce, M. B., Viswanathan, K., Shriver, Z. H., Raman, R., Cox, N. J.,

- Sasisekharan, R., Katz, J. M., Tumpey, T. M. (2009) Transmission and pathogenesis of swine-origin 2009 A(H1N1) influenza viruses in ferrets and mice. *Science* 325, 484-7.
99. Jayaraman, A., Pappas, C., Raman, R., Belser, J. A., Viswanathan, K., Shriver, Z., Tumpey, T. M., Sasisekharan, R. (2011) A Single Base-Pair Change in 2009 H1N1 Hemagglutinin Increases Human Receptor Affinity and Leads to Efficient Airborne Viral Transmission in Ferrets. *PLoS One* 6, e17616.
 100. Maher, J. A. and DeStefano, J. (2004) The ferret: an animal model to study influenza virus. *Lab Anim (NY)* 33, 50-3.
 101. Palese, P., Tumpey, T. M., Garcia-Sastre, A. (2006) What can we learn from reconstructing the extinct 1918 pandemic influenza virus? *Immunity* 24, 121-4.
 102. Tumpey, T. M., Garcia-Sastre, A., Taubenberger, J. K., Palese, P., Swayne, D. E., Basler, C. F. (2004) Pathogenicity and immunogenicity of influenza viruses with genes from the 1918 pandemic virus. *Proc Natl Acad Sci U S A* 101, 3166-71.
 103. Tumpey, T. M., Garcia-Sastre, A., Taubenberger, J. K., Palese, P., Swayne, D. E., Pantin-Jackwood, M. J., Schultz-Cherry, S., Solorzano, A., Van Rooijen, N., Katz, J. M., Basler, C. F. (2005) Pathogenicity of influenza viruses with genes from the 1918 pandemic virus: functional roles of alveolar macrophages and neutrophils in limiting virus replication and mortality in mice. *J Virol* 79, 14933-44.
 104. Pappas, C., Aguilar, P. V., Basler, C. F., Solorzano, A., Zeng, H., Perrone, L. A., Palese, P., Garcia-Sastre, A., Katz, J. M., Tumpey, T. M. (2008) Single gene reassortants identify a critical role for PB1, HA, and NA in the high virulence of the 1918 pandemic influenza virus. *Proc Natl Acad Sci U S A* 105, 3064-9.
 105. Comelli, E. M., Sutton-Smith, M., Yan, Q., Amado, M., Panico, M., Gilmartin, T., Whisenant, T., Lanigan, C. M., Head, S. R., Goldberg, D., Morris, H. R., Dell, A., Paulson, J. C. (2006) Activation of murine CD4+ and CD8+ T lymphocytes leads to dramatic remodeling of N-linked glycans. *J Immunol* 177, 2431-40.
 106. Uematsu, R., Furukawa, J., Nakagawa, H., Shinohara, Y., Deguchi, K., Monde, K., Nishimura, S. (2005) High throughput quantitative glycomics and glycoform-focused proteomics of murine dermis and epidermis. *Mol Cell Proteomics* 4, 1977-89.
 107. Manzi, A. E., Norgard-Sumnicht, K., Argade, S., Marth, J. D., van Halbeek, H., Varki, A. (2000) Exploring the glycan repertoire of genetically modified mice by isolation and profiling of the major glycan classes and nano-NMR analysis of glycan mixtures. *Glycobiology* 10, 669-89.
 108. Norgard-Sumnicht, K., Bai, X., Esko, J. D., Varki, A., Manzi, A. E. (2000) Exploring the outcome of genetic modifications of glycosylation in cultured cell lines by concurrent isolation of the major classes of vertebrate glycans. *Glycobiology* 10, 691-700.
 109. Bewley, C. A. (2008) Illuminating the switch in influenza viruses. *Nat Biotechnol* 26, 60-2.
 110. Srinivasan, A., Viswanathan, K., Raman, R., Chandrasekaran, A., Raguram, S., Tumpey, T. M., Sasisekharan, V., Sasisekharan, R. (2008) Quantitative

- biochemical rationale for differences in transmissibility of 1918 pandemic influenza A viruses. *Proc Natl Acad Sci U S A* 105, 2800-5.
111. Fraser, C., Donnelly, C. A., Cauchemez, S., Hanage, W. P., Van Kerkhove, M. D., Hollingsworth, T. D., Griffin, J., Baggaley, R. F., Jenkins, H. E., Lyons, E. J., Jombart, T., Hinsley, W. R., Grassly, N. C., Balloux, F., Ghani, A. C., Ferguson, N. M., Rambaut, A., Pybus, O. G., Lopez-Gatell, H., Alpuche-Aranda, C. M., Chapela, I. B., Zavala, E. P., Guevara, D. M., Checchi, F., Garcia, E., Hugonnet, S., Roth, C. (2009) Pandemic potential of a strain of influenza A (H1N1): early findings. *Science* 324, 1557-61.
 112. Cauchemez, S., Donnelly, C. A., Reed, C., Ghani, A. C., Fraser, C., Kent, C. K., Finelli, L., Ferguson, N. M. (2009) Household transmission of 2009 pandemic influenza A (H1N1) virus in the United States. *N Engl J Med* 361, 2619-27.
 113. Kida, H., Webster, R. G., Yanagawa, R. (1983) Inhibition of virus-induced hemolysis with monoclonal antibodies to different antigenic areas on the hemagglutinin molecule of A/seal/Massachusetts/1/80 (H7N7) influenza virus. *Arch Virol* 76, 91-9.
 114. Yoden, S., Kida, H., Kuwabara, M., Yanagawa, R., Webster, R. G. (1986) Spin-labeling of influenza virus hemagglutinin permits analysis of the conformational change at low pH and its inhibition by antibody. *Virus Res* 4, 251-61.
 115. Johansson, B. E., Bucher, D. J., Kilbourne, E. D. (1989) Purified influenza virus hemagglutinin and neuraminidase are equivalent in stimulation of antibody response but induce contrasting types of immunity to infection. *J Virol* 63, 1239-46.
 116. Chen, Z., Kadowaki, S., Hagiwara, Y., Yoshikawa, T., Matsuo, K., Kurata, T., Tamura, S. (2000) Cross-protection against a lethal influenza virus infection by DNA vaccine to neuraminidase. *Vaccine* 18, 3214-22.
 117. Johansson, B. E., Moran, T. M., Kilbourne, E. D. (1987) Antigen-presenting B cells and helper T cells cooperatively mediate intravirionic antigenic competition between influenza A virus surface glycoproteins. *Proc Natl Acad Sci U S A* 84, 6869-73.
 118. Powers, D. C., Kilbourne, E. D., Johansson, B. E. (1996) Neuraminidase-specific antibody responses to inactivated influenza virus vaccine in young and elderly adults. *Clin Diagn Lab Immunol* 3, 511-6.
 119. Stohr, K. (2002) Influenza--WHO cares. *Lancet Infect Dis* 2, 517.
 120. Gerber, P., Loosli, C. G., Hambre, D. (1955) Antigenic variants of influenza A virus, PR8 strain. I. Their development during serial passage in the lungs of partially immune mice. *J Exp Med* 101, 627-38.
 121. Taylor, R. M. (1949) Studies on survival of influenza virus between epidemics and antigenic variants of the virus. *Am J Public Health Nations Health* 39, 171-8.
 122. Archetti, I. and Horsfall, F. L., Jr. (1950) Persistent antigenic variation of influenza A viruses after incomplete neutralization in ovo with heterologous immune serum. *J Exp Med* 92, 441-62.

123. Yewdell, J. W., Caton, A. J., Gerhard, W. (1986) Selection of influenza A virus adsorptive mutants by growth in the presence of a mixture of monoclonal antihemagglutinin antibodies. *J Virol* 57, 623-8.
124. Yewdell, J. W., Webster, R. G., Gerhard, W. U. (1979) Antigenic variation in three distinct determinants of an influenza type A haemagglutinin molecule. *Nature* 279, 246-8.
125. Wilson, I. A., Skehel, J. J., Wiley, D. C. (1981) Structure of the haemagglutinin membrane glycoprotein of influenza virus at 3 Å resolution. *Nature* 289, 366-73.
126. Stevens, J., Corper, A. L., Basler, C. F., Taubenberger, J. K., Palese, P., Wilson, I. A. (2004) Structure of the uncleaved human H1 hemagglutinin from the extinct 1918 influenza virus. *Science* 303, 1866-70.
127. Xu, R., McBride, R., Paulson, J. C., Basler, C. F., Wilson, I. A. (2009) Structure, receptor binding and antigenicity of influenza virus hemagglutinins from the 1957 H2N2 pandemic. *J Virol*.
128. Gerhard, W., Yewdell, J., Frankel, M. E., Webster, R. (1981) Antigenic structure of influenza virus haemagglutinin defined by hybridoma antibodies. *Nature* 290, 713-7.
129. Caton, A. J., Brownlee, G. G., Yewdell, J. W., Gerhard, W. (1982) The antigenic structure of the influenza virus A/PR/8/34 hemagglutinin (H1 subtype). *Cell* 31, 417-27.
130. Lubeck, M. D. and Gerhard, W. (1981) Topological mapping antigenic sites on the influenza A/PR/8/34 virus hemagglutinin using monoclonal antibodies. *Virology* 113, 64-72.
131. Matrosovich, M. N., Gambaryan, A. S., Teneberg, S., Piskarev, V. E., Yamnikova, S. S., Lvov, D. K., Robertson, J. S., Karlsson, K. A. (1997) Avian influenza A viruses differ from human viruses by recognition of sialyloligosaccharides and gangliosides and by a higher conservation of the HA receptor-binding site. *Virology* 233, 224-34.
132. Harris, A., Cardone, G., Winkler, D. C., Heymann, J. B., Brecher, M., White, J. M., Steven, A. C. (2006) Influenza virus pleiomorphy characterized by cryoelectron tomography. *Proc Natl Acad Sci U S A* 103, 19123-7.
133. Gambaryan, A. S., Matrosovich, M. N., Bender, C. A., Kilbourne, E. D. (1998) Differences in the biological phenotype of low-yielding (L) and high-yielding (H) variants of swine influenza virus A/NJ/11/76 are associated with their different receptor-binding activity. *Virology* 247, 223-31.
134. Underwood, P. A., Skehel, J. J., Wiley, D. C. (1987) Receptor-binding characteristics of monoclonal antibody-selected antigenic variants of influenza virus. *J Virol* 61, 206-8.
135. Nelson, M. I., Simonsen, L., Viboud, C., Miller, M. A., Taylor, J., George, K. S., Griesemer, S. B., Ghedin, E., Sengamalay, N. A., Spiro, D. J., Volkov, I., Grenfell, B. T., Lipman, D. J., Taubenberger, J. K., Holmes, E. C. (2006) Stochastic processes are key determinants of short-term evolution in influenza a virus. *PLoS Pathog* 2, e125.

136. Jin, H., Zhou, H., Liu, H., Chan, W., Adhikary, L., Mahmood, K., Lee, M. S., Kemble, G. (2005) Two residues in the hemagglutinin of A/Fujian/411/02-like influenza viruses are responsible for antigenic drift from A/Panama/2007/99. *Virology* 336, 113-9.
137. Smith, D. J., Lapedes, A. S., de Jong, J. C., Bestebroer, T. M., Rimmelzwaan, G. F., Osterhaus, A. D., Fouchier, R. A. (2004) Mapping the antigenic and genetic evolution of influenza virus. *Science* 305, 371-6.
138. Nicholls, J. M., Chan, R. W., Russell, R. J., Air, G. M., Peiris, J. S. (2008) Evolving complexities of influenza virus and its receptors. *Trends Microbiol* 16, 149-57.
139. Roberts, P. C., Garten, W., Klenk, H. D. (1993) Role of conserved glycosylation sites in maturation and transport of influenza A virus hemagglutinin. *J Virol* 67, 3048-60.
140. Schulze, I. T. (1997) Effects of glycosylation on the properties and functions of influenza virus hemagglutinin. *J Infect Dis* 176 Suppl 1, S24-8.
141. Klenk, H. D., Wagner, R., Heuer, D., Wolff, T. (2002) Importance of hemagglutinin glycosylation for the biological functions of influenza virus. *Virus Res* 82, 73-5.
142. Ohuchi, R., Ohuchi, M., Garten, W., Klenk, H. D. (1997) Oligosaccharides in the stem region maintain the influenza virus hemagglutinin in the metastable form required for fusion activity. *J Virol* 71, 3719-25.
143. Reading, P. C., Pickett, D. L., Tate, M. D., Whitney, P. G., Job, E. R., Brooks, A. G. (2009) Loss of a single N-linked glycan from the hemagglutinin of influenza virus is associated with resistance to collectins and increased virulence in mice. *Respir Res* 10, 117.
144. Hebert, D. N., Zhang, J. X., Chen, W., Foellmer, B., Helenius, A. (1997) The number and location of glycans on influenza hemagglutinin determine folding and association with calnexin and calreticulin. *J Cell Biol* 139, 613-23.
145. Wang, C. C., Chen, J. R., Tseng, Y. C., Hsu, C. H., Hung, Y. F., Chen, S. W., Chen, C. M., Khoo, K. H., Cheng, T. J., Cheng, Y. S., Jan, J. T., Wu, C. Y., Ma, C., Wong, C. H. (2009) Glycans on influenza hemagglutinin affect receptor binding and immune response. *Proc Natl Acad Sci U S A* 106, 18137-42.
146. Gambaryan, A. S., Marinina, V. P., Tuzikov, A. B., Bovin, N. V., Rudneva, I. A., Sinitsyn, B. V., Shilov, A. A., Matrosovich, M. N. (1998) Effects of host-dependent glycosylation of hemagglutinin on receptor-binding properties on H1N1 human influenza A virus grown in MDCK cells and in embryonated eggs. *Virology* 247, 170-7.
147. Gao, Y., Zhang, Y., Shinya, K., Deng, G., Jiang, Y., Li, Z., Guan, Y., Tian, G., Li, Y., Shi, J., Liu, L., Zeng, X., Bu, Z., Xia, X., Kawaoka, Y., Chen, H. (2009) Identification of amino acids in HA and PB2 critical for the transmission of H5N1 avian influenza viruses in a mammalian host. *PLoS Pathog* 5, e1000709.
148. Wang, W., Lu, B., Zhou, H., Suguitan, A. L., Jr., Cheng, X., Subbarao, K., Kemble, G., Jin, H. (2010) Glycosylation at 158N of the hemagglutinin protein and receptor binding specificity synergistically affect the antigenicity and immunogenicity of a live attenuated H5N1 A/Vietnam/1203/2004 vaccine virus in ferrets. *J Virol* 84, 6570-7.

149. Wei, C. J., Boyington, J. C., Dai, K., Houser, K. V., Pearce, M. B., Kong, W. P., Yang, Z. Y., Tumpey, T. M., Nabel, G. J. (2010) Cross-neutralization of 1918 and 2009 influenza viruses: role of glycans in viral evolution and vaccine design. *Sci Transl Med* 2, 24ra21.
150. Smee, D. F., Wandersee, M. K., Checketts, M. B., O'Keefe, B. R., Saucedo, C., Boyd, M. R., Mishin, V. P., Gubareva, L. V. (2007) Influenza A (H1N1) virus resistance to cyanovirin-N arises naturally during adaptation to mice and by passage in cell culture in the presence of the inhibitor. *Antivir Chem Chemother* 18, 317-27.
151. O'Keefe, B. R., Smee, D. F., Turpin, J. A., Saucedo, C. J., Gustafson, K. R., Mori, T., Blakeslee, D., Buckheit, R., Boyd, M. R. (2003) Potent anti-influenza activity of cyanovirin-N and interactions with viral hemagglutinin. *Antimicrob Agents Chemother* 47, 2518-25.
152. Igarashi, M., Ito, K., Kida, H., Takada, A. (2008) Genetically destined potentials for N-linked glycosylation of influenza virus hemagglutinin. *Virology* 376, 323-9.
153. Kasson, P. M. and Pande, V. S. (2008) Structural basis for influence of viral glycans on ligand binding by influenza hemagglutinin. *Biophys J* 95, L48-50.
154. Garten, R. J., Davis, C. T., Russell, C. A., Shu, B., Lindstrom, S., Balish, A., Sessions, W. M., Xu, X., Skepner, E., Deyde, V., Okomo-Adhiambo, M., Gubareva, L., Barnes, J., Smith, C. B., Emery, S. L., Hillman, M. J., Rivaller, P., Smagala, J., de Graaf, M., Burke, D. F., Fouchier, R. A., Pappas, C., Alpuche-Aranda, C. M., Lopez-Gatell, H., Olivera, H., Lopez, I., Myers, C. A., Faix, D., Blair, P. J., Yu, C., Keene, K. M., Dotson, P. D., Jr., Boxrud, D., Sambol, A. R., Abid, S. H., St George, K., Bannerman, T., Moore, A. L., Stringer, D. J., Blevins, P., Demmler-Harrison, G. J., Ginsberg, M., Kriner, P., Waterman, S., Smole, S., Guevara, H. F., Belongia, E. A., Clark, P. A., Beatrice, S. T., Donis, R., Katz, J., Finelli, L., Bridges, C. B., Shaw, M., Jernigan, D. B., Uyeki, T. M., Smith, D. J., Klimov, A. I., Cox, N. J. (2009) Antigenic and Genetic Characteristics of Swine-Origin 2009 A(H1N1) Influenza Viruses Circulating in Humans. *Science*.
155. WHO (2010) H1N1 in post-pandemic period.
156. WHO (2010) Pandemic (H1N1) 2009 - Update 112.
157. Viboud, C., Tam, T., Fleming, D., Handel, A., Miller, M. A., Simonsen, L. (2006) Transmissibility and mortality impact of epidemic and pandemic influenza, with emphasis on the unusually deadly 1951 epidemic. *Vaccine* 24, 6701-7.
158. Maines, T. R., Chen, L. M., Matsuoka, Y., Chen, H., Rowe, T., Ortin, J., Falcon, A., Nguyen, T. H., Maile, Q., Sedyaningsih, E. R., Harun, S., Tumpey, T. M., Donis, R. O., Cox, N. J., Subbarao, K., Katz, J. M. (2006) Lack of transmission of H5N1 avian-human reassortant influenza viruses in a ferret model. *Proc Natl Acad Sci U S A* 103, 12121-6.
159. Lowen, A. C. and Palese, P. (2007) Influenza virus transmission: basic science and implications for the use of antiviral drugs during a pandemic. *Infect Disord Drug Targets* 7, 318-28.
160. Van Hoeven, N., Pappas, C., Belser, J. A., Maines, T. R., Zeng, H., Garcia-Sastre, A., Sasisekharan, R., Katz, J. M., Tumpey, T. M. (2009) Human HA and polymerase

- subunit PB2 proteins confer transmission of an avian influenza virus through the air. *Proc Natl Acad Sci U S A* 106, 3366-71.
161. Yen, H. L., Lipatov, A. S., Ilyushina, N. A., Govorkova, E. A., Franks, J., Yilmaz, N., Douglas, A., Hay, A., Krauss, S., Rehg, J. E., Hoffmann, E., Webster, R. G. (2007) Inefficient transmission of H5N1 influenza viruses in a ferret contact model. *J Virol* 81, 6890-8.
 162. Shelton, H., Ayora-Talavera, G., Ren, J., Loureiro, S., Pickles, R. J., Barclay, W. S., Jones, I. M. (2011) Receptor binding profiles of avian influenza virus hemagglutinin subtypes on human cells as a predictor of pandemic potential. *J Virol* 85, 1875-80.
 163. WHO (2009) Public health significance of virus mutation detected in Norway.
 164. Kilander, A., Rykkvin, R., Dudman, S. G., Hungnes, O. (2010) Observed association between the HA1 mutation D222G in the 2009 pandemic influenza A(H1N1) virus and severe clinical outcome, Norway 2009-2010. *Euro Surveill* 15.
 165. Yang, H., Carney, P., Stevens, J. (2010) Structure and Receptor binding properties of a pandemic H1N1 virus hemagglutinin. *PLoS Curr* 2, RRN1152.
 166. Liu, Y., Childs, R. A., Matrosovich, T., Wharton, S., Palma, A. S., Chai, W., Daniels, R., Gregory, V., Uhlenhorff, J., Kiso, M., Klenk, H. D., Hay, A., Feizi, T., Matrosovich, M. (2010) Altered receptor specificity and cell tropism of D222G hemagglutinin mutants isolated from fatal cases of pandemic A(H1N1) 2009 influenza virus. *J Virol* 84, 12069-74.
 167. Nicholls, J. M., Bourne, A. J., Chen, H., Guan, Y., Peiris, J. S. (2007) Sialic acid receptor detection in the human respiratory tract: evidence for widespread distribution of potential binding sites for human and avian influenza viruses. *Respir Res* 8, 73.
 168. Doyle, T. J. and Hopkins, R. S. (2011) Low secondary transmission of 2009 pandemic influenza A (H1N1) in households following an outbreak at a summer camp: relationship to timing of exposure. *Epidemiol Infect* 139, 45-51.
 169. Morens, D. M., Taubenberger, J. K., Fauci, A. S. (2010) The 2009 H1N1 Pandemic Influenza Virus: What Next? *MBio* 1.
 170. Barr, I. G., Cui, L., Komadina, N., Lee, R. T., Lin, R. T., Deng, Y., Caldwell, N., Shaw, R., Maurer-Stroh, S. (2010) A new pandemic influenza A(H1N1) genetic variant predominated in the winter 2010 influenza season in Australia, New Zealand and Singapore. *Euro Surveill* 15.
 171. Hensley, S. E., Das, S. R., Bailey, A. L., Schmidt, L. M., Hickman, H. D., Jayaraman, A., Viswanathan, K., Raman, R., Sasisekharan, R., Bennink, J. R., Yewdell, J. W. (2009) Hemagglutinin receptor binding avidity drives influenza A virus antigenic drift. *Science* 326, 734-6.
 172. Xu, Q., Wang, W., Cheng, X., Zengel, J., Jin, H. (2010) Influenza H1N1 A/Solomon Island/3/06 virus receptor binding specificity correlates with virus pathogenicity, antigenicity, and immunogenicity in ferrets. *J Virol* 84, 4936-45.
 173. Hussein, R. H., Sweet, C., Bird, R. A., Collie, M. H., Smith, H. (1983) Distribution of viral antigen with the lower respiratory tract of ferrets infected with a virulent

- influenza virus: production and release of virus from corresponding organ cultures. *J Gen Virol* 64 Pt 3, 589-98.
174. Suzuki, Y., Ito, T., Suzuki, T., Holland, R. E., Jr., Chambers, T. M., Kiso, M., Ishida, H., Kawaoka, Y. (2000) Sialic acid species as a determinant of the host range of influenza A viruses. *J Virol* 74, 11825-31.
 175. Garcia-Sastre, A. (2010) Influenza virus receptor specificity: disease and transmission. *Am J Pathol* 176, 1584-5.
 176. Perini, J. M., Vandamme-Cubadda, N., Aubert, J. P., Porchet, N., Mazzuca, M., Lamblin, G., Herscovics, A., Roussel, P. (1991) Multiple apomucin translation products from human respiratory mucosa mRNA. *Eur J Biochem* 196, 321-8.
 177. Rogers, D. F. (1994) Airway goblet cells: responsive and adaptable front-line defenders. *Eur Respir J* 7, 1690-706.
 178. Memoli, M. J., Davis, A. S., Proudfoot, K., Chertow, D. S., Hrabal, R. J., Bristol, T., Taubenberger, J. K. (2011) Multidrug-resistant 2009 pandemic influenza A(H1N1) viruses maintain fitness and transmissibility in ferrets. *J Infect Dis* 203, 348-57.
 179. Kirkeby, S., Martel, C. J., Aasted, B. (2009) Infection with human H1N1 influenza virus affects the expression of sialic acids of metaplastic mucous cells in the ferret airways. *Virus Res* 144, 225-32.
 180. Triana-Baltzer, G. B., Babizki, M., Chan, M. C., Wong, A. C., Aschenbrenner, L. M., Campbell, E. R., Li, Q. X., Chan, R. W., Peiris, J. S., Nicholls, J. M., Fang, F. (2010) DAS181, a sialidase fusion protein, protects human airway epithelium against influenza virus infection: an in vitro pharmacodynamic analysis. *J Antimicrob Chemother* 65, 275-84.
 181. WHO Influenza (Seasonal) Fact Sheet No. 211.
 182. Johansson, B. E. and Brett, I. C. (2007) Changing perspective on immunization against influenza. *Vaccine* 25, 3062-5.
 183. Gowen, B. B., Smee, D. F., Wong, M. H., Hall, J. O., Jung, K. H., Bailey, K. W., Stevens, J. R., Furuta, Y., Morrey, J. D. (2008) Treatment of late stage disease in a model of arenaviral hemorrhagic fever: T-705 efficacy and reduced toxicity suggests an alternative to ribavirin. *PLoS One* 3, e3725.
 184. Shapira, S. D., Gat-Viks, I., Shum, B. O., Dricot, A., de Grace, M. M., Wu, L., Gupta, P. B., Hao, T., Silver, S. J., Root, D. E., Hill, D. E., Regev, A., Hacohen, N. (2009) A physical and regulatory map of host-influenza interactions reveals pathways in H1N1 infection. *Cell* 139, 1255-67.
 185. Shibuya, N., Goldstein, I. J., Broekaert, W. F., Nsimba-Lubaki, M., Peeters, B., Peumans, W. J. (1987) The elderberry (*Sambucus nigra* L.) bark lectin recognizes the Neu5Ac(alpha 2-6)Gal/GalNAc sequence. *J Biol Chem* 262, 1596-601.
 186. Van Damme, E. J., Barre, A., Rouge, P., Van Leuven, F., Peumans, W. J. (1996) The NeuAc(alpha-2,6)-Gal/GalNAc-binding lectin from elderberry (*Sambucus nigra*) bark, a type-2 ribosome-inactivating protein with an unusual specificity and structure. *Eur J Biochem* 235, 128-37.
 187. Shahidi-Noghabi, S., Van Damme, E. J., Smagghe, G. (2008) Carbohydrate-binding activity of the type-2 ribosome-inactivating protein SNA-I from elderberry

- (*Sambucus nigra*) is a determining factor for its insecticidal activity. *Phytochemistry* 69, 2972-8.
188. Kaku, H., Kaneko, H., Minamihara, N., Iwata, K., Jordan, E. T., Rojo, M. A., Minami-Ishii, N., Minami, E., Hisajima, S., Shibuya, N. (2007) Elderberry bark lectins evolved to recognize Neu5Ac alpha2,6Gal/GalNAc sequence from a Gal/GalNAc binding lectin through the substitution of amino-acid residues critical for the binding to sialic acid. *J Biochem* 142, 393-401.
 189. Chen, Y., Rouge, P., Peumans, W. J., van Damme, E. J. (2002) Mutational analysis of the carbohydrate-binding activity of the NeuAc(alpha-2,6)Gal/GalNAc-specific type 2 ribosome-inactivating protein from elderberry (*Sambucus nigra*) fruits. *Biochem J* 364, 587-92.
 190. Maveyraud, L., Niwa, H., Guillet, V., Svergun, D. I., Konarev, P. V., Palmer, R. A., Peumans, W. J., Rouge, P., Van Damme, E. J., Reynolds, C. D., Mourey, L. (2009) Structural basis for sugar recognition, including the Tn carcinoma antigen, by the lectin SNA-II from *Sambucus nigra*. *Proteins* 75, 89-103.
 191. Mo, H., Winter, H. C., Goldstein, I. J. (2000) Purification and characterization of a Neu5Acalpha2-6Galbeta1-4Glc/GlcNAc-specific lectin from the fruiting body of the polypore mushroom *Polyporus squamosus*. *J Biol Chem* 275, 10623-9.
 192. Tateno, H., Winter, H. C., Goldstein, I. J. (2004) Cloning, expression in *Escherichia coli* and characterization of the recombinant Neu5Acalpha2,6Galbeta1,4GlcNAc-specific high-affinity lectin and its mutants from the mushroom *Polyporus squamosus*. *Biochem J* 382, 667-75.
 193. Matrosovich, M., Matrosovich, T., Carr, J., Roberts, N. A., Klenk, H. D. (2003) Overexpression of the alpha-2,6-sialyltransferase in MDCK cells increases influenza virus sensitivity to neuraminidase inhibitors. *J Virol* 77, 8418-25.
 194. Glycomics, C. f. F.
 195. Spackman, E. and Suarez, D. L. (2008) Type A influenza virus detection and quantitation by real-time RT-PCR. *Methods Mol Biol* 436, 19-26.
 196. Hartley, M. R. and Lord, J. M. (2004) Cytotoxic ribosome-inactivating lectins from plants. *Biochim Biophys Acta* 1701, 1-14.
 197. Hartley, M. R. and Lord, J. M. (2004) Genetics of ribosome-inactivating proteins. *Mini Rev Med Chem* 4, 487-92.
 198. Wei, C. J., Boyington, J. C., McTamney, P. M., Kong, W. P., Pearce, M. B., Xu, L., Andersen, H., Rao, S., Tumpey, T. M., Yang, Z. Y., Nabel, G. J. (2010) Induction of broadly neutralizing H1N1 influenza antibodies by vaccination. *Science* 329, 1060-4.
 199. Ekiert, D. C., Bhabha, G., Elsliger, M. A., Friesen, R. H., Jongeneelen, M., Throsby, M., Goudsmit, J., Wilson, I. A. (2009) Antibody recognition of a highly conserved influenza virus epitope. *Science* 324, 246-51.
 200. Swanson, M. D., Winter, H. C., Goldstein, I. J., Markovitz, D. M. (2010) A lectin isolated from bananas is a potent inhibitor of HIV replication. *J Biol Chem* 285, 8646-55.

201. Micewicz, E. D., Cole, A. L., Jung, C. L., Luong, H., Phillips, M. L., Pratikhya, P., Sharma, S., Waring, A. J., Cole, A. M., Ruchala, P. (2010) Grifonin-1: a small HIV-1 entry inhibitor derived from the algal lectin, Griffithsin. *PLoS One* 5, e14360.
202. Triana-Baltzer, G. B., Gubareva, L. V., Klimov, A. I., Wurtman, D. F., Moss, R. B., Hedlund, M., Larson, J. L., Belshe, R. B., Fang, F. (2009) Inhibition of neuraminidase inhibitor-resistant influenza virus by DAS181, a novel sialidase fusion protein. *PLoS One* 4, e7838.
203. Triana-Baltzer, G. B., Gubareva, L. V., Nicholls, J. M., Pearce, M. B., Mishin, V. P., Belser, J. A., Chen, L. M., Chan, R. W., Chan, M. C., Hedlund, M., Larson, J. L., Moss, R. B., Katz, J. M., Tumpey, T. M., Fang, F. (2009) Novel pandemic influenza A(H1N1) viruses are potently inhibited by DAS181, a sialidase fusion protein. *PLoS One* 4, e7788.
204. Fodor, E., Devenish, L., Engelhardt, O. G., Palese, P., Brownlee, G. G., Garcia-Sastre, A. (1999) Rescue of influenza A virus from recombinant DNA. *J Virol* 73, 9679-82.
205. Neumann, G., Watanabe, T., Ito, H., Watanabe, S., Goto, H., Gao, P., Hughes, M., Perez, D. R., Donis, R., Hoffmann, E., Hobom, G., Kawaoka, Y. (1999) Generation of influenza A viruses entirely from cloned cDNAs. *Proc Natl Acad Sci U S A* 96, 9345-50.
206. Hai, R., Martinez-Sobrido, L., Fraser, K. A., Ayllon, J., Garcia-Sastre, A., Palese, P. (2008) Influenza B virus NS1-truncated mutants: live-attenuated vaccine approach. *J Virol* 82, 10580-90.
207. Hinshaw, V. S., Webster, R. G., Easterday, B. C., Bean, W. J., Jr. (1981) Replication of avian influenza A viruses in mammals. *Infect Immun* 34, 354-61.
208. Stephenson, I., Wood, J. M., Nicholson, K. G., Charlett, A., Zambon, M. C. (2004) Detection of anti-H5 responses in human sera by HI using horse erythrocytes following MF59-adjuvanted influenza A/Duck/Singapore/97 vaccine. *Virus Res* 103, 91-5.